Analyses of juvenile hormone pathway governing environmental sex determination in the water flea *Daphnia pulex*

Kenji Toyota

Department of Basic Biology

School of Life Science

The Graduate University for Advanced Studies

2015

Table of Contents

List of Abbreviations

- AMPA (±)-α-amino-3-hydroxy-5-methyl-4-isoxazolepropionic acid
- BmPSI *Bombyx* homolog of P-element somatic inhibitor
- CYP Cytochrome P450
- DEG Differentially expressed gene
- DM domain Dsx/Mab-3 domain
- DMF Dimethylformamide
- Dsx Doublesex
- ESD Environmental sex determination
- EST Expressed sequence tag
- FA Farnesoic acid
- FAMeT FA *O*-methyltransferase
- FDR False discovery rate
- GC-MS Gas chromatography-mass spectrometry
- GO Gene ontology
- GSD Genotypic sex determination
- iGluR Ionotropic glutamate receptor
- JH Juvenile hormone
- JHAMT JH acid *O*-methyltransferase
- JHBP JH binding protein
- JHE JH esterase
- JHEBP JHE binding protein
- JHEH JH epoxide hydorase
- KEGG Kyoto Encyclopedia of Genes and Genomes
- LC-MS Liquid chromatography-mass spectrometry
- LD Long day condition (light 14 h : dark 10 h)
- MF Methyl farnesoate
- NMDA *N*-methyl-D-aspartic acid
- PKC Protein kinase C
- PFM Position frequency matrix
- RNAi RNA interference
- SAM S-adenosyl-methionine
- SD Short day condition (light 10 h : dark 14 h)
- Sxl Sex-lethal
- TALEN Transcription activator-like effector nuclease
- TF Transcription factor

- TFBS Transcription factor binding site
- TGFβ Transforming growth factor beta
- Tra Transformer
- Tra2 Transformer2
- TSS Transcription start site

General Introduction

Innate reproductive strategy is a fundamental aspect of life and an essential process that creates a new genetic variety in the next generation. In particular, sexual reproduction is responsible for the establishment of sexually dimorphic traits including the gonadal development (testis or ovary) and sex-specific differences in morphological, behavioral and physiological phenotypes. Mode of the sex determination can be generally divided into two major categories: genotypic sex determination (GSD) and environmental sex determination (ESD) (Bull, 1985; Marin and Baker, 1998; Zarkower, 2001). GSD occurs in the majority of organisms where a sex-determining gene residing on a sex chromosome establishes the development of male or female at conception (Kopp, 2012; Matson and Zarkower, 2012). On the other hand, the sex of ESD organisms is determined after fertilization in response to particular environmental conditions such as temperature in some reptiles (temperature-dependent sex determination: TSD) (Bull, 1985; Charnier, 1966), photoperiod in aphids and marine amphipods (Guler et al., 2012; Hardie, 1981; Lees, 1973), and social factors in shelf limpets (Warner et al., 1996). Although the trigger of sex determination is variable, a common three-step framework should be conserved in terms of sex determination mechanism: 1) sexes are primarily triggered by environmental (*e.g.*, temperature) or genetic (XX:XY, ZZ:ZW or X:autosome ratio) factors, which is organism-specific, 2) once such a trigger switches the sexual fate, sexually dimorphic gene cassettes (regulatory network of core sex-determining genes) is activated and lastly, 3) they proceed male- or female-specific developmental pathway and irreversibly forms testis or ovary (Crews and Bull, 2009). Of those steps, molecular mechanisms underlying the reception of primary environmental cues and the following signaling cascades for

sexual fate determination remains largely unclear throughout animal species, partly due to the absence of suitable experimental animals, that can contribute to our understanding of the role of environmental influences in ontogeny, and providing key insights into the mechanisms that environmental stimuli are translated into phenotypic alteration.

The Cladocera (commonly called water fleas) is a representative zooplanktonic crustacean ubiquitously found in components of inland aqueous habitats all around the world, and has an important role as a primary consumer in the food chain (Ebert, 2005). The Cladocera is an ancient clade of branchiopod crustaceans comprising 16 or 18 family lineages (Olesen, 1998; Stenderup et al., 2006). Among them, the well-studied species are the family Daphniidae, particularly genus *Daphnia*. To date, approximately 200 species consisted of three subgenus (*Daphnia*, *Ctenodaphnia* and *Australodaphnia*) have been described (Adamowicz et al., 2009; Kotov et al., 2013), and they in general employ the cyclical parthenogenesis, in which parthenogenesis and sexual reproduction are altered in response to plural environmental cues such as photoperiod, temperature, nutrients, population density and combination of these stimuli (Banta and Brown, 1929a; Hobæk and Larsson, 1990; Kleiven et al., 1992; Smith, 1915) **(Figure GI-1)**. During the favorable conditions, they parthenogenetically produce offspring that build up a population consisting of only females. On the other hand, when unfavorable conditions arise, they start to produce male offspring to employ the sexual reproduction. Once females mate with males exhibiting sexual (haploid) eggs, fertilized eggs, so-called resting eggs that protected by ephippium (modified carapace) are formed to tolerate extreme conditions (*e.g.*, drying and freezing) and to maintain viability for over 100 years (Caceres, 1998). The resting egg can hatch out and develop as females when favorable conditions are restored. In this way, daphnids take advantage of cyclical

parthenogenesis depending on environmental conditions; the parthenogenesis allows quick propagation during the favorable growing seasons, whereas the sexual reproduction contributes to an increase in the genetic diversity and survival rate (Barton and Charlesworth, 1998). Therefore, the trigger of sex determination and its regulating processes are fundamental to daphnids to appropriately employ their reproductive strategies in step with seasonally changing environments (Kleiven et al., 1992).

As representative and historically used model species in daphnids, there has been accumulated information for *D. pulex* (Leydig, 1860) and *D. magna* (Straus, 1820) in terms of evolutionary, ecological, physiological, developmental, ecotoxicological and genetic properties. In addition, due to the diploidy of parthenogenetic egg being maintained by mitosis-like meiosis, which skips a part of the first meiosis, individuals within a single strain are most likely genetically identical (Hiruta et al., 2010), allowing us to analyze environmental impacts on physiological and developmental processes under the identical genetic background. However, despite of a large efforts of studies for male induction of daphnids, reproducible induction system for male offspring have not been established (Banta and Brown, 1929a; Hobæk and Larsson, 1990; Kleiven et al., 1992; Smith, 1915). This is because multiple environmental cues (*e.g.*, short day length, low temperature, oligotrophy and overcrowding) seem to be integrally involved in the sex determination in daphnids, therefore, it makes difficult to reproduce such experimental conditions in the laboratory. Recently, several groups including us have been reported that exogenous administration of juvenile hormones (JHs: representative endocrine factors among arthropods) or their analogs can induce male offspring even under the female-producing condition (Olmstead and LeBlanc, 2002; Tatarazako et al., 2003). However, it has been elusive the contribution of endogenous JH signaling on the

male-fate determination, and this is due to a lack of suitable experimental system whose sex of offspring can be modified without JH treatment.

In this thesis, I successfully established a reliable induction system of male and female offspring responding to the photoperiod differences in a *D. pulex* strain, WTN6. Taking advantage of this system, I found that JH acid *O*-methyltransferase (JHAMT; a rate-limiting enzyme of JH biosynthesis) was significantly increased just prior to the JH-sensitive period for male production. Thus, I demonstrated the key role of innate JH signaling as a conductor between external environmental stimuli and the endogenous male developing pathway (Chapter I).

The above experimental system, combined with genome information in *D. pulex* (Colbourne et al., 2011) and EST database in *D. magna* (Watanabe et al., 2005), also enables me to identify the signaling pathway directly involving in the JH synthesis and/or male offspring induction. By RNA-seq analysis, I found that ionotropic glutamate receptors, including *N*-methyl-D-aspartate (NMDA) receptors, were significantly changed in the male-producing condition. By the pharmacological manipulation of the NMDA receptor, I demonstrated that this receptor induce male offspring production, probably by controlling the JH synthesis. This is the first demonstration of a possible molecular signaling cascade to direct JH signaling in response to the external environmental stimuli in *D. pulex* (Chapter II).

Furthermore, I also conducted microarray analysis to make a comprehensive catalogue of JH-responsive genes in response to JH analogs in newborns of *D. magna*. Exogenous JH administration might activate not only male pathway-related genes but also toxic response. Indeed, daphnids have been centrally used as sentinel species in ecological and toxicological studies for several decades, because they are highly

sensitive to environmental changes and artificial chemicals released into the environment (Ebert, 2005; Hebert, 1997). I thereby performed microarray experiment with clustering analysis and provide gene catalogues that allow me to distinguish the molecular signaling components between innate male induction and toxic effects in daphnids (Chapter III).

A *doublesex* (*dsx*) was originally identified in *Drosophila melanogaster* as a critical and terminal regulator in the sex-determining cascade (Burtis and Baker, 1989). *Dsx1* is specifically expressed in the male embryos of *D. magna*, and its expression is indispensable for male traits development and maintenance (Kato et al., 2011a). It is thus considered that *dsx1* is responsible innate masculinized factor in response to maternally produced JHs. Male induction by JH administration has been reported in various cladoceran species (Kim et al., 2006; Oda et al., 2005b; Sinev and Sanoamuang, 2011), however, it is elusive whether the downstream pathway, particularly *dsx1*–mediating male sexually dimorphic development, is conserved among cladoceran species. In this thesis, I identified orthologous genes of *dsx1* from closely related species of *D. magna* and the all *dsx* examined had similar amino acid structure containing highly conserved DM and oligomerization domains. In addition, they exhibited sexually dimorphic expression patterns, suggesting a possible conserved role of *dsx1* on the male traits development in the cladoceran species (Chapter IV).

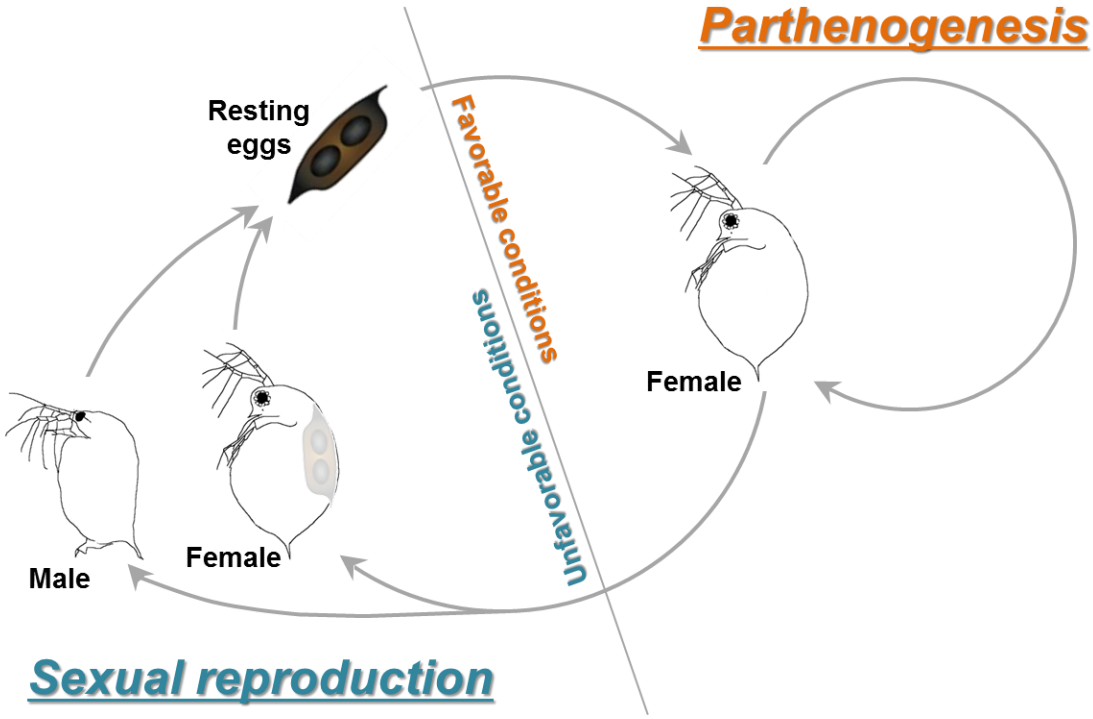

Figure GI-1. Schematic diagram of cyclical parthenogenesis in daphnids. They produce female offspring by parthenogenesis during favorable growing seasons. Males and females produce resting eggs only under unfavorable seasons. The resting eggs pass through the frozen and/or drying conditions.

Chapter I

Methyl farnesoate synthesis is necessary for the environmental sex determination in the water flea *Daphnia pulex*

Abstract

Sex-determination systems can be divided into two groups: genotypic sex determination (GSD) and environmental sex determination (ESD). ESD is an adaptive life-history strategy that allows control of sex in response to environmental cues in order to optimize fitness. However, the molecular basis of ESD remains largely unknown. The micro crustacean *Daphnia pulex* exhibits ESD in response to various external stimuli. Although methyl farnesoate (MF: putative juvenile hormone, JH, in daphnids) has been reported to induce male production in daphnids, the role of MF as a sex-determining factor remains elusive due to the lack of a suitable model system for its study. Here, I establish such a system for ESD studies in *D. pulex*. The WTN6 strain switches from producing females to producing males in response to the shortened day condition, while the MFP strain only produces females, irrespective of day-length. To clarify whether MF has a novel physiological role as a sex-determining factor in *D. pulex*, we demonstrate that a MF/JH biosynthesis inhibitor suppressed male production in WTN6 strain reared under the male-inducible condition, shortened day-length. Moreover, I show that juvenile hormone acid *O*-methyltransferase (JHAMT), a critical enzyme of MF/JH biosynthesis, displays MF-generating activity by catalyzing farnesoic acid. Expression of the *JHAMT* gene increased significantly just before the MF-sensitive period for male production in the WTN6 strain, but not in the MFP strain, when maintained under male-inducible conditions. These results suggest that MF synthesis regulated by JHAMT is necessary for male offspring production in *D. pulex*. My findings provide novel insights into the genetic underpinnings of ESD and they begin to shed light on the physiological function of MF as a male-fate determiner in *D. pulex*.

Introduction

Sex determination is the most fundamental developmental process contributing to the establishment of sexually dimorphic traits. The sex-determining systems can be phenomenologically divided into two groups: genotypic sex determination (GSD) and environmental sex determination (ESD) (Bull, 1985; Marin and Baker, 1998; Zarkower, 2001). GSD occurs in majority of organisms in which a sex-determining gene residing on a sex chromosome establishes the development of a male or a female (Kopp, 2012; Matson and Zarkower, 2012). In contrast, ESD is triggered by various external stimuli such as temperature in some reptiles (Merchant-Larios and Diaz-Hernandez, 2013), photoperiod in aphids and marine amphipods (Guler et al., 2012; Hardie, 1981; Lees, 1973), and social factors in shelf limpets (Warner et al., 1996), although the molecular mechanisms triggering these alternative sex determining programs remain largely unknown.

The cladoceran crustacean *Daphnia* exhibit unique reproductive strategy; in natural conditions they produce clonal female offspring by parthenogenesis (asexual reproduction). However, in response to unfavorable environmental cues such as shortened day-length, low temperature, lack of nutrients, overpopulation, and/or a combination thereof, they switch to sexual reproduction and produce male offspring (Banta and Brown, 1929a; Hobæk and Larsson, 1990; Kleiven et al., 1992; Smith, 1915). Sexual reproduction contributes to an increase in genetic diversity and survival rate, whereas parthenogenesis allows rapid propagation during favorable seasons (Barton and Charlesworth, 1998). Hence, the underlying regulatory mechanisms of sex-determining systems play a crucial role for daphnids to appropriately match their reproductive strategies with seasonally changing environments (Kleiven et al., 1992).

JHs are endocrine factors that regulate common fundamental biological processes such as metamorphosis, molting, and reproduction in insects and crustaceans (Nijhout, 1994). They also are responsible for generating alternative phenotypes in many cases of insect polyphenisms (Nijhout, 2003), for example, caste differentiations in social insects (Miura, 2005), male ornament developments in several coleopterans (Emlen and Nijhout, 1999; Gotoh et al., 2014), phase polyphenisms in locusts (Tanaka, 2001), and diapauses in mosquitoes (Denlinger, 2002). Unlike insect species, MF is thought to be a candidate molecule for innate JH in daphnids, since the *D. pulex* genome lacks an ortholog for CYP15A1, an epoxidase that catalyzes MF to JH III (an innate JH in insects) (Daimon and Shinoda, 2013; Miyakawa et al., 2014). In addition, chemicals with JH activities in insects are also known to be involved in the alteration of phenotypes in daphnids, such as facilitating inducible defense when co-treated with predatory kairomones (Miyakawa et al., 2013a; Oda et al., 2011), and the induction of male offspring under the female-producing conditions (Kim et al., 2006; Oda et al., 2005a; Olmstead and LeBlanc, 2002; Sinev and Sanoamuang, 2011; Tatarazako et al., 2003). While this experimental system has contributed to the elucidation of masculinization processes in daphnids (Kato et al., 2011a; Toyota et al., 2013), it remains elusive whether endogenous MF acts as a sex-determining factor in daphnids. This knowledge gap is largely due to a lack of a suitable daphnid strains in which sex can be experimentally modified without MF treatment for comparative study.

In the present study, I successfully establish two *D. pulex* strains for such evaluation: (1) the WTN6 strain, which produces male offspring in response to shortened day conditions, and (2) the MFP strain, which is unresponsive to shortened day conditions. I compared these strains to evaluate the molecular mechanisms

governing ESD in daphnids. I have demonstrate that the administration of MK-801, which is a specific antagonist of the ionotropic glutamate receptors and known as a JH biosynthesis inhibitor in several insects (Beguma et al., 2004; Chiang et al., 2002; Geister et al., 2008), suppresses male production in WTN6 strain under shortened day conditions, and that this inhibition is reversible when treated with an exogenous MF. I also identify genes involved in MF action and demonstrate that the *D. pulex* ortholog of the juvenile hormone acid *O*-methyltransferase (*Dp*JHAMT), an essential enzyme for JH biosynthesis in insects (Shinoda and Itoyama, 2003), generates MF by catalyzing farnesoic acid (FA) to MF. However, unlike insects, *Dp*JHAMT does not produce JH III from JH III acid (JHA III). Finally, I show that the *DpJHAMT* gene expression is significantly increased just prior to the MF-sensitive period for male production under shortened day conditions in the WTN6 strain, but not in the MFP strain. These results suggest that MF is needed for the male induction in response to external environmental cues, and that *Dp*JHAMT is a key gene responsible for the regulation of innate MF biosynthesis governing ESD in *D. pulex*.

Materials and Methods

Daphnia pulex strains and their rearing conditions

The *Daphnia pulex* WTN6 strain was obtained from Indiana University (West Trenton, collected in May 2006 by Sarah Schaak), and the MFP strain was collected in Japan (Miyakawa et al., submitted). The strains were individually maintained in bulk (40-45 individuals/L) as stock cultures in dechlorinated freshwater at 18°C under an artificial photoperiod (14-h light : 10-h dark). Culture medium was replaced every two days, and any neonates produced were removed from the culture. *Daphnia* were fed daily a 0.03-mL suspension of 4.3×10^5 cells/mL of *Chlorella vulgaris*. New cultures were established every week using neonates (< 24 h) produced by two-week-old adult females. To induce natural male neonates, one-month-old neonates of the WTN6 strain were reared under short day conditions (10-h light : 14-h dark photoperiod cycle).

For rearing experiments, one female neonate (< 24 h) collected from stock mothers (> 2 weeks old) was cultured in a 50 ml-centrifuge tube (Thermo Fisher Scientific Inc., Waltham, MA, USA) at 18°C under long day (14-h light : 10-h dark photoperiod cycle) or short day conditions. Dechlorinated and aerated freshwater was changed every two days. *Chlorella vulgaris* was provided daily as a 0.02-mL suspension of 4.3×10^5 cells/mL. The total number of offspring and their sexes were recorded throughtout the mother's lifetime and their sexes were recorded. The sex of the offspring was confirmed by the length of the first antenna (Olmstead and LeBlanc, 2000) using a Leica MZ FLIII microscope (Leica, Mannheim, Germany).

Chemicals and treatment procedures

A stock solution of 1 mg/mL MF (Echelon Bioscience, Salt Lake City, UT,

USA) was dissolved in dimethylformamide (DMF; analytical grade, Wako Pure Chemical Industries Ltd., Osaka, Japan) and kept at -20°C until use. This stock solution was directly added to 50 mL of culture water (final concentration: 0.8 μM) containing one adult female. This concentration is sufficient to induce male neonates in *D. magna* (Tatarazako et al., 2003). A stock solution of 15 mM MK-801 (Sigma-Aldrich, St. Louis, MO, USA) was dissolved in water and kept at 4°C until use. This stock solution was added to 5 mL of breeding water (final concentration: 20 μM) containing one adult female. Preliminarily, we confirmed that this concentration showed no toxic effects in *D. pulex*. Solvent concentration did not exceed 0.01% (v/v). A total of 15 individuals were used for these experiments. FA was purchased from Echelon Bioscience. Racemic JH III and farnesyl acetate (FAc) were purchased from Sigma-Aldrich. JH III was purified by HPLC before use. Racemic JHA III was prepared from purified JH III as described previously (Goodman and Adams, 1984; Ichikawa et al., 2007).

Identification and annotation of MF/JH pathway-related genes

Protein sequences of the red flour beetle (*Tribolium castaneum*) were used in BLAST searches querying wFleaBase (http://wfleabase.org/) and gene prediction software on wFleaBase was used to obtain and generate the predicted sequences encoding the *D. pulex* orthologs of JH pathway-related genes, except for *JHAMT* (described below). The retrieved sequences with e-values less than 1e-20 were examined, although the majority of hits had much lower e-values. Following this filter, putative orthologs were identified using the BLAST hits with the lowest e-values. However, for juvenile hormone esterase (JHE), the top 10 hits were selected as candidates, because multiple JHE-like sequences were identified and these sequences

might represent *D. pulex*-specific duplications. Furthermore, to improve reliability, these sequences were used as queries in BLASTX searches against the entire sequence repository on the NCBI server (http:// blast.ncbi.nlm.nih.gov/Blast.cgi). To further confirm the orthologs, I made multiple alignments of the related genes, including orthologs from closely related insects, using ClustalW program (Thompson et al., 1994), and constructed maximum likelihood trees of the protein sequences using MEGA version 6 (Tamura et al., 2013) and bootstrapping (1000x) to estimate confidence in the nodes.

Cloning of DpJHAMT

I searched wFleaBase for a *JHAMT* homolog using the tBlastn program using the peptide sequence of *Bombyx mori* JHAMT as a query and identified only a single putative homolog. I designated it as *D. pulex JAHMT (DpJAHMT).* Total RNA was extracted form the whole bodies of adult *D. pulex* using RNeasy Mini Kit (Qiagen, Valencia, CA, USA). cDNA was synthesized from the RNA using SuperScript II reverse transcriptase (Life Technologies, Carlsbad, CA, USA) and 3′-RACE CDS primer (Takara, Ohtsu, Japan). The full open reading frame of *DpJHAMT* was amplified from the cDNA by PCR using the Advantage 2 DNA polymerase (Takara) with *DpJHAMT*_start_*Nde*I (CATATGGAACTGCCTGAACTCTACGCTG) and *DpJHAMT*_stop_*Hind*III (TTAAGGTTTGCGAACGTGAGCGATC) primers, which were designed based on the predicted *DpJHAMT* sequence. The obtained amplicon was subcloned into pGEM-T plasmid (Promega, Madison, WI, USA) and sequenced. The sequence of *DpJHAMT* cDNA was deposited in GenBank (accession number: AB222845).

Expression of recombinant DpJHAMT protein

Full length *DpJHAMT* was excised from the pGEM-T plasmid with the restriction enzymes *Nde*I and *Not*I, and subcloned into the pET28a (+) expression vector (Merck, Darmstadt Germany). The resulting construct, *Dp*JHAMT/pET28a (+) was transformed into the *Escherichia coli* BL21 (DE3) strain. The expression and purification of *N*-terminal 6xHis-tagged recombinant *Dp*JHAMT protein were performed as previously described (Shinoda and Itoyama, 2003). The purity of the recombinant protein was confirmed by SDS/PAGE and the concentration was quantified as previously described (Shinoda et al., 2001). The purified protein was stored as a 50% glycerol stock solution (745 ng/μL) at -80°C until use. Under these conditions, the protein showed no significant decline in enzymatic activity for more than 5 years.

Enzyme assay

Enzymatic activity of the recombinant *Dp*JHAMT was measured as previously described (Minakuchi et al., 2008). To compare substrate specificity, the same conditions as previously used for recombinant JHAMT of *T. castaneum* was employed (Minakuchi et al., 2008). Briefly, purified recombinant *Dp*JHAMT (6.5 μg) was incubated in a siliconized glass tube (10 × 120 mm) with 500 μL of 50 mM Tris/Cl buffer (pH 7.5) containing S-adenosyl-methionine (SAM) (500 μM) and one of the following acids as a substrate: FA (50 μM), or racemic JH III acid (JHA III) (50 μM). After 10 min of incubation at 25°C, the reactions were stopped by the addition of 500 μL CH_3CN. After removing the precipitate from samples by centrifugation, the supernatants (10 μL) were directly subjected to RP-HPLC to quantify the generated MF

or JH III from FA or JHA III, respectively. RP-HPLC was performed with a Shimadzu LC-10 HPLC system (column: Shiseido ODS UG80, 3 × 150 mm; solvent: 90% CH_3CN for MF and 60% CH_3CN for JH III, 0.5 mL/min; detection: UV 219 nm) (Shimadzu, Kyoto, Japan). Assays were performed in triplicate. To evaluate the kinetics, recombinant *Dp*JHAMT protein (final concentration was 1 ng/μL) was incubated in a siliconized glass tube (10 mm i.d. × 120 mm) with 500 μL of 50 mM HEPES buffer (pH 7.0) containing 500 μM SAM, 0.01% BSA, and various concentrations of FA (0.3125, 0.625, 1.25, 2.5, 5 and 10 μM). After 6 min of incubation, the reactions were stopped by the addition of 500 μL of CH_3CN containing FAc (100 ng/mL) as an internal standard. Incubation times were adjusted so as not to consume more than 15% of the initial substrates. Assays were performed in triplicate. The reaction was added to 1 ml of 2% NaCl solution and extracted with 750 μL of *n*-hexane. The extract was dried with an N_2 stream, dissolved in 50 μL of *n*-hexane, and 1 μL of samples were analyzed by GC-MS. The GC-MS system (GCMS-QP2010 Plus, Shimadzu) was equipped with an on-column sample injection unit (OCI/PTV-2010, Shimadzu) fitted with a deactivated fused silica tubing (15 cm × 0.53 mm i.d.) connected to a deactivated fused silica retention gap (1 m × 0.25 mm i.d.) and then to a GC column DB-35MS (30 m × 0.25 mm i.d. × 0.25 μm film; Agilent Technologies, Santa Clara, CA, USA). The temperature profile of the column oven was 40°C for 1 min, and then 15°C increase per min to 250°C. The injector temperature profile was 40°C for 0.5 min, then 170°C increase per min to 250°C. Helium carrier gas was set at a flow rate 1.3 mL/min. The mass selective detector was set in electron impact ionization mode with an ionizing energy of 70-eV. The peaks of MF and FAc were monitored by selective-ion mode using m/z 69, 93, 114, 136, and 207, and the peak areas of m/z 69 were used for quantification. Retention

times of MF and FAc were 13.5 and 13.8 min, respectively. The amount of MF and FAc in each sample was determined using standard curves prepared with authentic MF and FAc (5, 50, 500, and 5000 pg). The total amount of MF generated in the reaction was estimated by compensating the extraction loss with the amount of internal standard (FAc). The Michaelis-Menten constant (*Km*) and the kinetic constant (*Vmax, kcat*) were determined by nonlinear regression analysis using Prism 4 (Graphpad software, San Diego, CA, USA).

Real-time quantitative RT-PCR

Adult *D. pulex* (> one-month of age) were sampled at eight time points with 10-h intervals during the 70-h reproductive cycle. Developing embryos in the dorsal chamber were removed. All samples were pooled from three individuals, and three replicates were prepared for each time point in each experiment. Total RNA was extracted and treated with DNase using the RNAqueous-Micro Kit (Life Technologies). cDNA was synthesized from 0.5 μg of total RNA using Super Script III with random primers (Life Technologies). PCR was conducted with SYBR-Green PCR Master Mix using the ABI Prism 7000 thermocycler (Life Technologies). The primer sequences used for the quantitative PCR analyses are shown in **Table 1-1**. Among four housekeeping genes (*actin*, *α-tubulin*, *GAPDH* and *capon*) (Miyakawa et al., 2010; Spanier et al., 2010), *D. pulex actin* was selected as the reference gene calculated by geNorm (Vandesompele et al., 2002) and NormFinder (Andersen et al., 2004). Statistical analyses of gene expression at each time point were performed by two-way ANOVA followed by the Tukey-Kramer post-hoc test using Excel 2010 (Microsoft Corp., Redmond, WA, USA) fitted with add-in software, Statcel 3 (Yanai, 2011).

Results

Induction of male offspring by photoperiod changes

I searched for a *D. pulex* strain in which male offspring could be induced in the laboratory by altering or manipulating the rearing conditions (i.e., photoperiod, temperature, nutrition, population density, and/or a combination thereof), and discovered the photoperiod-dependent WTN6 strain. Experiments conducted over the course of the daphnids lifespan demonstrated that the WTN6 strain produces female offspring under long day conditions (14-h light : 10-h dark) **(Figure 1-1A)**, whereas male offspring were produced under short day conditions (10-h light : 14-h dark) **(Figure 1-1B)**. Notably, after 5-6 ovipositions (about one-month of age), parental parthenogenetic females reared under the short day conditions continuously and exclusively produced male progeny **(Figure 1-1B)**. In addition, I found that the MFP strain did not produce male offspring in response to short day conditions **(Figures 1-1C, D)**. Administration of MF to parental WTN6 and MFP females at 40-60 h post ovulation induced male offspring, although the rate of male induction was slightly lower in the WTN6 strain. These results also confirm that the MF-sensitive period for male sex determination corresponds to the oocyte maturation period (40-60 h post ovulation) **(Figure 1-2)**, which is consistent with *D. magna* (Ignace et al., 2011).

MK-801 suppresses male production in WTN6 strain under the short day conditions

To investigate whether the MF pathway is involved in the induction and production of male offspring in response to short day conditions, I treated the WTN6

strain with MK-801, an ionotropic glutamate receptors specific antagonist that has a known inhibitory effect upon the JH biosynthesis in several insects (Beguma et al., 2004; Chiang et al., 2002; Geister et al., 2008). When the WTN6 strain was exposed to MK-801 during short day conditions only female offspring were produced, thus reversing the effects of short day conditions **(Figures 1-3, 1-4)**. In contrast, co-administration of MK-801 and MF during short day conditions resulted in the production of male offspring, which is typical response to short day conditions for this strain **(Figure 1-3)**.

JH pathway-related genes in the *D. pulex* genome

In insects, the fluctuation of endogenous JH levels in hemolymph is generally regulated by various mechanisms such as JH biosynthesis, degradation, and/or sequestration (Goodman and Cusson, 2012). To better understand the regulatory processes of the MF pathway and its downstream signaling in the WTN6 strain reared under short day conditions, I investigated the expression patterns of the genes involved. For this purpose, I successfully identified orthologs of genes related to JH biosynthesis, degradation and downstream pathways from the *D. pulex* genome (see Materials and methods), which are listed in **Table 1-1** and described in detail below.

JHAMT and farnesoic acid *O*-methyltransferase (FAMeT) have been reported to catalyze the methylation of FA to MF using SAM in insects and crustaceans. A putative *JHAMT* has been identified in *D. pulex* (Hui et al., 2010; Miyakawa et al., 2010). In addition, I identified a putative *FAMeT*. Phylogenetic analysis indicated that the putative *Dp*JHAMT and *Dp*FAMeT are clearly separated into different clades from orthologs of insects and other crustaceans, respectively **(Figures 1-5, 1-6)**.

As JH degradation-related genes, I identified three kinds of potential *JH esterase* (*JHE*s) **(Figure 1-7)** chosen from 10 candidates based on the presence of four conserved JHE motifs in insects (RF, DQ, GQSAG, and GxxHxxD/E, **Table 1-2**) (Ward et al., 1992). In addition, I identified a putative *JHE binding protein* (*JHEBP*), known to influence JHE transportation, degradation, and regulation of JH levels indirectly through hydrolysis of JHE **(Figure 1-8)** (Hao et al., 2013), and a putative *JH epoxide hydrolase* (*JHEH*). JHEH can be classified into one of two forms (Arand et al., 1999); soluble epoxide hydrolase (sEH) that is found in various organisms or microsomal EH (mEH) that is found in mammals and insects. A previous study in the pea aphid, *Acyrthosiphon pisum*, revealed that *JHEH-like* sequences could be distinguished by constructing a phylogenetic tree with mEHs and sEHs (Ishikawa et al., 2012). Based on this criterion, a phylogenetic analysis categorized the putative *JHEH* in *D. pulex* into the mEH with other insect *JHEHs* **(Figure 1-9)**.

As for the genes involved in the transportation and sequestration of JH, I sought three gene families in the *D. pulex* genome: (1) *hexamerin* that act as a regulator of the JH level in hemolymph by binding to JHs (Zhou et al., 2007), (2) *JH binding protein* (*JHBP*) that act as a transporter of JH (Saito et al., 2006; Suzuki et al., 2011; Vermunt et al., 2001), and (3) cytosolic *JHBP* that act as the cytoplasmic receptor of JH in insects (Chang et al., 1980). Surprisingly, no putative *hexamerins*, *JHBP*s or cytosolic *JHBP*s were found in the *D. pulex* genome **(Figures 1-10, 1-11, 1-12)**.

Methoprene-tolerant (*Met*) and *steroid receptor coactivator* (*SRC*) are the main components of JH receptors in insects (Charles et al., 2011; Li et al., 2011; Zhang et al., 2011). These genes have recently been identified in *D. pulex* and *D. magna* (Miyakawa et al., 2013b). In addition, I have identified *D. pulex* orthologs of *Krüppel homolog 1*

(*kr-h1*) and *broad*, which are known as JH-responsive genes in insects. Phylogenetic analyses show that *kr-h1* and *broad* are clustered with their orthologs in insect species **(Figures 1-13, 1-14)**.

Enzymatic activity and kinetics of JHAMT

JHAMT (*DpJHAMT*) was identified in the reference genome of *D. pulex* as a single copy gene **(Figure 1-5)**. I conducted enzymatic assays using a recombinant protein produced by *E. coli* to clarify whether the product of the *DpJHAMT* gene is functionally involved in MF synthesis. The enzymatic activity of recombinant *Dp*JHAMT was examined against two potential substrates, FA and JHA III. HPLC analysis showed that *Dp*JHAMT clearly catalyzed FA and generated MF; however, generation of JH III from JHA III by *Dp*JHAMT was not detected **(Figure 1-15A)**. In the same experimental conditions, recombinant protein of *T. castaneum* JHAMT (*Tc*JHAMT) catalyzed the methylation of both FA and JHA III with similar activities **(Figure 1-15A)**, as was previously reported (Minakuchi et al., 2008). Kinetic analysis of *Dp*JHAMT against FA gave a *Km* value of 1.13 μM with a *kcat* (*Vmax*) of 4.4×10^{-3} s^{-1} **(Figure 1-15B)**.

Expression profiles of MF synthesis-related genes during reproductive cycle under the long and short day conditions in the WTN6 and MFP strains

I quantified the relative expression levels of genes involved in the MF synthesis, *DpJHAMT* and *DpFAMeT*, at 10-h intervals during a 70-h reproductive cycle under long day and short day conditions. *DpJHAMT* expression was transiently activated at 30-h after ovulation under short day conditions in the WTN6 strain, which

corresponds to just prior to the MF-sensitive period for male offspring production **(Figure 1-16A)**. In contrast, there were no changes in the expression of *DpJHAMT* at any time point tested in the MFP strain **(Figure 1-16B)**. *DpFAMeT* expression levels showed no differences at 30-h after ovulation between the short day and long day conditions in both strains **(Figure 1-17)**.

Discussion

Although a variety of experimental conditions can incidentally induce male offspring production in daphnids (Banta and Brown, 1929a; Hobæk and Larsson, 1990; Kleiven et al., 1992; Smith, 1915), previous studies have used different *Daphnia* strains under the control of a complex combination of environmental conditions. Consequently, no culture conditions have yet been developed that would completely and reproducibly manipulate offspring sex in laboratory conditions. In this study, I have successfully established a stable experimental system for ESD studies that uses the *D. pulex* WTN6 strain in which offspring sex can be controlled by changing day-length. Furthermore, I describe a complementary strain, MFP, which unlike WTN6 does not produce male offspring in short day conditions, and therefore, provides a negative control for ESD studies. Thus, these strains are the first experimental models that enable the evaluation of factors involved in the primary signal cascades governing ESD. With this system, I determined that WTN strain reared under short day conditions failed to produce male offspring following treatment with MF/JH biosynthesis inhibitor, MK801 (Beguma et al., 2004; Chiang et al., 2002; Geister et al., 2008). However, male offspring were produced following co-treatment with MF and MK801, indicating the specificity of MK-801 to MF synthesis in daphnids. This is the first evidence showing that the activation of MF signaling is necessary for male induction, which is elicited by environmental stimuli in daphnids.

Although I identified MF as a male induction hormone responding to the environmental stimuli, the molecular components involved in the function of MF in the crustaceans have not been well elucidated. In this study, I identified putative MF pathway genes in the *D. pulex* genome related to, among others functions synthesis,

transportation/sequestration, degradation, and downstream signaling. However, I found no orthologs of *hexamerins*, *JHBP*s, and *cytosolic JHBP*s. I identified multiple gene copies of *JHE* (JH degradation enzyme), which seem to have arisen by gene duplication in *D. pulex*, suggesting that there are unique mechanisms playing roles in the MF degradation processes in *Daphnia*. Further studies based on a biochemical assay of these genes will be necessary for understanding the molecular basis of MF action in daphnids. During screening, a homologous *JHAMT* (*DpJHAMT*) gene was found in the *D. pulex* reference genome. Recombinant JHAMTs of several insect species such as *B. mori* (Shinoda and Itoyama, 2003), *Drosophila melanogaster* (Niwa et al., 2008), and *Aedes aegypti* (Defelipe et al., 2011; Mayoral et al., 2009) exhibited robust activities in methylating JHA III to JH III, and comparable activities in methylating FA to MF. However, it remains elusive whether the *Dp*JHAMT functions to generate MF in *D. pulex* as observed in insects. In the current study, I demonstrated that the *Dp*JHAMT clearly catalyzed FA and generated MF, whereas the *Dp*JHAMT failed to generate JH III from JHA III, suggesting that the *Dp*JHAMT does not catalyze JHA III. I also demonstrated that the *T. castaneum* JHAMT, which was used as a positive control, can catalyze JHA III (Minakuchi et al., 2008). Thus, *Dp*JHAMT is an *O*-methyltransferase highly specific to FA, but not JHA III, which further supports the hypothesis that MF acts as an innate JH in daphnids, as in other arthropods (Nagaraju, 2011).

JHAMT is known to play critical roles in JH synthesis in many insect species (Hui et al., 2010). During the caste differentiation in honey bees, JHAMT expression is responsible for the high JH levels necessary for the queen's development (Li et al., 2013). In the current study, I found that the *DpJHAMT* gene expression was transiently elevated at 30-h after ovulation in the WTN6 strain, which corresponds to just prior to

the MF-sensitive period for sex determination under short day conditions. In the MFP strain, however, *DpJHAMT* showed no changes in expression among all time points in either short day or in long day conditions. Therefore, the transient peak of *DpJHAMT* in the WTN6 strain is likely to be responsible for male production. In contrast, the *FAMeT* gene, which encodes an enzyme that is known to catalyze the methylation of FA to MF in crustaceans (Kuballa et al., 2007), showed no differences in expression among all time points and day length conditions in either strain. These results suggest that FAMeT is not likely involved in MF synthesis in daphnids **(Figure 1-17)**. Similarly, the genes involved in MF degradation showed no significant differences in expression **(Figure 1-18)**, suggesting that the MF degradation pathway is not responsible for the assumed high MF titers under the short day conditions. The present results suggest that DpJHAMT regulates innate MF levels for male production in response to the short day conditions.

I demonstrated that both WTN6 and MFP strains have the ability to induce male offspring in response to exogenous MF treatment, suggesting that the downstream events in MF signaling are conserved in these strains. In addition, the real-time qPCR analyses of genes involved in MF reception and its downstream pathway showed no differences in expression **(Figure 1-19)**, implying that the MF signaling pathway might not be a candidate regulating primary sexual fate under the short day conditions. I reported that as in insects Met and SRC act as components of the MF/JH receptors in *Daphnia* species (Miyakawa et al., 2013b). I also showed that male induction by exogenous chemicals with MF/JH activity is likely to be caused by the MF signaling pathway via these MF receptors (Miyakawa et al., 2013b). However, the expression level of *kr-h1*, the primary target of Met in several insects (Cui et al., 2014; Kayukawa

et al., 2012; Kayukawa et al., 2013; Song et al., 2014), did not change under either long day or short day conditions, although the MF titer was predicted to be high **(Figure 1-19C)**. This observation suggests that *D. pulex kr-h1* is not an MF-responsive gene. These results indicate that the factors involved in the MF signaling cascades for sex determination in *D. pulex* are quite distinct from the canonical JH signaling pathway in insect species.

Recently, it has been reported in the pea aphid that a low JH III titer is indispensable for the induction of sexual morph (producing a male and oviparous female)**.** In addition, JHE was identified as a key regulator responsible for the decrease of the JH III titer in response to sexual morph-inducing conditions (Ishikawa et al., 2012). Although the ESD system of daphnids and pea aphid are thought to be acquired independently through evolution, it is interesting that the MF/JH system seems to be co-opted as a sex-determining factor in both species, although in opposing titers. The integration of findings from these species sheds light on variation in the common principles underlying the survival strategies of organisms living in changing natural environments.

Recent progress in instrumental analytical technologies such as liquid or gas chromatography-mass spectrometry (LC- or GC-MS) have allowed the innate methyl farnesoids (including MF) and JH levels to be quantified in the extracts and hemolymphs of several insect species (Jones et al., 2010; Jones et al., 2013). However, my attempts to measure MF in *D. pulex* using LC- and GC-MS methods have not yet been successful. One possibility is that endogenous MF concentrations in daphnids are apparently lower than that in the insect species previously analyzed. Detailed quantification of endogenous MF levels during the sex determination period is essential

to reveal the relationship between MF titers and sexual fate in daphnids.

In conclusion, I established a reliable induction system of female and male offspring in *D. pulex* using the WTN6 strain in response to photoperiod differences, and the MFP strain that only produces females irrespective of day-length. I confirmed that MF is an innate JH in *D. pulex*. In a pharmacological experiment using MK-801 as a MF biosynthesis inhibitor, I demonstrated for the first time that endogenous MF is indispensable for male induction in response to external stimuli in daphnids. I identified *JHAMT* ortholog in *D. pulex* and demonstrated that it is responsible for MF synthesis and is transiently expressed just before the critical period for sex determination under the male-inducible condition **(Figure 1-20)**. My findings not only provide novel insights into the physiological function of MF as a male-fate determinant in *D. pulex*, but also contribute to understanding the endocrinological basis underlying the regulation of various fundamental biological processes such as metamorphosis, reproduction, and molting in crustaceans.

Tables

Table 1-1 Protein ID and primer sequences for real-time qPCR

Gene name (abbreviation)	*Daphnia pulex* gene ID	Accession number	Forward primer (5’ to 3’)	Reverse primer (5’ to 3’)
juvenile hormone acid O-methyltransferase (JHAMT)	DappuDraft_300180	AB222845	GGCTGCGCGAGAGCTATCTA	CGGAGCCTTCAGTTTTTGGA
farnesoic acid O-methyltransferase (FAMeT)	DappuDraft_208220	-	GGGTAAGAAGCCGTTCTATCG	TCTCTCCCGATGTGTCAACTC
juvenile hormone esterase 1 (JHE1)	DappuDraft_53255, DappuDraft_245878	-	CAAGGGTGGTGCTACCTGTAA	CGGCTGGGATATTGACGTAT
juvenile hormone esterase 2 (JHE2)	DappuDraft_312876	-	TTCACGATAGACAGGCCGTA	GCTGAGCAGGTCAACTGATTC
juvenile hormone esterase 3 (JHE3)	DappuDraft_97670	-	CTCACGCTGAATGTCTACACG	ACCAGGGATCCATACCAAGAC
juvenile hormone esterase binding protein (JHEBP)	DappuDraft_335104	-	TTTAAGGGCATCAGCGGTAT	TTGAGCCAACTGTTCACTGC
juvenile hormone epoxide hydrolase (JHEH)	DappuDraft_301203	-	TCGTTGCCTAGCTGTTGTTG	TATCAGGTCCCCAGTTCTCG
hexamerin	Not found	-	-	-
juvenile hormone binding protein (JHBP)	Not found	-	-	-
cytosolic juvenile hormone binding protein	Not found	-	-	-
methoprene-tolerant (Met)	-	BAM83853	CTTGGTGCGCATTCTTCAAA	GCTTGCATGATGGTCAATGG
steroid receptor coactivator (SRC)	-	BAM83854	CGTCTACGACTCCAACGGT	GGTGGAGACTTGAGGTG

kruppel homolog 1 (Kr-h1)	DappuDraft_49585	-	AA GAAGAAGCTCATCGCTGT GAC	AGTG ACCTGTGTGCGTTCGGT AGT
broad	DappuDraft_39364	-	CACTTGCATGTGAAGGTC AG	GGTGTTTGCATGGTGTT GTC

Table 1-2 Conserved domain comparison of JHE-like genes

Gene name	*D. pulex* gene ID	Name on wFleaBase	Motif				Match motif No.
			RF	DQ	GQSAG	GxxHxxD/E	(Max 4)
JHE1	DappuDraft_53255, DappuDraft_245878	NCBI_GNO_480334	+	+	+	+	4
JHE2	DappuDraft_312876	NCBI_GNO_344074	+	+	GCSAG (+)	SxxHxxE (+)	4
JHE3	DappuDraft_97670	NCBI_GNO_404074	+	+	GCSAG (+)	SxxHxxD (+)	4
	DappuDraft_105042	NCBI_GNO_486334	+	+	+	-	3
	DappuDraft_307908	NCBI_GNO_648074	+	+	GESSG (-)	+	3
	DappuDraft_305140	NCBI_GNO_508334	+	+	GESAG (-)	+	3
	DappuDraft_305141	NCBI_GNO_510334	+	+	GESAG (-)	+	3
	DappuDraft_320238	NCBI_GNO_512334	+	+	GESAG (-)	+	3
	DappuDraft_105048	NCBI_GNO_492334	+	+	GESTG (-)	+	3
	DappuDraft_192973	NCBI_GNO_472074	+	+	GSSAG (+)	-	3

(+): synonymous substitution

(-): non-synonymous substitution

Figures

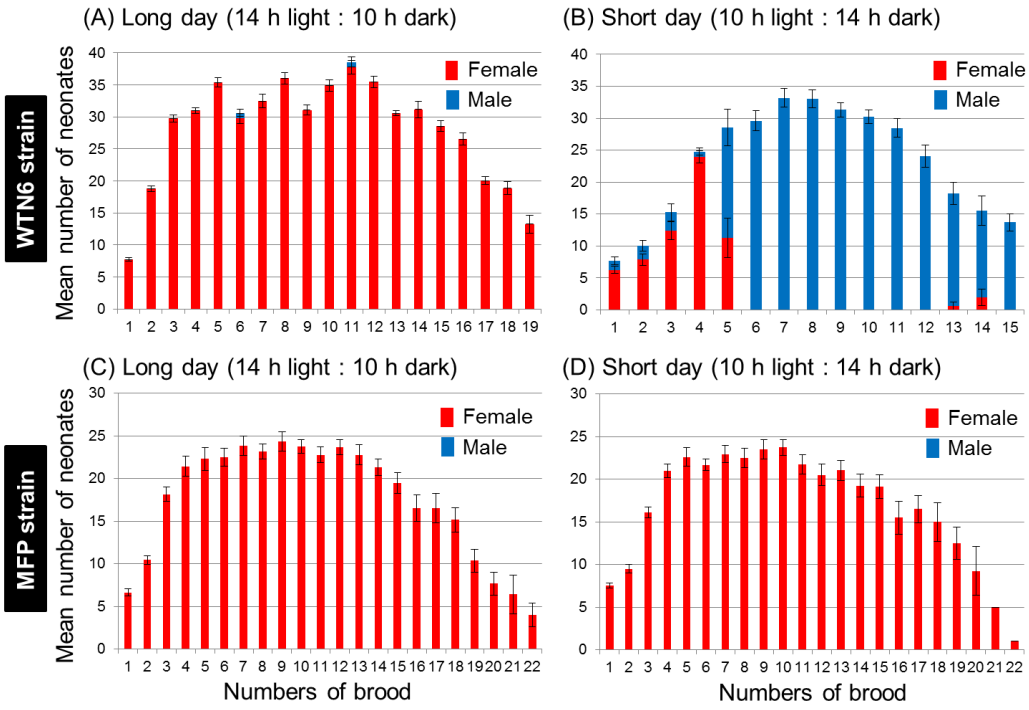

Figure 1-1. Number of broods in the lifespan of *D. pulex* WTN6 and MFP strains under 18°C. Mean number and standard error (SE) of neonates produced by mothers under (A) long day (14-h light : 10-h dark) and (B) short day (10-h light : 14-h dark) conditions (n=25) in WTN6 strain, and by mothers under (C) long day and (D) short day conditions (n=27 and 24, respectively) in the MFP strain are indicated. Short day conditions, after 5-6 ovipositions, induce the production of male offspring in females of the WTN6 strain, but not in females of the MFP strain.

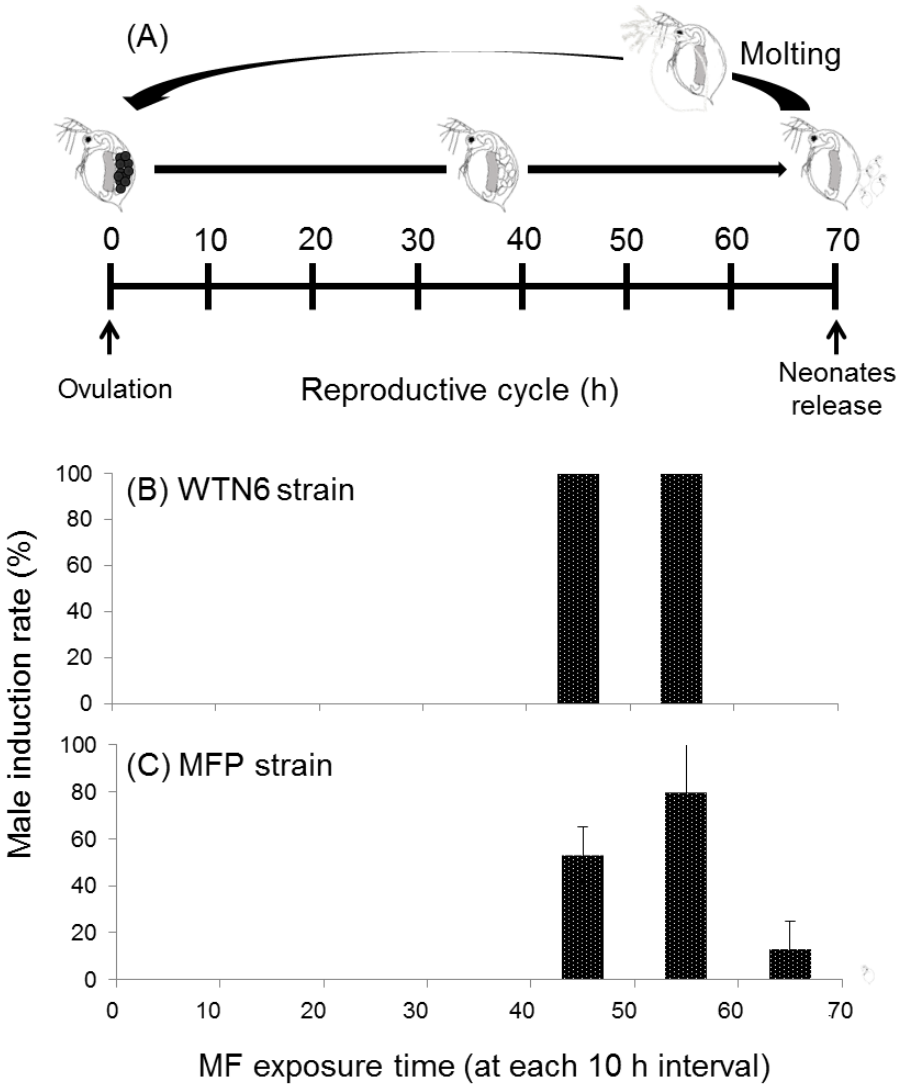

Figure 1-2. MF-sensitive period in the reproductive cycle of *D. pulex*. Upper panel shows reproductive cycle in both WTN6 and MFP strains (A). Lower panel shows that administration of MF, between 40-50 or 50-60 h under long day conditions, induces male offspring in the WTN6 (B) and MFP (C) strains. Daphnids under long day conditions were exposed to MF (0.8 μM) for each of the 10 h intervals indicated during the reproductive cycle. Mean ± SD, n=15.

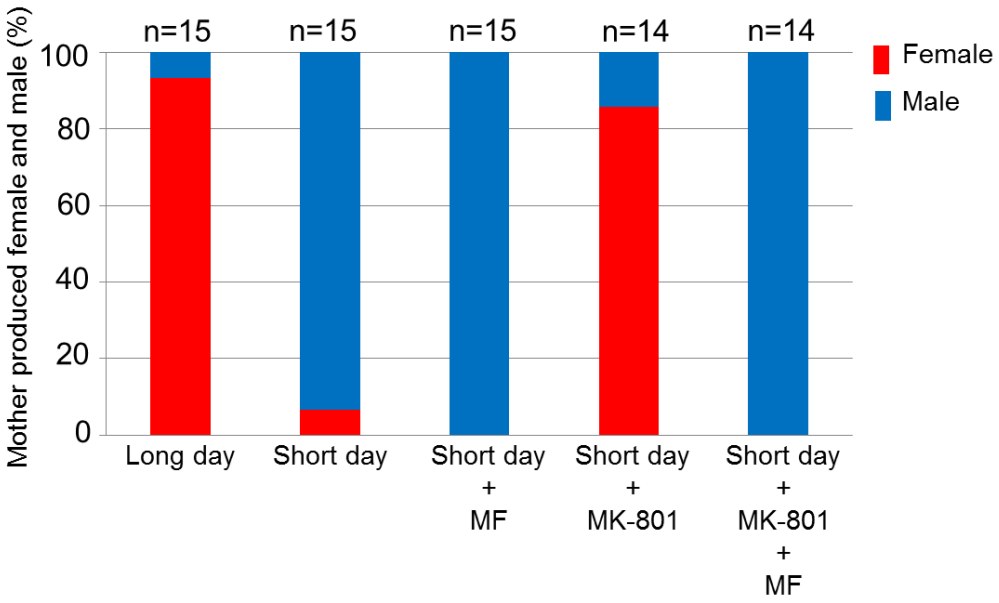

Figure 1-3. Effects of MF/JH biosynthesis inhibitor on sex ratio of neonates. WTN6 strain treated with MK-801 or MK-801 + MF reared under short day conditions. The concentration of MK-801 and MF was 20 µM and 0.8 µM, respectively.

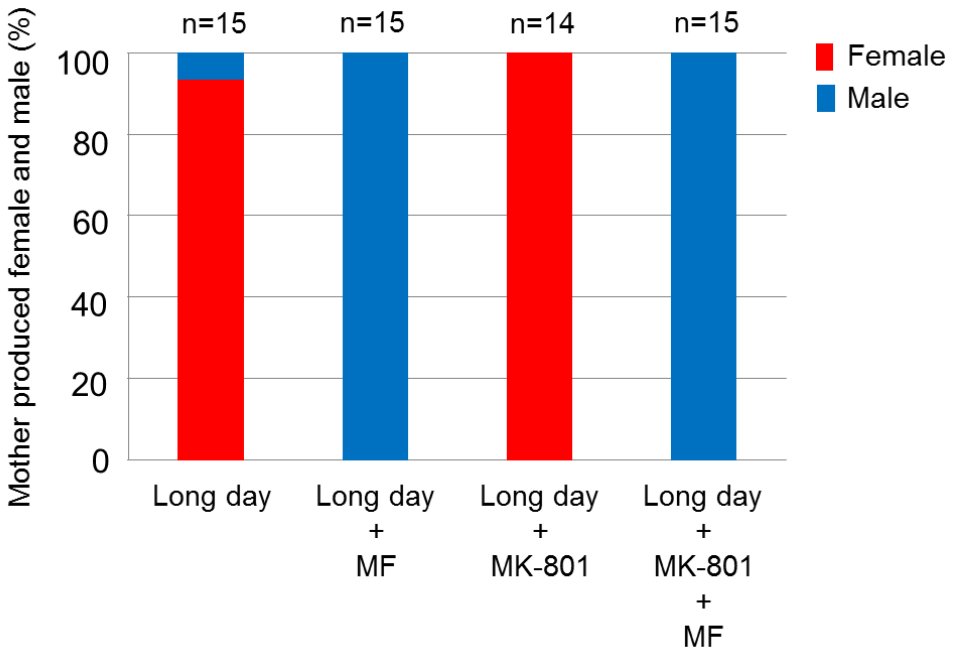

Figure 1-4. Effects of MF/JH biosynthesis inhibitor on sex ratio of neonates. WTN6 strain treated with MK-801 and reared under the long day conditions. The concentration of MK-801 and MF was 20 µM and 0.8 µM, respectively.

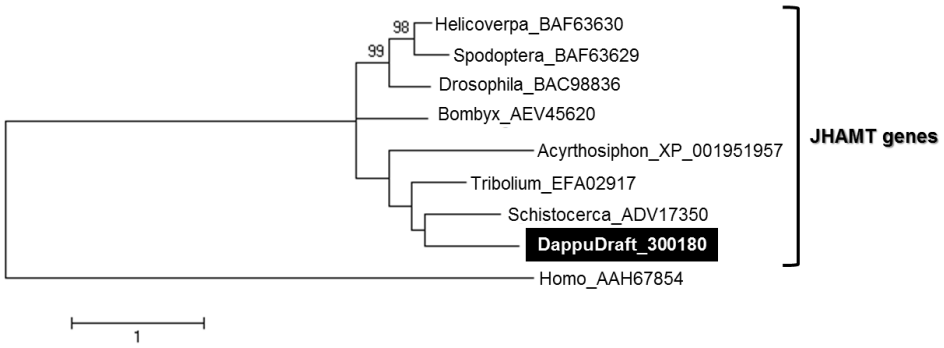

Figure 1-5. Phylogeny of JHAMT. Figure legend is below.

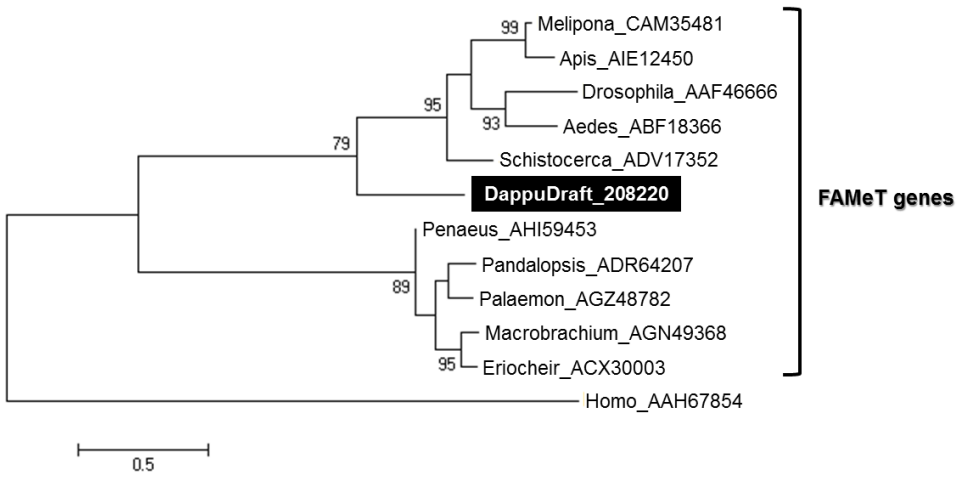

Figure 1-6. Phylogeny of FAMeT. Figure legend is below.

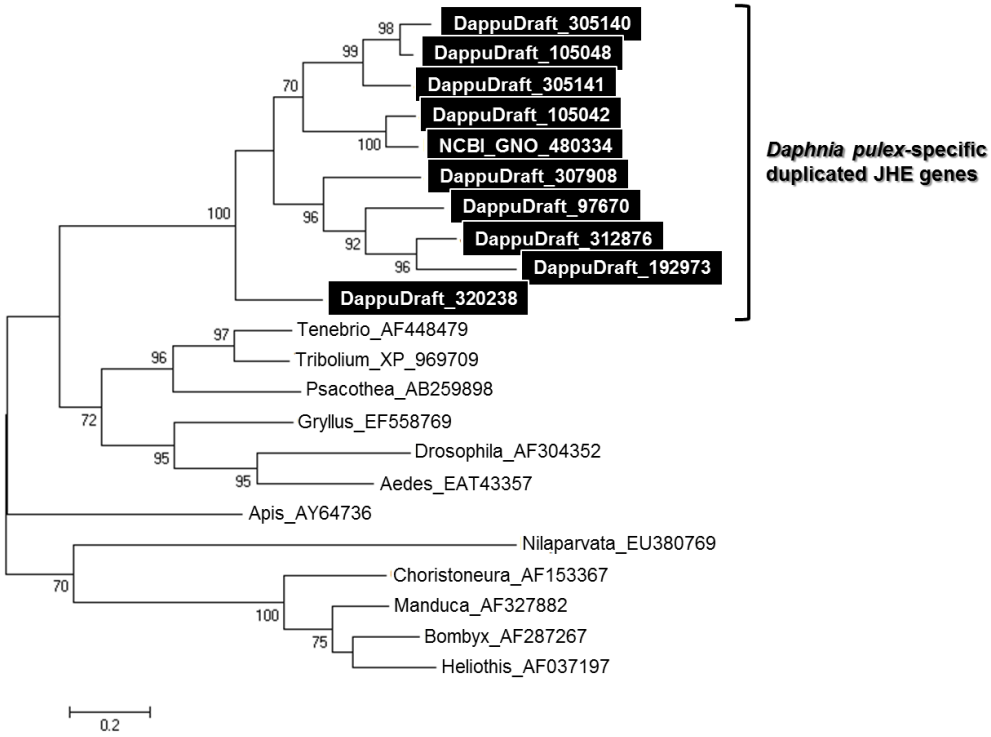

Figure 1-7. Phylogenies of JHE. Figure legend is below.

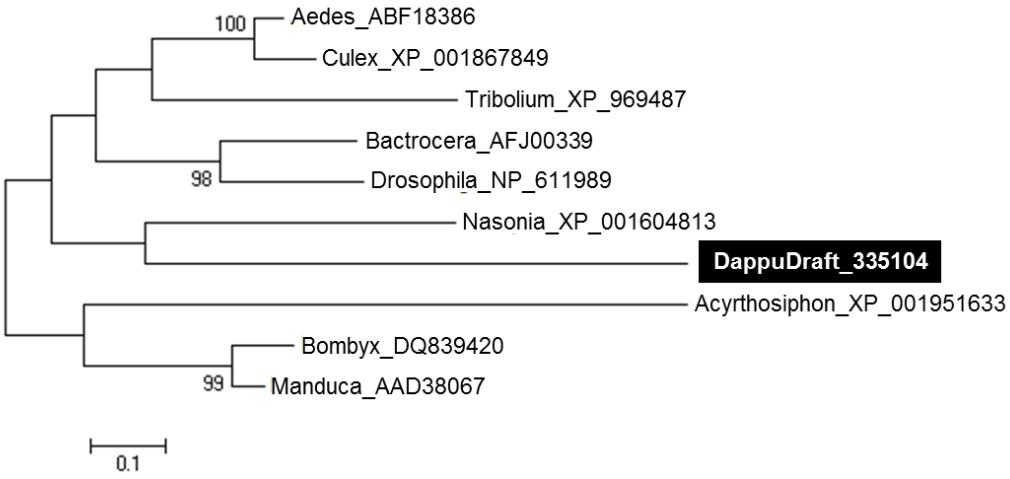

Figure 1-8. Phylogenies of JHEBP. Figure legend is below.

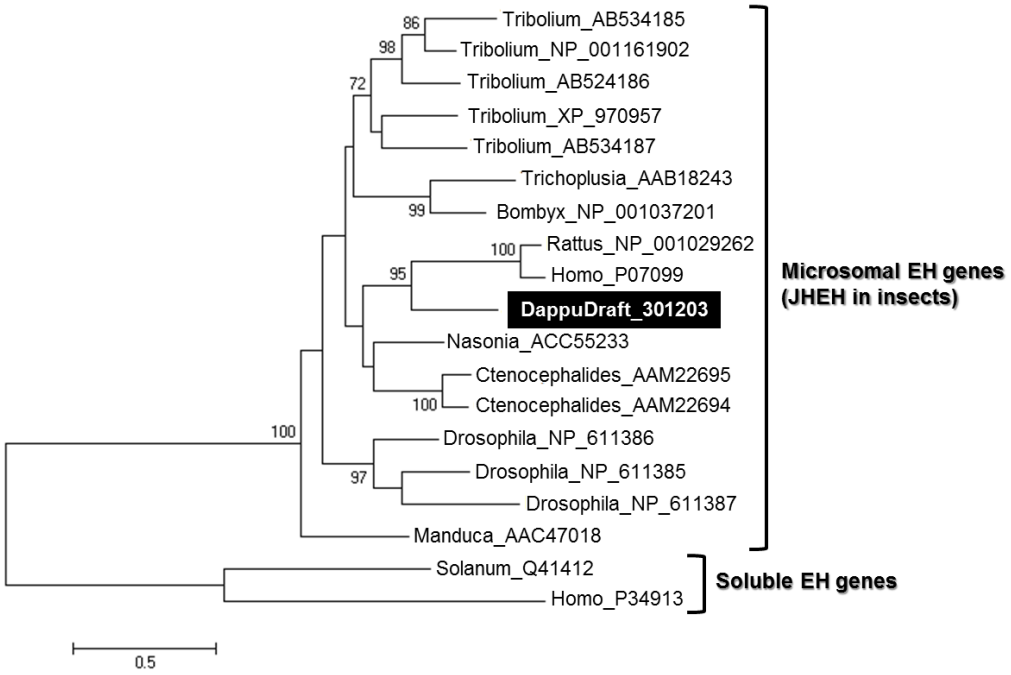

Figure 1-9. Phylogenies of JHEH. Figure legend is below.

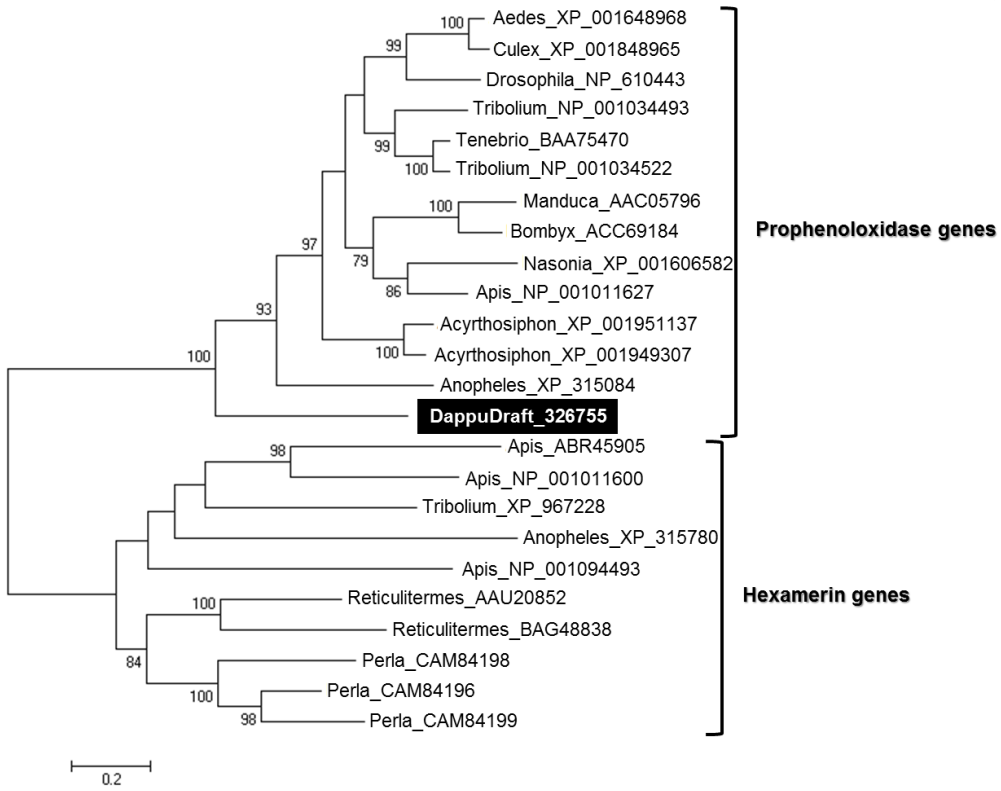

Figure 1-10. Phylogenies of hexamerin. Figure legend is below.

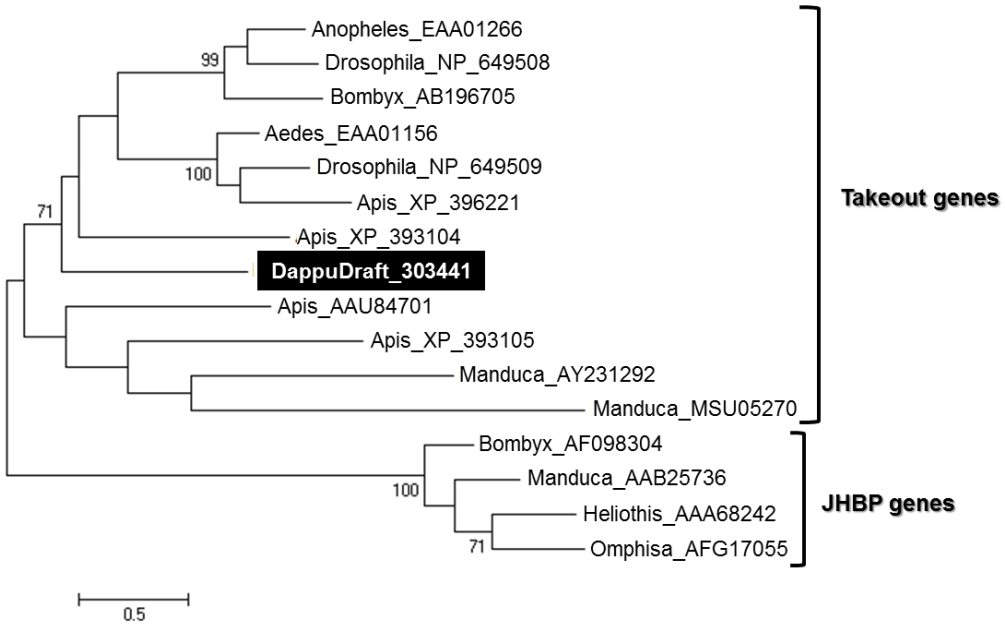

Figure 1-11. Phylogenies of JHBP. Figure legend is below.

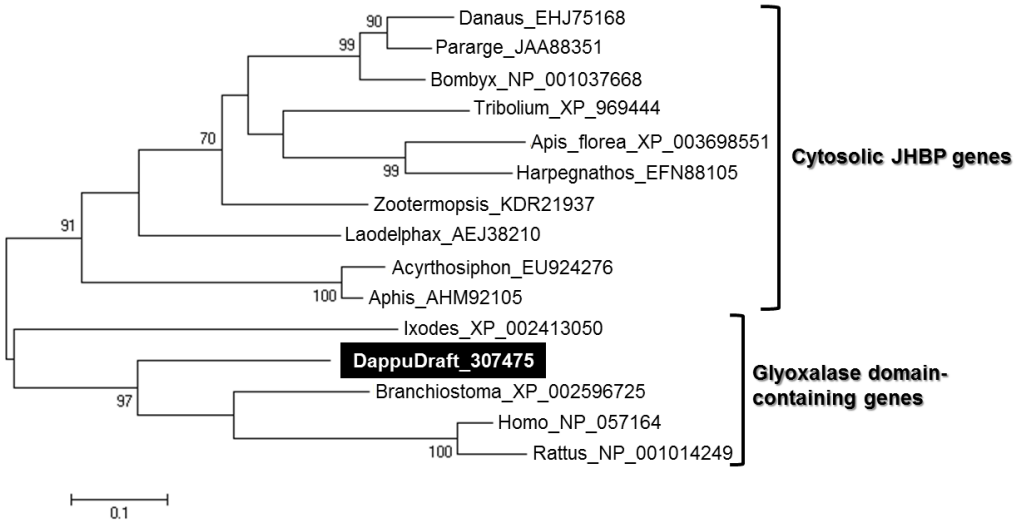

Figure 1-12. Phylogenies of cytosolic JHBP. Figure legend is below.

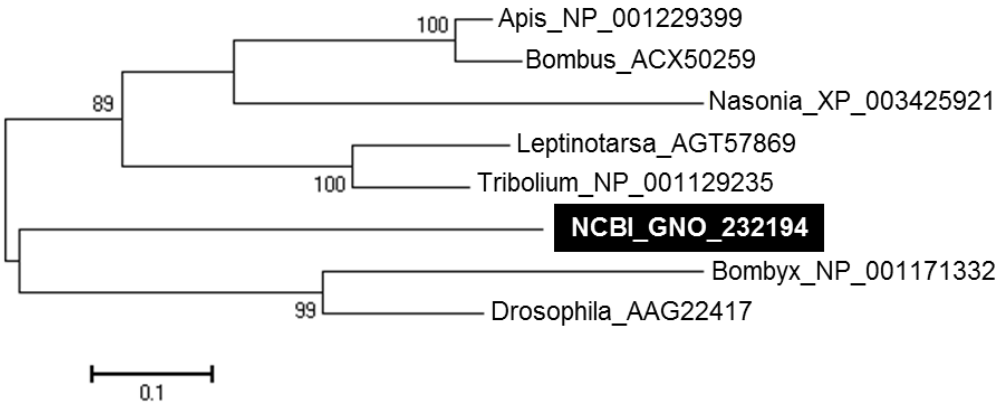

Figure 1-13. Phylogenies of kr-h1. Figure legend is below.

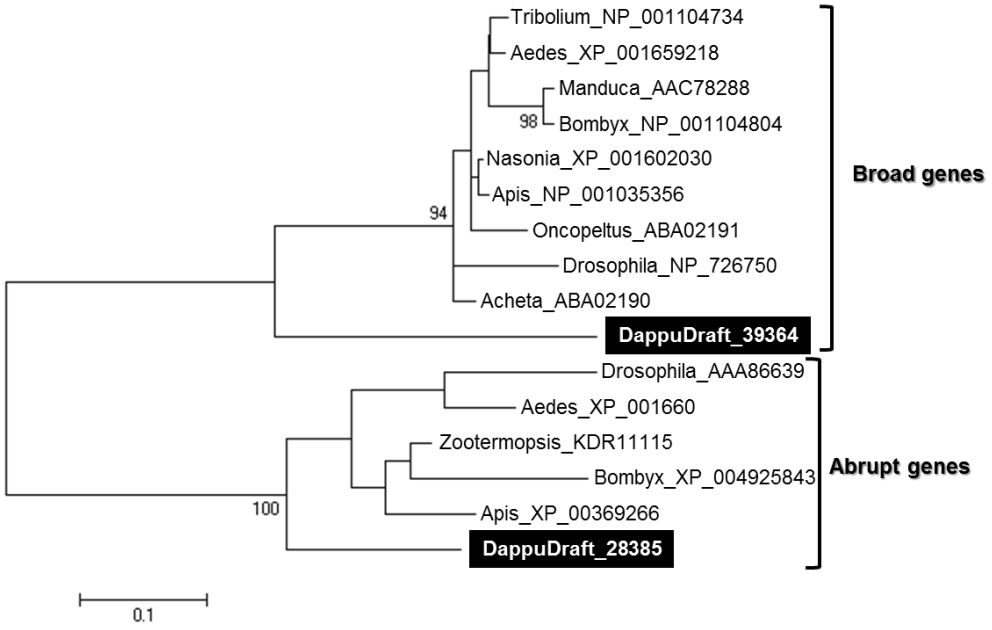

Figure 1-14. Phylogenies of broad. Figure legend is below.

Figures 1-5. ~14. Phylogenies of JHAMT (Figure 1-5), FAMeT (Figure 1-6), JHE (Figure 1-7), JHEBP (Figure 1-8), JHEH (Figure 1-9), hexamerin (Figure 1-10), JHBP (Figure 1-11), cytosolic JHBP (Figure 1-12), kr-h1 (Figure 1-13) and broad (Figure 1-14). Sequences were aligned by ClustalW, and the trees were generated by MEGA6 (Tamura et al., 2013). There were bootstrapped 1000 times to estimate confidence in the nodes and values hide lower than 70. Species names are as follows: DappuDraft (*Daphnia pulex*), Tenebrio (*Tenebrio malitor*), Tribolium (*Tribolium castaneum*), Psacothea (*Psacothea hilaris*), Gryllus (*Gryllus assimilis*), Drosophila (*Drosophila melanogaster*), Bombyx (*Bombyx mori*), Apis (*Apis mellifera*), Aedes (*Aedes aegypti*), Acyrthosiphon (*Acyrthosiphon pisum*), Choristoneura (*Choristoneura fumiferana*), Heliothis (*Heliothis virescens*), Nilaparvata (*Nilaparvata lugens*), Manduca (*Manduca sexta*), Culex (*Culex quinquefasciatus*), Bactrocera (*Bactrocera dorsalis*), Nasonia (*Nasonia vitripennis*), Trichoplusia (*Trichoplusia ni*), Rattus (*Rattus norvegicus*), Ctenocephalides (*Ctenocephalides felis*), Solanum (*Solanum tuberosum*), Anopheles (*Anopheles gambiae*), Reticulitermes (*Reticulitermes flavipes*), Perla (*Perla marginata*), Danaus (*Danaus plexippus*), Pararge (*Pararge aegeria*), Apis (*Apis florea*), Harpegnathos (*Harpegnathos saltator*), Zootermopsis (*Zootermopsis nevadensis*), Laodelphax (*Laodelphax striatella*), Aphis (*Aphis gossypii*), Branchiostoma (*Branchiostoma floridae*), Ixodes (*Ixodes scapularis*), Bombus (*Bombus terrestris*), Leptinotarsa (*Leptinotarsa decemlineata*), Oncopeltus (*Oncopeltus fasciatus*), Acheta (*Acheta domesticus*), Omphisa (*Omphisa fuscidentalis*), Blattella (*Blattella germanica*), and Homo (*H. sapiens*).

(A)

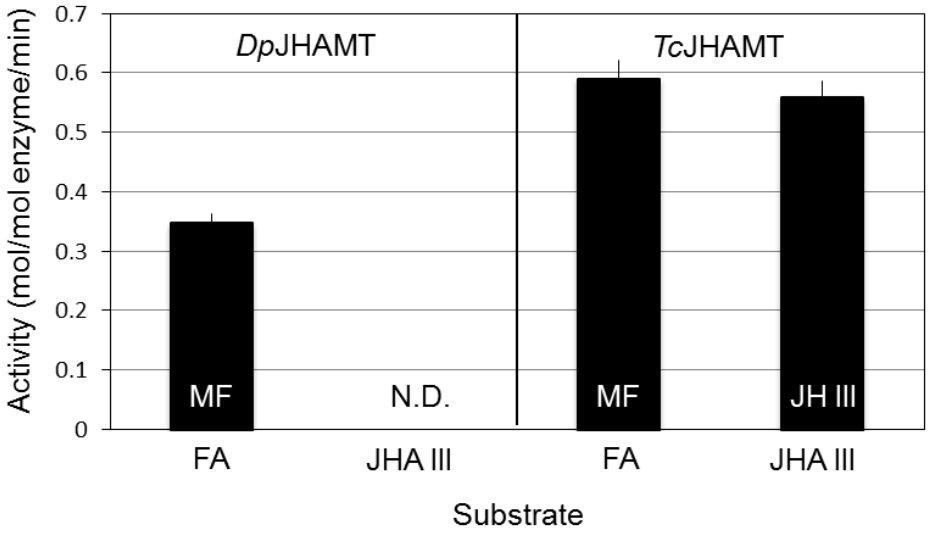
Activity (mol/mol enzyme/min)
0.7
0.6
0.5
0.4
0.3
0.2
0.1
0
DpJHAMT
TcJHAMT
MF
N.D.
MF
JH III
FA
JHA III
FA
JHA III
Substrate

(B)

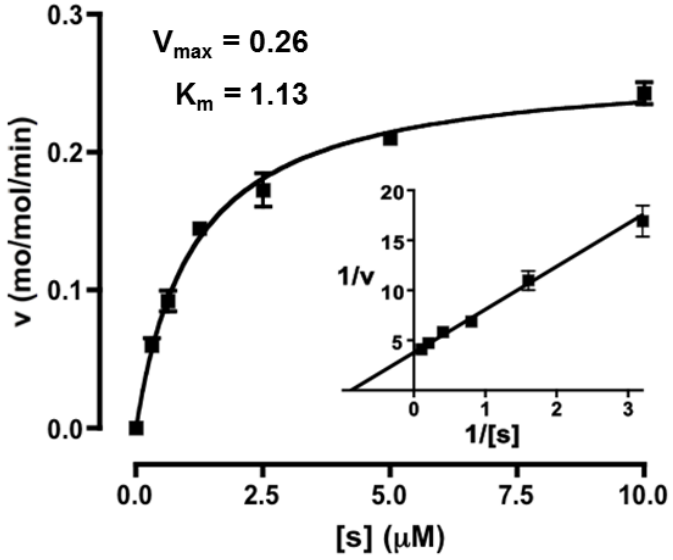
V_{max} = 0.26
K_m = 1.13
v (mo/mol/min)
0.3
0.2
0.1
0.0
1/v
20
15
10
5
0
1
2
3
1/[s]
0.0
2.5
5.0
7.5
10.0
[s] (μM)

Figure 1-15. Enzymatic activity and kinetics of JHAMTs. Relative enzymatic activities of recombinant *Dp*JHAMT and *T. castaneum* JHAMT against FA and JHA III (A). The *Dp*JHAMT catalyzes FA and generates MF, however, it does not generate JH III from JHA III. The activities are indicated as mol product/mol enzyme/min. N.D.; not detected. Mean ± SE, n=3. Substrate-velocity curve of *Dp*JHAMT with FA as substrate (B). *Km* and *Kcat* values obtained from the data by non-linear regression analysis using the Michaelis-Menten equation are indicated. The inset indicates Lineweaver-Burk plot. Mean ± SD, n=3.

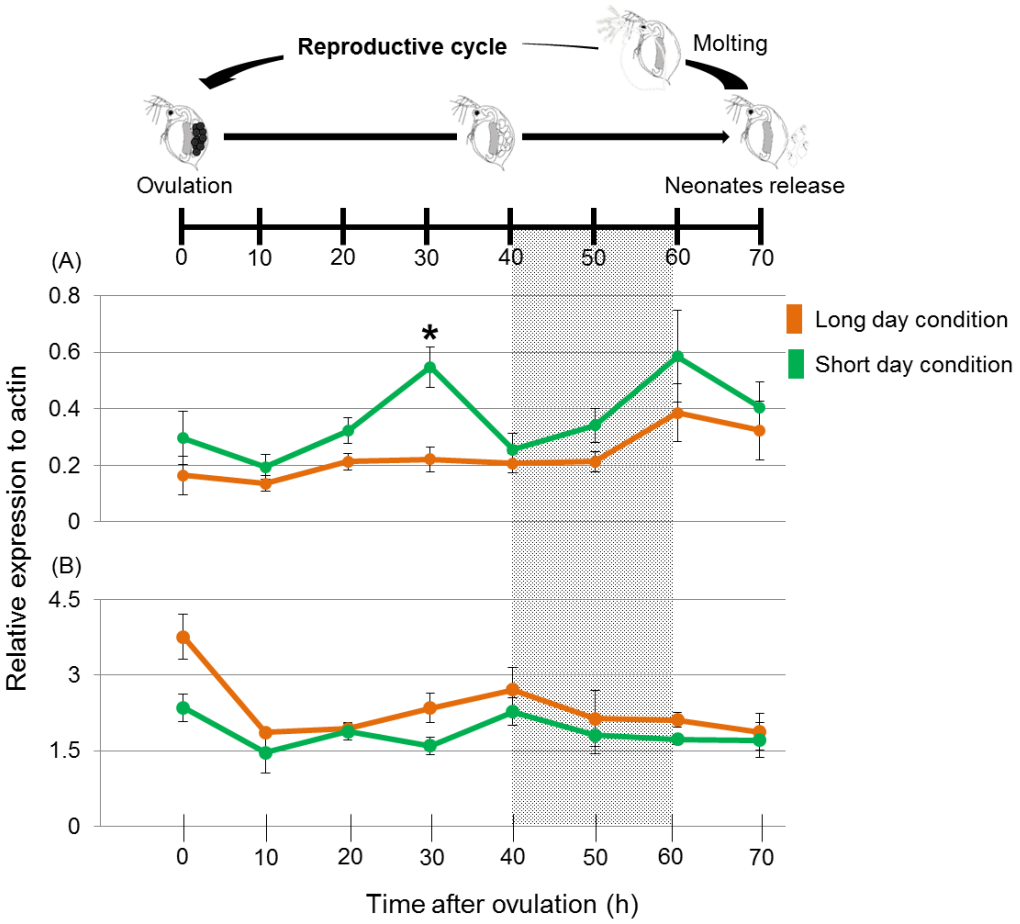

Figure 1-16. Expression profiles of *DpJHAMT* gene under long day (female-inducing) and short day (male-inducing) conditions in WTN6 and MFP strains. The expression of *DpJHAMT* is transiently upregulated just prior to the sex determining period (dotted area; see also **Figure 1-2**) in the WTN6 strain (A), but such peak does not appear in the MFP strains (B). Mean ± SEM, n=3. The asterisks denote significant differences between long day and short day conditions (two-way ANOVA, post-hoc the Tukey–Kramer test, $p < 0.05$).

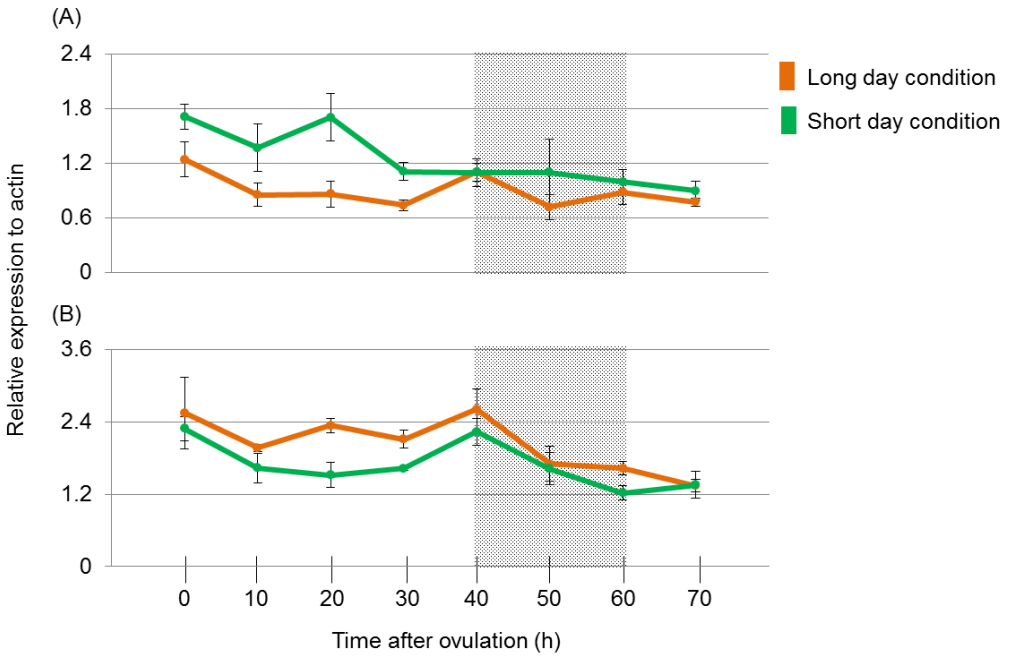

Figure 1-17. Expression profiles of *FAMeT* under long day (female-inducing) and short day (male-inducing) conditions in (A) WTN6 and (B) MFP strains. Mean ± SE, n=3. Dotted area indicates the sex determining period in daphnids.

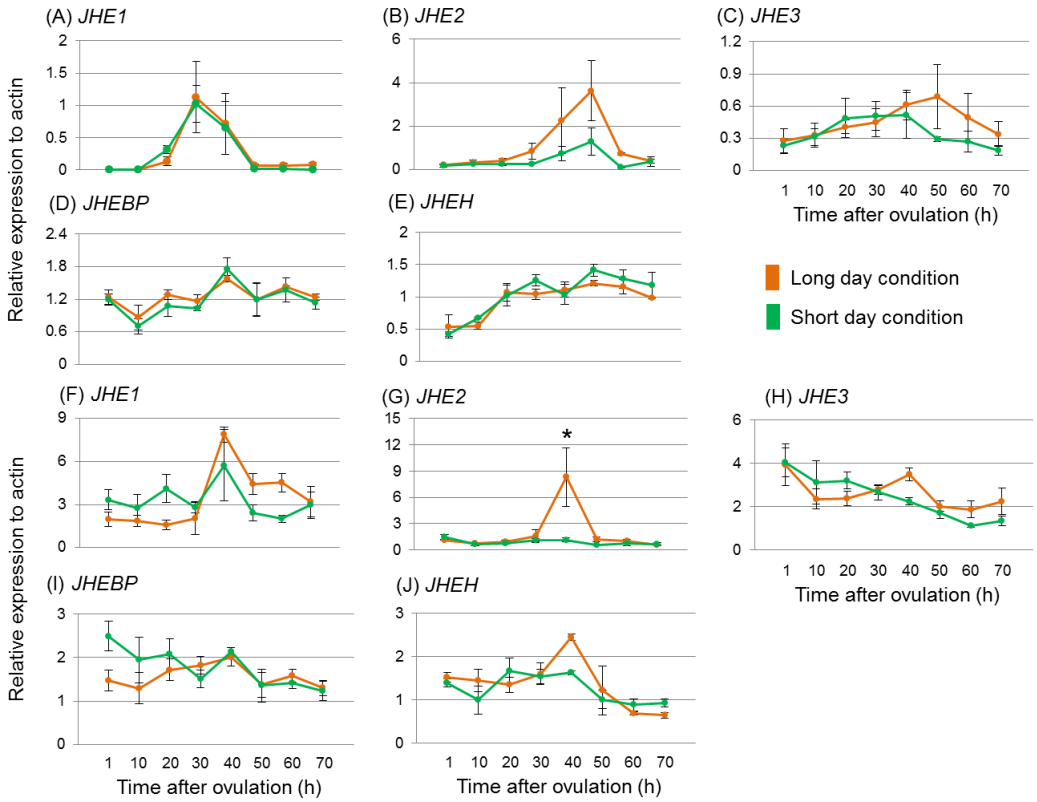

Figure 1-18. Expression profiles of genes encoding the *JHE1*, *JHE2*, *JHE3*, *JHEBP* and *JHEH* under long day (female-inducing) and short day (male-inducing) conditions in WTN6 (A-E) and MFP strains (F-J). Mean ± SE, n=3. The asterisks denote significant differences between long day and short day conditions (two-way ANOVA, post-hoc the Tukey–Kramer test, $p < 0.05$).

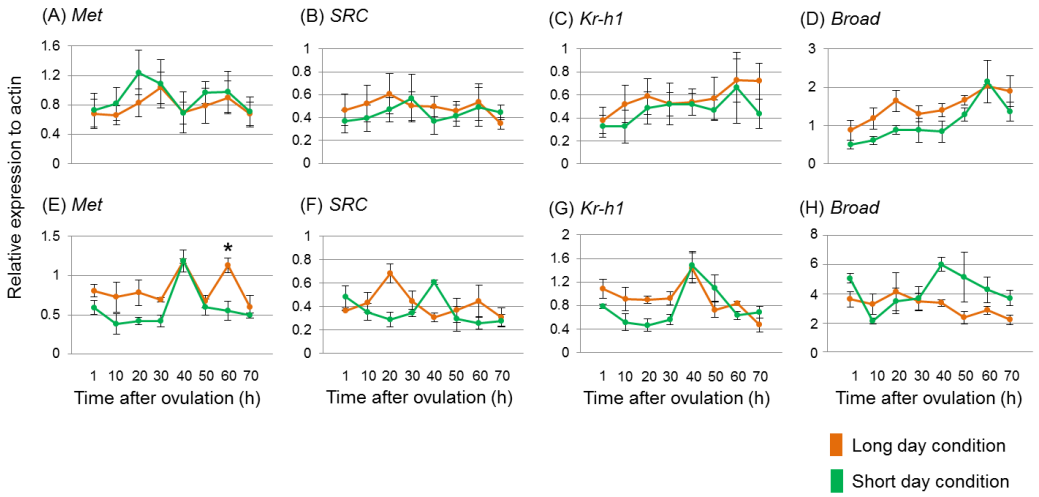

Figure 1-19. Expression profiles of genes encoding the *Met*, *SRC*, *kr-h1* and *broad* under long day (female-inducing) and short day (male-inducing) conditions in WTN6 (A-D) and MFP (E-H) strains. Mean ± SE, n=3. The asterisks denote significant differences between long day and short day conditions (two-way ANOVA, post-hoc the Tukey–Kramer test, $p < 0.05$).

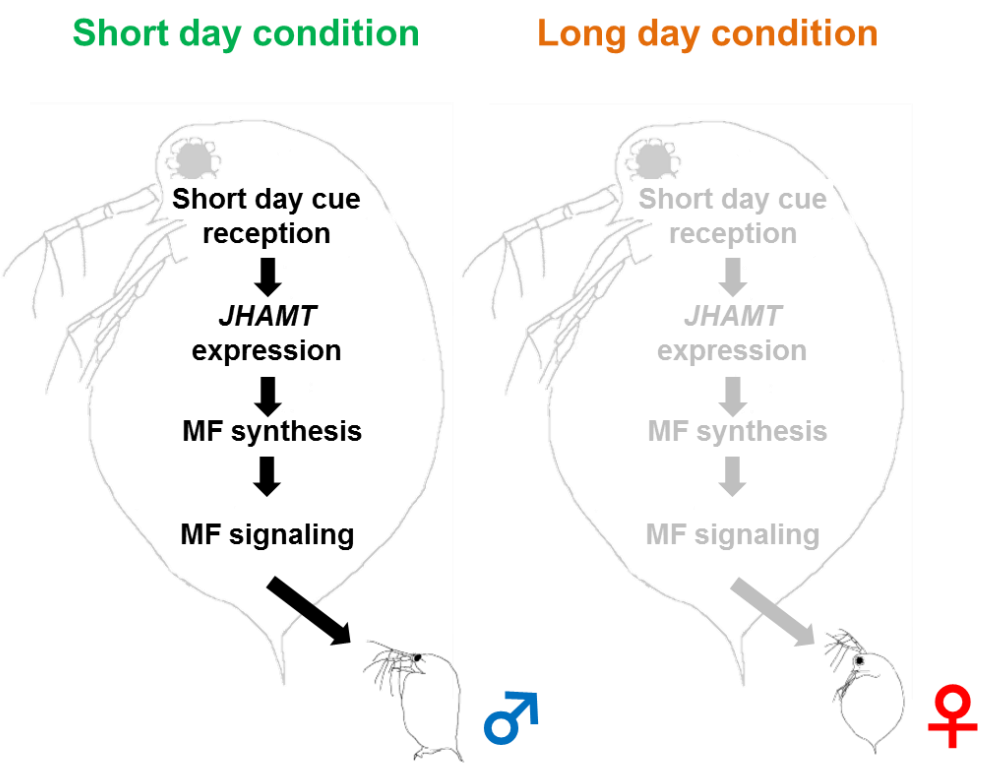

Figure 1-20. Schematic diagram of putative signal cascades regulating male offspring production responding to the short day stimuli in *D. pulex* WTN6 strain.

Chapter II

NMDA receptor activation upstream of methyl farnesoate signaling for short day-induced male offspring production in the water flea, *Daphnia pulex*

Abstract

The cladoceran crustacean *Daphnia pulex* produces female offspring by parthenogenesis under favorable conditions, but in response to various unfavorable external stimuli, it produces male offspring (ESD). I recently established an innovative system for ESD studies using *D. pulex* WTN6 strain, in which the sex of the offspring can be controlled simply by changes in the photoperiod: the long-day and short-day conditions can induce female and male offspring, respectively. Taking advantage of this system, I demonstrated that *de novo* MF synthesis is necessary for male offspring production. These results indicate the key role of innate MF signaling as a conductor between external environmental stimuli and the endogenous male developmental pathway. Despite these findings, the molecular mechanisms underlying up- and downstream signaling of MF have not yet been well elucidated in *D. pulex*. To elucidate up- and downstream events of MF signaling during sex determination processes, I compared the transcriptomes of daphnids reared under the long-day (female) condition with short-day (male) and MF-treated (male) conditions. I found that genes involved in ionotropic glutamate receptors, known to mediate the vast majority of excitatory neurotransmitting processes in various organisms, were significantly activated in daphnids by the short-day condition but not by MF treatment. Administration of specific agonists and antagonists, especially for the *N*-methyl-D-aspartic acid (NMDA) receptor, strongly increased or decreased, respectively, the proportion of male-producing mothers. Moreover, I also identified genes responsible for male production (e.g., protein kinase C pathway-related genes). Such genes were generally shared between the short-day reared and MF-treated daphnids. I identified several candidate genes regulating ESD which strongly suggests that these genes may be essential factors for male offspring production

as an upstream regulator of MF signaling in *D. pulex*. This study provides new insight into the fundamental mechanisms underlying how living organisms alter their phenotypes in response to various external environments.

Introduction

Sex determination is a fundamental developmental process that contributes to the establishment of sexually dimorphic traits, including the sexual differentiation of gonads, and leads to sex-specific differences in behavior and physiology. Sex determination systems can be divided into two major categories: GSD and ESD (Bull, 1985; Marin and Baker, 1998; Zarkower, 2001). GSD is attributed to the genetic segregation of genes, often residing on sex chromosomes that initially trigger and govern the alteration of sex-specific developmental pathways. In contrast, ESD, which has been repeatedly acquired during animal evolution (Organ and Janes, 2008), is initiated by plural external environmental cues such as temperature, photoperiod and population density, that trigger alternative genetic cascades, resulting in the activation of male or female fate-determining genes (Crews and Bull, 2009; Korpelainen, 1990).

The cladoceran crustacean genus *Daphnia* is a representative organism bearing the ESD system. Under natural favorable environmental conditions, *Daphnia* produce female offspring by parthenogenesis. However, when an adult female receives unfavorable environmental cues such as low temperature, low food quality, high individual density, or short day-length, *Daphnia* produce male offspring, thus altering their reproductive mode to sexual reproduction (Banta and Brown, 1929a; Hobæk and Larsson, 1990; Kleiven et al., 1992; Smith, 1915). Parthenogenesis allows rapid proliferation during favorable seasons whereas sexual reproduction contributes to an increase in genetic diversity and fitness to deal with changing habitat conditions (Barton and Charlesworth, 1998). Thus, the mechanisms underlying sexual fate determination that depend on external environmental conditions are important for daphnids as these will allow them to fit reproductive strategies appropriately to seasonally changing

environments (Kleiven et al., 1992).

Previous studies demonstrated that daphnids administrated with JHs or their analogs induced male offspring even under female-producing conditions (Olmstead and LeBlanc, 2002; Tatarazako et al., 2003). In response to parental activation of MF signaling, *doublesex1* is specifically expressed in the male embryos, and is indispensable for the development of male traits such as testis formation and first antenna elongation (Kato et al., 2011a). These results suggest that parental MF signaling activated by unfavorable environmental cues affects the developing oocytes during the oocyte maturation stage (Ignace et al., 2011) and determines their sexual fate (Ignace et al., 2011; Kato et al., 2011a; Kim et al., 2006; Oda et al., 2005b; Sinev and Sanoamuang, 2011; Toyota et al., 2013). However, the regulatory mechanisms of MF signaling and the following downstream pathway for male offspring production have not been clarified yet.

We have successfully established an innovative experimental system using *D. pulex* WTN6 strain. In this strain, the offspring sex can be controlled by simply changing the day length conditions; a mother produces female progeny reared under long-day conditions (14 h light : 10 h dark), whereas male progeny emerges under short-day conditions (10 h light : 14 h dark) (Toyota et al., in press).

In this study, to investigate the up- and downstream events of MF signaling, I reared adult *D. pulex* WTN6 strain under the following conditions: long-day (female-inducing), short-day (male-inducing) and long-day with MF treatment (male-inducing). The gene expression profiles of the ovary and whole body of these adults at the MF-sensitive period for male offspring production were compared by RNA-seq analysis. I found that the expression levels of ionotropic glutamate

receptor-related genes had changed significantly in response to the short-day condition, but not to MF treatment. Using pharmacological manipulation of ionotropic glutamate receptors, I demonstrated that *N*-methyl-D-aspartic acid (NMDA) receptors (a type of ionotropic glutamate receptor) are essential factors for male offspring production in *D. pulex* acting as an upstream regulator of MF signaling. My findings not only provide a molecular component to explain the ESD mechanism but also contribute to elucidate how organisms convert environmental information into phenotypic changes.

Materials and Methods

Female- and male-inducing conditions in *Daphnia pulex* strain

The *D. pulex* WTN6 strain was obtained from the Center for Genomics and Bioinformatics (Indiana University, IN, USA). This strain was maintained in dechlorinated freshwater, which was aerated and filtered through activated carbon for 2 weeks, at 18°C. A 0.04-ml suspension of 4.3×10^8 cells ml^{-1} of chlorella (*Chlorella vulgaris*) was added daily to each culture (40 individuals/2 L). To induce male offspring by exogenous administration of MF (Echelon Bioscience, Salt Lake City, UT, USA), I prepared a stock solution of 1 mg/ml MF dissolved in dimethylformamide (DMF; analytical grade, Wako, Osaka, Japan) and kept it at -20°C until use. This stock solution was added directly to each 50 ml of breeding water (final concentration: 0.8 μM) containing one adult female at 30 h after ovulation **(Figure 2-1A)**. I confirmed the sex of offspring based on the length of the first antenna (Olmstead and LeBlanc, 2000) using a Leica MZ FLIII microscope (Leica, Mannheim, Germany).

Chemicals and treatment procedures

I used three agonists of ionotropic glutamate receptors; *N*-methyl-D-asparatic acid (NMDA) (≥98%; Sigma-Aldrich, St. Louis, MO), (±)-α-Amino-3-hydroxy-5-methyl-4-isoxazolepropionic acid (AMPA), (≥98%; Sigma-Aldrich), and kainic acid *n*-hydrate (Kainate) (≥98%; Wako), and two antagonists; (+)-MK-801 hydrogen maleate (MK-801) (≥98%; Sigma-Aldrich) and 2,3-dioxo-6-nitro-1,2,3,4-tetrahydrobenzo[f]quinoxaline-7-sulfonamide disodium salt hydrate (NBQX) (≥98%; Sigma-Aldrich). Chemicals dissolved in water were stored as 10 mM stock solutions, and kept at 4°C until use. This stock solution was added to each

5 ml of breeding water containing one adult female (one-month old or older) at 30 h after ovulation in a 5-ml sampling tube (INA OPTICA, Osaka, Japan). A total of 15 individuals were used for these experiments. The concentrations of MF, agonists and antagonists used are as follows: MF (0.8 μM), MK-801 (20 μM), NBQX (100 and 200 μM), NMDA, AMPA and Kainate (100 μM). Differences between treatments were statistically analyzed by Fisher's exact probability test with Holm's correction using R 2.15.3 (Team, 2013).

RNA extraction and sequencing

One individual was cultured in 50 ml of rearing water under the long-day, short-day conditions and long-day condition with MF treatment. They were sacrificed when one month old (i.e., at least 8 times ovulated) during the MF-sensitive period for sex determination of the embryos (50 h after ovulation, **Figure 2-1A**). Whole body samples with developing embryos removed from the dorsal chamber and ovary samples consisted of three individuals/replicate, and triplicates were prepared for each experimental condition (long-day, short-day and MF-treated conditions), using a total of 54 individuals. Total RNA was extracted using the RNAqueous-Micro kit (Life Technologies, Carlsbad, CA, USA) according to the manufacturer's protocol. The RNA treated with RNase-free DNase was cleaned up using the RNeasy Mini kit (Qiagen, Valencia, CA, USA) according to the manufacturer's protocol. The quality and concentration of total RNA was validated by NanoDrop (Thermo Fisher Scientific, Waltham, MA, USA), Qubit (Life Technologies), and 2100 Bioanalyzer (Agilent Technologies, Santa Clara, CA, USA). The samples for transcriptome analyses were prepared from 1.0 μg of total RNA using TruSeq RNA Sample Preparation v2 kit

(Illumina, San Diego, CA, USA) following the manufacturer's protocols with minor modifications: RNA fragmentation was conducted for 4 min instead of 8 min at 94^{o}C and the number of PCR cycles was reduced to 6. We validated the cDNA libraries using the Bioanalyzer High Sensitivity DNA Assay (Agilent Technologies) and KAPA Library Quantification kits (Kapa Biosystems, Woburn, MA USA) according to the manufacturers' protocols. Multiplex sequencing of 101 bp paired-end reads was performed on an Illumina HiSeq2500 instrument. The output sequence quality was inspected using the FastQC program (Kodama et al., 2014). The RNA-Seq reads are available through DRA under the accession number DRA002725.

RNA-seq *de novo* assembly and annotation

The reads were cleaned up with cutadapt (Martin, 2011), trimming low-quality ends (< QV30) and adapter sequences, and reads shorter than 50 bp were discarded. Cleaned reads from all libraries were assembled together using the RNA-seq *de novo* assembler Trinity (Grabherr et al., 2011) in the paired-end mode with the options '–min_kmer_cov = 2, --dnorm_max_cov = 100'. ORFs larger than 150 bp were extracted from the Trinity contigs using TransDecorder, which is included in the Trinity suite. The translated protein sequences were subjected to similarity searches against NCBI nr using the BLASTP program and assigned the functional annotations of the most similar protein sequences. In most cases, the top hits were *D. pulex* proteins deposited in the RefSeq database. Gene model and annotation were assigned to each constructed transcripts according to *D. pulex* genome project data (Colbourne et al., 2011).

Differential expression analysis

To identify differentially expressed sequences, I first mapped the reads back to the contigs assembled by Trinity using Bowtie 2 version 2.1.0 (Langmead and Salzberg, 2012). For read mapping, I used a reporting option "-a" in Bowtie 2. Then transcript abundance was estimated by using eXpress version 1.5.1 (Roberts and Pachter, 2013). I used the edgeR package (Robinson et al., 2010) of Bioconductor to identify genes that are differentially expressed between each condition following the developer's manual (false discovery rate: FDR < 0.05). To adjust for library sizes and skewed expression of transcripts, the estimated abundance values were normalized using the Trimmed Mean of M-values (TMM) normalization method included in the edgeR package (Robinson and Oshlack, 2010). Based on a negative binomial model implemented in edgeR, DEGs among the long-day, short-day and MF-treated conditions were selected in the whole body and ovary, separately.

Gene ontology enrichment analysis

GO terms were assigned to each gene model according to the genome project in *D. pulex* (Colbourne et al., 2011). GO enrichment analysis was carried out using the gene score resampling method in ErmineJ (v3.0.2) (Lee et al., 2005), with full resampling of fold change used as gene scores. Among 7,860 constructed transcripts (total 70,229 transcripts) bearing at least one GO term, GO subsets containing between 5 and 150 genes were used in this analysis, and GO terms with the Benjamini-Hochberg FDR < 0.1 were considered as significant (Benjamini and Hochberg, 1995). QuickGO was used to provide co-occurrence GO terms which are most often annotated to the same proteins as the selected term (Binns et al., 2009).

Results and discussion

Differentially expressed genes in response to short-day and MF treatment

At first, I screened differentially expressed genes (DEGs) between female- and male-producing mothers as follows. The focal *D. pulex* strain, WTN6, can rigorously discriminate the sexual fate of its offspring (Toyota et al., in press). Briefly, under the long-day condition, it produces 100% female offspring **(Table 2-1)**. In contrast, the offspring sex ratio reaches 100% male under the short-day condition or exogenous treatment with MF under the long-day condition **(Table 2-1)** (Toyota et al., in press). RNA-seq analysis was performed using the aforementioned three types of conditioned mothers at a MF-sensitive period, *i.e.*, long-day (female-producing), short-day (male-producing) and long-day with MF treatment (male-producing) conditions **(Figure 2-1A)**. Prior to RNA sampling, we confirmed that all mothers were strictly conditioned in this way **(Figure 2-1B)**.

Illumina HiSeq2500 sequencing yielded a total of 530,174,848 paired-end reads (265,087,424 read pairs). The transcriptome assembly process produced 70,229 putative transcripts using Trinity. The N50 value and the mean length of assembled contigs, which are representative statistics of transcriptome assembly, are 3,043 bp and 1,591 bp, respectively. These scores are consistent with recent studies of some insect and crustacean species (Chauhan et al., 2014; Ghaffari et al., 2014; Zhang et al., 2014), suggesting that my transcriptome data provides a good resource for investigating the molecular mechanisms of ESD in *D. pulex*. We identified 55,466 ORFs (N50: 1,488 bp; mean length: 856 bp) in the assembled transcript sequences. Among them, 21,191 had significant BLAST similarity hits with publicly available protein sequences, 7,860 were assigned GO terms according to the genome project in *D. pulex* (Colbourne et al., 2011),

and 17,185 were consistent with gene models constructed by the *Daphnia* Genomics Consortium (Colbourne et al., 2011).

Among 70,229 constructed transcripts, 37 and 1,562 were differentially expressed in the ovary in response to the short-day condition and MF treatment, respectively **(Figures 2-2A, 2-3A, 2-3B)**. Similarly, in the whole body, I found 135 and 1,229 DEGs responding to the short-day condition and MF treatment, respectively **(Figures 2-2D, 2-3C, 2-3D)**.

Upstream factors of MF signaling

In this experimental design, I first compared the female-producing long-day condition, male-producing short-day condition and male-producing MF-treated condition. Genes differentially expressed exclusively in the short-day condition were designated as candidates for upstream of MF signaling, whereas mutual genes differentially expressed in both the short-day and MF-treated conditions were designated as candidates for downstream of MF signaling **(Figure 2-1A)**. Based on these criteria, I identified 16 and 33 DEGs responding to the short-day condition in the ovary and whole body, respectively, as the candidate transcripts regulating the upstream process of MF signaling **(Figures 2-2A, 2-2D)**. In response to short-day (male-producing) condition, four transcripts (*e.g.*, E3 ubiquitin ligase) were more abundant in ovary with $\log_2$-transformed fold change (FC) values between 2.42 and 11.19, whereas nineteen transcripts (*e.g.*, rho-associated coiled-coil containing protein kinase, cytochrome P450 CYP4/19/26 subfamilies, and ER-Golgi vesicle-tethering protein p115) were differentially expressed in whole body with $\log_2$-transformed FC values between 2.31 and 9.50 **(Tables 2-2, 2-3)**. However, not only approximately 80%

of the candidate genes in both sample categories could be classified into functionally unknown groups **(Figures 2-2B, 2-2E)**, but also molecular functions of these genes annotated with the regulation of the MF signaling remain largely unclear. Then, we next performed gene ontology (GO) enrichment analysis (Lee et al., 2005) to provide an overview of the potential candidate gene sets involved in the upstream of MF signaling governing male offspring production in *D. pulex*.

In comparison with the long-day and short-day conditions, GO terms (molecular function) corresponding to *ionotropic glutamate receptor activity*, *extracellular-glutamate-gated ion channel activity* and *glutamate receptor activity* showed significant differences in both the ovary and the whole body. The upper-hierarchy of these terms also varied significantly **(Table 2-4)**. This finding was strongly consistent with our previous study in which administration of MK-801, a specific antagonist of ionotropic glutamate receptors, suppressed male offspring production in *D. pulex* (Toyota et al., in press).

Intriguingly, intracellular calcium signaling might be activated in response to the short-day condition, because the expression levels of genes associated with intracellular calcium influx, such as *calcium channel activity*, changed significantly in both the ovary and whole body categories **(Table 2-4)**. Previous studies in several insects reported that an elevation of free intracellular calcium modulated by ionotropic glutamate receptors is necessary for increasing JH biosynthesis in the corpora allata, which is a JH-synthesizing organ in insects (Pszczolkowski et al., 1999; Rachinsky and Tobe, 1996). Therefore, ionotropic glutamate receptors might regulate the intracellular calcium concentration to modulate endogenous MF levels in daphnids as well as in insect species.

Also, among the GO category of biological process, I revealed that the expression levels of genes labeled with *cell surface receptor signaling pathway*, *sensory perception* and *neurological system process* showed significant changes only in the ovary in response to the short-day condition, but not to MF treatment **(Table 2-5)**. The terms of the *cell surface receptor signaling pathway* belong to an upper-hierarchy term of *glutamate receptor signaling pathway* (GO:0007215). Besides, the co-occurrence statistics for *sensory perception* and *neurological system process* using QuickGO (see Methods) indicated that *sensory perception* co-occurs with *regulation of N-methyl-D-aspartate selective glutamate receptor activity* (GO:2000310), while *neurological system process* co-occurs with *glutamate binding* (GO:0016595) and *glutamate receptor activity* (GO:0008066). These results suggest that genes assigned with *cell surface receptor signaling pathway*, *sensory perception* and *neurological system process* might be involved in the regulation of ionotropic glutamate receptors. On the other hand, expression changes in genes annotated with *regulation of N-methyl-D-aspartate selective glutamate receptor activity* and/or *glutamate binding* were not observed between the long-day and short-day conditions. These data also implied a possibility that genes related to *sensory perception* and *neurological system process* might be involved in the reception mechanism of the short-day cues acting as primary environmental signals for ESD in the WTN6 strain.

I also found that *sulfotransferase activity* and its upper-hierarchy terms (*transferase activity, transferring sulfur-containing groups and fucosyltransferase activity*, and *galactosyltransferase activity*), which are terms that belong to the molecular function category, varied significantly only in the ovary in response to the short-day condition **(Table 2-4)**. Although sulfotransferase-related genes might be one

of the candidates for the upstream element of MF signaling, a causal relationship between those genes and the regulatory mechanism of MF remains largely unknown. Further analyses will be required to elucidate the molecular functions of sulfotransferase-related genes in the regulation of MF signaling for the ESD system in *D. pulex*. These findings provide important clues about the molecular signaling cascade regulating male offspring production in response to the short-day condition in *D. pulex*.

Administration of agonists and antagonists of ionotropic glutamate receptor subtypes

The ionotropic glutamate receptors are divided into three subtypes based on their pharmacological characteristics; NMDA-type, (±)-α-amino-3-hydroxy-5-methyl-4-isoxazolepropionic acid (AMPA)-type and Kainate-type receptors. As described above, we previously reported that administration of MK-801 suppresses male offspring production in *D. pulex* WTN6 strain reared under the short-day condition (Toyota et al., in press); however, MK-801 can only block the NMDA-type among these subtypes. To investigate the molecular functions of ionotropic glutamate receptors and the contribution of each subtype to male induction, I performed detailed exposure experiments using several specific agonists and antagonists of ionotropic glutamate receptors. First, we exposed mothers reared under the long-day or short-day conditions to MK-801 or 2,3-dioxo-6-nitro-1,2,3,4-tetrahydrobenzo[f]quinoxaline-7-sulfonamide (NBQX), a specific antagonist for AMPA and Kainate receptors. Treatment of these antagonists did not affect the proportion of female-producing mothers reared under the long-day condition **(Figure 2-4A)**. On the other hand, administration of MK-801 to daphnids

reared under the short-day condition strongly suppressed the proportion of male-producing mothers and importantly, its phenotype was restored when treated with exogenous MF **(Figure 2-4B)**, which is highly reproducible data with a previous study (Toyota et al., in press). In addition to MK-801, NBQX treatment seemed to suppress the proportion of male-producing mothers, although the effect was not significant **(Figure 2-4B)**. A reduction in the proportion of male-producing mothers following the administration of NBQX was also recovered by co-treatment with MF **(Figure 2-4B)**. In this experiment, mothers always produced either female or male offspring in a clutch **(Table 2-6)**.

I then applied agonists for ionotropic glutamate receptors (NMDA, AMPA and Kainate) to daphnids reared under the long-day condition, and found that the proportion of male-producing mothers increased in response to treatment of each single agonist and their combinations **(Figure 2-5A)**. Although not statistically significant, NMDA administration showed the strongest effect on male induction among them **(Figure 2-5A)**. On the other hand, all agonists showed no effect on the proportion of male-producing mothers reared under the short-day condition **(Figure 2-5B)**. As in antagonist treatment experiments, mothers always produced either female or male offspring in a clutch **(Table 2-7)**. Taken together, the current results suggest that the activation of ionotropic glutamate receptors is essential for male offspring production in *D. pulex*, and that the process of male induction might be primarily mediated by NMDA receptors, although some contributions of AMPA and Kainate receptors should also be considered.

The present results suggest that NMDA receptors act on the upstream of MF signaling, however, signal cascades connecting NMDA receptors and the activation of

MF signaling remain largely unknown. Previously, the TGFβ signaling pathway was identified as a potential candidate connecting NMDA receptor to JH synthesis in *D. melanogaster* (Huang et al., 2011). In the corpora allata of *D. melanogaster*, TGFβ signaling, which is mediated by *decapentaplegic* (a TGFβ ligand), *thickveins* and *Mothers against decapentaplegic* (main components of its pathway), contributes to the regulation of JH biosynthesis via induction of JHAMT, a critical enzyme of JH synthesis (Huang et al., 2011). In chapter I, I revealed that JHAMT is a key factor for modulating the innate MF levels governing the ESD in *D. pulex* (Toyota et al., in press). Although the expression of TGFβ signaling pathway-related genes did not change between the short-day and the long-day conditions in our RNA-seq experiments, further investigations concerning TGFβ signaling are necessary to elucidate the signal cascades between NMDA receptors and activation of *JHAMT* expression in *D. pulex*.

Most aphid species are known to exhibit cyclical parthenogenesis and ESD in a manner much like the daphnids. It has been reported that the autumnal shortened day-length induce the sexual morph that produces male and oviparous female (Lees, 1959), and topical application of JH to oviparous producer induces the parthenogenetic female in pea aphid *Acyrthosiphon pisum* (Corbitt and Hardie, 1985). Moreover, recent progress in omics technologies (*e.g.*, genomics, transcriptomics and proteomics) have allowed the large-scale screening of candidate factors responsible for the switch from parthenogenetic morph to sexual morph induced by shortening of the photoperiod (Consortium, 2010; Gallot et al., 2012; Ishikawa et al., 2012; Le Trionnaire et al., 2009; Trionnaire et al., 2013). Interestingly, JHE (JH degradation enzyme) was identified as a key element for the induction of sexual morph by the JH III titer decrease in response to short-day condition (Ishikawa et al., 2012). This finding indicates relationship between

endogenous JH III/MF titer in the mothers and sexual outcome of the offspring is an opposite phenomenon in pea aphids and daphnids: high innate JH III titer induces female progeny in pea aphids and male progeny in daphnids. NMDA receptor might act in the singling pathway between receptions of shortened day-length and regulation of innate JH III titer in pea aphids as well as in daphnids. To investigate the common principle of ESD system among them, further comparative analyses will be necessary.

Downstream factors of MF signaling

Finally, I screened the downstream candidates of MF signaling as the mutual DEGs in response to both the short-day condition and MF treatment **(Figure 2-1A)**. I obtained 21 and 102 DEGs in the ovary and whole body, respectively **(Figures 2-2A, 2-2D)**. In response to short-day condition, seventeen transcripts (*e.g.*, drebrins and related actin binding proteins) were more enriched in ovary with $\log_2$-transformed FC values between 2.46 and 8.76, whereas twenty-five transcripts (*e.g.*, low-density lipoprotein receptors containing Ca^{2+}-binding EGF-like domains) were differentially expressed in whole body with $\log_2$-transformed FC values between 2.11 and 9.06 **(Tables 2-8, 2-9)**. Further, candidate genes in the whole body contained several serine protease and hemoglobin-related genes, known as MF-responsive genes in daphnids (Abe et al., 2015; Toyota et al., 2014), implying that this experimental design possesses higher reliability to select factors involved in downstream of MF signaling. In addition, more than 50% of the candidate genes could not be attributed to any annotations **(Fig.ures2-2C, 2-2F)**, suggesting that those genes might be novel candidates for sexual fate determination via MF signaling in *D. pulex* **(Tables 2-8, 2-9)**.

GO enrichment analysis showed that expression levels of genes associated

with *protein tyrosine kinase activity* and *calcium ion transmembrane transporter activity* terms varied significantly in response to the short-day condition and MF treatment, especially in the ovary **(Table 2-4)**. Although recent studies indicated that JH acts via intracellular-type receptors to modulate downstream gene expression (Charles et al., 2011; Kayukawa et al., 2012; Li et al., 2011; Miyakawa et al., 2013c; Miyakawa et al., 2014; Shin et al., 2012), some studies implied that JH actions are mediated via plasma membrane-type receptors involving calcium ion and protein kinase C in *D. melanogaster* (Yamamoto et al., 1988) and two crustaceans, barnacle *Balanus amphitrite* (Yamamoto et al., 1997) and the crayfish *Cherax quadricarinatus* (Soroka et al., 2000). Based on this knowledge, it is suggested that MF signal transduction from the mother (ovarian tissues) to oocytes is regulated by not only transcriptional gene cascades via intracellular-type JH receptors but also by phosphorylation cascades through the protein kinase C family in the ovary of daphnids. To prove this hypothesis, further exposure experiments using activators and inhibitors of protein kinase C will be required.

Conclusion

I conducted transcriptome analyses using RNA-seq to shed light on the signaling cascades underlying the ESD system in *D. pulex*. I identified several candidate gene sets of the MF pathway regulating the ESD of *D. pulex*, including NMDA receptors, as a primary upstream regulator of MF signaling **(Figure 2-6)**. Moreover, the phosphorylation signaling cascades via protein kinase C might be implicated in the downstream pathway of MF signaling **(Figure 2-6)**. Although further investigation concerning the characterization of NMDA receptors and protein kinase C gene families will be required, my findings not only provide important clues involved in the molecular signaling cascade regulating male offspring production in response to the short-day condition in *D. pulex*, but also contribute to elucidate how animals transmit information from the external environmental and transform it into phenotypic alterations.

Tables

Table 2-1 Male induction rates under the long day, short day and MF-treated conditions.

Rearing conditions	Replicates	No. of offspring		Male induction rate
		Female	Male	
Long day	1	30	0	0%
	2	42	0	0%
	3	40	0	0%
	4	32	0	0%
	5	24	0	0%
	6	16	0	0%
	7	14	0	0%
	8	17	0	0%
Short day	1	0	29	100%
	2	0	23	100%
	3	0	43	100%
	4	0	37	100%
	5	0	16	100%
	6	0	40	100%
	7	0	37	100%
	8	0	52	100%
	9	0	29	100%
	10	0	23	100%
	11	0	43	100%
	12	0	37	100%
	13	0	20	100%
MF treatment	1	0	41	100%
	2	0	19	100%
	3	0	34	100%
	4	0	34	100%
	5	0	38	100%
	6	0	25	100%
	7	0	16	100%
	8	0	26	100%
	9	0	33	100%

Table 2-2. Annotation of up- and downregulated genes in response to the short day condition in the ovary

Trinity_ID	Protein_ID	Short day/long day		MF-treated/long day		Description
		logFC	FDR	logFC	FDR	
Up-regulation						
c21268_g2_i8	Not available	11.19	<0.001	-0.02	1	No hits
c21268_g1_i6	Not available	7.18	<0.001	-1.17	1	No hits
c21268_g2_i9	Not available	5.27	0.0278	0.31	1	No hits
c22027_g1_i5	JGI_V11_255909	2.42	0.0495	1.96	0.32	E3 ubiquitin ligase. Cullin 2 component
Down-regulation						
c17218_g1_i3	JGI_V11_228636	-1.48	0.0182	-1.06	0.2783	No hits
c20607_g1_i10	Not available	-3.04	0.0032	-1.72	0.0942	No hits
c20607_g1_i5	Not available	-3.62	<0.001	-1.26	0.4622	No hits
c20607_g1_i9	Not available	-3.89	<0.001	-1.15	0.378	No hits
c20970_g1_i2	Not available	-4.35	0.0099	-0.04	1	No hits
c21362_g2_i3	Not available	-4.66	0.0130	1.25	0.5872	No hits
c16528_g1_i4	Not available	-4.74	0.0099	-1.15	0.8207	No hits
c19122_g1_i4	Not available	-5.43	0.0441	-3.43	0.0828	No hits
c21993_g1_i17	Not available	-7.41	0.0108	-2.95	0.2726	No hits
c18509_g1_i6	Not available	-8.44	0.0142	-1.17	1	No hits
c20897_g1_i4	JGI_V11_191054	-8.56	0.0313	-1.48	0.9956	Serine proteinase inhibitor (KU family) with thrombospondin repeats
c22111_g1_i5	Not available	-9.09	0.0085	-2.7	0.3999	No hits

Table 2-3. Annotation of up- and downregulated genes in response to the short day condition in the whole body

Trinity_ID	Protein_ID	SD/LD		MF/LD		Description
		logFC	FDR	logFC	FDR	
Up-regulated						
c19191_g3_i5	N.A.	9.50	0.0014	7.41	0.1153	No hits
c19857_g1_i17	JGI_V11_300342	7.65	0.0142	5.86	0.0588	Rho-associated. coiled-coil containing protein kinase
c19940_g1_i4	N.A.	7.62	0.0498	3.58	1.0000	No hits
c19048_g3_i1	JGI_V11_244715	6.93	0.0025	4.61	0.0784	No hits
c20548_g3_i11	N.A.	6.91	0.0438	3.60	1.0000	No hits
c19557_g2_i5	JGI_V11_309953	6.40	0.0378	5.28	0.0731	No hits
c21857_g2_i8	N.A.	5.93	0.0065	4.81	0.1481	No hits
c20592_g1_i14	N.A.	5.28	0.0347	4.63	0.1356	No hits
c17628_g3_i2	JGI_V11_312048	4.91	0.0092	3.49	0.1525	Cytochrome P450 CYP4/CYP19/CYP26 subfamilies
c18466_g1_i12	JGI_V11_299568	4.71	<0.001	2.37	0.2495	No hits
c16366_g1_i2	N.A.	4.64	0.0169	2.58	0.4318	No hits
c17429_g1_i2	N.A.	3.65	0.0346	-0.32	1.0000	No hits
c9854_g1_i1	JGI_V11_300203	3.65	0.0454	0.73	1.0000	ER-Golgi vesicle-tethering protein p115

c19716_g1_i1	JGI_V11_226169	3.39	0.0011	0.51	1.0000	No hits
c19716_g4_i1	JGI_V11_244645	3.32	0.0011	0.78	1.0000	No hits
c19716_g6_i1	N.A.	3.20	0.0437	0.66	1.0000	No hits
c11657_g1_i1	JGI_V11_226094	2.91	0.0378	1.82	0.3303	No hits
c20997_g1_i2	JGI_V11_211890	2.70	0.0492	1.12	0.9551	No hits
c20997_g1_i12	N.A.	2.31	0.0357	0.97	0.9922	No hits
Down-regulated						
c20996_g1_i10	N.A.	-3.00	0.0408	-1.47	0.6914	No hits
c20242_g1_i3	N.A.	-3.12	0.0017	-2.67	0.1817	No hits
c22029_g1_i22	JGI_V11_312878	-3.29	0.0416	0.85	1.0000	Na+:iodide/myo-inositol/multivitamin symporters
c13372_g1_i4	JGI_V11_309303	-3.33	0.0166	-2.27	0.1190	No hits
c19467_g1_i1	JGI_V11_243454	-3.35	0.0177	-2.38	0.0615	Peptidyl-dipeptidase A. ,Angiotensin I-converting enzymes - M2 family peptidases
c14848_g1_i5	JGI_V11_240002	-3.70	0.0177	-0.86	1.0000	Phosphogluconate dehydrogenase (decarboxylating). Pentose phosphate pathway,6-phosphogluconate dehydrogenase
c19114_g2_i11	N.A.	-3.83	0.0402	-2.99	0.0678	No hits

c19726_g1_i5	N.A.	-5.13	0.0166	-1.64	0.8193	No hits
c12920_g1_i1	N.A.	-5.27	0.0385	-3.84	0.0753	No hits
c22007_g1_i5	N.A.	-5.48	0.0430	-3.03	0.2308	No hits
c14347_g1_i4	JGI_V11_219600	-5.57	0.0080	-1.09	1.0000	DHHC-type Zn-finger proteins
c21824_g1_i1	N.A.	-5.69	0.0071	-3.02	0.1791	No hits
c15747_g1_i1	N.A.	-7.10	0.0028	0.82	1.0000	No hits
c21437_g1_i3	Not available	-8.39	0.0027	-4.34	0.0641	No hits

Table 2-4 List of GO terms in molecular function significantly changed in response to the short day and MF-treated conditions.

Name	ID	Same as*	False discovery rate			
			Short day/long day		MF-treated/long day	
			Ovary	Whole body	Ovary	Whole body
receptor activity	GO:0004872		0.025	0.080	0.081	0.245
signaling receptor activity	GO:0038023		0.008	0.085	0.035	0.220
transmembrane signaling receptor activity	GO:0004888		0.006	0.022	0.045	0.180
glutamate receptor activity	GO:0008066	GO:0005234, GO:0004970	0.056	0.100	0.441	0.410
ionotropic glutamate receptor activity	GO:0004970	GO:0005234, GO:0008066	0.056	0.100	0.441	0.410
passive transmembrane transporter activity	GO:0022803	GO:0015267	0.018	0.015	0.110	0.335
channel activity	GO:0015267	GO:0022803	0.018	0.015	0.110	0.335
gated channel activity	GO:0022836		0.064	0.078	0.184	0.393
ligand-gated channel activity	GO:0022834	GO:0015276	0.048	0.073	0.282	0.389
ligand-gated ion channel activity	GO:0015276	GO:0022834	0.048	0.073	0.282	0.389
extracellular ligand-gated ion channel activity	GO:0005230		0.067	0.068	0.303	0.392
excitatory extracellular ligand-gated ion channel activity	GO:0005231		0.091	0.154	0.568	0.546
extracellular-glutamate-gated ion channel activity	GO:0005234	GO:0004970, GO:0008066	0.056	0.100	0.441	0.410
substrate-specific channel activity	GO:0022838	**GO:0005216**	0.018	0.015	0.110	0.335
ion channel activity	**GO:0005216**	GO:0022838	0.018	0.015	0.110	0.335
cation channel activity	**GO:0005261**		0.090	0.111	0.177	0.636
calcium channel activity	**GO:0005262**		0.027	0.067	0.112	0.417
molecular transducer activity	GO:0060089	**GO:0004871**	0.025	0.089	0.054	0.356

signal transducer activity	**GO:0004871**	GO:0060089	0.025	0.089	0.054	0.356
protein kinase activity	GO:0004672		0.002	0.003	0.022	0.139
protein serine/threonine kinase activity	GO:0004674		0.002	0.010	0.031	0.127
protein tyrosine kinase activity	GO:0004713		0.002	0.013	0.024	0.064
divalent inorganic cation transmembrane transporter activity	GO:0072509	GO:0015085	0.058	0.069	0.086	0.511
calcium ion transmembrane transporter activity	GO:0015085	GO:0072509	0.058	0.069	0.086	0.511
monooxygenase activity	GO:0004497		0.001	0.076	0.066	0.028
galactosyltransferase activity	GO:0008378		0.074	0.283	0.305	0.421
fucosyltransferase activity	GO:0008417		0.425	0.063	0.629	0.325
transferase activity, transferring sulfur-containing groups	GO:0016782		0.016	0.415	0.032	0.322
sulfotransferase activity	GO:0008146		0.016	0.355	0.023	0.241
lipid binding	GO:0008289		0.094	0.279	0.105	0.051
phospholipid binding	GO:0005543		0.093	0.762	0.181	0.727
calcium-dependent phospholipid binding	GO:0005544		0.070	0.667	0.148	0.626
metallopeptidase activity	GO:0008237		0.089	0.739	0.101	0.390
exopeptidase activity	GO:0008238		0.315	1.000	0.067	0.226
carboxypeptidase activity	GO:0004180		0.092	0.991	0.024	0.105
chitin binding	GO:0008061		1.000	0.987	0.028	0.531
lipid transporter activity	GO:0005319		0.809	0.826	0.046	0.209
phosphopantetheine binding	GO:0031177		0.656	0.146	0.070	0.224
structural constituent of cuticle	GO:0042302		0.648	0.299	0.013	0.032
extracellular matrix structural constituent	GO:0005201		0.596	0.171	0.003	0.037

*These GO terms were contained in the same gene with terms listed under ID column.

Red letters indicate the ionotropic glutamate receptor-related terms.

Bold letters indicate the co-occurring terms with ionotropic glutamate receptor-related terms.

Values in shaded cells indicate the FDR < 0.1.

Table 2-5 List of GO terms in biological processes that changed significantly in response to short day and MF-treated conditions.

Name	ID	Same as*	False discovery rate			
			Short day/long day		MF-treated/long day	
			Ovary	Whole body	Ovary	Whole body
cell surface receptor signaling pathway**	GO:0007166		0.094	0.265	0.117	0.455
neurological system process	**GO:0050877**	**GO:0007600**	**0.072**	**1.000**	**0.568**	**1.000**
sensory perception	**GO:0007600**	**GO:0050877**	**0.072**	**1.000**	**0.568**	**1.000**
protein phosphorylation	GO:0006468		0.019	0.012	0.102	0.543
amino sugar metabolic process	GO:0006040	GO:1901071	1.000	1.000	0.064	1.000
glucosamine-containing compound metabolic process	GO:1901071	GO:0006040	1.000	1.000	0.064	1.000
aminoglycan metabolic process	GO:0006022	GO:0006030	1.000	1.000	0.039	1.000
chitin metabolic process	GO:0006030	GO:0006022	1.000	1.000	0.039	1.000
anion transport	GO:0006820		1.000	1.000	0.134	0.049
inorganic anion transport	GO:0015698		1.000	0.460	0.126	0.013
phosphate ion transport	GO:0006817		1.000	0.415	0.043	0.017

*These GO terms were contained in the same gene with terms listed under the ID column.

**Term of cell surface receptor signaling pathway is an upper-hierarchy term of glutamate receptor signaling pathway (GO:0007215).

Bold letters indicate the co-occurring terms with ionotropic glutamate receptor-related terms.

Values in shaded cells indicate an FDR < 0.1.

Table 2-6 Male induction rates by administration of ionotropic glutamate receptor antagonists

Treatment	Replicates	Long day condition			Short day conditon		
		No. of offspring		Male induction rate	No. of offspring		Male induction rate
		Female	Male		Female	Male	
Control	1	35	0	0%	0	22	100%
	2	32	0	0%	0	30	100%
	3	27	0	0%	0	21	100%
	4	41	0	0%	0	20	100%
	5	34	0	0%	0	23	100%
	6	31	0	0%	0	42	100%
	7	27	0	0%	0	33	100%
	8	28	0	0%	0	34	100%
	9	32	0	0%	0	9	100%
	10	27	0	0%	0	32	100%
	11	28	0	0%	0	33	100%
	12	29	0	0%	0	37	100%
	13	21	0	0%	0	31	100%
	14	34	0	0%	0	35	100%
	15	27	0	0%	0	27	100%
MK-801	1	23	0	0%	34	0	0%
	2	24	0	0%	27	0	0%

	3	27	0	0%	31	0	0%
	4	27	0	0%	28	0	0%
	5	28	0	0%	31	0	0%
	6	30	0	0%	24	0	0%
	7	32	0	0%	30	0	0%
	8	30	0	0%	23	0	0%
	9	23	0	0%	21	0	0%
	10	24	0	0%	25	0	0%
	11	23	0	0%	29	0	0%
	12	26	0	0%	25	0	0%
	13	27	0	0%	0	38	100%
	14	27	0	0%	30	0	0%
	15	30	0	0%	24	0	0%
NBQX (100 µM)	1	32	0	0%	0	28	100%
	2	29	0	0%	34	0	0%
	3	26	0	0%	0	31	100%
	4	24	0	0%	28	0	0%
	5	25	0	0%	28	0	0%
	6	14	0	0%	30	0	0%
	7	21	0	0%	0	28	100%
	8	26	0	0%	25	0	0%
	9	30	0	0%	0	30	100%
	10	23	0	0%	0	26	100%

	11	28	0	0%	24	0	0%
	12	23	0	0%	0	35	100%
	13	27	0	0%	0	38	100%
	14	26	0	0%	0	36	100%
	15	25	0	0%	0	32	100%
NBQX (200 µM)	1	26	0	0%	0	7	100%
	2	23	0	0%	0	12	100%
	3	24	0	0%	20	0	0%
	4	25	0	0%	0	17	100%
	5	30	0	0%	0	12	100%
	6	21	0	0%	0	21	100%
	7	32	0	0%	0	23	100%
	8	27	0	0%	0	21	100%
	9	35	0	0%	0	26	100%
	10	26	0	0%	0	24	100%
	11	21	0	0%	0	21	100%
	12	24	0	0%	25	0	0%
	13	23	0	0%	16	0	0%
	14	26	0	0%	19	0	0%
	15	26	0	0%	0	22	100%
MK-801 +	1	0	28	100%	0	30	100%
	2	0	31	100%	0	31	100%

MF	3	0	32	100%	0	27	100%
	4	0	28	100%	0	32	100%
	5	0	27	100%	0	38	100%
	6	0	28	100%	0	32	100%
	7	0	28	100%	0	30	100%
	8	0	36	100%	0	23	100%
	9	0	31	100%	0	22	100%
	10	0	30	100%	0	25	100%
	11	0	33	100%	0	25	100%
	12	0	26	100%	0	30	100%
	13	0	31	100%	0	27	100%
	14	0	32	100%	0	24	100%
	15	0	34	100%	0	22	100%
NBQX (100µM) + MF	1	0	36	100%	0	29	100%
	2	0	33	100%	0	24	100%
	3	0	34	100%	0	28	100%
	4	0	27	100%	0	23	100%
	5	0	26	100%	0	27	100%
	6	0	27	100%	0	26	100%
	7	0	31	100%	0	25	100%
	8	0	36	100%	0	24	100%
	9	0	32	100%	0	27	100%

	10	0	34	100%	0	26	100%
	11	0	30	100%	0	28	100%
	12	0	36	100%	0	28	100%
	13	0	32	100%	0	32	100%
	14	0	30	100%	0	24	100%
	15	0	25	100%	0	21	100%

Table 2-7 Male induction rates by administration of ionotropic glutamate receptor agonists

Treatment	Replicates	Long day condition			Short day condition		
		No. of offspring		Male induction rate	No. of offspring		Male induction rate
		Female	Male		Female	Male	
Control	1	35	0	0%	0	22	100%
	2	32	0	0%	0	30	100%
	3	27	0	0%	0	21	100%
	4	41	0	0%	0	20	100%
	5	34	0	0%	0	23	100%
	6	31	0	0%	0	42	100%
	7	27	0	0%	0	33	100%
	8	28	0	0%	0	34	100%
	9	32	0	0%	0	9	100%
	10	27	0	0%	0	32	100%
	11	28	0	0%	0	33	100%
	12	29	0	0%	0	37	100%
	13	21	0	0%	0	31	100%
	14	34	0	0%	0	35	100%
	15	27	0	0%	0	27	100%
NMDA	1	0	35	100%	0	27	100%
	2	0	26	100%	0	32	100%
	3	0	28	100%	0	34	100%

	4	0	31	100%	0	39	100%
	5	0	34	100%	0	33	100%
	6	0	25	100%	0	40	100%
	7	0	24	100%	0	28	100%
	8	0	34	100%	0	32	100%
	9	0	32	100%	0	36	100%
	10	0	31	100%	0	30	100%
	11	0	28	100%	0	28	100%
	12	0	26	100%	0	23	100%
	13	0	34	100%	0	29	100%
	14	0	35	100%	0	24	100%
	15	0	28	100%	0	23	100%
AMPA	1	0	30	100%	0	32	100%
	2	0	37	100%	0	29	100%
	3	0	39	100%	0	30	100%
	4	0	41	100%	0	28	100%
	5	34	0	0%	0	26	100%
	6	0	34	100%	0	27	100%
	7	0	15	100%	0	29	100%
	8	0	28	100%	0	31	100%
	9	0	30	100%	0	25	100%
	10	0	32	100%	0	23	100%
	11	34	0	0%	0	27	100%

	12	0	28	100%	0	27	100%
	13	0	29	100%	0	29	100%
	14	0	26	100%	0	31	100%
	15	0	25	100%	0	36	100%
Kainate	1	0	25	100%	0	28	100%
	2	0	54	100%	0	27	100%
	3	0	32	100%	0	30	100%
	4	36	0	0%	0	25	100%
	5	0	33	100%	0	23	100%
	6	31	0	0%	0	14	100%
	7	25	0	0%	0	28	100%
	8	0	34	100%	0	26	100%
	9	0	28	100%	0	29	100%
	10	0	26	100%	0	31	100%
	11	0	29	100%	0	38	100%
	12	0	33	100%	0	34	100%
	13	0	34	100%	0	35	100%
	14	0	28	100%	0	32	100%
	15	24	0	0%	0	30	100%
NMDA + AMPA	1	0	26	100%	0	31	100%
	2	0	24	100%	0	32	100%
	3	0	31	100%	0	34	100%
	4	0	36	100%	0	33	100%

	5	0	32	100%	0	30	100%
	6	0	24	100%	0	35	100%
	7	0	33	100%	0	36	100%
	8	0	28	100%	0	31	100%
	9	0	26	100%	0	28	100%
	10	0	24	100%	0	27	100%
	11	0	25	100%	0	30	100%
	12	0	29	100%	0	38	100%
	13	0	31	100%	0	31	100%
	14	0	28	100%	0	26	100%
	15	0	25	100%	0	25	100%
NMDA + Kainate	1	0	21	100%	0	34	100%
	2	0	23	100%	0	38	100%
	3	0	29	100%	0	25	100%
	4	0	24	100%	0	29	100%
	5	0	22	100%	0	31	100%
	6	0	36	100%	0	39	100%
	7	0	36	100%	0	43	100%
	8	0	26	100%	0	42	100%
	9	0	25	100%	0	22	100%
	10	0	31	100%	0	26	100%
	11	0	24	100%	0	31	100%
	12	0	32	100%	0	27	100%

	13	0	31	100%	0	24	100%
	14	0	26	100%	0	23	100%
	15	0	32	100%	0	38	100%
AMPA + Kainate	1	0	33	100%	0	14	100%
	2	42	0	0%	0	28	100%
	3	0	30	100%	0	29	100%
	4	0	25	100%	0	24	100%
	5	0	29	100%	0	28	100%
	6	24	0	0%	0	25	100%
	7	0	31	100%	0	23	100%
	8	0	26	100%	0	24	100%
	9	0	24	100%	0	24	100%
	10	0	24	100%	0	24	100%
	11	23	0	0%	0	37	100%
	12	0	28	100%	0	35	100%
	13	0	34	100%	0	27	100%
	14	0	27	100%	0	28	100%
	15	-	-	-	0	24	100%
NMDA + AMPA + Kainate	1	0	20	100%	0	24	100%
	2	0	26	100%	0	27	100%
	3	0	24	100%	0	26	100%
	4	0	32	100%	0	27	100%
	5	0	25	100%	0	27	100%

	6	0	31	100%	0	11	100%
	7	0	20	100%	0	26	100%
	8	0	19	100%	0	23	100%
	9	0	27	100%	0	27	100%
	10	0	24	100%	0	29	100%
	11	0	29	100%	0	21	100%
	12	0	31	100%	0	23	100%
	13	0	28	100%	0	16	100%
	14	0	26	100%	0	23	100%
	15	-	-	-	0	29	100%

Table 2-8. Annotation of up- and downregulated genes in response to the short day and MF-treated conditions in the ovary

Trinity_ID	Protein_ID	Short day/long day		MF-treated/long day		Description
		logFC	FDR	logFC	FDR	
Up-regulation						
c21172_g5_i3	Not available	8.76	0.0273	9.85	<0.001	No hits
c21682_g1_i5	Not available	7.51	0.0441	8.23	<0.001	No hits
c20517_g1_i4	JGI_V11_306849	7.36	<0.001	7.68	<0.001	Uncharacterized conserved protein. Contains ZZ-type Zn-finger.
c20663_g1_i12	Not available	5.94	0.0064	6.37	<0.001	No hits
c14897_g1_i1	JGI_V11_304685	5.91	0.0032	6.54	<0.001	Drebrins and related actin binding proteins
c19246_g4_i3	JGI_V11_272839	5.65	0.0099	6.75	<0.001	No hits
c15081_g1_i1	Not available	5.34	<0.001	6.42	<0.001	No hits
c20994_g1_i1	JGI_V11_243159	5.08	0.0306	5.79	<0.001	Predicted RNA-binding polyribonucleotide nucleotidyltransferase
c16934_g1_i2	JGI_V11_101079	5.00	0.0028	6.84	<0.001	No hits
c13610_g1_i1	JGI_V11_198492	4.72	0.0182	6.35	<0.001	Sulfate/bicarbonate/oxalate exchanger SAT-1 and related transporters (SLC26 family)
c22006_g1_i8	JGI_V11_302548	4.70	0.0304	6.11	<0.001	No hits

c21942_g1_i15	Not available	4.48	0.0357	4.4	0.0117	No hits
c19246_g2_i1	JGI_V11_220682	4.43	<0.001	6.08	<0.001	Clathrin assembly protein AP180 and related proteins. Contain ENTH domain.
c19246_g4_i4	JGI_V11_220682	4.30	0.0032	6.15	<0.001	Clathrin assembly protein AP180 and related proteins. Contain ENTH domain.
c21356_g1_i8	Not available	4.03	0.0019	4.95	<0.001	No hits
c20193_g3_i1	Not available	3.24	0.0091	4.81	<0.001	No hits
c18773_g4_i7	JGI_V11_222984	2.46	0.0130	3.29	<0.001	ER-Golgi vesicle-tethering protein p115
Down-regulation						
c16351_g1_i1	JGI_V11_223021	-1.77	0.0206	-3.4	<0.001	No hits
c20771_g1_i10	Not available	-2.66	<0.001	-3.61	<0.001	No hits
c21175_g1_i12	Not available	-6.24	0.0125	-11.34	<0.001	No hits
c21175_g1_i10	Not available	-8.16	0.0019	-8.42	<0.001	No hits

Table 2-9. Annotation of up- and downregulated genes in response to the short day and MF-treated conditions in the whole body

Trinity_ID	Protein_ID	SD/LD		MF/LD		Description
		logFC	FDR	logFC	FDR	
Up-regulated						
c19940_g1_i1	JGI_V11_319910	9.06	0.0029	6.63	0.0361	Ubiquitin thiolesterase. Ubiquitin-specific protease
c20826_g1_i9	JGI_V11_309160	7.99	<0.001	7.38	<0.001	No hits
c15642_g1_i3	Not available	7.83	<0.001	6.27	<0.001	No hits
c19624_g1_i3	JGI_V11_303856	7.69	<0.001	8.84	<0.001	Low-density lipoprotein receptors containing Ca2+-binding EGF-like domains
c21920_g6_i4	JGI_V11_303168	7.32	0.0293	6.79	0.0206	Adaptor protein PACSIN
c20715_g2_i3	JGI_V11_318320	6.33	<0.001	5.56	<0.001	Low-density lipoprotein receptors containing Ca2+-binding EGF-like domains
c20715_g2_i4	JGI_V11_318320	5.88	<0.001	5.11	<0.001	Low-density lipoprotein receptors containing Ca2+-binding EGF-like domains
c20715_g2_i5	Not available	5.69	<0.001	4.66	<0.001	No hits
c19048_g3_i2	JGI_V11_244715	5.24	0.0011	3.46	0.0123	No hits
c21157_g1_i2	Not available	4.88	0.0346	4.83	0.0156	No hits
c20975_g3_i3	JGI_V11_325159	4.62	0.0100	4.62	0.0021	Uncharacterized conserved protein
c21302_g1_i15	Not available	4.52	<0.001	4.68	<0.001	No hits
c20715_g1_i13	Not available	4.42	0.0011	3.35	0.0017	No hits
c20715_g1_i10	Not available	4.18	<0.001	5.42	<0.001	No hits
c22033_g1_i5	JGI_V11_303190	4.09	0.0042	3.65	0.0044	Propionate--CoA ligase. Propanoate metabolism, Acyl-CoA synthetase

c17728_g1_i8	Not available	3.96	0.0431	3.41	0.0311	No hits
c19857_g1_i8	JGI_V11_300342	3.86	0.0011	2.48	0.0033	Rho-associated. Coiled-coil containing protein kinase.
c20715_g3_i2	JGI_V11_318319	3.78	0.0085	2.64	0.0465	Low-density lipoprotein receptors containing Ca2+-binding EGF-like domains
c20715_g1_i5	JGI_V11_318320	3.24	<0.001	4.15	<0.001	Low-density lipoprotein receptors containing Ca2+-binding EGF-like domains
c22055_g1_i8	JGI_V11_103181	2.99	0.0342	3.64	<0.001	Serine/threonine protein kinase and endoribonuclease ERN1/IRE1. Sensor of the unfolded protein response pathway
c20309_g1_i6	JGI_V11_308669	2.99	0.0022	3.46	<0.001	DNA-directed RNA polymerase subunit E'
c21345_g1_i3	Not available	2.50	0.0153	3.05	<0.001	No hits
c17718_g1_i1	JGI_V11_303858	2.40	0.0011	4.38	<0.001	Low-density lipoprotein receptors containing Ca2+-binding EGF-like domains
c13924_g1_i1	JGI_V11_327978	2.40	0.0028	2.69	<0.001	No hits
c20607_g1_i7	Not available	2.11	0.0201	2.05	0.0012	No hits
Down-regulated						
c19494_g2_i2	Not available	-1.66	0.0462	-4.45	<0.001	No hits
c17279_g1_i1	Not available	-1.99	0.0478	-3.02	<0.001	No hits
c19494_g2_i3	Not available	-2.22	0.0040	-3.69	<0.001	No hits
c20691_g4_i5	JGI_V11_110684	-2.27	0.0175	-5.09	<0.001	Isovaleryl-CoA dehydrogenase
c21100_g1_i2	JGI_V11_308059	-2.39	0.0028	-2.13	0.0026	No hits

c20664_g2_i1	JGI_V11_313736	-2.59	0.0015	-3.40	<0.001	Collagens (type IV and type XIII) and related proteins
c19574_g1_i5	JGI_V11_96311	-2.68	0.0267	-4.34	<0.001	Globins and related hemoproteins
c9466_g1_i1	Not available	-2.69	0.0025	-3.91	<0.001	No hits
c21238_g2_i16	Not available	-2.74	0.0077	-2.47	0.0030	No hits
c19574_g1_i3	JGI_V11_96311	-2.77	<0.001	-4.16	<0.001	Globins and related hemoproteins
c14663_g1_i1	JGI_V11_236051	-3.06	0.0020	-4.35	<0.001	No hits
c19467_g1_i2	Not available	-3.22	0.0166	-3.48	0.0016	No hits
c19572_g1_i1	JGI_V11_309090	-3.30	0.0408	-3.82	0.0013	Collagens (type IV and type XIII) and related proteins
c19922_g1_i1	JGI_V11_300138	-3.39	0.0208	-5.03	<0.001	No hits
c19179_g1_i1	JGI_V11_308992	-3.45	0.0385	-4.86	<0.001	No hits
c19574_g1_i2	JGI_V11_230332	-3.48	0.0074	-4.64	<0.001	Globins and related hemoproteins
c19574_g1_i1	JGI_V11_96311	-3.84	<0.001	-5.53	<0.001	Globins and related hemoproteins
c17220_g1_i9	Not available	-3.95	0.0015	-4.74	<0.001	No hits
c17060_g5_i3	JGI_V11_204061	-3.98	0.0273	-5.75	<0.001	Predicted methyltransferase
c19488_g2_i1	JGI_V11_331396	-4.00	0.0385	-4.80	0.0053	No hits
c17422_g1_i2	Not available	-4.02	<0.001	-7.29	<0.001	No hits
c19814_g1_i4	Not available	-4.14	0.0113	-5.26	<0.001	No hits
c16896_g1_i1	Not available	-4.18	0.0059	-4.49	<0.001	No hits
c21115_g1_i9	Not available	-4.44	0.0077	-4.63	<0.001	No hits
c20464_g2_i11	JGI_V11_314997	-4.66	0.0177	-4.57	0.0049	No hits
c19572_g4_i1	JGI_V11_309090	-4.67	<0.001	-5.70	<0.001	Collagens (type IV and type XIII) and related

						proteins
c19720_g5_i5	Not available	-4.70	0.0282	-7.51	<0.001	No hits
c21077_g1_i1	JGI_V11_224074	-4.74	0.0074	-6.29	<0.001	Chitinase
c16088_g3_i6	Not available	-4.76	0.0032	-6.72	<0.001	No hits
c21857_g2_i9	Not available	-5.04	<0.001	-5.13	<0.001	No hits
c19488_g3_i1	JGI_V11_302196	-5.10	0.0173	-5.54	0.0099	No hits
c19880_g2_i2	Not available	-5.11	0.0046	-6.13	<0.001	No hits
c16088_g3_i4	Not available	-5.24	0.0060	-5.98	<0.001	No hits
c12359_g1_i1	JGI_V11_315116	-5.37	0.0028	-10.19	<0.001	No hits
c19179_g4_i1	JGI_V11_237265	-5.61	0.0459	-9.73	<0.001	C-type lectin
c17830_g1_i1	JGI_V11_235069	-5.66	<0.001	-5.94	<0.001	Microtubule-associated proteins
c20664_g2_i3	JGI_V11_216236	-5.76	<0.001	-5.08	<0.001	No hits
c21285_g6_i1	JGI_V11_320659	-5.92	0.0052	-8.33	<0.001	Serine endopeptidases. Trypsin
c21671_g2_i1	JGI_V11_307923	-6.00	0.0011	-7.67	<0.001	No hits
c2924_g1_i1	JGI_V11_224357	-6.00	0.0028	-6.30	<0.001	No hits
c16636_g1_i2	Not available	-6.22	<0.001	-10.81	<0.001	No hits
c19915_g1_i1	JGI_V11_238835	-6.26	0.0015	-6.05	<0.001	Chitinase
c18138_g2_i1	JGI_V11_239781	-6.26	<0.001	-9.44	<0.001	No hits
c21285_g1_i2	JGI_V11_320659	-6.50	0.0052	-8.70	<0.001	Serine endopeptidases. Trypsin
c17684_g3_i2	JGI_V11_312323	-6.79	0.0014	-10.91	<0.001	Cysteine proteinase Cathepsin L
c17684_g1_i4	JGI_V11_312323	-6.80	0.0164	-10.10	<0.001	Cysteine proteinase Cathepsin L
c18138_g1_i2	Not available	-6.90	0.0086	-8.98	<0.001	No hits
c14516_g1_i1	JGI_V11_306621	-6.99	0.0013	-10.42	<0.001	β-1,6-N-acetylglucosaminyltransferase. Contains

						WSC domain.
c28623_g1_i1	JGI_V11_302599	-7.11	<0.001	-10.02	<0.001	No hits
c20664_g2_i4	JGI_V11_216236	-7.11	<0.001	-9.94	<0.001	No hits
c14729_g1_i3	Not available	-7.28	0.0011	-5.18	0.0021	No hits
c13211_g1_i2	JGI_V11_309301	-7.36	0.0031	-7.17	<0.001	No hits
c20664_g2_i2	JGI_V11_216236	-7.40	<0.001	-8.83	<0.001	No hits
c21285_g4_i1	Not available	-7.42	<0.001	-9.22	<0.001	No hits
c21202_g1_i1	JGI_V11_301647	-7.53	<0.001	-7.92	<0.001	FOG: Low-complexity
c17043_g1_i1	JGI_V11_224885	-7.71	0.0252	-9.79	0.0016	Neurexin IV
c21285_g7_i1	JGI_V11_225480	-7.73	<0.001	-8.92	<0.001	Chymotrypsin C. Trypsin
c15952_g1_i2	JGI_V11_309075	-7.75	<0.001	-12.21	<0.001	No hits
c7221_g1_i1	JGI_V11_312322	-7.89	0.0028	-7.31	<0.001	Cysteine proteinase. Cathepsin L.
c19048_g1_i14	JGI_V11_225026	-7.93	0.0103	-9.09	<0.001	Trypsin
c21285_g5_i3	Not available	-8.14	<0.001	-5.76	0.0013	No hits
c19048_g1_i9	JGI_V11_244721	-8.89	0.0014	-12.71	<0.001	Trypsin
c21202_g1_i2	JGI_V11_301647	-9.03	<0.001	-9.24	<0.001	FOG: Low-complexity
c13438_g1_i1	JGI_V11_43928	-9.24	0.0373	-6.85	0.0217	Trypsin
c21736_g1_i7	JGI_V11_101703	-9.26	0.0273	-9.15	0.0054	Cytoskeleton-associated protein and related proteins
c16746_g1_i1	JGI_V11_112082	-9.53	0.0373	-9.42	0.0077	No hits
c1435_g1_i1	JGI_V11_312323	-9.77	0.0035	-9.66	<0.001	Cysteine proteinase. Cathepsin L.
c19697_g2_i1	JGI_V11_236108	-9.88	<0.001	-8.81	<0.001	Trypsin
c19697_g2_i2	JGI_V11_236108	-9.94	<0.001	-14.05	<0.001	Trypsin

c15952_g1_i1	JGI_V11_309075	-9.98	<0.001	-12.89	<0.001	No hits
c14516_g1_i2	JGI_V11_306621	-10.06	<0.001	-7.68	<0.001	β-1,6-N-acetylglucosaminyltransferase. Contains WSC domain.
c17268_g2_i6	JGI_V11_191625	-10.22	<0.001	-6.46	<0.001	Phytoene desaturase
c19697_g1_i1	JGI_V11_236105	-10.36	<0.001	-10.02	<0.001	Serine endopeptidases. Trypsin
c19048_g1_i10	Not available	-10.37	<0.001	-7.71	0.0015	No hits
c19048_g1_i5	JGI_V11_244721	-10.63	0.0047	-10.51	<0.001	Trypsin
c19048_g1_i13	Not available	-11.25	0.0018	-11.13	<0.001	No hits
c19880_g2_i12	JGI_V11_225495	-12.83	<0.001	-12.79	<0.001	Serine endopeptidases. Trypsin

Figure 2-1. Experimental design of RNA-seq analysis. Upper part shows an illustration of the reproductive cycle in *D. pulex* WTN6 strain and sampling method for RNA-seq. The space between dotted lines indicates the JH-sensitive period for male offspring production by exogenous MF treatment (40-60 h after ovulation). At 50 h after ovulation, all daphnids were sacrificed and prepared as two kinds of samples; the ovary and whole body (A). Bar graph indicates the proportion of male-producing mothers by photoperiod changes and exogenous MF administration (B).

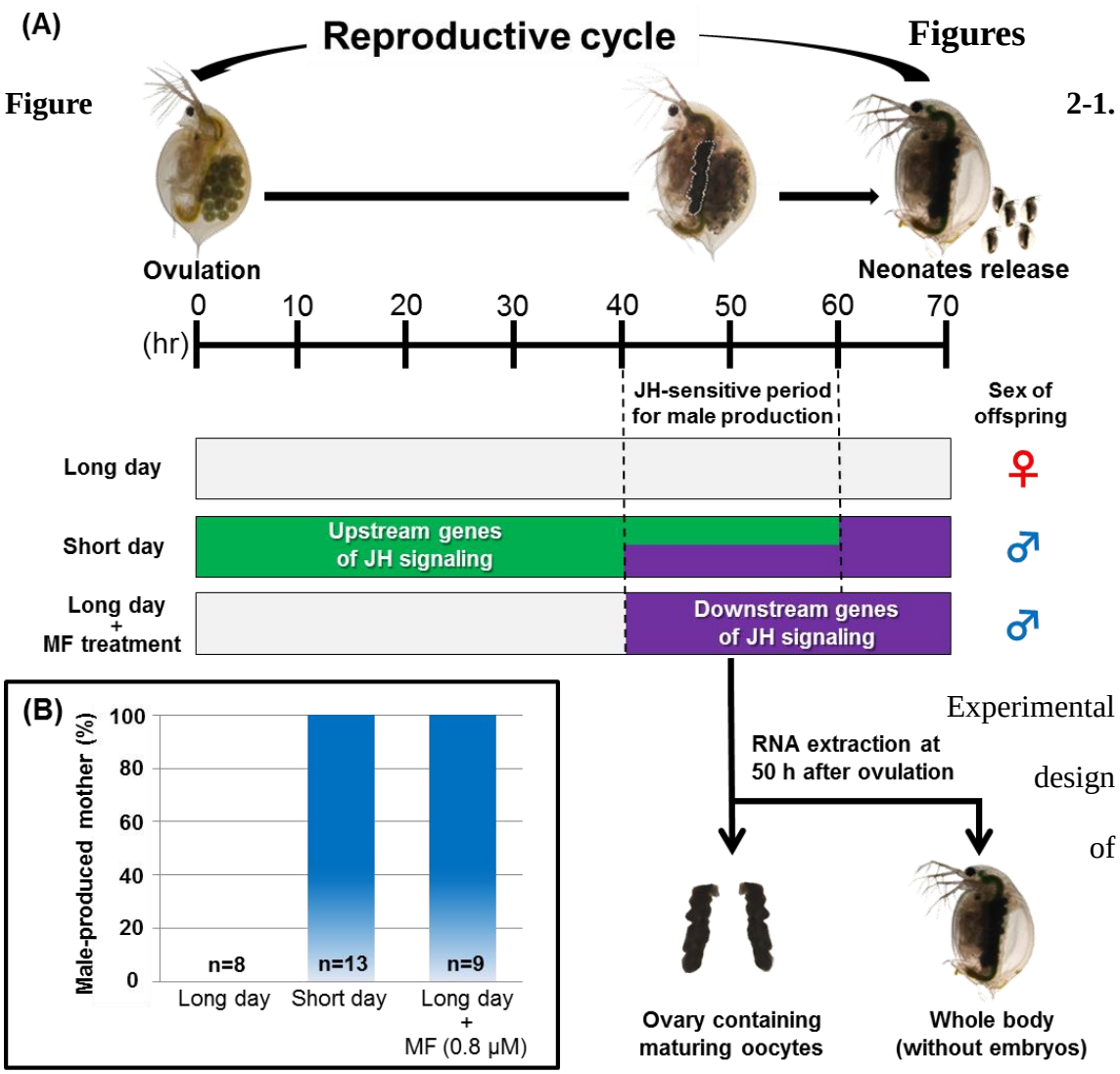

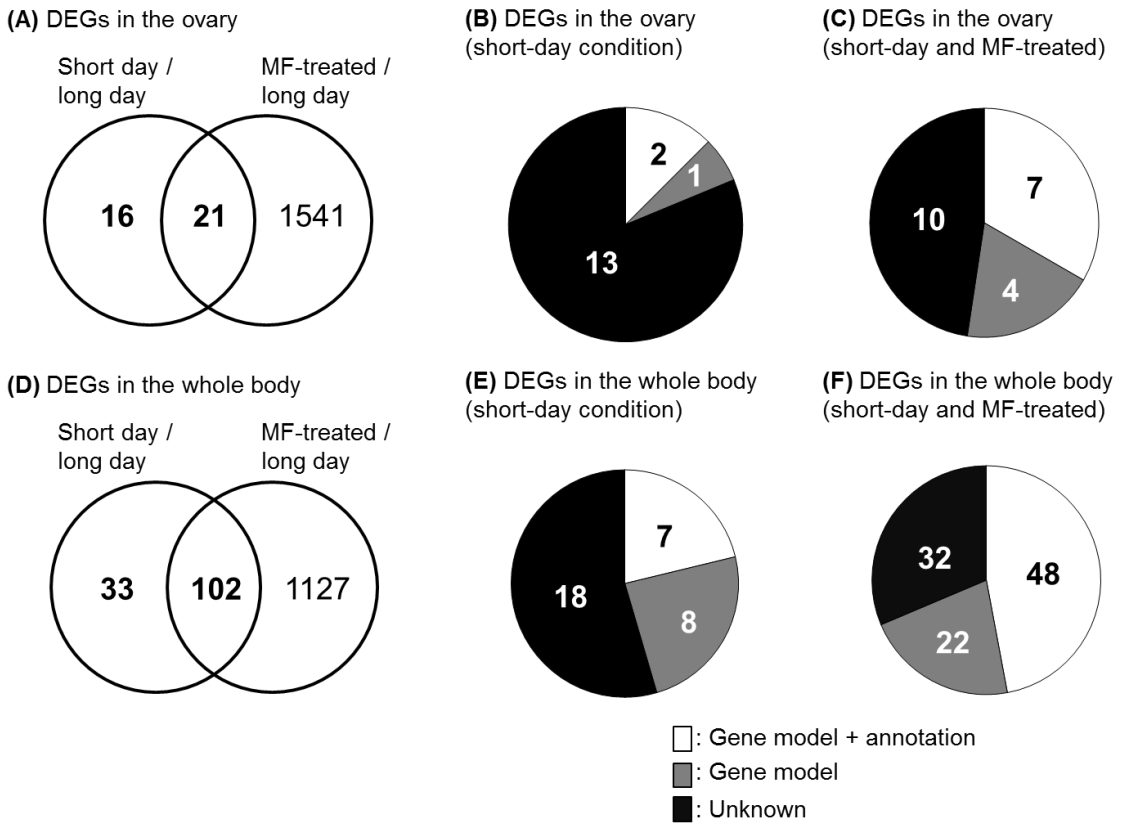

Figure 2-2. DEGs in the ovary and whole body. Venn diagrams show the number of DEGs between *D. pulex* WTN6 strain reared under the long-day and short-day conditions, and long-day and MF-treated conditions in the ovary (A) and whole body (D), respectively (FDR < 0.05). Pie graphs show the proportion of DEGs in response to the short-day condition in the ovary (C) and whole body (F), and in response to both the short-day and MF-treated conditions in the ovary (B) and whole body (E), respectively. White, grey and black colors indicate the genes bearing putative transcript model and annotation, only putative transcript model, and no information, respectively.

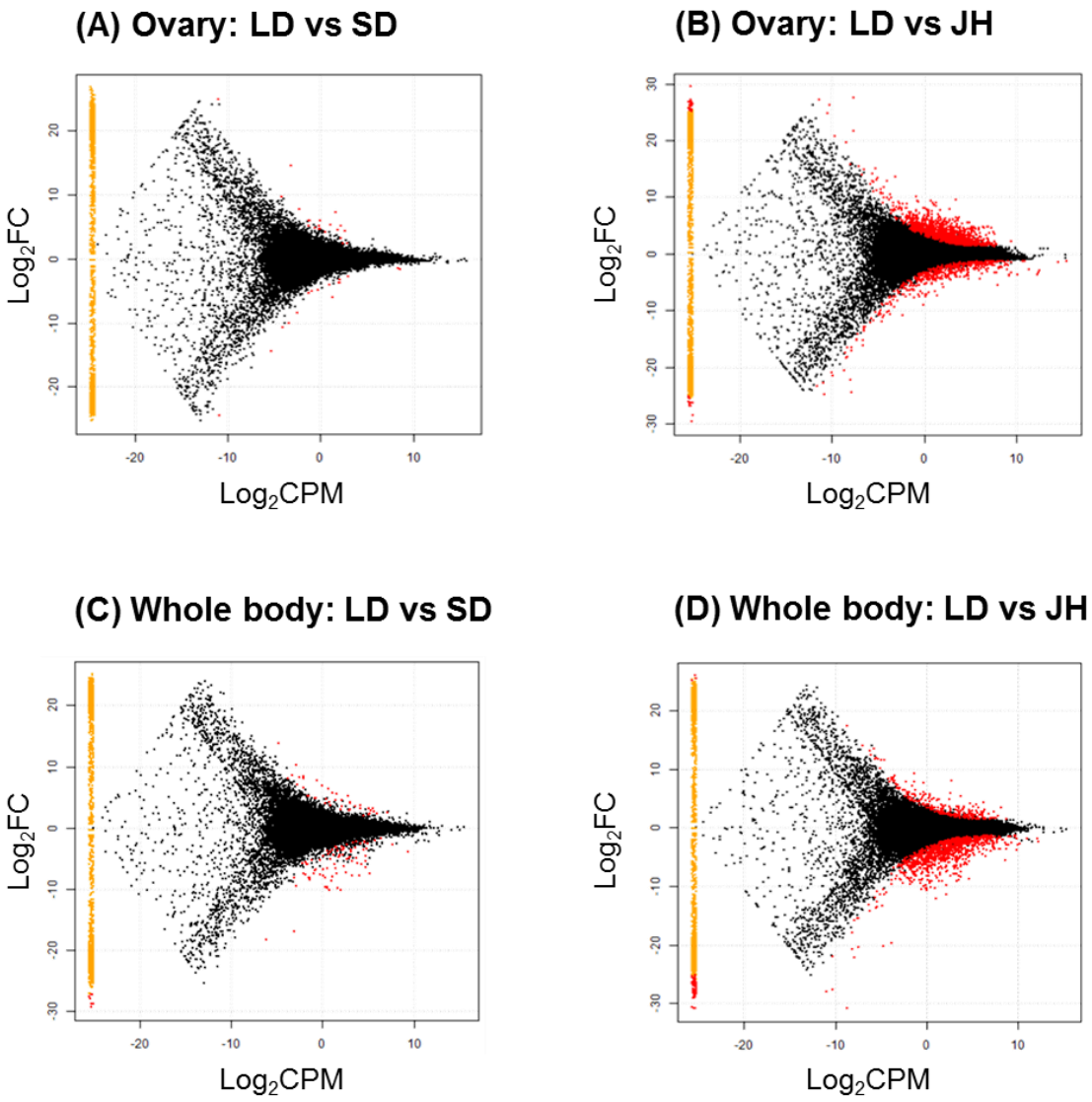

Figure 2-3. MA plots for each comparison. These plots show the tagwise log fold change (FC) against the log counts per million (CPM) for each gene in the ovary and whole body libraries. Each dot on the graph represents an individual gene. All red points show DEGs with a FDR < 0.05, and all black dots are genes that were not significantly differentially expressed. LD and SD indicate the long-day and short-day conditions.

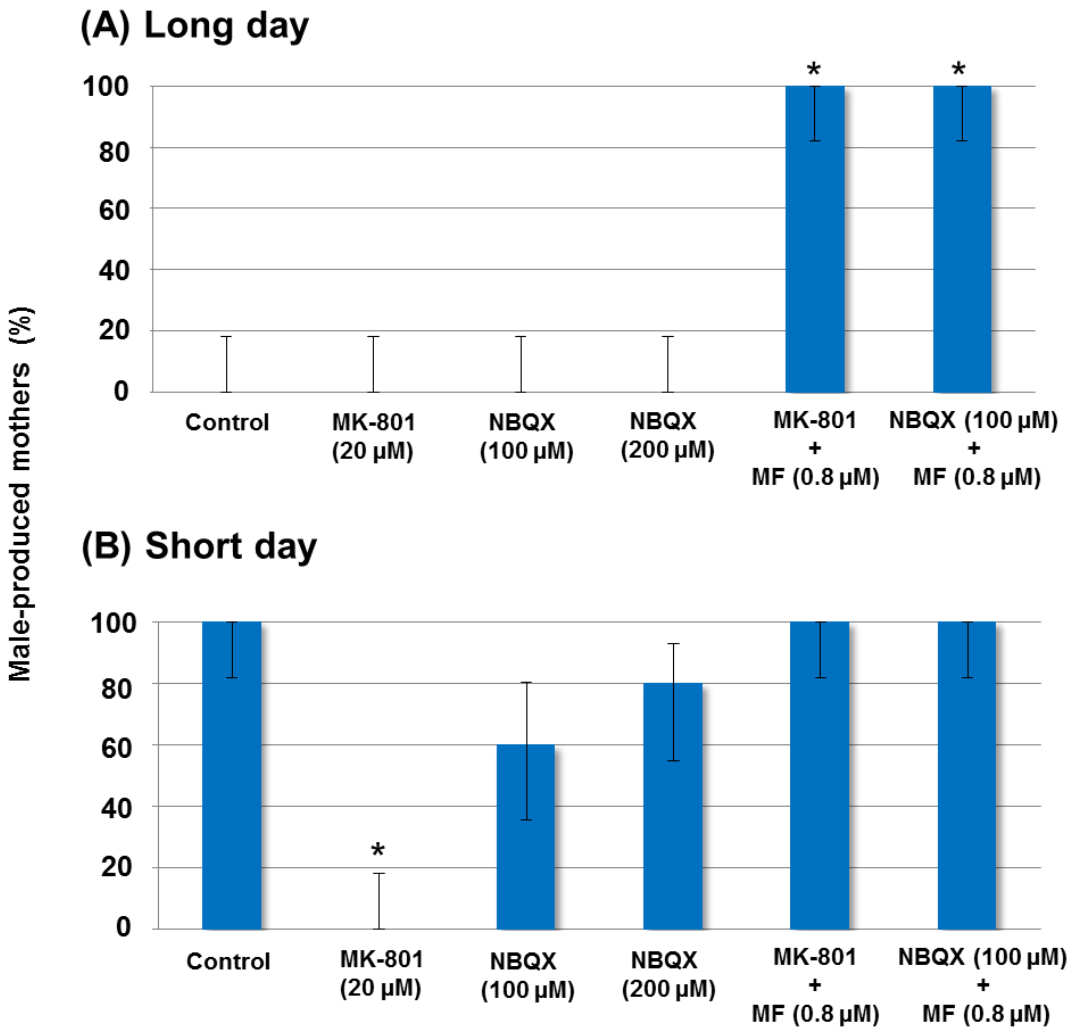

Figure 2-4. Effects of antagonists of ionotropic glutamate receptors (MK-801 and NBQX) on the inducibility of male offspring by mothers. Upper and lower panels show the effect of these antagonists on *D. pulex* reared under the (A) long-day and (B) short-day conditions, respectively. Vertical values indicate the proportion of male-producing mothers (n = 15). Bars indicate the 95 % confidence interval. The asterisks indicate significant differences compared to respective controls (Fisher's exact probability test with Holm's correction, $p<0.01$). Concentrations of MF and antagonists used are as follows: MF (0.8 μM), MK-801 (20 μM), and NBQX (100 and 200 μM).

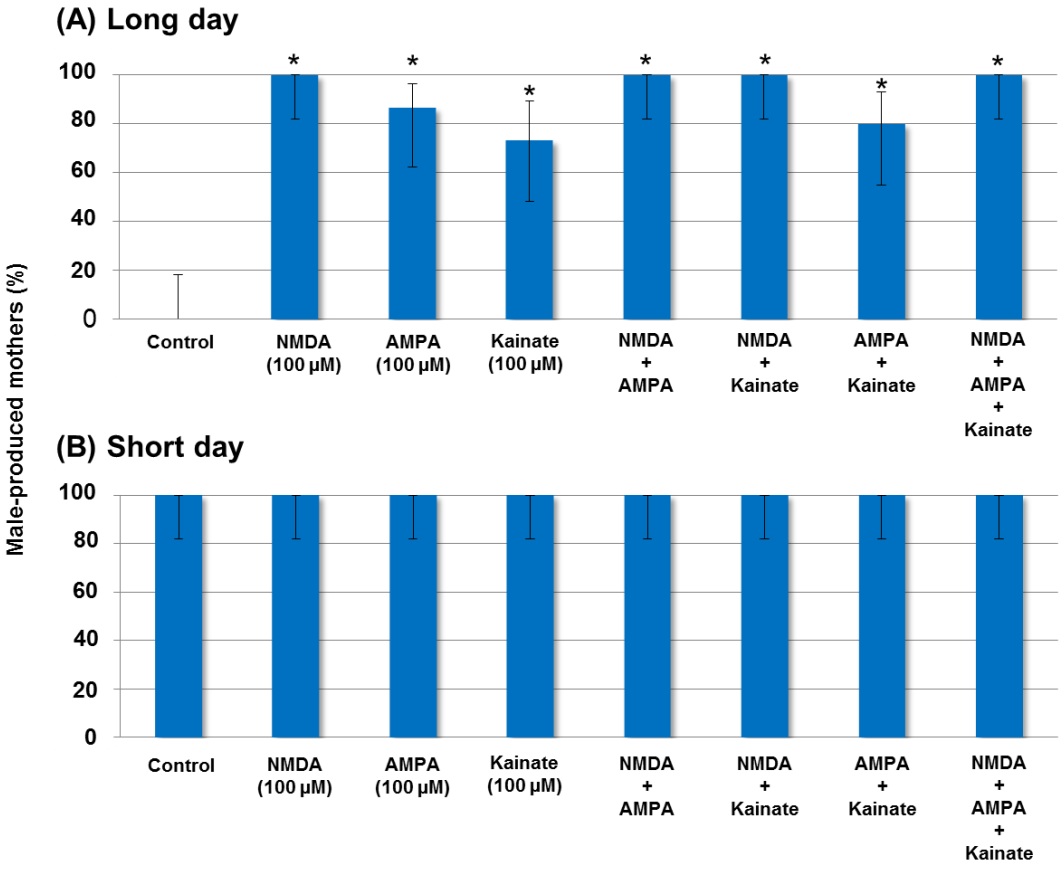

Figure 2-5. Effects of agonists of ionotropic glutamate receptors (NMDA, AMPA and Kainate) on the inducibility of male offspring by mothers. Upper and lower panels show the effect of agonists on the *D. pulex* reared under the (A) long-day and (B) short-day conditions, respectively. Vertical values indicate the proportion of male-producing mothers (n = 15). Bars indicate the 95% confidence interval. Asterisks indicate significant differences compared to respective controls (Fisher's exact probability test with Holm's correction, $p<0.01$). Concentrations of MF and agonists used are as follows: MF (0.8 μM), NMDA, AMPA and Kainate (100 μM, respectively).

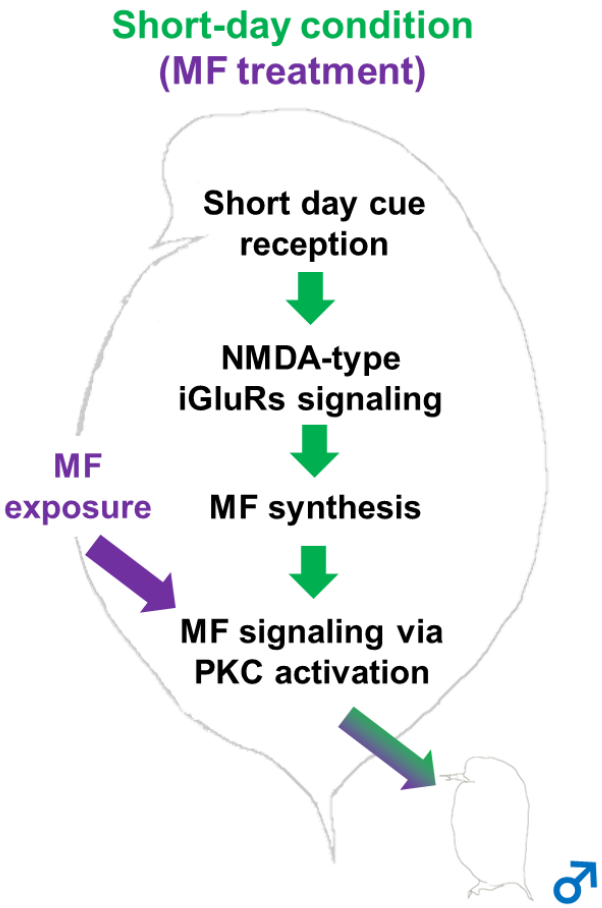

Figure 2-6. A model for the function of NMDA receptors and PKC signaling in the JH signaling pathway for male production of *D. pulex* in response to the short-day and MF-treated conditions.

Chapter III

Molecular impact of juvenile hormone agonists on neonatal *Daphnia magna*

Abstract

Daphnia magna has been used extensively to evaluate organism and population level responses to pollutants in acute toxicity and reproductive toxicity tests. Our group has previously reported that exposure to JH agonists results in a reduction of reproductive function and production of male offspring in a cyclic parthenogenesis. Recent advances in molecular techniques have provided tools to better understand the responses to pollutants in aquatic organisms including *D. magna*. DNA microarray was used to evaluate gene expression profiles of neonatal daphnids exposed to JH agonists; methoprene (125, 250 and 500 ppb), fenoxycarb (0.5, 1 and 2 ppb), and epofenonane (50, 100 and 200 ppb). Exposure to these JH analogs resulted in chemical specific patterns of gene expression. The heat map analyses based on hierarchical clustering revealed a similar pattern between treatments with a high dose of methoprene and with epofenonane. In contrast, treatment with low to middle doses of methoprene resulted in similar profiles to fenoxycarb treatments. Hemoglobin and JHEH genes clustered to be JH-responsive genes. These data suggest that fenoxycarb has high activity as a JH agonist, methoprene shows high toxicity and epofenonane works through a different mechanism compared with other JH analogs, agreeing with data of previously reported toxicity tests. In conclusion, *D. magna* DNA microarray is useful for classification of JH analogs and identification of JH-responsive genes.

Introduction

The Cladoceran crustacean *D. magna* has been used extensively to evaluate organism and population based responses of invertebrates to pollutants. In the field, daphnids are widely distributed and are important as a basic link in the food chain. Like other aquatic organisms, they are constitutively exposed to multiple chemicals and it is thought that they are sensitive to environmental chemicals. In the laboratory, *D. magna* is easy to maintain and manipulate because of its short generation time, and thus, has been used as a model organism in the Organization for Economic Co-operation and Development (OECD, 1998, 2004). Based on standard and other related toxicological tests, data on the effect of a large number of chemicals on daphnids has been accumulated (Liess and Ohe, 2005). However, the accumulated data are mainly related to effective concentrations and there is very limited information as yet as to the mode of action.

In order to understand the effect of chemicals on an organism, it is important to elucidate the specific mode of action of the toxic effects. Recent progress in genomics is expected to be useful for the understanding of these modes of action, and this field of study has been named “toxicogenomics”, which facilitate understanding of the relationship between chemical exposure and adverse effects; identification of useful biomarkers of exposure to toxic substances; and elucidation of the molecular mechanisms of toxicity (Waters et al., 2003; Waters and Fostel, 2004). In general, cells respond to chemical stresses, and then a phenotype emerges. Thus, the toxicogenomic approach can be expected to provide multiple clues for understanding the molecular pathways that result in the phenotypic changes which occur in response to chemicals, because the same pathways are not always affected. The application of toxicogenomics

to ecotoxicology has been termed “ecotoxicogenomics” (Iguchi et al., 2006; Snapea et al., 2004).

The application of the ecotoxicogenomic approach to *D. magna* has the potential to increase our knowledge and understanding of ecotoxicity, since the current mechanistic understanding of chemical toxicity in invertebrates is rather limited, and useful biomarkers have not been identified. Recently, our group has established an ecotoxicogenomic assessment of *D. magna* (Watanabe et al., 2007; Watanabe et al., 2005). Although other groups also have reported the usefulness of *D. magna* gene expression analysis as an ecotoxicogenomic approach (Cannon et al., 2008; Poynton et al., 2007; Soetaert et al., 2006; Soetaert et al., 2007a; Soetaert et al., 2007b), the number of genes on the arrays have been rather limited. Our group has increased the number of genes, and modified the designs on the microarray (Watanabe et al., 2008).

D. magna is known to switch between sexual and asexual reproduction depending on the environmental conditions. Generally, they reproduce asexually when they have sufficient food and an appropriate photoperiod along with proper population density. Once the environmental conditions decline as the result of a shortening of the photoperiod, a lack of food, and/or an increase in population density, they changes reproductive strategy and begins to produce males, which allows sexual reproduction. The egg generated by mating is called the resting egg which can survive for a long period even in the absence of water. This form of ESD is well known and it is considered to be a robust system for maintaining the species (Stross and Hill, 1965).

Recent studies have focused on morphological development and sex ratio in the testing of chemicals in *D. magna*. Changes in sex ratio of offspring have been reported in *D. pulicaria* populations exposed to atrazine (Dodson et al., 1999). MF has

been demonstrated to be an inducer of male offspring in *D. magna* (Olmstead and LeBlanc, 2002). Our research group also has demonstrated that induction of male offspring in *D. magna* by exposure of JHs, MF, JH III and their analogs, methoprene, pyriproxyfen and fenoxycarb at lower concentrations, and also production of 100% males by pyriproxyfen and fenoxycarb (Tatarazako et al., 2003). Our group also have demonstrated that JH I, JH II and the JH mimicking insecticides, kinoprene, hydroprene, epofenonane or fenoxycarb induce male offspring and reduce reproduction in *D. magna* (Oda et al., 2005a). Even in *D. magna*, genetic differences in induction of male neonates by JH agonist are present (Oda et al., 2006). JHs and their analogs result in the production of male neonates in a concentration-dependent manner in four different species of Cladoceran, including *Moina. macrocopa*, *M. micrura*, *Ceriodaphnia. dubia* and *C. reticulata.* In these four species, fenoxycarb could induce male neonates and reduce rates of reproduction (Oda et al., 2005b). Tatarazako and Oda (2007) compared the potency of four JHs and 6 insect growth regulators (JH agonists) in the induction of male neonates using NIES strain of *D. magna* and demonstrated that all JHs and these agonists induced male neonate production and reduction of reproduction, except for epofenonane which induced male neonate production with a small reduction in reproductive rate. Exposure to chlordane (Manar et al., 2009) and endosulfan sulfate (Palma et al., 2009) has been reported to induce male offspring and developmental abnormalities in *D. magna*. Ignace et al. (2011) also has reported male production by toxaphene in *D. magna*.

In chapter III, I examine JH-responsive genes and toxicity-related genes in newborn daphnids exposed three JH agonists, fenoxycarb, methoprene and epofenonane to neonate (less than 24 hours after release from mother).

Materials and Methods

Daphnia strain and culture conditions

The *D. magna* strain (NIES clone) was obtained from the National Institute for Environmental Studies (NIES; Tsukuba, Japan) (Tatarazako et al., 2003). The strain originated from the Environmental Protection Agency (USA) and was maintained for more than 15 years at NIES. Culture medium was prepared using charcoal-filtered tap water maintained at room temperature overnight prior to use. Cultures of 20 individuals per liter were incubated at 21 ± 1°C under a 14-h light/10-h dark photoperiod. A 0.01-ml suspension of 4.3 x 10^8 cells ml^{-1} *C. vulgaris* was added daily to each culture. The water hardness was between 72 and 83 mg L^{-1}, the pH between 7.0 and 7.5, and the dissolved oxygen concentration between 80 and 99%.

Chemicals and concentrations

Based on previous studies (Oda et al., 2005a; Tatarazako and Oda, 2007; Tatarazako et al., 2003), I selected three chemicals as JH agonists, fenoxycarb, methoprene and epofenonane. Chemical structures of these JH agonists are shown in **Figure 3-1**. I chose these agonists because fenoxycarb induced male induction at low concentration, methoprene showed high toxicity and male induction, and epofenonane showed very low toxicity and high male induction capacity. Fenoxycarb (technical grade 96.6% pure) and methoprene (98.0% pure), were obtained from Wako Pure Chemical Industries Led. (Osaka, Japan). Epofenonane (95.0% pure) was obtained from Fluka BioChemika (Buchs, Swizerland).

Experiments were conducted at the nominal concentrations of 0.5, 1 and 2 ppb for fenoxycarb, 125, 250 and 500 ppb for methoprene, and 50, 100 and 200 ppb for

epofenonane dissolved in DMF (analytical grade, WAKO, Osaka, Japan), based on the LOEC values for reduction in reproduction rate and induction of male neonates in the former studies (Tatarazako and Oda, 2007). Solvent concentration in all test solutions was less than 0.01% v/v.

Sample preparation

Experiments were conducted on the basis of the "*Daphnia magna* reproduction test", as described in the test guideline 211 of the OECD (OECD, 1998). Eight newborn animals released from the mother for less than 24 h old were cultured in 100 ml of water with or without JH agonists for 24 h. At least 20 individuals were used for one set of samples for each chemical concentration and controls. Harvested daphnids were briefly washed and homogenized using the physcotron NS-310E (Nichion, Tokyo, Japan). Total RNA was purified with TRIZOL reagent (Invitrogen, Tokyo, Japan), and purified using the RNeasy Micro Kit (Qiagen, Valencia, CA, USA) according to the manufacturer's protocols. The quality of total RNA was analyzed using the Agilent 2100 Bioanalyzer (Agilent Technologies, Santa Clara, CA, USA). RIN values are shown in **Table 3-1**. Three experiments were conducted independently (biological triplicates).

***Daphnia magna* oligonucleotide microarray**

Custom 44k oligonucleotide arrays representing ~11k transcripts were produced by Agilent Technologies (Agilent Technologies, Santa Clara, CA, eARRAY Design ID: 020-586). A custom daphnia oligo-microarray was designed starting from the EST database containing ~11k transcripts (Watanabe et al., 2005). Four probes were generally designed per sequence and the oligonucleotides (60 mers) were selected using

the Agilent web design application (http://earray.chem.agilent.com/earray). A 4×44 k oligo-microarray format was chosen according to the number of unique sequences identified, and therefore four replicates of each probe per microarray and four microarrays were fitted on each slide. Probes were placed in a random layout using the Agilent methodology. The probes were uploaded and the oligo-microarray ordered via the Agilent web design application (http://earray.chem.agilent.com/earray). Details of the platform design of the *D. magna* microarray and raw intensity values for each microarray are available at Gene Expression Omnibus (GEO) (http://www.ncbi.nlm.nih.gov/geo/) with accession number GPL17297, series GSE47990.

Microarray hybridization

500 ng of total RNA were prepared for microarray hybridization using the Quick Amp Labeling Kit and One-color RNA Spike-in kit (Agilent Technologies), and purified using the RNeasy Micro Kit (Qiagen) following the manufacturer's protocol. The quality of Cyanine3-labeled complementary RNA (cRNA) was analyzed using the Agilent 2100 Bioanalyzer (Agilent Technologies). 165 μg of Cyanine3-labeled cRNA were hybridized to the custom 4x44k *D. magna* microarray using the protocols of Agilent Technologies. After 17 h incubation with rotation, the microarrays were washed with Gene Expression Wash Buffer Kit (Agilent Technologies) according to the manufacturer's protocols. DNA microarrays were scanned using a GenePix 4000B scanner (Molecular Devices, Sunnyvale, CA, USA) at 5 μm resolution. The signal intensity of the spots was digitized using the microarray imager software (Combimatrix Molecular Diagnostics, Irvine, CA, USA).

Identification of candidate DEGs

Gene expression and statistical analyses were performed using the Subio Platform (Subio Inc. Nagoya, Japan). Data files generated by the Agilent Feature Extraction Software were imported into Subio Platform. The digitized raw data were normalized by the mean value of all spots of signal intensity in each array. Signal intensities (gProcessedSignal) were normalized by 75th percentile, and transformed into log ratios (base 2) against the averages of un-treated samples. I merged triplicates of each experimental condition and applied statistical analysis on the averages. I removed 15,408 probes with too low signals, which gIsWellAboveBG values are 0 in 2 out of 3 replicates in all experimental conditions, and 13,844 unvarying probes, which mean log ratios are between -0.5 and 0.5 in all groups. As a result, 10,938 probes remained and these were used for further analysis. Subsequently, these data were assessed by *t*-test ($p < 0.05$) to identify DEGs between treatment groups. The *q*-value is a measure of significance in terms of FDR. For all our analyses, q-values were estimated with the 'qvalue' Bioconductor package in the statistical programming environment R (Gentleman et al., 2004).

Gene ontology assignment

For GO classification (Conesa et al., 2005), DEGs determined by the microarray analysis were further analyzed using Blast2GO software v2.5.1 (http://blast2go.org). The following steps were performed to annotate the sequences: (1) BLAST using the NCBI nr database (All non-redundant GenBank CDS translations + PDB + SwissProt + PIR + PRF) with an e-value cut-off of 1e-3. (2) Mapping where Accessions retrieved through BLAST were used to search the GO database to identify GO terms. (3) Annotation where GO terms were selected from the GO term pool

obtained in the mapping step based on an Annotation Score. In this step, the annotation configuration was set to the following parameters: pre e-value filter: $1e^{-3}$, annotation cut off: 55 and GO-weight: 5. (4) Enzyme code annotation was performed through the Go-database. (5) The KEGG pathway annotation was also conducted.

Results

Gene expression of newborns in response to JH analogs

DNA microarray analysis was performed among 10 experimental groups: neonates exposed to DMF (0.01% v/v) as a solvent control, methoprene (125, 250 and 500 ppb), fenoxycarb (0.5, 1 and 2 ppb), and epofenonane (50, 100 and 200 ppb). The aim of this study was to overview the JH-responsive genes among JH analogs with differing physiological and toxicological actions. Transcriptome in neonates exposed to each JH analog at three concentrations, respectively, and solvent control were also analyzed by microarray analysis.

The numbers of DEGs compared with solvent control were 510 for neonates exposed to methoprene 125 ppb (320 upregulated and 190 downregulated), 489 for 250 ppb (239 upregulated and 250 downregulated), 658 for 500 ppb (279 upregulated and 379 downregulated), 185 for neonates exposed to fenoxycarb 0.5 ppb (157 upregulated and 28 downregulated), 281 for 1 ppb (204 upregulated and 77 downregulated), 295 for 2 ppb (184 upregulated and 111 downregulated), 102 for neonates exposed to epofenonane 50 ppb (69 upregulated and 33 downregulated), 236 for 100 ppb (167 upregulated and 69 downregulated), and 600 for 200 ppb (230 upregulated and 370 downregulated **(Figure 3-2)**. The DEGs in each treatment are summarized in **Tables 3-2, 3-3, 3-4**. Moreover, the heat map analyses based on hierarchical clustering UPGMA (Unweighted Pair Group Method with Arithmetic mean, un-centered correlation) method revealed a similarity between treatments with methoprene at high dose and with epofenonane. In contrast, methoprene at low to middle doses resulted in similar profiles to fenoxycarb treatments **(Figure 3-2)**.

In addition, for the expression of a number of common genes, treatment with methoprene, fenoxycarb and epofenonane at three concentrations resulted in 33 upregulated and 70 downregulated in methoprene treatments, 124 upregulated and 7 downregulated in fenoxycarb treatments, and 22 upregulated and 6 downregulated in epofenonane treatments **(Tables 3-2, 3-3, 3-4)**. 33 upregulated common genes in methoprene treatments included JHEH, vitellogenin fused with superoxide dismutase and so on **(Table 3-2)**. 124 upregulated common genes in fenoxycarb treatments included hemoglobin-related genes, cuticle protein and so on **(Table 3-3)**. 22 upregulated common genes in epofenonane treatments included hemoglobin-related genes, cuticle protein, JHEH and so on **(Table 3-4)**.

I compared the gene expression at the highest concentrations of the three JH agonists. 11 genes encoding hemoglobin, JHEH, adipose specific protein and 4-aminobutyrate aminotransferase were commonly up-regulated **(Figure 3-3A)**, and 6 genes encoding sec14-like protein, negative elongation factor and pancreatic alpha-amylase were down-regulated **(Figure 3-3B)**.

Hemoglobin-related genes are JH-responsive in *Daphnia*

Hemoglobin genes are known as one of the representative JH-responsive (up-regulated) genes in daphnids (Eads. et al., 2008; Gorr et al., 2006). Fenoxycarb up-regulated 15 hemoglobin-related genes **(Table 3-3)**. Epofenonane up-regulated 8, 2, 3 genes at 50, 100 and 200 ppb, respectively **(Table 3-4)**. In contrast, methoprene at 125 ppb did not fluctuate expression of those genes, although concentration at 250 and 500 ppb up-regulated those of 2 and 10 genes, respectively **(Table 3-2)**. Interestingly, hemoglobin-related genes were down-regulated by methoprene at 125 and 250 ppb, and

epofenonane at 100 ppb.

Expression of other well-known JH-responsive genes involving the acute and chronic toxicity in *D. magna*

Although JH-responsive genes involving the acute toxicity in daphnids have not reported, a few JH-responsive genes encoding the serine protease and glutathione s-transferase has already identified in insects (Horst et al., 2007; Zou et al., 2011). Expression of most of glutathione s-transferase gene was not fluctuated by JH analogs. However, one gene was commonly up-regulated by both methoprene and epofenonane treatment **(Table 3-5)**. In addition, serine protease related genes showed chemical specific expression pattern. Most genes were down-regulated by methoprene, not changed by fenoxycarb and up-regulated by epofenonane **(Table 3-5)**.

On the other hands, JH-responsive genes involving the chronic (reproductive) toxicity in daphnids have been reported as cuticle and vitellogenin related genes (Kim et al., 2011). Most of cuticle related genes were upregulated by 250 ppb methoprene and 100 ppb epofenonane, although expression of those genes was down-regulated by 50 ppb fenoxycarb and 200ppb epofenonane. In addition, expression levels of cuticle related genes were not changed by methoprene at 125 and 500 ppb **(Table 3-5)**. Moreover, vitellogenin related genes, which are essential for the oocyte maturation and embryo development, showed dose-dependent expression pattern by methoprene treatment **(Table 3-5)**. Although **Table 3-5** showed that tendency of expression pattern of some candidates of JH-responsive elements, most of them showed no significant expression change.

Functional attributes of JH-responsive genes

To determine the biological process disturbed by three JH agonists treatment, Blast2GO was used to map differently expressed genes based on GO terms, and annotate genes in KEGG analysis. In genes commonly up-regulated by methoprene, a total of 12 genes were successfully assigned 27 biological process terms from the third level of the GO, and 5 were annotated with enzyme codes for KEGG analysis. The majority of the terms were for metabolic processes (63.0%), which included primary metabolism, macromolecule metabolism and so on. Other predominant biological process was related to localization (14.8%) and physiological processes (7.4%) that specify a reaction to external stimuli or stresses **(Figure 3-4A)**. In genes commonly up-regulated by epofenonane, a total of 15 genes were assigned to 36 biological process terms from the third level of the GO and 6 were annotated with enzyme codes for KEGG analysis. The predominant biological process was metabolic processes (66.7%), localization (11.1%) and physiological processes (5.6%) **(Figure 3-5A)**. In genes commonly up-regulated by fenoxycarb, a total of 38 genes were assigned 105 biological process terms from the third level of the GO and 6 were annotated with enzyme codes for KEGG analysis. The predominant biological process was metabolic processes (48.6%), localization (15.2%), physiological processes (11.4%) and developmental process (8.6%) **(Figure 3-6A)**.

Similarly, in genes commonly down-regulated by methoprene, a total of 50 genes were successfully assigned to 124 biological process terms from the third level of the GO and 9 were annotated with enzyme codes for KEGG analysis. The majority of the terms were metabolic processes (59.7%), which included primary metabolism, macromolecule metabolism and so on. Other predominant biological process was

related to localization (11.3%), multicellular organismal process (8.1%) and physiological processes (5.6%) that specify a reaction to external stimuli or stresses **(Figure 3-4B)**. In genes commonly down-regulated by epofenonane and fenoxycarb, a total of 4 and 5 genes were successfully assigned 28 and 8 biological process terms from the third level of the GO, respectively **(Figures 3-5B, 3-6B)**, and 5 genes in fenoxycarb treatments were annotated with enzyme codes for KEGG analysis. The KEGG pathway list involved for the three chemicals is shown in **Table 3-6**. Interestingly, GO terms involved in reproduction were assigned in up-regulation by epofenonane (reproductive process, multicellular organism reproduction and sexual reproduction), and down-regulation by methoprene (reproductive process, multicellular organism reproduction, sexual reproduction and viral reproductive process) (data not shown).

Discussion

I conducted studies using newly developed *D. magna* DNA microarray to investigate the transcriptome in the response of daphnids to three JH agonists. The microarray technologies have been successfully used to identify genes responding to JH analogs in several insects, for which there are an abundant amount of sequence information (Willis et al., 2010; Zhu et al., 2010; Zou et al., 2013). This study revealed that the gene response provides insight into the biological and potentially toxicological responses to JH analogs, which are endocrine disrupting chemicals for daphnids.

Previous studies (Oda et al., 2007; Oda et al., 2005b; Tatarazako et al., 2003) demonstrated that fenoxycarb reduces reproduction and induces male neonates even at the lowest concentration (0.5 ppb), methoprene was toxic at higher concentrations (250 and 500 ppb) and induced male offspring at the highest concentration (500 ppb), and epofenonane did not affect the reproduction at 100 ppb, but only induced a slight reduction at the highest concentration (200 ppb). Epofenonane induced male neonates even at the lowest concentration (50 ppb). I exposed newborn daphnids to the same concentrations of each chemical to in the present experiment as used in the previous studies (Oda et al., 2005b; Tatarazako et al., 2003).

I focused on hemoglobin-related genes, which are a representative JH-responsive gene cluster and are highly diverged in daphnids (Colbourne et al., 2011). In addition, a previous study indicated that the promoter region of hemoglobin gene has candidate JH receptor binding *cis*-element (Gorr et al., 2006). Although hemoglobin-related genes have known to be up-regulated by MF treatment (Eads et al., 2008), some subtypes of them seem to have been down-regulated in juveniles of *D. pulex* by MF administration (Miyakawa et al., unpublished data). Similarly, in this study,

some hemoglobin-related genes are down-regulated by methoprene at 125 and 250 ppb, and epofenonane at 100 ppb. Although exposure of 500 ppb methoprene to daphnids showed a great reduction of the number of offspring and high mortality, the methoprene concentration necessary to induce male production is more than 500 ppb (Tatarazako et al., 2003). It is suggested that methoprene has high toxicity more than JH actions **(Figure 3-7)**. For most JH analogs, moreover, physiological roles are not only male induction, but also a great reduction of neonate number. However, epofenonane shows a slight reduction in brood size (Oda et al., 2005a). In addition, previous studies involved in a JH receptor complex of daphnids indicated that male production by epofenonane is driven by different mechanisms from the other juvenoids and their synthetic derivatives (Miyakawa et al., 2013c). Therefore, it is likely that down-regulation of hemoglobin genes by epofenonane are also caused by different mechanisms from other JH analogs **(Figure 3-7)**. Moreover, the venn diagram comparing the three JH agonists at the highest concentrations shows that only a few common genes are expressed between fenoxycarb and methoprene, and fenoxycarb and epofenonane (20 and 5 genes, respectively), unlike that of methoprene and epofenonane (142 genes), although hemoglobin-related genes and JHEH were up-regulated. This result also might support the above speculation.

Moreover, JHEH may play pivotal roles in regulating insect JH titers along with JHE (Terashima and Bownes1, 2005; Touhara and Prestwich, 1993). In the present study, JHEH gene was up-regulated by all treatments except for fenoxycarb at the lowest concentration **(Tables 3-2, 3-3, 3-4)**, but not JHE **(Table 3-5)**. These data imply that daphnids might upregulate JHEH in order to maintain normal JH titers, and were consistent in result when our group exposed MF to juveniles of *D. pulex* (Miyakawa et

al., unpublished data). Genes encoding the adipose specific protein and 4-aminobutyrate aminotransferase, which were up-regulated by three JH analogs at the highest concentration, might be novel JH-responsive genes. Further analysis will be necessary to determine whether these genes are functionally related to the JH response.

Interestingly, four GO terms involved in reproduction could be categorized in down-regulation by methoprene treatments, which showed a great reduction of neonate number. In contrast, three GO terms could be assigned in the up-regulation by epofenonane, which showed a slight change in neonate number. These data suggest that functional annotation based on GO terms supports the previous studies involved in the relationship between JH treatment and reproduction rate.

In this chapter, I created an overview of daphnid's transcriptome by exposure to three JH analogs. Moreover, these transcriptome data linked with previous toxicity tests (Oda et al., 2005a; Tatarazako et al., 2003). This approach called Adverse Outcome Pathway, which is a new conceptual framework to support ecotoxicological research and risk assessment (Ankley et al., 2010). This study suggested that transcriptome data of different physiological JH analogs could be associated with chronic toxicity tests of each chemical studied previously. In the future, further analysis will be required to understand the molecular basis of toxicology using various omics and computational approaches. Taken together, these results suggest that *D. magna* DNA microarray can be applied for categorization of JH analogs depending on their physiological function, and to discover novel JH-responsive genes.

Tables

Table 3-1 Summary of RIN scores

Chemical	Dose (ppb)	RIN_Average	SEM
Methoprene	125	6.4	0.033
	250	6.4	0.033
	500	6.5	0.088
Fenoxycarb	0.5	6.4	0.000
	1	6.3	0.088
	2	6.4	0.088
Epofenonane	50	6.5	0.100
	100	6.5	0.133
	200	6.4	0.088

Table 3-2 33 and 70 genes commonly up- and downregulated in response to methoprene.

#seq	Hit name	Fold change (Met-125)	Fold change (Met-250)	Fold change (Met-500)	Hit description
4	Contig4912	214.50	137.65	26.56	cre-nas-8 protein
1	Contig3936	151.72	145.06	66.75	conserved uncharacterized protein
3	IGU001_0045_A04.f	60.94	41.16	19.95	Unknown
4	Contig1602	13.84	12.68	7.86	hypothetical protein DAPPUDRAFT_315189 [Daphnia pulex]
4	Contig713	11.91	11.22	5.17	hypothetical protein DAPPUDRAFT_300387 [Daphnia pulex]
2	IGU001_0054_G10.f	10.92	6.01	3.28	hypothetical protein DAPPUDRAFT_301004 [Daphnia pulex]
1	dm039a15.r	10.31	5.90	2.82	clip-domain serine protease subfamily d (agap008183-pa)
3	dm050c02.f	9.92	6.99	3.62	Unknown
7	Contig3305	9.21	8.75	5.61	hypothetical protein DAPPUDRAFT_315189 [Daphnia pulex]
1	IGU001_0013_D10.f	7.28	6.60	3.96	protein
1	Contig2716	4.96	4.12	3.23	histone h2a
1	Contig1494	3.87	4.75	6.37	chitinase 1
3	Contig602	3.68	3.69	3.21	Unknown
1	Contig312	3.34	18.84	29.15	kinesin-like protein klp1
2	dm014m12.r	3.24	3.22	4.65	vitellogenin fused with superoxide dismutase
3	Contig1807	2.90	2.91	4.05	senescence-associated protein
1	WTH001_000	2.84	2.70	3.55	senescence-associated protein

	9_K03.f				
2	dm008i09.r	2.61	2.58	3.40	vitellogenin fused with superoxide dismutase
3	Contig594	2.57	2.65	2.58	a chain structural consequences of accommodation of four non-cognate amino-acid residues in the s1 pocket of bovine trypsin and chymotrypsin
3	dm018a06.f	2.56	16.69	26.25	kinesin-like protein klp1
1	WTH001_0001_N06.r	2.42	2.48	3.41	Unknown
1	Contig5076	2.33	2.85	7.38	glutathione s-
1	dm029o15.f	2.32	2.49	3.54	disintegrin and metalloproteinase domain-containing protein 12-like
3	Contig5103	2.29	2.26	2.05	beta- -glucanase
1	Contig913	2.24	3.46	3.89	isoform e
1	Contig3045	2.24	2.71	2.68	Unknown
1	Contig1889	2.21	2.22	2.63	hypothetical protein DAPPUDRAFT_325062 [Daphnia pulex]
2	Contig2707	2.17	3.37	7.09	complement component q subcomponent-like 4
3	Contig4577	2.10	2.14	3.53	hypothetical protein DAPPUDRAFT_236902 [Daphnia pulex]
1	Contig4584	2.06	2.04	2.10	juvenile hormone epoxide hydrolase
1	Contig1448	2.05	2.65	2.92	Unknown
1	Contig456	2.02	2.35	2.52	Unknown
1	Contig4482	2.01	4.73	10.05	Unknown
2	dm049h23.f	0.48	0.46	0.35	glycolipid-transport protein
2	Contig141	0.48	0.49	0.43	lipophorin precursor
1	Contig5004	0.47	0.43	0.33	pancreatic triacylglycerol lipase

1	dm019p08.f	0.47	0.48	0.43	chromosome segregation protein smc
1	dm045b23.f	0.47	0.49	0.46	conserved protein
2	dm010k23.f	0.43	0.36	0.22	chymotrypsin-like protein
1	Contig1708	0.43	0.40	0.40	4-hydroxyphenylpyruvate dioxygenase
1	Contig4535	0.42	0.38	0.29	carboxypeptidase a2
1	dm069l20.f	0.40	0.40	0.29	beta-galactosidase
1	Contig3044	0.39	0.39	0.44	oxidase peroxidase
2	dm053b04.r	0.39	0.46	0.42	cytoplasmic 2
1	Contig942	0.38	0.46	0.45	vitellogenin-like protein
2	Contig3323	0.38	0.32	0.15	carboxylesterase
1	Contig93	0.38	0.33	0.42	hypothetical protein DAPPUDRAFT_308770 [Daphnia pulex]
1	Contig2729	0.37	0.49	0.35	membrane glycoprotein lig-
3	Contig4988	0.37	0.46	0.30	cellobiohydrolase i-i
1	Contig3434	0.37	0.43	0.29	contactin associated protein 1
1	dm012n14.f	0.36	0.35	0.31	hypothetical protein DAPPUDRAFT_309226 [Daphnia pulex]
1	dm025j01.f	0.35	0.34	0.17	juvenile hormone esterase
2	Contig354	0.34	0.38	0.23	protease m1 zinc metalloprotease
6	Contig1775	0.33	0.33	0.20	endoribonuclease-like protein
1	Contig4266	0.33	0.46	0.40	t-cell ecto-adp-ribosyltransferase 2 precursor
1	Contig5034	0.33	0.28	0.15	chymotrypsin-like protein
1	Contig1844	0.33	0.37	0.22	hypothetical protein DAPPUDRAFT_239371 [Daphnia pulex]
1	WTH001_0014_B10.f	0.32	0.45	0.41	mib2 protein

1	Contig2240	0.32	0.46	0.43	synaptobrevin homolog ykt6
1	dm007f10.f	0.31	0.44	0.42	---NA---
1	Contig2312	0.31	0.39	0.31	nuclear transcription factor tfp1
2	Contig1102	0.29	0.43	0.23	trypsin
3	Contig1229	0.28	0.35	0.22	carboxypeptidase b-like
1	Contig2230	0.27	0.43	0.20	hypothetical protein DAPPUDRAFT_325973 [Daphnia pulex]
1	Contig4997	0.27	0.24	0.17	chymotrypsin-like protein
3	Contig3061	0.27	0.42	0.27	hypothetical protein DAPPUDRAFT_302224 [Daphnia pulex]
1	dm066f17.f	0.27	0.37	0.43	condensin complex subunit 1
2	dm022p15.f	0.26	0.30	0.24	gamma-glutamyltranspeptidase 1
4	Contig4700	0.26	0.31	0.15	cathepsin d
1	Contig2665	0.25	0.50	0.31	dolichol-phosphate mannosyltransferase
2	Contig1536	0.25	0.33	0.24	pancreatic triacylglycerol lipase
6	Contig2421	0.25	0.43	0.25	carboxylesterase
2	Contig2696	0.25	0.33	0.24	asialoglycoprotein receptor
3	dm074a03.r	0.25	0.36	0.23	angiotensin-converting enzyme 2
1	Contig1086	0.24	0.24	0.18	carboxyl choline esterase cce016b
1	dm045m07.r	0.24	0.36	0.11	hypothetical protein DAPPUDRAFT_305228 [Daphnia pulex]
3	Contig2429	0.23	0.29	0.10	hypothetical protein DAPPUDRAFT_301975 [Daphnia pulex]
2	Contig3613	0.23	0.33	0.16	angiotensin converting enzyme
5	Contig717	0.23	0.43	0.28	vertebrate gliacolin-like protein
4	Contig1835	0.22	0.32	0.22	chymotrypsin-like protein
4	Contig4772	0.22	0.28	0.17	carboxypeptidase a1

2	Contig2711	0.21	0.34	0.19	lysosomal alpha-mannosidase
1	Contig1984	0.21	0.28	0.23	lysosomal alpha-mannosidase (mannosidase alpha class 2b member 1)
2	dm073g02.r	0.21	0.20	0.18	trypsin
1	dm001a12.f	0.20	0.41	0.25	probable oxidoreductase c10orf33
1	Contig3091	0.20	0.20	0.18	lipase 1 precursor
2	dm022j06.f	0.18	0.15	0.16	hypothetical protein DAPPUDRAFT_308463 [Daphnia pulex]
3	Contig3100	0.16	0.20	0.16	moxd1 protein
1	Contig5162	0.16	0.29	0.10	hypothetical protein DAPPUDRAFT_113071 [Daphnia pulex]
1	dm069i15.f	0.15	0.35	0.21	aldose reductase
4	Contig4259	0.15	0.20	0.13	salivary secreted protein
3	Contig4751	0.13	0.23	0.06	alcohol dehydrogenase
4	Contig529	0.12	0.24	0.12	carboxypeptidase a2
2	Contig818	0.12	0.32	0.09	dipeptidase 1-like
2	dm011n11.f	0.11	0.20	0.12	sec14-like protein
1	Contig1559	0.10	0.25	0.14	negative elongation factor b
2	Contig1407	0.10	0.15	0.09	sec14-like protein
2	dm013n05.r	0.09	0.11	0.08	trypsin
3	dm010l20.f	0.09	0.11	0.08	pancreatic alpha-amylase
2	Contig1547	0.08	0.40	0.14	cre-nas-15 protein
2	dm021k17.r	0.06	0.16	0.05	trypsin [Daphnia pulex]
2	Contig1454	0.05	0.13	0.04	trypsin
2	Contig1885	0.02	0.11	0.02	sec14-like 2 (cerevisiae) partial

Table 3-3 124 and 7 genes commonly up- and downregulated in response to fenoxycarb.

#seq	Hit name	Fold change (Fx-0.5)	Fold change (Fx-1.0)	Fold change (Fx-2.0)	Hit description
1	dm026i12.f	13.04	14.35	15.76	2-domain hemoglobin protein subunit
4	Contig3394	12.39	12.81	14.24	2-domain hemoglobin
1	dm032i01.r	11.85	12.49	13.62	hemoglobin
1	dm045j14.f	10.48	22.18	12.05	hypothetical protein DAPPUDRAFT_306723 [Daphnia pulex]
3	dm053h04.r	10.12	10.44	6.64	hypothetical protein DAPPUDRAFT_309224 [Daphnia pulex]
2	dm031i03.r	8.99	9.47	9.00	hemoglobin
2	Contig4203	7.47	8.95	6.44	hypothetical protein DAPPUDRAFT_309625 [Daphnia pulex]
7	Contig2082	6.70	6.36	5.65	hypothetical protein DAPPUDRAFT_209471 [Daphnia pulex]
1	dm002a05.f	6.31	5.00	4.73	hypothetical protein DAPPUDRAFT_107086 [Daphnia pulex]
2	Contig2545	5.93	8.07	6.43	frrs1_drome ame: full= ferric-chelate reductase 1 homolog short= 2
1	dm075a23.f	5.85	5.26	5.04	hypothetical protein DAPPUDRAFT_311119 [Daphnia pulex]
5	Contig801	5.79	4.78	4.57	Unknown
1	dm051g20.r	5.79	7.05	5.07	Unknown
2	Contig4580	5.76	6.80	5.00	Unknown
3	Contig4751	5.73	5.08	4.81	alcohol dehydrogenase
1	Contig2684	5.71	5.52	6.43	2-domain hemoglobin
3	Contig278	5.48	5.43	4.73	hypothetical protein DAPPUDRAFT_300507 [Daphnia pulex]
1	IGU001_0030_A09.f	5.47	4.59	4.57	Unknown
1	Contig4138	5.14	5.76	4.69	hypothetical protein DAPPUDRAFT_312824 [Daphnia pulex]

1	Contig5238	5.10	7.98	5.79	hypothetical protein DAPPUDRAFT_304743 [Daphnia pulex]
3	dm035h01.f	5.09	4.86	4.05	Unknown
4	dm042d06.f	5.08	4.88	4.36	Unknown
1	Contig5097	5.03	6.28	4.32	hypothetical protein DAPPUDRAFT_306181 [Daphnia pulex]
3	Contig279	4.93	4.59	3.92	Unknown
3	Contig1769	4.81	5.66	4.05	hypothetical protein DAPPUDRAFT_306144 [Daphnia pulex]
1	dm065p16.f	4.67	4.00	3.56	Unknown
3	Contig269	4.62	6.25	4.61	hypothetical protein DAPPUDRAFT_224136 [Daphnia pulex]
2	dm004l01.r	4.61	4.70	3.47	hypothetical protein DAPPUDRAFT_309203 [Daphnia pulex]
2	Contig2196	4.59	3.88	3.41	hypothetical protein DAPPUDRAFT_225089 [Daphnia pulex]
4	dm074k05.f	4.59	4.81	3.47	hypothetical protein DAPPUDRAFT_316390 [Daphnia pulex]
3	Contig4150	4.47	4.49	3.70	hypothetical protein DAPPUDRAFT_319515 [Daphnia pulex]
2	Contig4766	4.41	4.47	3.66	growth and transformation-dependent protein
1	Contig4165	4.37	3.86	4.07	hypothetical protein DAPPUDRAFT_307285 [Daphnia pulex]
4	Contig2659	4.36	3.70	3.95	hypothetical protein DAPPUDRAFT_329459 [Daphnia pulex]
1	dm001e01.r	4.25	4.39	3.16	set domain and mariner transposase fusion gene
1	Contig4662	4.21	5.00	3.80	hypothetical protein DAPPUDRAFT_234969 [Daphnia pulex]
1	IGU001_0006_H04.f	4.15	3.96	4.50	2-domain hemoglobin protein subunit
2	Contig4308	4.07	3.96	3.45	Unknown
1	IGU001_0030_C09.f	4.06	3.97	2.89	Unknown
4	Contig4086	3.99	4.29	3.14	hypothetical protein DAPPUDRAFT_309625 [Daphnia pulex]

1	Contig4906	3.97	5.80	4.97	hypothetical protein DAPPUDRAFT_101459 [Daphnia pulex]
3	dm009p02.f	3.91	4.18	3.16	Unknown
4	Contig1649	3.91	3.82	3.21	techylectin-5b isoform
1	dm050a21.r	3.91	4.58	3.21	Unknown
2	dm050c02.f	3.87	3.87	4.72	Unknown
3	dm071o04.f	3.83	3.97	3.23	Unknown
1	Contig809	3.81	4.04	4.55	2-domain hemoglobin
1	Contig5249	3.80	4.78	3.22	hypothetical protein DAPPUDRAFT_309625 [Daphnia pulex]
2	Contig955	3.78	4.27	2.86	hypothetical protein DAPPUDRAFT_308928 [Daphnia pulex]
8	Contig3094	3.76	3.92	4.11	2-domain hemoglobin
1	IGU001_0049_F06.f	3.69	3.89	4.06	2-domain hemoglobin protein subunit
5	Contig4586	3.66	5.68	3.56	hypothetical protein DAPPUDRAFT_233998 [Daphnia pulex]
1	IGU001_0030_C09.r	3.62	3.86	2.76	Unknown
5	Contig344	3.61	3.20	2.83	hypothetical protein DAPPUDRAFT_309288 [Daphnia pulex]
3	dm010g22.r	3.58	3.61	2.66	hypothetical protein DAPPUDRAFT_315173 [Daphnia pulex]
1	WTH001_0006_G23.f	3.57	3.27	2.54	hypothetical protein DAPPUDRAFT_311119 [Daphnia pulex]
2	Contig5250	3.56	3.35	3.10	atp-binding sub-family a member 3
1	dm044p05.f	3.55	4.42	3.26	hypothetical protein DAPPUDRAFT_305523 [Daphnia pulex]
1	Contig4118	3.51	3.83	3.24	hypothetical protein DAPPUDRAFT_314230 [Daphnia pulex]
2	dm003c12.f	3.48	3.94	2.98	hypothetical protein DAPPUDRAFT_113492 [Daphnia pulex]

3	IGU001_0003_B07.f	3.43	3.30	2.70	Unknown
1	Contig4822	3.43	4.13	3.10	low mw proline-rich protein
2	Contig3214	3.39	3.51	3.60	2-domain hemoglobin
3	Contig2544	3.38	3.65	3.16	heme-binding protein 2
3	Contig4417	3.35	3.37	3.54	2-domain hemoglobin protein subunit
3	Contig381	3.35	3.73	3.07	hypothetical protein DAPPUDRAFT_94071 [Daphnia pulex]
7	dm050l19.f	3.34	3.30	3.35	2-domain hemoglobin
1	Contig2501	3.32	3.61	3.25	60s acidic ribosomal protein p1
3	Contig255	3.26	3.10	2.86	Unknown
8	Contig4119	3.22	3.13	2.82	hypothetical protein DAPPUDRAFT_192749 [Daphnia pulex]
6	Contig3216	3.18	3.92	3.67	vertebrate gliacolin-like protein
1	dm049n05.f	3.15	4.10	2.94	Unknown
1	Contig1904	3.15	2.83	2.64	Unknown
2	dm049a03.r	3.15	3.26	3.38	2-domain hemoglobin
3	Contig2392	3.13	3.32	2.66	cuticular protein analogous to peritrophins 1-g
5	Contig387	3.13	2.78	2.63	dusky- isoform a
3	Contig4267	3.10	3.23	2.67	hypothetical protein DAPPUDRAFT_328924 [Daphnia pulex]
3	Contig2270	3.09	3.51	3.73	hypothetical protein DAPPUDRAFT_110156 [Daphnia pulex]
4	Contig2288	3.08	2.83	2.59	hypothetical protein DAPPUDRAFT_307846 [Daphnia pulex]
5	Contig1093	3.08	3.14	2.63	c-type lectin
2	Contig1164	3.06	2.77	2.33	Unknown
2	Contig4581	2.99	3.55	2.75	hypothetical protein DAPPUDRAFT_305522 [Daphnia pulex]

2	Contig1804	2.98	3.00	2.55	hypothetical protein DAPPUDRAFT_315173 [Daphnia pulex]
1	Contig314	2.98	2.88	2.28	mitochondrial dimethyladenosine transferase 1
2	dm012f24.f	2.94	3.30	3.04	hypothetical protein DAPPUDRAFT_305568 [Daphnia pulex]
3	IGU001_0045_A04.f	2.93	2.59	2.86	Unknown
4	dm002j02.r	2.92	2.91	2.86	2-domain hemoglobin protein subunit
1	Contig4793	2.91	2.70	2.35	hypothetical protein DAPPUDRAFT_244841 [Daphnia pulex]
1	Contig5041	2.87	3.16	2.60	Unknown
3	WTH001_0010_I13.f	2.81	2.72	2.42	cystatin
2	Contig348	2.79	2.61	2.39	Unknown
2	Contig2271	2.77	2.70	2.60	matrix metalloproteinase 1
1	dm061b11.f	2.76	3.02	2.23	hypothetical protein DAPPUDRAFT_306131 [Daphnia pulex]
1	Contig4044	2.75	2.65	2.51	hypothetical protein DAPPUDRAFT_239768 [Daphnia pulex]
1	Contig4006	2.73	2.47	2.09	follistatin
3	dm047h19.f	2.70	2.84	2.27	positive regulatory domain b-lymphocyte induced maturation protein version a
2	Contig1061	2.67	2.92	2.04	hypothetical protein DAPPUDRAFT_220756 [Daphnia pulex]
1	dm006b03.f	2.64	2.83	2.75	procollagen- 2-oxoglutarate 5-dioxygenase 3
1	dm074k05.r	2.64	2.63	2.15	Unknown
2	dm049g05.f	2.61	3.09	2.49	retinoblastoma-binding protein 5
1	Contig4312	2.60	3.71	2.42	hypothetical protein DAPPUDRAFT_304488 [Daphnia pulex]
3	dm036f17.r	2.56	2.59	2.28	Unknown

1	dm041b21.f	2.56	2.72	2.23	Unknown
4	dm073g02.r	2.54	2.66	2.69	trypsin
1	dm007k05.f	2.54	2.28	2.16	spatzle 6
2	Contig1600	2.50	2.94	2.33	hypothetical protein DAPPUDRAFT_109962 [Daphnia pulex]
1	IGU001_0013_D10.f	2.49	2.89	2.56	protein
2	Contig3795	2.49	2.61	2.29	hypothetical protein DAPPUDRAFT_305522 [Daphnia pulex]
1	Contig5068	2.47	3.37	2.81	hypothetical protein DAPPUDRAFT_322265 [Daphnia pulex]
2	Contig2381	2.46	2.58	2.16	Unknown
1	Contig192	2.45	2.71	2.47	Unknown
2	Contig371	2.45	2.29	2.18	cathepsin l-like
3	dm061m16.f	2.43	2.59	2.19	Unknown
2	Contig2946	2.42	2.75	2.47	c1q-like adipose specific protein
2	Contig5232	2.41	2.40	2.16	midline fasciclin
2	dm022e01.f	2.39	3.45	2.46	hypothetical protein DAPPUDRAFT_109961 [Daphnia pulex]
2	Contig3481	2.39	3.17	2.96	Unknown
2	Contig4996	2.37	2.74	2.18	cub and sushi multiple domains 2-like
3	Contig1019	2.31	2.43	2.64	Unknown
2	Contig653	2.26	2.55	2.31	Unknown
1	IGU001_0003_B07.r	2.24	2.16	2.03	Unknown
1	WTH001_0003_E15.f	2.24	2.96	2.16	Unknown

1	dm004k07.r	2.21	2.40	2.07	argininosuccinate synthase
1	Contig1715	2.12	2.23	2.05	steroid dehydrogenase
1	Contig5076	0.50	0.48	0.47	glutathione s-
1	Contig3052	0.41	0.42	0.43	ubiquitin c
1	Contig2861	0.35	0.35	0.36	btb poz domain-containing protein kctd10
2	Contig1561	0.30	0.28	0.37	Unknown
1	Contig1985	0.29	0.41	0.36	hypothetical protein DAPPUDRAFT_302370 [Daphnia pulex]
1	Contig1709	0.26	0.27	0.24	hypothetical protein DAPPUDRAFT_315291 [Daphnia pulex]
1	Contig1559	0.16	0.15	0.17	negative elongation factor b

Table 3-4 22 and 6 genes commonly up- and downregulated in response to epofenonane.

#seq	Hit name	Fold change (Ep-50)	Fold change (Ep-100)	Fold change (Ep-200)	Hit description
1	Contig2351	5.54	6.23	7.92	trypsin
1	Contig91	5.53	5.66	6.08	trypsin
1	Contig3477	5.07	5.43	6.35	trypsin [Daphnia pulex]
6	dm053a24.f	4.87	5.39	6.56	trypsin
1	Contig3394	4.52	2.53	2.85	2-domain hemoglobin
1	dm026i12.f	4.07	2.18	2.60	2-domain hemoglobin protein subunit
1	Contig4577	4.00	3.42	2.01	hypothetical protein DAPPUDRAFT_236902 [Daphnia pulex]
3	Contig2991	3.34	5.30	5.91	vitelline membrane outer layer protein 1 homolog precursor
1	Contig1819	2.99	3.00	3.20	trypsin
1	dm040b05.f	2.79	3.01	7.31	Unknown
3	Contig441	2.50	3.63	10.04	hypothetical protein DAPPUDRAFT_229387 [Daphnia pulex]
5	Contig1278	2.48	2.70	4.09	cuticular protein analogous to peritrophins 3-a2
1	Contig1375	2.48	2.46	5.29	pancreatic triacylglycerol lipase-like
3	Contig4186	2.42	2.41	4.08	serine proteinase
1	Contig5008	2.37	3.84	3.27	moxd1 homolog 2-like
1	Contig4334	2.30	2.23	2.15	liver basic fatty acid binding protein
1	Contig4099	2.28	3.35	3.90	hypothetical protein DAPPUDRAFT_195649 [Daphnia pulex]
3	Contig5076	2.28	3.26	9.24	glutathione s-
3	Contig4253	2.11	2.13	2.34	hypothetical protein DAPPUDRAFT_232076 [Daphnia pulex]
1	Contig3998	2.09	4.34	4.23	clip-domain serine protease subfamily d (agap008183-pa)

1	Contig4584	2.09	2.53	2.45	juvenile hormone epoxide hydrolase
1	Contig3436	2.08	2.45	2.76	microsomal glutathione s-transferase 3
1	Contig1985	0.39	0.35	0.34	hypothetical protein DAPPUDRAFT_302370 [Daphnia pulex]
2	Contig3100	0.28	0.21	0.07	moxd1 protein
2	Contig1407	0.27	0.35	0.08	sec14-like protein
2	Contig1885	0.25	0.35	0.02	sec14-like 2 (cerevisiae) partial
1	Contig1709	0.25	0.27	0.26	hypothetical protein DAPPUDRAFT_315291 [Daphnia pulex]
1	Contig1559	0.11	0.09	0.11	negative elongation factor b

Table 3-5 Expression of well-known JH-responsive genes involving the acute and chronic toxicity in *D. magna*

JH responsive gene	ID	Hit name	Mt 125 ppb		Mt 250 ppb		Mt 500 ppb		Fx 0.5 ppb		Fx 1.0 ppb		Fx 2.0 ppb		Ep 50 ppb		Ep 100 ppb		Ep 200 ppb	
			FC	q value	FC	q value	FC	q value	FC	q value	FC	q value	FC	q value	FC	q value	FC	q value	FC	q value
	DM00747_1	Contig4704	1.18	0.618	3.90	0.139	1.07	0.427	0.84	0.632	0.65	0.520	1.99	0.383	0.21	0.303	8.17	0.311	0.86	0.624
	DM01898_1	Contig1762	1.18	0.462	1.01	0.530	1.15	0.119	0.90	0.254	0.90	0.444	0.91	0.292	0.86	0.202	0.93	0.496	0.97	0.565
	DM01898_2	Contig3396	0.60	0.505	0.77	0.489	0.52	0.190	0.56	0.484	0.34	0.323	0.31	0.152	0.40	0.259	0.85	0.582	0.67	0.484
	DM02191_3	dm035l05.r	0.73	0.595	2.16	0.280	0.95	0.430	0.81	0.617	0.38	0.423	0.74	0.467	0.25	0.303	2.11	0.471	0.79	0.588
	DM02348_3	Contig4274	0.46	0.510	0.93	0.545	0.53	0.349	0.33	0.518	0.09	0.327	0.07	0.167	0.22	0.317	0.37	0.474	0.34	0.445
	DM02515_2	Contig5089	0.50	0.513	1.04	0.547	0.66	0.349	0.47	0.526	0.26	0.370	0.44	0.361	0.20	0.252	1.53	0.481	0.45	0.452
	DM02560_2	Contig3721	0.91	0.570	1.46	0.196	0.89	0.387	1.04	0.630	0.82	0.498	0.93	0.526	0.77	0.393	1.22	0.489	1.06	0.620
cuticle	DM02680_1	Contig4434	1.17	0.610	2.10	0.212	0.63	0.374	0.84	0.623	0.78	0.502	1.06	0.544	0.24	0.270	3.89	0.342	0.65	0.561
protein	DM02749_2	Contig4572	0.69	0.548	1.29	0.458	0.65	0.298	0.60	0.550	0.19	0.260	0.31	0.253	0.30	0.283	0.75	0.552	0.45	0.387
(Kim et	DM02979_2	dm068e06.r	1.13	0.627	10.9	0.171	1.39	0.414	0.61	0.620	0.14	0.442	0.42	0.470	0.07	0.341	6.73	0.367	0.71	0.618
al., 2011)	DM03143_3	Contig2179	0.45	0.441	0.91	0.511	1.34	0.206	0.66	0.467	0.47	0.375	0.64	0.285	0.42	0.240	1.20	0.512	0.99	0.636
	DM04371_1	Contig4104	2.98	0.131	2.73	0.212	1.00	0.432	1.84	0.325	1.90	0.306	1.75	0.201	0.94	0.507	0.85	0.561	0.73	0.383
	DM05553_1	dm074m16.f	1.29	0.602	3.29	0.169	1.00	0.436	0.84	0.628	0.61	0.465	1.01	0.555	0.23	0.283	5.06	0.321	0.86	0.618
	DM05811_1	Contig4013	0.77	0.588	2.32	0.147	0.89	0.416	0.80	0.614	0.71	0.504	0.94	0.542	0.32	0.303	2.60	0.311	0.83	0.607
	DM05969_1	Contig4536	0.87	0.594	1.96	0.234	0.95	0.424	0.93	0.637	0.64	0.472	0.95	0.542	0.43	0.347	1.84	0.335	1.02	0.636
	DM06160_2	Contig4052	0.88	0.619	2.80	0.252	0.86	0.417	0.69	0.604	0.36	0.444	0.92	0.528	0.18	0.291	3.00	0.385	0.71	0.585
	DM06252_2	Contig1244	0.52	0.483	1.44	0.374	0.77	0.337	0.71	0.554	0.24	0.215	0.46	0.269	0.31	0.227	1.38	0.514	0.38	0.275
	DM06459_1	Contig1445	0.59	0.575	2.75	0.265	0.76	0.404	0.63	0.603	0.46	0.481	1.22	0.503	0.18	0.326	4.40	0.321	0.57	0.571

DM06508_2	Contig4661	0.80	0.617	5.23	0.157	1.14	0.423	0.73	0.626	0.44	0.489	0.94	0.549	0.09	0.293	9.73	0.311	0.87	0.628
DM06537_2	dm056h20.f	0.92	0.033	1.05	0.430	1.20	0.118	0.95	0.354	0.91	0.448	0.90	0.222	0.90	0.236	0.94	0.523	0.99	0.619
DM06768_2	Contig1473	1.14	0.250	1.12	0.224	1.26	0.112	1.02	0.553	1.07	0.394	1.06	0.169	0.99	0.380	1.08	0.445	1.16	0.131
DM06785_1	Contig3967	1.05	0.631	6.09	0.146	1.11	0.427	0.79	0.634	0.54	0.512	1.12	0.544	0.11	0.319	7.39	0.311	0.81	0.623
DM06955_2	Contig2782	0.80	0.520	1.01	0.550	0.95	0.396	0.40	0.184	0.52	0.399	0.85	0.486	0.40	0.180	0.97	0.620	0.89	0.597
DM07501_2	Contig4248	1.04	0.630	2.56	0.261	0.99	0.435	1.14	0.629	0.49	0.461	0.86	0.530	0.19	0.290	4.26	0.345	0.64	0.567
DM08040_1	Contig3710	0.88	0.587	1.32	0.394	0.77	0.348	0.66	0.525	0.98	0.568	1.10	0.530	0.53	0.341	1.81	0.311	0.77	0.549
DM09211_1	Contig1129	0.57	0.211	0.67	0.278	0.56	0.105	0.85	0.219	0.72	0.293	0.88	0.129	1.02	0.527	0.96	0.542	0.84	0.398
DM12302_1	Contig2554	0.76	0.601	2.42	0.278	0.88	0.418	0.60	0.583	0.30	0.434	0.52	0.448	0.16	0.273	3.29	0.345	0.62	0.567
DM12548_2	Contig5098	0.84	0.036	1.00	0.552	1.11	0.162	0.88	0.277	0.85	0.423	0.81	0.171	0.88	0.234	0.87	0.452	0.90	0.409
DM12571_2	Contig4355	1.04	0.599	1.00	0.543	1.13	0.142	0.91	0.281	0.87	0.440	0.85	0.175	0.88	0.229	0.88	0.464	0.92	0.442
DM14064_2	Contig1496	0.76	0.334	1.04	0.504	1.50	0.162	0.71	0.313	0.69	0.307	0.69	0.172	0.84	0.225	0.66	0.269	1.13	0.271
DM14565_2	Contig4146	1.93	0.358	1.68	0.199	0.73	0.359	1.16	0.575	0.72	0.406	0.88	0.461	0.41	0.227	1.70	0.469	0.47	0.460
DM15160_1	dm073j01.r	0.94	0.428	1.20	0.193	1.50	0.142	0.93	0.361	0.89	0.443	0.87	0.188	0.91	0.326	0.91	0.484	1.15	0.486
DMAG0001S00000088	Contig88	1.19	0.294	2.35	0.180	3.18	0.112	1.15	0.485	1.08	0.440	1.15	0.285	1.19	0.228	1.14	0.486	3.17	0.133
DMAG0001S00000392	Contig392	1.11	0.535	0.90	0.319	1.00	0.425	1.19	0.534	1.05	0.552	0.90	0.443	1.05	0.500	1.40	0.488	0.91	0.535
DMAG0001S00000447	Contig447	0.85	0.615	2.52	0.224	0.91	0.423	0.72	0.600	0.48	0.447	0.85	0.518	0.23	0.284	3.39	0.337	0.73	0.584
DMAG0001S00000588	Contig588	1.33	0.379	1.08	0.430	0.70	0.151	1.18	0.412	1.10	0.448	1.13	0.293	1.21	0.205	1.50	0.347	1.04	0.310
DMAG0001S	Contig977	0.99	0.625	0.74	0.264	0.55	0.115	1.00	0.641	1.00	0.538	0.87	0.296	0.93	0.469	0.67	0.321	0.64	0.292

	00000977																		
	DMAG0001S00000989	Contig989	0.79	0.605	2.44	0.316	1.03	0.432	0.52	0.558	0.18	0.335	0.39	0.352	0.20	0.291	2.40	0.441	0.73	0.593
	DMAG0001S00001760	Contig1760	1.05	0.593	1.27	0.372	1.15	0.115	0.98	0.641	0.83	0.440	0.82	0.225	0.84	0.193	1.05	0.572	1.14	0.276
	DMAG0001S00002122	Contig2122	0.78	0.601	2.57	0.272	1.19	0.407	0.71	0.595	0.37	0.437	0.58	0.443	0.29	0.277	2.41	0.428	0.65	0.554
	DMAG0001S00002221	Contig2221	0.61	0.496	1.13	0.511	0.90	0.383	0.78	0.569	0.87	0.534	1.27	0.411	0.70	0.440	1.74	0.466	1.45	0.462
	DMAG0001S00002295	Contig2295	1.51	0.529	2.08	0.216	1.04	0.429	0.99	0.651	0.52	0.380	0.82	0.483	0.27	0.239	2.37	0.401	0.64	0.539
	DMAG0001S00002452	Contig2452	0.66	0.568	1.54	0.409	0.76	0.374	0.50	0.515	0.43	0.442	0.56	0.419	0.26	0.254	2.22	0.429	0.49	0.451
	DMAG0001S00002527	Contig2527	1.06	0.629	3.89	0.169	1.06	0.430	0.86	0.637	0.52	0.483	0.94	0.548	0.18	0.305	4.98	0.324	0.76	0.603
	DMAG0001S00002629	Contig2629	0.73	0.545	1.18	0.516	0.74	0.311	1.54	0.308	0.77	0.513	1.52	0.311	0.89	0.512	1.50	0.487	1.63	0.482
	DMAG0001S00002838	Contig2838	0.84	0.613	3.02	0.146	0.95	0.430	0.81	0.625	0.63	0.496	0.97	0.551	0.22	0.290	3.89	0.311	0.74	0.596
	DMAG0001S00002842	Contig2842	0.82	0.580	1.23	0.464	0.89	0.386	0.90	0.613	0.91	0.534	1.17	0.449	0.62	0.389	1.79	0.455	1.12	0.589
	DMAG0001S00003076	Contig3076	0.80	0.604	2.59	0.158	0.88	0.418	0.79	0.616	0.71	0.501	0.95	0.547	0.25	0.276	3.54	0.321	0.73	0.584

	DMAG00015S00003494	Contig3494	0.47	0.434	0.81	0.503	0.69	0.334	0.57	0.528	0.33	0.381	0.38	0.172	0.32	0.245	0.48	0.459	0.34	0.304
	DMAG00015S00004813	Contig4813	1.64	0.565	3.91	0.145	1.33	0.390	1.09	0.643	1.51	0.523	2.34	0.425	0.24	0.231	12.31	0.311	1.30	0.602
	DMAG00015S00004821	Contig4821	0.63	0.057	0.70	0.149	0.81	0.110	0.62	0.184	0.76	0.382	0.60	0.131	0.85	0.431	0.60	0.311	0.63	0.165
	DMAG00015S00004990	Contig4990	0.63	0.522	1.38	0.411	0.70	0.329	0.88	0.616	0.68	0.442	0.66	0.344	0.60	0.336	1.45	0.493	0.72	0.531
	DMAG00015S00005022	Contig5022	0.59	0.504	0.99	0.549	0.81	0.347	0.76	0.523	0.58	0.403	0.83	0.417	0.63	0.375	1.50	0.488	0.88	0.583
	DMAG00015S00005165	Contig5165	0.72	0.452	0.91	0.417	0.87	0.283	0.79	0.457	0.72	0.381	0.84	0.350	0.85	0.292	1.20	0.457	0.90	0.505
	DMAG00015S00006758	dm002h16.f	0.90	0.625	4.30	0.150	1.07	0.429	0.74	0.621	0.52	0.480	1.13	0.535	0.15	0.288	5.36	0.319	0.71	0.599
	DMAG00015S00009485	dm047o01.r	0.68	0.542	1.86	0.256	0.95	0.421	0.89	0.628	0.61	0.452	0.82	0.503	0.36	0.276	2.23	0.334	1.29	0.590
	DMAG00015S00009631	dm050j13.f	1.96	0.536	4.62	0.139	1.68	0.347	1.33	0.620	1.45	0.524	1.71	0.491	0.27	0.311	22.22	0.311	1.32	0.605
	DMAG00015S00009638	dm050k18.f	0.88	0.613	1.69	0.409	0.79	0.395	0.85	0.614	0.60	0.344	0.62	0.229	0.32	0.299	0.99	0.627	0.51	0.484
	DMAG00015S00009827	dm055g23.f	0.80	0.509	0.51	0.153	0.59	0.114	0.65	0.402	0.70	0.388	0.56	0.202	0.51	0.218	0.49	0.407	0.79	0.385
vitellogeni	DM00429_1	dm050o09.f	0.96	0.495	0.97	0.452	1.00	0.430	0.92	0.325	0.92	0.442	0.92	0.229	0.93	0.240	0.90	0.485	0.93	0.299

n (Kim et al., 2011)	DM00429_3	dm046j18.f	0.90	0.043	1.06	0.415	1.19	0.134	1.84	0.496	0.90	0.446	0.87	0.173	0.92	0.243	0.94	0.517	0.97	0.578
	DM01546_3	Contig1655	0.90	0.397	0.99	0.516	1.12	0.135	0.96	0.515	0.84	0.437	0.82	0.175	0.84	0.228	0.84	0.417	0.89	0.366
	DM01774_1	Contig942	0.60	0.079	0.46	0.143	0.48	0.134	0.82	0.241	0.76	0.299	0.80	0.165	0.99	0.432	0.82	0.342	0.58	0.177
	DM01793_2	dm014m12.r	2.01	0.056	1.96	0.179	2.35	0.115	1.23	0.271	1.58	0.322	1.41	0.131	1.36	0.230	1.54	0.341	1.94	0.162
	DM01857_1	dm043j10.r	2.11	0.148	1.74	0.224	1.31	0.213	1.75	0.313	1.09	0.526	1.56	0.305	1.57	0.231	0.97	0.607	1.45	0.483
	DM02213_3	dm006i16.r	0.92	0.250	0.97	0.263	1.02	0.396	0.90	0.274	0.90	0.438	0.89	0.335	0.90	0.180	0.93	0.517	0.96	0.501
	DM02350_1	dm011h08.f	0.96	0.422	0.97	0.431	0.98	0.402	0.94	0.308	0.94	0.443	0.91	0.312	0.92	0.231	0.95	0.518	1.02	0.545
	DM02636_1	dm008i09.r	2.65	0.040	2.58	0.175	3.42	0.108	1.31	0.243	1.92	0.328	1.59	0.140	1.54	0.217	1.78	0.321	2.54	0.142
	DM03168_3	dm050g02.r	0.89	0.095	1.03	0.470	1.16	0.116	0.92	0.272	0.90	0.443	0.88	0.211	0.89	0.228	0.92	0.488	0.97	0.559
	DM03613_1	dm026o19.f	0.93	0.064	1.06	0.415	1.22	0.121	0.96	0.380	0.92	0.453	0.90	0.228	0.91	0.244	0.96	0.546	1.00	0.638
	DM06812_1	Contig2149	0.88	0.073	1.05	0.419	1.18	0.115	0.91	0.322	0.98	0.432	0.85	0.200	1.31	0.349	0.91	0.489	1.12	0.505
	DM06892_1	dm027m21.f	1.41	0.080	1.20	0.323	0.83	0.219	1.21	0.297	1.27	0.257	1.25	0.129	1.22	0.219	1.24	0.349	0.89	0.357
	DM07205_2	Contig1684	0.84	0.321	0.80	0.336	0.47	0.108	1.02	0.620	0.96	0.461	0.94	0.413	0.98	0.455	0.85	0.395	0.72	0.146
	DM07853_2	Contig1801	0.93	0.481	1.00	0.552	1.03	0.358	0.75	0.302	0.73	0.345	0.74	0.253	0.90	0.340	1.25	0.378	1.32	0.162
	DM10679_2	Contig1914	1.43	0.462	1.07	0.401	1.82	0.202	1.05	0.549	0.94	0.469	0.92	0.249	1.20	0.441	1.22	0.508	1.16	0.435
	DM11336_1	Contig2007	0.84	0.065	0.99	0.520	1.10	0.169	0.90	0.281	0.87	0.441	0.84	0.163	0.87	0.230	0.88	0.455	0.90	0.384
	DM11670_2	Contig1851	0.74	0.448	0.62	0.165	1.21	0.301	0.84	0.255	1.19	0.510	1.18	0.466	0.61	0.180	0.55	0.311	1.02	0.631
	DMAG0001S00000327	Contig327	0.94	0.276	1.06	0.473	0.51	0.208	0.83	0.494	0.93	0.442	0.90	0.422	0.87	0.401	0.82	0.433	0.99	0.625
	DMAG0001S00000727	Contig727	0.69	0.218	0.62	0.218	0.87	0.162	0.56	0.296	1.12	0.514	0.76	0.383	0.96	0.471	1.28	0.485	0.83	0.369
	DMAG0001S00001693	Contig1693	1.12	0.427	1.05	0.470	1.11	0.232	1.05	0.608	1.07	0.471	1.09	0.364	1.05	0.477	0.87	0.408	1.15	0.286

DMAG00015 00001734	Contig1734	1.15	0.395	0.87	0.409	0.89	0.115	1.45	0.213	0.96	0.548	1.12	0.471	1.69	0.248	1.04	0.618	0.98	0.618
DMAG00015 00002172	Contig2172	2.33	0.130	1.03	0.534	0.32	0.108	1.71	0.332	1.77	0.342	1.31	0.307	0.85	0.206	0.60	0.319	0.30	0.146
DMAG00015 00002355	Contig2355	0.61	0.229	0.93	0.506	0.67	0.108	0.56	0.233	0.52	0.258	0.63	0.221	0.54	0.180	0.52	0.311	0.85	0.560
DMAG00015 00003658	Contig3658	1.10	0.621	1.62	0.386	1.30	0.366	0.65	0.548	0.23	0.255	0.64	0.421	0.33	0.242	2.52	0.379	1.02	0.625
DMAG00015 00005208	Contig5208	0.93	0.481	0.99	0.514	1.10	0.197	0.89	0.241	0.86	0.430	0.83	0.162	0.87	0.229	0.88	0.462	0.90	0.384
DMAG00015 00005674	IGU001_0051_E12.f	0.83	0.511	1.20	0.448	0.97	0.410	1.07	0.608	1.36	0.335	0.81	0.321	0.90	0.463	1.28	0.500	1.19	0.522
DMAG00015 00006441	WTH001_0011_P11.f	0.65	0.134	0.62	0.137	0.61	0.153	0.92	0.486	0.84	0.304	0.83	0.170	1.15	0.272	0.89	0.525	0.74	0.224
DMAG00015 00007020	dm018p20.f	0.63	0.167	0.32	0.124	0.43	0.116	0.91	0.615	0.74	0.473	0.84	0.395	1.00	0.541	0.58	0.481	0.56	0.209
DMAG00015 00007057	dm006p15.f	0.61	0.027	0.48	0.193	0.61	0.160	0.84	0.586	0.69	0.444	0.76	0.341	0.85	0.345	0.64	0.487	0.53	0.268
DMAG00015 00008161	dm022k23.r	0.63	0.017	0.74	0.166	0.82	0.123	0.66	0.184	0.64	0.303	0.62	0.129	0.65	0.183	0.66	0.321	0.67	0.169
DMAG00015 00009002	dm037o04.f	1.10	0.564	1.02	0.531	1.40	0.109	1.92	0.184	1.44	0.340	1.79	0.130	1.18	0.422	1.59	0.418	1.72	0.179
DMAG00015	dm045f09.f	0.53	0.212	0.58	0.253	0.65	0.159	0.72	0.373	0.76	0.289	0.62	0.230	0.98	0.519	0.72	0.427	0.95	0.584

	00009352																		
	DMAG0001S00009385	dm045p05.r	0.83	0.026	1.01	0.531	1.12	0.154	0.88	0.313	0.88	0.442	0.89	0.227	0.90	0.277	0.91	0.494	0.94	0.517
	DMAG0001S00009543	dm048p19.f	1.92	0.173	1.04	0.531	0.36	0.112	1.45	0.334	1.43	0.381	1.24	0.352	0.83	0.340	0.63	0.347	0.38	0.155
	DMAG0001S00009618	dm050g02.f	0.94	0.160	1.31	0.401	1.50	0.161	0.92	0.280	0.91	0.447	0.91	0.223	1.09	0.476	0.94	0.512	0.97	0.559
	DMAG0001S00009929	dm058b09.f	0.81	0.032	0.98	0.500	1.09	0.179	1.30	0.520	0.84	0.411	0.79	0.183	1.14	0.422	0.86	0.451	0.90	0.408
	DMAG0001S00010416	dm071d16.f	0.95	0.252	1.06	0.399	1.23	0.108	0.92	0.325	0.91	0.447	1.03	0.510	0.92	0.293	0.94	0.507	0.97	0.555
Glutathione S-transferases (Zou et al., 2011)	DM01138_1	dm032l08.r	0.84	0.036	1.26	0.271	1.31	0.145	0.89	0.274	0.86	0.432	0.83	0.199	1.05	0.494	1.30	0.510	1.61	0.301
	DM01679_3	Contig3436	0.61	0.269	0.72	0.224	1.29	0.137	1.10	0.557	1.38	0.347	0.96	0.463	1.16	0.397	1.05	0.571	1.08	0.584
	DM01694_1	Contig3246	0.99	0.617	0.99	0.521	1.00	0.436	0.96	0.244	1.01	0.523	1.02	0.451	1.07	0.228	1.02	0.571	1.06	0.145
	DM01799_2	dm074g23.f	1.05	0.524	1.22	0.170	1.00	0.430	1.31	0.341	1.19	0.438	1.14	0.222	1.34	0.213	1.10	0.319	1.03	0.587
	DM02206_2	Contig4437	1.00	0.634	0.80	0.452	0.68	0.162	1.12	0.562	1.00	0.571	1.01	0.538	0.82	0.398	0.59	0.327	0.54	0.166
	DM02407_1	Contig1667	0.78	0.140	0.72	0.213	0.56	0.108	0.88	0.410	1.27	0.444	0.99	0.522	1.01	0.517	0.99	0.622	0.66	0.146
	DM02984_1	Contig5076	2.33	0.033	2.85	0.160	7.38	0.108	0.78	0.324	0.85	0.470	0.84	0.285	2.64	0.180	3.04	0.319	8.79	0.107
	DM03187_1	Contig4599	1.00	0.633	0.95	0.340	0.87	0.132	0.96	0.388	1.02	0.469	0.99	0.466	1.11	0.246	0.95	0.498	1.00	0.626
	DM04701_1	Contig3831	1.06	0.461	1.11	0.308	1.05	0.252	0.98	0.577	1.09	0.378	1.07	0.165	1.09	0.283	1.11	0.393	1.09	0.132
	DM04855_1	Contig4647	0.60	0.227	0.58	0.146	0.74	0.119	0.67	0.333	0.91	0.524	0.71	0.224	1.13	0.429	1.07	0.587	1.06	0.608
	DM05021_1	dm029i03.f	0.80	0.145	0.76	0.205	0.77	0.115	0.96	0.496	0.87	0.388	0.91	0.354	0.94	0.359	0.74	0.334	0.83	0.182
	DM06311_1	Contig1450	0.89	0.254	0.52	0.325	0.87	0.281	0.89	0.536	0.93	0.366	0.86	0.173	0.90	0.422	0.76	0.439	0.80	0.195

	DM13800_1	Contig20	0.97	0.609	0.73	0.430	0.99	0.434	1.06	0.631	0.84	0.444	0.81	0.401	1.15	0.451	0.97	0.612	1.00	0.634
	DMAG0001S00002248	Contig2248	0.79	0.090	0.71	0.235	0.99	0.408	0.81	0.339	1.25	0.456	0.92	0.463	1.06	0.384	1.34	0.437	1.06	0.459
	DMAG0001S00002613	Contig2613	1.01	0.621	1.01	0.546	1.06	0.326	0.79	0.204	0.86	0.452	0.80	0.169	1.00	0.540	0.97	0.590	0.80	0.232
	DMAG0001S00003140	Contig3140	0.72	0.138	0.90	0.165	1.13	0.218	1.00	0.648	1.10	0.453	1.06	0.425	1.43	0.202	1.79	0.346	1.87	0.135
	DMAG0001S00003342	Contig3342	0.88	0.322	0.90	0.206	0.95	0.223	0.99	0.634	1.02	0.531	1.13	0.208	2.01	0.364	0.98	0.599	1.23	0.147
	DMAG0001S00004504	Contig4504	1.00	0.631	1.05	0.406	1.25	0.136	0.95	0.284	0.95	0.426	0.90	0.203	1.05	0.223	1.01	0.480	1.17	0.195
	DMAG0001S00004924	Contig4924	0.93	0.536	0.91	0.385	1.05	0.294	0.82	0.212	0.81	0.393	0.83	0.197	0.86	0.271	0.82	0.399	0.86	0.339
	DMAG0001S00007902	dm019d10.r	1.03	0.570	0.95	0.407	1.07	0.352	1.13	0.413	1.01	0.516	1.12	0.162	1.08	0.215	0.92	0.377	1.04	0.449
Juvenile	DM01516_1	Contig1405	1.11	0.546	2.04	0.316	1.31	0.115	1.10	0.528	0.93	0.478	0.90	0.290	0.86	0.204	0.88	0.455	1.03	0.611
hormone	DM02746_3	dm025j01.f	0.37	0.126	0.20	0.112	0.60	0.178	0.67	0.274	1.70	0.442	0.73	0.415	1.21	0.357	1.79	0.413	0.62	0.359
esterase (Vermunt et al., 1999)	DMAG0001S00001645	Contig1645	0.87	0.622	5.22	0.124	1.10	0.426	1.23	0.637	1.33	0.548	7.60	0.167	0.09	0.295	5.85	0.311	0.54	0.563
	DMAG0001S00002906	Contig2906	1.37	0.230	1.18	0.311	0.86	0.210	1.16	0.222	1.27	0.268	1.17	0.158	1.20	0.204	1.15	0.403	1.00	0.640
serine	DM00934_3	Contig2561	1.06	0.573	1.23	0.397	1.28	0.113	0.92	0.334	0.88	0.442	0.89	0.195	0.94	0.452	1.39	0.485	1.05	0.581
protease	DM01296_3	Contig3860	0.94	0.094	1.07	0.401	1.25	0.115	1.12	0.507	1.05	0.516	0.91	0.236	1.60	0.338	0.95	0.530	1.00	0.636

(Sui et al., 2009, Horst et al., 2007)	DM01553_2	dm062o12.r	1.08	0.433	1.03	0.472	1.01	0.413	1.10	0.469	1.03	0.520	1.06	0.147	1.09	0.327	1.04	0.515	1.07	0.282
	DM01701_3	Contig1133	0.29	0.137	0.18	0.142	0.29	0.108	0.91	0.423	1.32	0.444	0.95	0.516	1.05	0.449	1.08	0.479	0.22	0.223
	DM01783_1	Contig1454	0.19	0.125	0.07	0.137	0.13	0.115	0.93	0.515	1.68	0.437	1.07	0.487	0.97	0.509	0.81	0.533	0.23	0.188
	DM01879_2	Contig2097	1.66	0.078	1.59	0.155	1.37	0.164	1.33	0.305	1.19	0.442	1.23	0.247	0.73	0.194	0.87	0.488	0.95	0.563
	DM02129_3	Contig1102	0.41	0.070	0.21	0.158	0.29	0.108	0.67	0.320	1.49	0.445	0.88	0.474	0.78	0.286	1.12	0.557	0.39	0.180
	DM02236_1	dm073g02.r	0.53	0.297	0.43	0.225	0.48	0.108	1.19	0.571	1.24	0.405	0.80	0.458	1.70	0.253	2.25	0.369	0.72	0.498
	DM02473_3	Contig5193	0.68	0.360	0.97	0.535	1.45	0.154	1.07	0.603	0.57	0.327	0.77	0.338	1.22	0.476	0.66	0.370	1.24	0.462
	DM02712_1	dm026m04.f	1.01	0.629	0.97	0.522	2.22	0.115	0.69	0.487	1.03	0.559	1.16	0.479	1.20	0.413	1.73	0.366	1.86	0.329
	DM02712_2	Contig3807	0.75	0.436	0.86	0.484	0.88	0.331	0.65	0.327	0.64	0.258	1.46	0.354	1.38	0.263	1.29	0.540	1.54	0.497
	DM02908_3	Contig3998	0.81	0.464	0.79	0.222	0.91	0.301	0.73	0.347	0.92	0.447	0.73	0.320	0.61	0.180	0.68	0.337	0.78	0.307
	DM02990_3	Contig1854	0.80	0.555	0.89	0.490	1.89	0.214	1.13	0.617	0.81	0.486	0.88	0.484	0.67	0.360	0.70	0.464	1.09	0.543
	DM03029_1	Contig4436	9.05	0.093	4.71	0.173	1.18	0.115	1.10	0.574	1.16	0.445	1.40	0.401	1.98	0.231	7.24	0.425	5.22	0.210
	DM06032_1	Contig534	1.06	0.386	1.07	0.418	0.80	0.115	0.96	0.586	0.98	0.505	0.90	0.270	1.06	0.367	0.89	0.510	0.92	0.436
	DM06299_1	Contig4915	0.84	0.247	0.89	0.288	1.00	0.436	0.97	0.621	0.91	0.349	0.96	0.519	0.88	0.360	0.85	0.489	1.02	0.625
	DM06319_2	dm013n05.r	0.10	0.068	0.09	0.110	0.10	0.105	0.59	0.335	1.48	0.386	0.82	0.432	0.96	0.487	0.49	0.491	0.08	0.107
	DM06884_1	Contig1188	0.81	0.562	0.82	0.485	0.85	0.335	0.98	0.633	0.47	0.347	0.58	0.243	0.60	0.367	0.54	0.466	0.66	0.242
	DM07545_1	Contig4	0.93	0.590	1.21	0.491	0.40	0.288	0.81	0.601	0.56	0.433	0.37	0.129	0.36	0.249	0.29	0.327	0.14	0.323
	DM07929_1	Contig4106	0.82	0.430	0.78	0.362	1.68	0.192	1.08	0.325	1.43	0.438	1.26	0.231	1.79	0.180	1.53	0.344	1.51	0.180
	DM08152_2	Contig4161	0.72	0.154	0.62	0.268	0.71	0.114	1.37	0.334	1.12	0.442	1.21	0.174	1.16	0.269	0.82	0.311	0.75	0.163
	DM08607_1	Contig1835	0.33	0.077	0.20	0.121	0.20	0.078	0.73	0.248	1.21	0.453	0.78	0.271	0.94	0.414	0.73	0.476	0.18	0.120
	DM09252_1	IGU001_0042_A12.r	0.89	0.046	1.04	0.448	1.16	0.137	0.92	0.298	0.89	0.442	0.88	0.239	0.90	0.234	0.91	0.487	0.95	0.512
	DM09746_2	WTH001_00	1.18	0.540	1.09	0.496	1.13	0.294	1.05	0.622	1.95	0.288	1.87	0.184	1.44	0.264	1.34	0.400	1.70	0.191

	05_K11.f																	
DM10493_1	Contig1697	1.55	0.047	1.46	0.191	1.05	0.126	0.85	0.348	0.96	0.467	0.85	0.270	0.87	0.205	0.69	0.322	0.85	0.141
DM12902_2	dm063h14.r	0.74	0.278	0.78	0.335	1.11	0.142	0.79	0.384	1.20	0.458	0.90	0.439	1.11	0.349	1.44	0.401	1.10	0.464
DMAG00015 00000091	Contig91	0.39	0.327	0.80	0.444	3.43	0.138	1.72	0.286	1.97	0.366	1.51	0.151	5.53	0.180	5.66	0.311	6.08	0.131
DMAG00015 00000388	Contig388	0.37	0.060	0.31	0.194	1.25	0.263	0.89	0.453	1.65	0.433	1.09	0.460	1.67	0.209	1.64	0.336	1.20	0.499
DMAG00015 00000485	Contig485	0.59	0.184	0.69	0.224	1.39	0.174	0.82	0.336	1.75	0.432	1.11	0.499	1.27	0.227	1.63	0.432	1.69	0.211
DMAG00015 00000594	Contig594	2.53	0.048	2.66	0.141	2.75	0.107	1.05	0.534	1.03	0.520	1.08	0.313	0.96	0.300	0.88	0.444	1.36	0.138
DMAG00015 00000964	Contig964	1.09	0.340	0.98	0.494	1.04	0.376	0.96	0.521	0.98	0.498	1.04	0.359	1.20	0.233	1.14	0.473	1.25	0.263
DMAG00015 00000965	Contig965	1.45	0.410	0.96	0.509	0.62	0.162	1.16	0.373	0.96	0.540	1.29	0.226	1.15	0.232	0.87	0.475	1.29	0.278
DMAG00015 00001306	Contig1306	0.85	0.228	0.89	0.303	0.87	0.230	0.97	0.614	0.91	0.398	0.87	0.184	0.84	0.202	0.79	0.379	0.89	0.265
DMAG00015 00001683	Contig1683	1.57	0.040	1.32	0.192	1.16	0.190	1.16	0.322	1.15	0.435	1.13	0.201	1.23	0.202	1.16	0.481	1.21	0.263
DMAG00015 00001819	Contig1819	0.35	0.223	0.48	0.277	1.84	0.214	1.29	0.286	1.86	0.397	1.32	0.243	2.99	0.180	3.00	0.325	3.20	0.136
DMAG00015 00002351	Contig2351	0.67	0.484	1.11	0.521	4.22	0.139	2.33	0.184	3.18	0.378	1.97	0.268	5.54	0.180	6.23	0.311	7.92	0.129

DMAG00015000002515	Contig2515	0.69	0.323	0.77	0.340	1.14	0.371	0.78	0.394	0.62	0.380	0.48	0.208	1.37	0.230	1.46	0.311	2.08	0.123
DMAG00015000002576	Contig2576	0.65	0.044	0.54	0.152	0.51	0.108	0.88	0.524	0.75	0.356	0.83	0.309	0.69	0.180	0.57	0.321	0.47	0.217
DMAG00015000002816	Contig2816	0.59	0.187	0.54	0.247	0.95	0.161	0.60	0.334	1.05	0.550	0.80	0.400	0.94	0.471	1.31	0.488	1.28	0.362
DMAG00015000002824	Contig2824	1.97	0.187	0.91	0.470	0.23	0.108	1.63	0.352	1.57	0.399	1.10	0.500	0.61	0.291	0.52	0.321	0.23	0.172
DMAG00015000002866	Contig2866	0.41	0.162	0.23	0.151	0.62	0.158	1.29	0.433	2.61	0.331	1.49	0.305	1.56	0.202	1.53	0.466	0.70	0.207
DMAG00015000002972	Contig2972	0.33	0.131	0.24	0.219	1.07	0.396	0.91	0.595	2.17	0.387	1.13	0.418	0.83	0.357	0.65	0.408	0.62	0.374
DMAG00015000003098	Contig5034	0.27	0.077	0.18	0.137	0.33	0.115	0.95	0.471	1.18	0.447	1.08	0.470	1.26	0.202	1.07	0.560	0.56	0.180
DMAG00015000003477	Contig3477	0.45	0.334	0.94	0.519	3.80	0.132	1.63	0.277	1.89	0.370	1.41	0.173	5.07	0.180	5.43	0.311	6.35	0.122
DMAG00015000003817	Contig3817	2.36	0.039	2.19	0.132	1.52	0.106	1.29	0.245	1.23	0.382	1.12	0.283	0.86	0.280	0.91	0.545	0.91	0.411
DMAG00015000004791	Contig4791	0.97	0.544	0.94	0.359	1.08	0.223	0.91	0.280	0.91	0.442	0.92	0.185	1.05	0.396	0.99	0.606	1.11	0.235
DMAG00015000004902	Contig4902	1.12	0.356	2.31	0.131	3.12	0.106	1.09	0.533	0.97	0.501	1.04	0.424	1.43	0.218	1.15	0.504	2.01	0.180
DMAG00015	Contig4997	0.24	0.101	0.17	0.156	0.27	0.106	1.13	0.455	1.84	0.348	1.20	0.314	3.98	0.180	2.71	0.311	0.57	0.244

00004997																			
DMAG0001S00005217	Contig5217	1.22	0.258	1.23	0.196	1.23	0.239	1.29	0.284	1.15	0.323	1.15	0.171	1.15	0.202	0.91	0.536	1.26	0.132
DMAG0001S00005714	IGU001_0055_G07.f	1.25	0.293	1.37	0.118	1.74	0.108	1.13	0.385	1.08	0.306	1.14	0.266	1.08	0.361	0.90	0.489	1.34	0.221
DMAG0001S00006070	WTH001_0005_K11.r	0.70	0.031	0.78	0.173	0.92	0.122	0.70	0.185	0.77	0.235	0.69	0.129	0.64	0.180	0.69	0.319	1.21	0.546
DMAG0001S00007307	dm010k23.f	0.44	0.092	0.30	0.169	0.62	0.113	0.71	0.310	1.32	0.444	0.92	0.486	1.10	0.418	1.15	0.478	0.46	0.146
DMAG0001S00007878	dm018n22.r	0.88	0.358	0.88	0.433	1.13	0.168	0.82	0.339	1.08	0.492	0.93	0.478	1.08	0.349	1.33	0.407	1.11	0.403
DMAG0001S00007885	dm018p12.r	1.83	0.155	1.36	0.268	0.85	0.229	1.47	0.322	1.29	0.377	1.43	0.135	0.94	0.425	0.76	0.441	0.80	0.237
DMAG0001S00008092	dm021k17.r	0.18	0.048	0.06	0.124	0.05	0.108	0.76	0.184	1.10	0.469	0.92	0.452	0.92	0.400	0.60	0.388	0.15	0.173
DMAG0001S00009047	dm039a15.r	1.12	0.425	1.87	0.264	1.21	0.113	1.14	0.511	0.89	0.443	1.22	0.422	1.39	0.315	0.89	0.466	0.94	0.482
DMAG0001S00009524	dm048j11.f	0.24	0.127	0.14	0.142	0.34	0.115	0.81	0.413	1.66	0.427	1.04	0.529	1.23	0.234	1.44	0.468	0.57	0.227
DMAG0001S00009668	dm051e05.r	1.04	0.547	1.04	0.499	0.73	0.182	1.30	0.470	0.88	0.464	0.94	0.337	0.86	0.445	0.71	0.458	1.24	0.529
DMAG0001S00009733	dm053a24.f	0.48	0.358	1.06	0.526	4.36	0.132	1.54	0.314	1.77	0.388	1.41	0.241	5.03	0.180	6.14	0.311	7.42	0.123

Table 3-6 List of KEGG pathways in response to methoprene, fenoxycarb and epofenonane, respectively.

Chemical	Up- or down-regulated	KEGG ID	Pathway Name
Methoprene	Up	00480	Glutathione metabolism
		00590	Arachidonic acid metabolism
		00625	Chloroalkane and chloroalkene degradation
		00980	Metabolism of xenobiotics by cytochrome P450
		00982	Drug metabolism - cytochrome P450
	Down	00130	Ubiquinone and other terpenoid-quinone bioshynthesis
		00350	Tyrosine metabolism
		00360	Phenylalanine metabolism
		00430	Taurine and hypotaurine metabolism
		00460	Cyanoamino acid metabolism
		00480	Glutathione metabolism
		00511	Other glycan degradation
		00590	Arachidonic acid metabolism
		00620	Pyruvate metabolism
Fenoxycarb	Up	00230	Purine metabolism
		00250	Alanine, aspartate and glutamine metabolism
		00310	Lysine degradation
		00330	Arginine and proline metabolism
		00625	Chloroalkane and chloroalkene degradation
		00910	Nitrogen metabolism
	Down	00230	Purine metabolism
		00480	Glutathione metabolism
		00980	Metabolism of xenobiotics by cytochrome P450
		00982	Drug metabolism - cytochrome P450
Epofenonane	Up	00480	Glutathione metabolism
		00520	Amino sugar and nucleotide sugar metabolism
		00590	Arachidonic acid metabolism
		00625	Chloroalkane and chloroalkene degradation

	00980	Metabolism of xenobiotics by cytochrome P450
	00982	Drug metabolism - cytochrome P450
Down	None	None

Figures

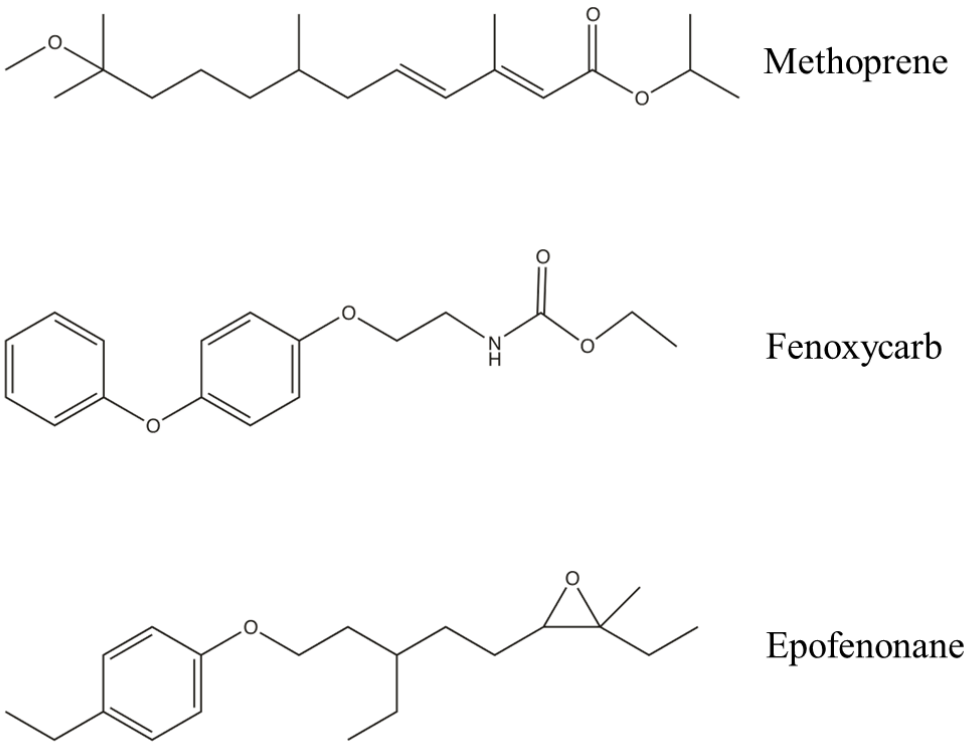

Figure 3-1. Chemical structures of methyl farnesoate, fenoxycarb and epofenonane.

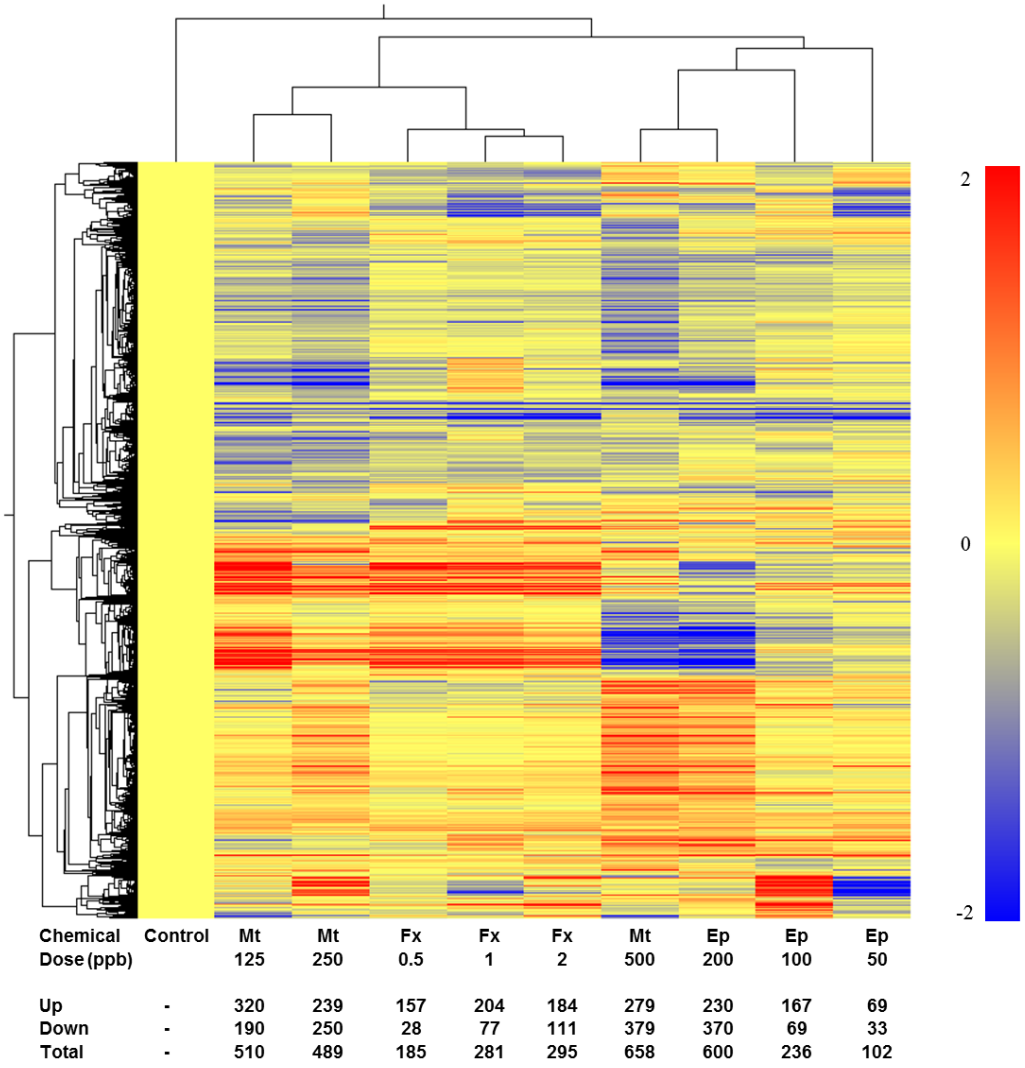

Figure 3-2. A heat map with hierarchical clustering of the selected genes after three independent microarray analyses. Lower table indicates that the number of up- and downregulated genes in response to three JH analogs at three concentrations.

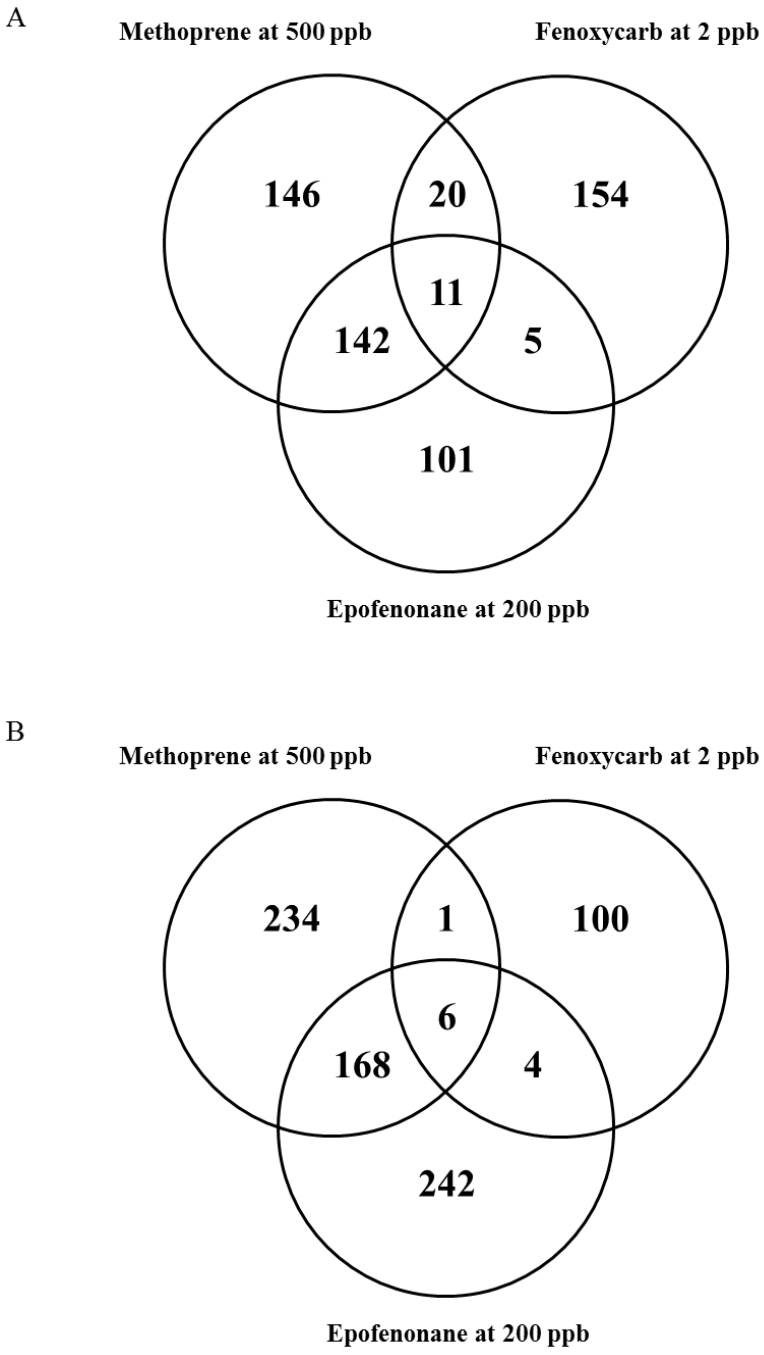

Figure 3-3. Venn diagram showing number of up-regulated (A) and down-regulated (B) genes with significant expression change among the three JH analogs at highest concentrations.

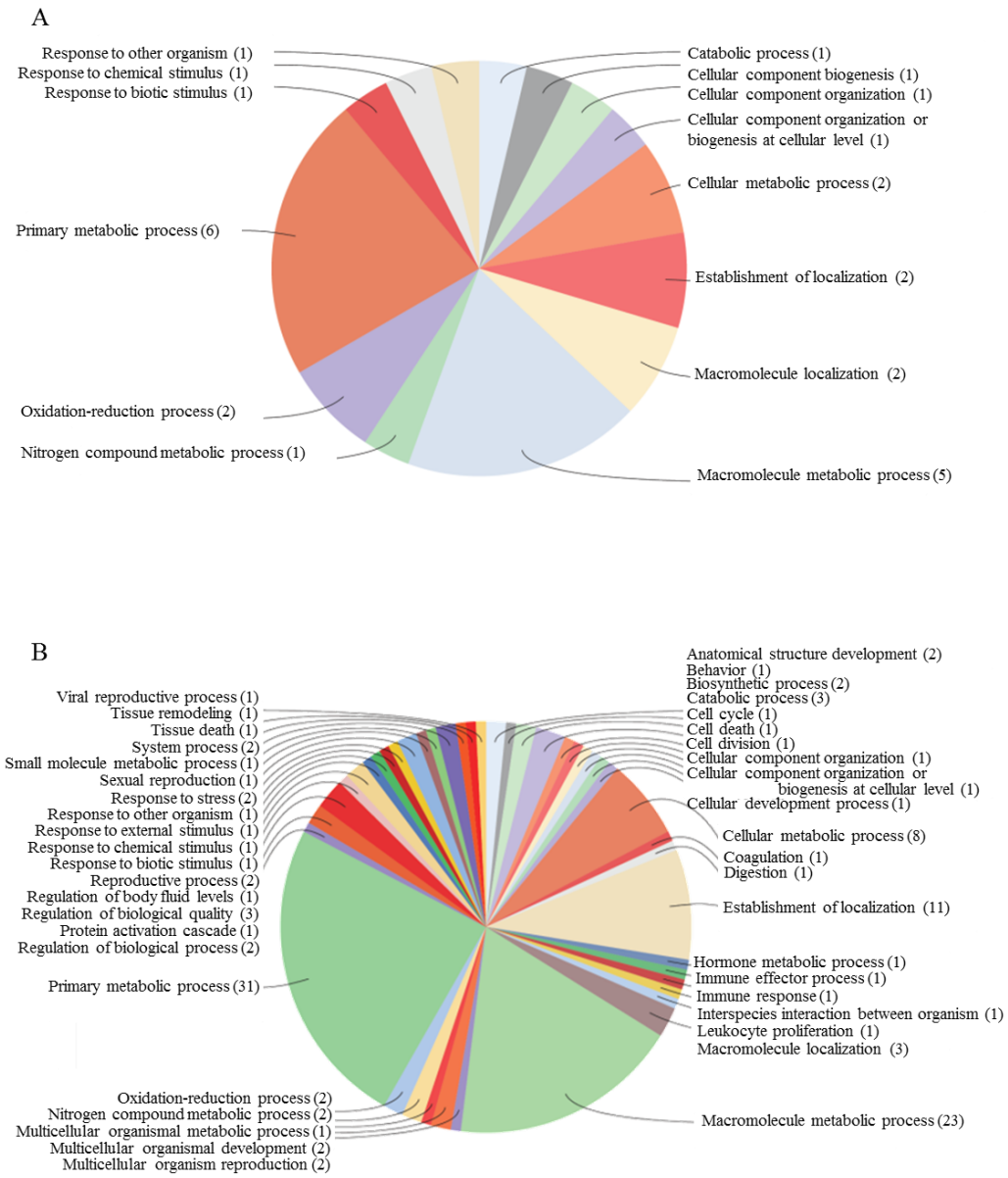

Figure 3-4. Biological processes up-regulated and down-regulated by exposure to JH analogs at three concentrations determined by gene ontology annotation. Blast2GO was utilized to map differentially expressed genes to gene ontology (GO) terms. Major GO terms representing biological processes are shown for common up-regulated (A) and down-regulated (B) genes to give an overview of the processes that are disrupted by methoprene treatment. Biological processes were shown in GO terms at level 3.

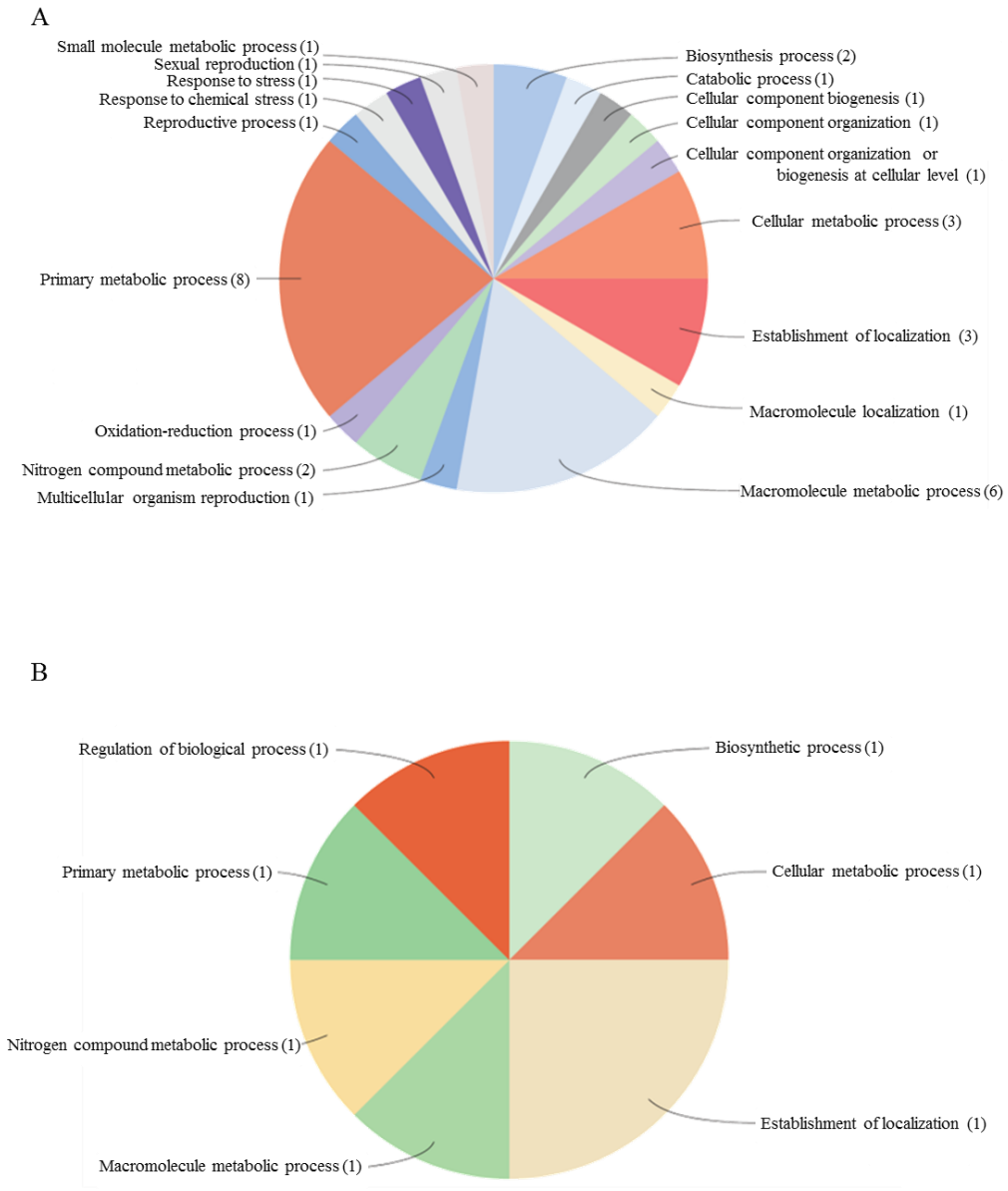

Figure 3-5. Major GO terms representing biological processes are shown for common up-regulated (A) and down-regulated (B) genes to give an overview of the processes that are disrupted by epofenonane treatment. Biological processes were shown in GO terms at level 3.

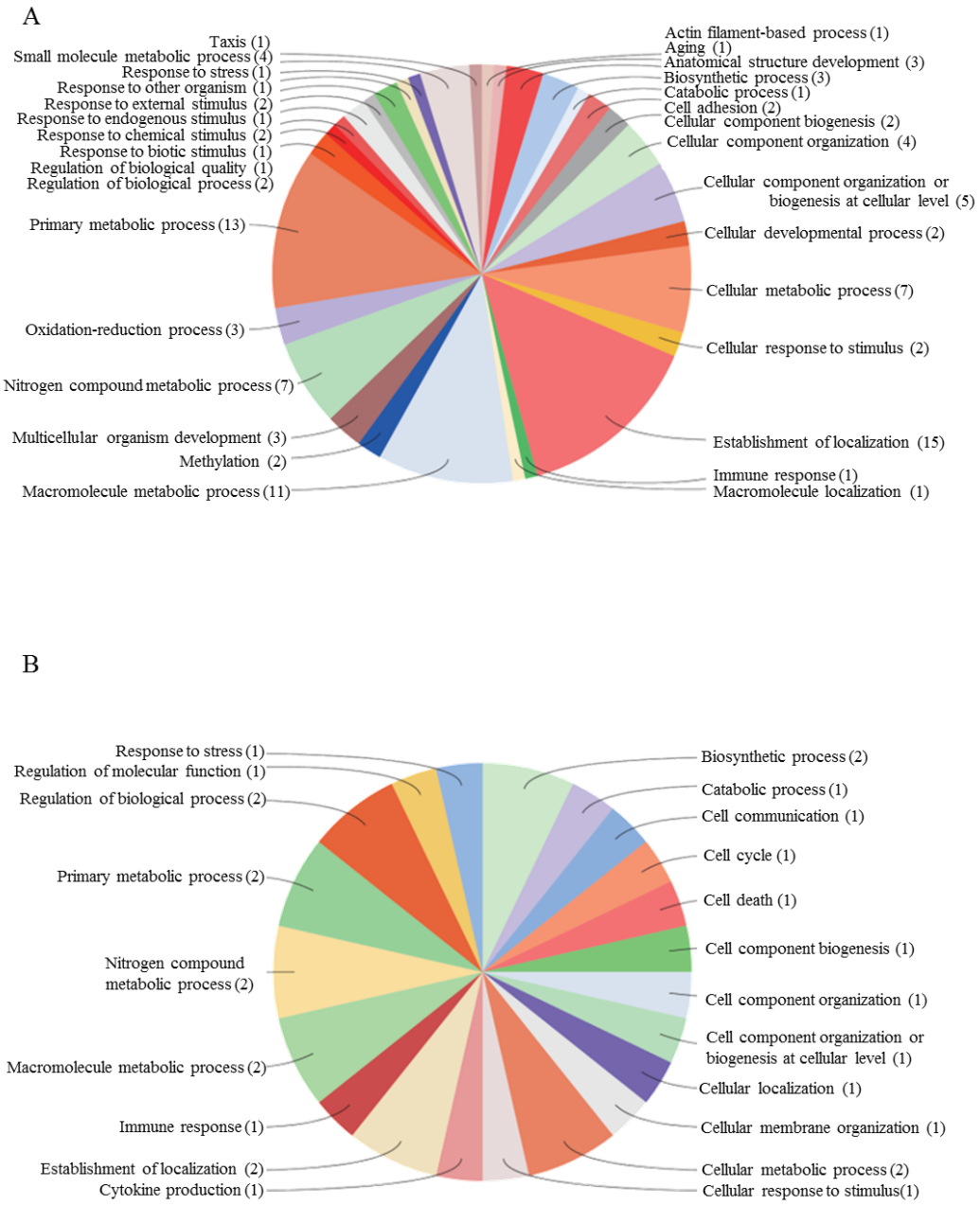

Figure 3-6. Major GO terms representing biological processes are shown for common up-regulated (A) and down-regulated (B) genes to give an overview of the processes that are disrupted by fenoxycarb treatment. Biological processes were shown in GO terms at level 3.

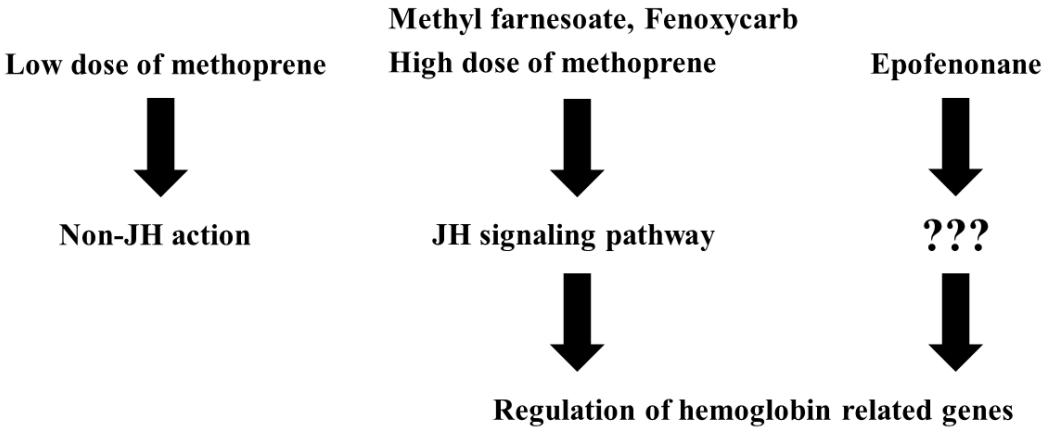

Figure 3-7. Schematic depicting the putative regulation cascades of hemoglobin-related genes by JH analogs.

Chapter IV

Molecular cloning of *doublesex* genes of four cladocera (water flea) species

Abstract

The gene *doublesex* (*dsx*) is known as a key factor regulating genetic sex determination in many organisms. Our group previously identified two *dsx* genes (*DapmaDsx1* and *DapmaDsx2*) from a freshwater branchiopod crustacean, *Daphnia magna,* which are expressed in males but not in females. *Daphnia magna* produces males by parthenogenesis in response to environmental cues, and showed that *DapmaDsx1* expression during embryonic stages is responsible for the male trait development. The *Dapmadsx* genes are thought to have arisen by a lineage-specific duplication; therefore, to investigate evolutionary conservation of sex specific expression of *dsx* genes and to further assess their functions in the ESD, I searched for *dsx* homologs in four closely-related cladoceran species. I identified both *dsx* genes from, *D. pulex, D. galeata*, and *Ceriodaphnia dubia,* yet only a single *dsx* gene was found from *Moina macrocopa*. Molecular phylogenetic analysis suggested that the *dsx* gene duplication occurred prior to the divergence of these cladoceran species, therefore I infer that *M. macrocopa* lost *dsx2* gene secondarily. Furthermore, all *dsx* genes identified in this study showed male-biased expression levels, yet only half of the putative 5' upstream regulatory elements are preserved in *D. magna* and *D. pulex*. The functions of the *dsx* genes are likely conserved among cladoceran species, yet the differences in putative regulatory elements and expression levels observed do suggest a divergence in *dsx2* gene functions, although still associated with ESD.

Introduction

Sex determination is a fundamental developmental process, affecting the sexual differentiation of gonads, and leads to sex-specific differences in behavior, physiology and morphology. Sex-determining systems can be divided into two categories: GSD and ESD (Bull, 1985; Marin and Baker, 1998; Zarkower, 2001). GSD is attributed to the genetic segregation of genes, often residing on sex chromosomes that initiate alternate sex-determining developmental pathways. In contrast, ESD has repeatedly arisen during animal evolution (Organ and Janes, 2008) and is initiated by diverse environmental cues, such as temperature, photoperiod, nutrition and population density, that trigger alternative genetic signals, resulting in the regulation of male or female sex-determining genes (Crews and Bull, 2009; Korpelainen, 1990).

Natural selection of rare mutational variants has been suggested to mediate the transitions between GSD and ESD (Bull, 1981; Bulmer and Bull, 1982). A previous phylogenetic analysis revealed that there have been at least three independent switches from GSD to ESD in lizards, and six transitions from ESD to GSD in turtles (Chandler et al., 2009). Moreover, previous experiments using temperature-sensitive mutations created artificially in *Caenorhabditis elegans* demonstrated how GSD could rapidly evolve into ESD as a consequence of a mutation in key sex-determining genes (Chandler et al., 2009). Orthologs of GSD genes such as *dmrt1*, *sox9* and *cyp19a* (aromatase) are expressed in the gonads during the temperature-sensitive period in TSD of reptiles (Shoemaker and Crews, 2009). Thus, according to the current interpretation of these data, TSD mechanisms are likely to share many sex-determining components with GSD (Crews and Bull, 2009).

Sex determination systems in insects vary considerably in key factors and

regulatory mechanisms to develop sex-specific traits. The sex determination mechanism in *D. melanogaster* is best understood. The ratio of X chromosomes to autosomes (X:A ratio) is thought to provide the initial signal for the activation of *sex-lethal* (*sxl*), a master gene of the sex determination cascade. Then, *sxl* is produced the sex-specific splicing isoforms. *Sxl* in female acts on the pre-mRNA of *transformer* (*tra*) resulting in reproduction of functional Tra. The functional Tra in the female, in concert with Tra2, regulates the production of female-specific *dsx* mRNA, which is a critical and terminal transcription factor in the fly sex determining cascade. *Dsx* is spatially and temporally transcribed into two sex-specific splice forms conferring sexually dimorphic traits during development (Burtis and Baker, 1989; Robinett et al., 2010). The male-specific splice form of *dsx* mRNA is the default splice variant in *D. melanogaster*. *Dsx* regulates the various sex-specific traits such as gonads. Recently, sex determination mechanisms have also been demonstrated in various insect lineages such as Diptera (*M. domestica* and *C. capitata*), Hymenoptera (*A. mellifera* and *N. vitripennnis*) and Coleoptera (*T. castaneum*). These studies revealed that *tra* and *dsx* are highly conserved among insects (Gempe and Beye, 2011; Sanchez, 2008; Shukla and Nagaraju, 2010; Shukla and Palli, 2012). However, in case of Lepidoptera, *B. mori*, *tra* and *tra2* are assumed not to be required for the sex-specific splicing of *Bmdsx* pre-mRNA, because *Bmdsx* has no Tra/Tra2 binding motif. Recently, it has been revealed that binding of the *BmPSI*, a *Bombyx* homolog of *P-element* somatic inhibitor, to the exonic splicing suppressor sequence on expected region is involved in sex-specific splicing of *Bmdsx* (Shukla and Nagaraju, 2010). These data suggest that upstream genetic cascades of *dsx* might be diverse among insects.

The cladocera (commonly called water fleas) is an ancient clade of

branchiopod crustaceans comprising 16 or 18 family lineages (Olesen, 1998; Stenderup et al., 2006) that all reproduce by cyclical parthenogenesis (Taylor et al., 1999). The well-studied species are from the family Daphniidae, particularly of the genus *Daphnia*. *Daphnia* inhabit freshwater ponds and lakes on all continents and are known to switch between parthenogenetic and sexual reproduction when environmental conditions for growth and reproduction deteriorate. During normal growing conditions, populations are most often entirely composed of females. However, shortened photoperiod, a lack of food and/or increased population density all lead to the clonal production of males that are genetically identical to their sisters and mothers (Kleiven et al., 1992). First instar male juveniles are easily distinguished from the females (Olmstead and LeBlanc, 2000). During maturation, daphnids undergo morphological sexual differentiation of various somatic tissues, including the armament of a first thoracic leg with the copulatory hook in males, which becomes larger during the fifth instar (Mitchell, 2001). Gonads develop and finally settle at both sides of the gut during embryogenesis in both sexes (Sagawa et al., 2005). The appearance of males allows sexual reproduction to occur (Hebert, 1987; Stross and Hill, 1965), when females begin producing haploid eggs requiring fertilization.

Recently, our group and others found that male production occurred independently of environmental cues by treatment with exogenous JH or its analogs (Olmstead and LeBlanc, 2002; Tatarazako et al., 2003). Exposure of *D. magna* to JH analogs at the stage corresponding to the environmentally-sensitive period for sex determination of a cladoceran species of the family Moinidae (Banta and Brown, 1929b), produced exclusively male broods, suggesting that JH could be a key molecule for understanding mechanisms of the ESD (Kato et al., 2010; Olmstead and LeBlanc,

2002; Tatarazako et al., 2003).

A *dsx* gene was originally identified in *D. melanogaster* as a critical and terminal transcription factor in the fly sex determining cascade. *Dsx* is spatially and temporally transcribed into two sex-specific splice forms conferring sexually dimorphic traits during development (Burtis and Baker, 1989; Robinett et al., 2010). The *dsx* gene contains two conserved domains: the Dsx/Mab-3 (DM) domain at the N-terminus and the oligomerization domain at the C-terminus (Bayrer et al., 2005). Genes encoding DM-domain (DM-domain genes) were discovered to play a related role in *C. elegans* (Raymond et al., 1998; Shen and Hodgkin, 1988) and also in vertebrates (Kopp, 2012; Matson and Zarkower, 2012; Raymond et al., 2000). In contrast, results from numerous studies have shown that other genes in the genetic sex-determination cascade widely diversified among species (Marin and Baker, 1998; Williams and Carroll, 2009; Zarkower, 2001).

To understand the molecular and evolutionary relationships between GSD and ESD, our group previously identified and analyzed three DM-domain genes (DMRT11E, DMRT93B and DMRT99B) from *D. magna*, displaying sexual dimorphic gene expression patterns in adult gonads (Kato et al., 2008). However, none of these DM-domain genes exhibited sexually dimorphic expression patterns during embryonic development, suggesting that they are not involved in sex determination (Kato et al., 2008). Two additional DM-domain genes were later found in the *D. magna* ESTs database (Watanabe et al., 2005). Therefore, they analyzed the function of these two genes from *D. magna* using gene manipulation (Kato et al., 2011b). These experiments revealed that two *dsx* genes in *D. magna* were obtained by lineage-specific duplication, and then one of the paralogs, *D. magna dsx1* (*DapmaDsx1*), plays an important role in

directing the major sexually dimorphic development of *D. magna* (Kato et al., 2011a). In contrast, specific function of *D. magna dsx2* (*DapmaDsx2*) remains unknown. These newly identified *dsx* genes showed greater sequence similarity at the amino acid sequence level to known insect *dsx* genes than to the previously identified DM-domain containing genes in *D. magna*. A genome-wide study of gene functions in *D. pulex* suggested that lineage-specific duplicated genes are most responsive to varying environmental conditions (Colbourne et al., 2011).

In the chapter, I investigated the sequence and functional conservations of the two *dsx* genes identified from broader taxonomic cladocerans consist of representing two families and three genera; *D. pulex, D. galeata, C. dubia,* and *M. macrocopa*. I also analyzed the genomic structures of cloned *dsx* genes of *D. magna* and *D. pulex* including their putative regulatory motifs and putative transcription factor binding sites at the 5' upstream regions of these duplicated *dsx* genes.

Materials and Methods

Daphnia strain and culture conditions

Isoclonal strains of *D. magna* (NIES and Belgium strains), *D. galeata*, *C. dubia* and *M. macrocopa* were obtained from the NIES (Tsukuba, Japan) (Oda et al., 2011; Oda et al., 2005b). *Daphnia pulex* was obtained from Hokkaido University, Sapporo, Japan (Hiruta et al., 2010), and maintained as described previously (Tatarazako et al., 2003). Briefly, culture medium was prepared using charcoal-filtered tap water and cultures of 20 individuals per liter were incubated at 21±1°C under a 14-h light/10-h dark photoperiod. A 0.01-ml suspension of 4.3 x 10^8 cells ml^{-1} Chlorella (*Chlorella vulgaris*) was added daily to each culture. The water hardness was between 72 and 83 mg L^{-1}, the pH between 7.0 and 7.5, and the dissolved oxygen concentration between 80 and 99%. To obtain natural male embryos, adult *D. magna* (Belgium clone) was reared in crowded conditions, and *D. pulex* was incubated at 18°C under a 10-h light/14-h dark photoperiod, and a 0.01-ml suspension of 4.3 x 10^8 cells ml^{-1} Chlorella was added every two days. To induce male offspring of *D. magna* (NIES clone), *D. galeata, C. dubia and M. macrocopa*, in which natural males are rarely seen, adult individuals (about 2 weeks of age) were chemically induced to produce males by treating them with a synthetic JH analog, fenoxycarb (1 μg/L) (technical grade 96.6% pure, Wako Pure Chemical Industries, Ltd., Osaka, Japan) (Oda et al., 2005b). I confirmed the offspring sexes by the length of the first antenna (Olmstead and LeBlanc, 2000) observed and photographed using a Leica MZ APO dissecting microscope (Leica, Mannheim, Germany).

Cloning of *dsx* genes

The nucleotide sequences of the *D. magna dsx* genes were used for designing primers that amplify *dsx* genes in four different species. The harvested animals were homogenized using the Micro Smash MS-100R (Tomy, Tokyo, Japan). Total RNA was extracted with ISOGEN reagent according to the manufacturer's protocol (NIPPON GENE, Tokyo, Japan). Poly (A)+ RNA was isolated from purified total RNA using Fast Track (Life Science, Carlsbad, CA) and converted to cDNA using Superscript III and random primers (Life Science) according to the manufacturer's protocol. cDNAs corresponding to the EST sequences were obtained by PCR amplification, and full-length cDNAs were obtained by RACE (Cap Fishing; SeeGene, Seoul, South Korea) using the oligonucleotide sequences as shown in **Table 4-1**.

Phylogenetic analysis of the DM-domain genes

A phylogenetic tree of DM-domain genes including newly cloned *D. pulex*, *D. galeata*, *C. dubia* and *M. macrocopa dsx* genes were constructed using amino acid sequences of DM-domain genes used in the previous study (Kato et al., 2008) **(Table 4-2)**. A multiple alignment was constructed using Clustal W (Tamura et al., 2011; Thompson et al., 1994) with the following settings (pairwise alignment parameters: gap opening penalty 15, gap extension penalty 6.66, identity protein weight matrix; multiple alignment parameters: delay divergent cutoff 30%, gap separation distance 4). Phylogenetic reconstruction was performed using the maximum likelihood and the neighbor-joining methods implemented in MEGA version 5 (Tamura et al., 2011).

Quantitative PCR analysis

Two to three weeks old male and female individuals of the five cladoceran species were used in quantitative-PCR assays of gene expression levels. mRNAs were quantified as described previously (Kato et al., 2008). Animals were washed briefly and soaked in RNAlater (Life Science, Austin, TX) for 10 min. Total RNA was purified and cDNA was synthesized as described above except that a random oligonucleotide was used as the primer. PCR was performed in an ABI Prism 7000 (Life Science) using the SYBR-Green PCR core reagents kit (Life Science), in the presence of appropriate primers. PCR amplifications were performed using the following conditions: 2 min at 50°C and 10 min at 95°C, followed by a total of 40 two-temperature cycles (15 sec at 95°C and 1 min at 60°C).

The primers were chosen to amplify short PCR products of 150 bp; the primer sequences are listed in **Table 4-3**. Ribosomal protein L32 gene was used for normalization purposes (Kato et al., 2007; Sagawa et al., 2005). Data acquisition and analysis were performed by ABI Prism 7000 SDS software ver. 1.1 (Applied Biosystems). The baseline and threshold for the Ct (cycle threshold) were set automatically. Each gene was tested in technical triplicate samples by the relative standard curve method. In the case of *D. magna* and *D. pulex*, each experiment was performed in biological triplicate and statistical analyses were performed.

***Doublesex* gene annotations**

The genomic locations of *DapmaDsx1-α*, *DapmaDsx1-β*, and *DapmaDsx2* mRNA transcripts were identified using BLASTN sequence similarity searches against a reference BLAST database of the *D. magna* genome assembly v2.4 scaffolds, and

against a reference BLAST database of the *D. pulex* genome assembly v1.1 scaffolds. The best BLAST matches were analyzed and used to map the gene exons onto the *D. magna* and *D. pulex* scaffolds. ESTs mapped onto the genome assembly with PASA (Haas et al., 2003), microarray tiling path expression data, and RNA-Seq data from wFleaBase (Colbourne et al., 2005) were used as supporting evidence for exon annotations. The *dsx* gene annotation figures were created with AnnotationSketch (Steinbiss et al., 2009) **(Figure 4-1)**.

Transcription factor map alignments

Matscan (Blanco et al., 2006) was used to search for matches to 125 JASPAR core insect transcription factor binding site (TFBS) matrices and 44 TRANSFAC insect TFBS matrices in each *dsx* promoter region in *D. magna* and *D. pulex*. A threshold of 0.85 matrix similarities was used to find TFBS matrix matches in the promoter sequences. For each promoter sequence, the collection of TFBS matrix matches is referred to as its TF-map. Meta (Blanco et al., 2006) was then used to find the best meta-alignment of the orthologous promoters TF-maps (with parameters: a=0.5, l=0.1, m=0.1).

***De novo* conserved promoter motifs**

The 5' upstream region of 1.0 Kbp was extracted from all *D. pulex* gene models and used to create a background frequency model for 8 bp length motifs in *Daphnia* promoter regions. WeederH (Pavesi et al., 2007) was used to search for conserved regulatory motifs of length 8 bp present in all 6 *dsx* promoters in *D. magna* and *D. pulex*. That algorithm measures conservation based on the sequence conservation as well as the

motif occurrence's positions relative to the transcription start site (TSS). WeederH produces a χ^2 score assessing how conserved the motif is compared to the rest of the homologous sequences. I used a χ^2 score threshold of 3, discarding motifs with a χ^2 score less than 3.

Results and Discussion

Molecular cloning of *dsx* genes from cladocerans

To verify whether paralogs of *dsx* genes among daphnids are conserved, I first identified *dsx* genes from four cladocerans (*D. pulex*, *D. galeata*, *C. dubia* and *M. macrocopa*), then characterized them by comparison with *dsx* genes of *D. magna* and several insect species (Kato et al., 2011a; Oliveira et al., 2009) **(Figure 4-2)**. As a result, two *dsx* paralogs were identified from *D. pulex*, *D. galeata* and *C. dubia*, while only one was isolated from *M. macrocopa* **(Figures 4-2B, 4-3)**. The deduced amino acid sequences of all 9 homologs contained the expected DM- and oligomerization-domains, which are characteristic for all arthropod DSX family members (Bayrer et al., 2005; Volff et al., 2003) (**Figures 4-4, 4-5**). Phylogenetic analysis with other known DSX of various species revealed that DSX of cladocerans grouped into two distinct monophyletic groups: DSX1 and DSX2 **(Figure 4-6)**. Because DSX of the giant tiger prawn *Penaeus monodon* is rooted ancestrally to both DSX1 and DSX2, the gene duplication event likely occurred after the divergence of Branchiopoda and Malacostraca **(Figure 4-6)**. In the present study, only *dsx1*, but not *dsx2* gene, was identified from *M. macrocopa*. To test whether another copy might exist, I performed reverse transcription PCR assays using primers corresponding to highly conserved region of *dsx1* and *dsx2* genes among Daphniidae. Only a single amplified DNA could be detected from both sexes in *M. macrocopa* **(Figure 4-3)**. These results suggest that the *dsx* gene duplication occurred prior to the divergence of these cladoceran species, therefore I infer that the *M. macrocopa dsx2* gene was secondarily lost.

By comparing the DapmaDsx1 sequence to paralogs from the four studied species (*D. pulex*, *D. galeata*, *C. dubia* and *M. macrocopa*), I found that DapmaDsx1

shows 88-58%, 100-95%, 88-48%, 100-78% and 96-61% sequence identities to the A, B (DM-domain), C, D (oligomerization-domain) and E domains, respectively **(Figure 4-4A)**. Similarly, by comparing the DapmaDsx2 sequence with identified paralogs, I observed that DapmaDsx2 shows comparable relative ratios among each of the domains: 74-66%, 98-97%, 88-67%, 100-78% and 92-69% sequence identities to the A, B, C, D and E domains, respectively **(Figure 4-5A)**. These results suggest that putative amino acids of both the DM- and oligomerization-domains are highly conserved among the Cladocera. On the other hand, amino acid similarities outside of these domains are lower, and are proportional to the evolutionary distance between each genus; *Daphnia*, *Ceriodaphnia* and *Moina* (Swain and Taylor, 2003) **(Tables 4-4, 4-5)**.

The DM-domain contains zinc chelating residues, and among the insects studied to date, two highly conserved amino acid residues, threonine and glutamine **(**Boxed in **Figures 4-4B, 4-5B)**, distinguish the DM-domain of DSX from DM-domains of other insect proteins (Oliveira et al., 2009). Therefore, I searched for similar highly conserved amino acid residues within the DSX DM-domains of cladocerans. Indeed, all zinc chelating residues are found to be conserved in the DM domains of DSX1 and DSX2 among the five cladoceran species **(Figures 4-4B, 4-5B)**. Yet, although the threonine and glutamine residues were conserved in DSX2, the glutamine residue in DSX1 was substituted by arginine in all cladoceran species examined **(Figures 4-4B, 4-5B)**. These results suggest that DSX1 in cladocerans might have gained a novel function affecting in sex determination by amino acid replacement after duplication of *dsx* in branchiopoda lineage.

Compared to the DM-domains, more amino acid variation is observed in alignments of the oligomerization-domains **(Figures 4-4C, 4-5C)**. Dimerization, which

enhances specific DNA binding, is mediated by several residues in a non-polar interface that is conserved within oligomerization-domains. Previous study has revealed that, in DSX2 of *D magna*, two of three nonpolar amino acids indispensable for formation of the nonpolar interface are substituted with the polar acidic amino acid, aspartic acid (Kato et al., 2011a). This suggests that the daphnid DSX2 proteins are unable to dimerize and may not be functional or may have a different, unknown functions.

Sex-specific expression of *dsx* genes in five cladoceran species

Our group previously reported that both *dsx* genes in *D. magna* were transcriptionally up-regulated in males and showed no sex-specific splice isoforms. Our and other groups also reported that exposure to JH analogs reliably produces male daphnids (Olmstead and LeBlanc, 2002; Tatarazako et al., 2003). Moreover, by using gene knock-down (RNAi) and overexpression methods in *D. magna* (Kato et al., 2011a; Kato et al., 2011b), our group discovered that *DapmaDsx1* is necessary and sufficient for sex determination in *D. magna*, whereas the tandemly duplicated *DapmaDsx2* gene does not determine sex, even though its transcription is equally sex-biased (Kato et al., 2011a). In this study, I confirmed that expression patterns of *DapmaDsx1* and *DapmaDsx2* homologous genes are conserved in other cladocerans, by studying steady state mRNA levels for *dsx* transcripts in adult females and males by quantitative PCR. I found that the mRNA levels of these *dsx* genes range from 7 to 40-fold greater in males than in females **(Figure 4-7)**. This data indicates that the sexual dimorphic mRNA expression patterns of *dsx* are conserved among cladocerans.

Annotation of *dsx* gene structures in *D. magna* and *D. pulex*

Our group previously cloned and described the mRNA transcripts of the *DapmaDsx1* and *DapmaDsx2* genes (Kato et al., 2011a). *DapmaDsx1* produces two mRNA, *DapmaDsx1-α* and *DapmaDsx1-β*, which are expressed in both sexes and differ only in their 5' UTR, while *DapmaDsx2* produces only one mRNA transcript. The *D. pulex* draft genome sequence was recently published (Colbourne et al., 2011), and the *D. magna* genome sequencing project is currently in progress by the *Daphnia* Genomics Consortium. The *DapmaDsx1-α*, *DapmaDsx1-β*, and *DapmaDsx2* mRNA transcripts were aligned to the genome and used to annotate the *dsx1* and *dsx2* gene models in the *D. magna* and *D. pulex* genomes **(Figure 4-8)**.

The *D. magna dsx* gene cluster is located on scaffold 2,190 of the *D. magna* genome assembly v2.4 with a ~10 Kbp intergenic region between the *DapmaDsx1* (~16.1 Kbp length) and *DapmaDsx2* (~1.6 Kbp length) genes **(Figure 4-8A)**. The second exon of the *DapmaDsx1-β* mRNA transcript fell within an assembly gap in scaffold 2,190, but was located on scaffold 521. I conclude that scaffold 521 (~5.8 Kbp length) characterizes a ~3.1 Kbp gap in scaffold 2,190, located in the intragenic region of *DapmaDsx1*.

The *D. pulex dsx* gene cluster is located on scaffold 32 of the *D. pulex* genome assembly v1.1 with a ~9.6 Kbp intergenic region between the *DappuDsx1* (~21.5 Kbp length) and *DappuDsx2* (~1.6 Kbp length) genes **(Figure 4-8B)**. The *D. pulex* v1.1 gene model predictions did not correctly identify the *dsx1* and *dsx2* duplicate gene cluster. This annotations improved the *dsx* gene models in both *D. magna* and *D. pulex* genomes.

Potential transcriptional regulatory elements in the 5' upstream promoter regions of the *dsx* genes

To further annotate putative functional and conserved elements of the *dsx* genes, I searched and compared transcriptional promoter regions of the genes in *D. magna* and *D. pulex*. The 1.0 Kbp upstream of the TSS of *dsx1-α, dsx1-β,* and *dsx2* were extracted as transcriptional regulatory regions. This interval spans the predicted intergenic region between adjacent loci. Promoter sequences are challenging for multiple alignment algorithms, because upstream regulatory regions are not well conserved compared to protein coding regions of genes (Blanco et al., 2006; Erb et al., 2012). I aligned orthologous promoter sequences from *D. magna* and *D. pulex* using Pro-Coffee (Erb et al., 2012), an alignment algorithm specifically designed for homologous promoter regions **(Figures 4-9, 4-10, 4-11)**. The *DapmaDsx1-α* and *DappuDsx1-α* promoter alignment showed 46% sequence identity **(Figure 4-9)**, the *DapmaDsx1-β* and *DappuDsx1-β* promoter alignment showed 60% sequence identity **(Figure 4-10)**, and the *DapmaDsx2* and *DappuDsx2* promoter alignment showed 62% sequence identity **(Figure 4-11)**. The promoter regions of *dsx1* and *dsx2* have much less conservation than their respective protein coding regions, which have 84% and 83% sequence identity, respectively.

I characterized putative known TFBS in the *dsx* upstream promoter regions using TF-map alignments (Blanco et al., 2006) between orthologous *dsx* promoter regions in *D. magna* and *D. pulex*, based on matches to position frequency matrices (PFMs) from JASPAR (Bryne et al., 2008) and TRANSFAC TFBS databases (Matys et al., 2003). The optimal *dsx1-α* promoter TF-map alignment contains 20 putative known TFBSs **(Figure 4-1A; Table 4-6)**. The optimal *dsx1-β* promoter TF-map alignment

contains 31 putative known TFBSs **(Figure 4-1C; Table 4-7)**. The optimal *dsx2* promoter TF-map alignment contains 39 putative known TFBSs **(Figure 4-1E; Table 4-8)**. The positions of the putative TFBS pairs (between orthologous promoters) are well aligned when annotated onto the promoter sequence Pro-Coffee alignments **(Figure 4-1)**, suggesting these predicted putative TFBSs are conserved between *D. magna* and *D. pulex*.

I compared the number of unique predicted TFs shared amongst the *dsx* promoter regions **(Figure 4-12A)**. In total, 32 unique TFs were predicted in the *dsx* promoters; half (16) are present in at least two of the promoters **(Table 4-9)**. Six unique TFs were predicted in all three *dsx* promoters; an additional six unique TFs were also shared between *dsx1-β* and *dsx2* promoter regions. Interestingly, 11 unique TFs were predicted in the *dsx2* promoter but not in either *dsx1* promoters. Our group previously showed that *dsx1-β* mRNA expression levels are three times greater than expression levels of *dsx1-α* during male *D. magna* development, and that transcription of *dsx2* is even greater than both *dsx1* mRNAs combined (Kato et al., 2011a). The shared TF motifs suggest a duplication history involving in at least part of the 5' region upstream of *dsx1-β,* while numeric differences observed among *dsx* promoter regions are reflective of these expression level differences. Based on the promoter sequence conservation between *D. magna* and *D. pulex*, and the greater number of predicted TFs, the *dsx1-β* promoter seems to be the more widely used and evolutionarily conserved, while the *dsx1-α* promoter has experienced more sequence divergence and loss of TFBSs.

Since our group previously reported that *DapmaDsx1* and *DapmaDsx2* are paralogs, and that both *DapmaDsx1* and *DapmaDsx2* mRNAs are transcriptionally

up-regulated in male *D. magna* (Kato et al., 2011a), I searched for *de novo* conserved motifs present in all *dsx* promoter regions in *D. magna* and *D. pulex* (*DapmaDsx1-α, DappuDsx1-α, DapmaDsx1-β, DappuDsx1-β, DapmaDsx2,* and *DappuDsx2*), without reference to TFBS sequence databases. I identified 14 conserved motifs in the *Daphnia dsx* promoters **(Table 4-10)**, which can later be functionally investigated as potential TFBSs and/or potential transcriptional promoters of *Daphnia dsx*. The motifs were labeled M1 through M14 and annotated onto the *D. magna/D. pulex dsx* promoter alignments **(Figures 4-1B, D, F)**. Motifs 1 through 9 were also found in the *D. melanogaster dsx* upstream promoter region, supporting the conservation and potential regulatory functions of these motifs.

In order to assess whether these *de novo* conserved motifs are similar to any known TFBSs, I scanned the individual motif sequences for matches to TFBS PFMs and compared each motif consensus sequence to known TFBS consensus sequences. Several of the conserved motifs showed similarity to known TFBSs **(Figures 4-12B-F)**. Motif 3 matches the TFBS of Mirr, a homeobox transcription factor in the Iroquois complex, which is predicted in all three *dsx* promoter TF-map alignments **(Figure 4-12B)**. Motif 4 matches the TFBS of Vvl, a homeobox transcription factor which is predicted in both *dsx1-β* and *dsx2* TF-map alignments **(Figure 4-12C)**. Motif 7 matches the TFBS of Gsc/Bcd/Oc, three homeobox transcription factors with nearly identical binding sites **(Figure 4-12D)**, with four of the Motif 7 sequences matching the Gsc/Bcd/Oc consensus TAATC exactly. Gsc was also predicted in the *dsx2* TF-map alignment, and Oc was predicted in the *dsx1-α* TF-map alignment. Motif 8 matches the TFBS of Pan, a high mobility group transcription factor, which is predicted in both *dsx1-β* and *dsx2* TF-map alignments **(Figure 4-12E)**. Motif 12 also matches the TFBS

of Pan, but with the reverse complement of the binding site **(Figure 4-12F)**. The similarity of these *de novo* conserved motifs to known TFBSs that were also predicted by the TF-map alignment further supports our results describing the regulatory elements of the *Daphnia dsx* genes.

Conclusions

In this chapter, I identified the orthologs of *DapmaDsx1* and *DapmaDsx2* genes from closely-related species belonging to two cladoceran families and three genera: *D. pulex*, *D. galeata*, *C. dubia* (Daphniidae) and *M. macrocopa* (Moinidae), with highly conserved DM- and oligomerization-domains. All five species examined exhibited sexually dimorphic expression pattern of *dsx* genes, suggesting that these genes may have similar functions for sex determination in cladocerans **(Figure 4-13)**. Daphnids are unique animals that exhibit ESD and are; therefore, attractive for understanding the evolution of ESD. I also identified potential regulatory motifs and transcription factor binding sites in the putative promoter regions of these genes in *D. magna* and *D. pulex*. This information will facilitate future study of molecular mechanisms underlying sex determination in cladocerans.

Tables

Table 4-1 Primer sequences for 5’ and 3’ RACE in *D. galeata*, *C. dubia* and *M. macrocopa*.

	First primer (5’ to 3’)	Nested primer (5’ to 3’)
D. galeata-Dsx1 (5'RACE)	GGGCCACTTGCTCCGCATTTATCTTTCG	GTGCCCTTTGAGCGTGCTTATCGTTTG
D. galeata-Dsx1 (3'RACE)	GCACGCTCAAAGGGCACAAAAGATACTG	GATAAATGCGGAGCAAGTGGCCCTGAG
D. galeata-Dsx2 (5'RACE)	GACACAAGTCACAACTGCACCGCCCAAA	CTGCACCGCCCAAATGGACAGTAACG
D. galeata-Dsx2 (3'RACE)	CCATTTGGGCGGTGCAGTTGTGACTTG	GGGCGGTGCAGTTGTGACTTGTGTCGAG
C. dubia-Dsx1 (5'RACE)	AGACACAGTTTCGCCAGGGACAGT	CCGTAGCACAGTTCACAGACACAGTT
C. dubia-Dsx1 (3'RACE)	GGTGGCAATGTTTGCTGAATTGGGGA	TGGAAACGAGACGAAGGAACGATGAG
C. dubia-Dsx2 (5'RACE)	TTTTTCTGCTTCTTGCGAGTGACCCTG	AGCGGCCAAATGGACAGTATCGCTT
C. dubia-Dsx2 (3'RACE)	GCGCCCTAGCATCCAGAACGTTATT	CCACTGTCTACATTCATTTTCCCTCC
M. macrocopa-Dsx (5'RACE)	CCTGCTCGGCATTGATCTTGCGCTTC	
M. macrocopa-Dsx (3'RACE)	ACCATCAGCACGCTCAAAGGCCACAA	

Table 4-2 Accession numbers of the sequences for phylogenetic analysis

Organism	Gene name in phylogenetic tree (definition in NCBI)	Accession No.
Human (*Homo sapiens*)	DMRT1 (doublesex and mab-3-related transcription factor 1b)	AAR89619
	DMRT2 (doublesex and mab-3-related transcription factor 2 isoform 1)	NP_006548
	DMRT3 (doublesex and mab-3-related transcription factor 3)	NP_067063
	DMRT4 (DMRT-like family A1)	NP_071443
	DMRT5 (predicted: similar to doublesex and mab-3-related transcription factor-like family A2)	XP_946699
African clawed frog (*Xenopus laevis*)	DMRT1 (doublesex- and mab-3-related transcription factor 1)	Q3LH63
	DMRT4 (DMRT4)	AAV66322
	DMRT5 (doublesex and mab-3-related transcription factor 5)	ABC55871
Japanese medaka (*Oryzias latipes*)	DMY (DMY protein)	BAB92012
	DMRT2 (DMRT2)	AAL02163
	DMRT4 (OlaDMRT4)	BAB63259
	DMRT5 (doublesex and mab-3-related transcription factor 5)	BAD00703
Pufferfish (*Takifugu rubripes*)	DMRT1 (doublesex and mab-3-related transcription factor 1)	NP_001033038
	DMRT2 (doublesex and mab-3-related transcription factor 2)	NP_001033035
	DMRT3 (doublesex and mab-3-related transcription factor 3)	NP_001033034
	DMRT4 (doublesex and mab-3-related transcription factor 4)	NP_001033037
	DMRT5 (doublesex and mab-3-related transcription factor 5)	NP_001033039
Zebrafish (*Danio rerio*)	DMRT3 (doublesex and mab-3-related transcription factor 3)	AAU89440
Honeybee (*Apis mellifera*)	DMRT93B (predicted: similar to CG5737-PA)	XP_392966
	doublesex	NP_001104725

Beetle (*Tribolium castaneum*)	DMRT93B (predicted: similar to CG5737-PA)	XP_971604
	DMRT99B (predicted: similar to CG15504-PA)	XP_975675
	PREDICTED: similar to CG11094-PB, isoform B	XP_971776
Silkworm (*Bombyx mori*)	doublesex isoform M	NP_001104815
African malaria mosquito (Anopheles gambiae)	DMRT93B (ENSANGP00000016774)	XP_321748
	DMRT99B (ENSANGP00000020063)	XP_310668
	AGAP004050-PC	XP_560052
Yellow fever mosquito (*Aedes aegypti*)	DMRT93B (conserved hypothetical protein)	EAT43900
	male specific 1 protein	ABD96573
Fruit fly (*Drosophila melanogaster*)	DMRT11E (doublesex-Mab-related 11E CG15749-PA)	NP_511146
	DMRT93B (doublesex-Mab-related 93B CG5737-PA)	NP_524428
	DMRT99B (doublesex-Mab-related 99B CG15504-PA)	NP_524549
	doublesex CG11094-PA, isoform A	NP_731197
Fruit fly (*Drosophila pseudoobscura*)	DMRT11E (GA13932-PA)	XP_001355530
	DMRT93B(GA19095-PA)	XP_001360059
	DMRT99B(GA13771-PA)	XP_001357766
House fly (*Musca domestica*)	DSXM	AAR23813
Fruit fly (*Anastrepha obliqua*)	doublesexM	AAY25167
Fruit fly (*Bactrocera oleae*)	male-specific doublesex protein	CAD67987
Eriocheir sinensis	Dmrt-like protein	ADH15934
Penaeus monodon	testis-specific DMRT1	ACC94178
Daphnia magna	doublesex-Mab related 99B	BAG12873

	doublesex-Mab related 11E	BAG12871
	doublesex-Mab related 93B	BAG12872
	doublesex1-a	AB569296
	doublesex1-b	AB569297
	doublesex2	AB569298
Daphnia pulex	DMRT-99B-like protein	EFX84867
	Doublesex and mab-3 related transcription factor 3	EFX89054
	DM DNA-binding protein	EFX74782
	doublesex1	AB693158
	doublesex2	AB693159
Daphnia galeata	doublesex1	AB693160
	doublesex2	AB693161
Ceriodaphnia dubia	doublesex1	AB693162
	doublesex2	AB693163
Moina macrocopa	doublesex	AB693164

Table 4-3 Primer sequences for quantitative PCR

Organism	Gene name	Forward primer (5’ to 3’)	Reverse primer (5’ to 3’)
D. magna	*Dsx1*	CCATTCATCATTACCAAATCCCTTC	AAGTTTGGTGTAGGGGAGGATGAG
D. magna	*Dsx2*	TCTAATGCCAGTGCGAAATCC	CTAAACGCATCTTCCGTCGTC
D. magna	*RpL32*	GACCAAAGGGTATTGACAACAGA	CCAACTTTTGGCATAAGGTACTG
D. pulex	*Dsx1*	GCGATGCAGAAGAGTTGTCC	AACGCTGCTCGATCCTTCTT
D. pulex	*Dsx2*	TCGGAGGAGGCTTTTAGTGTC	CGGATAAACAGGAAGCGAAA
D. pulex	*RpL32*	TTTCGCGGAGTTGGATTTAC	TTGGGGTCTCTCTTGGGAAT
D. galeata	*Dsx1*	AGACAGCGACGCAGAAGAGT	TTGAAGTCGAAACGCTGCTC
D. galeata	*Dsx2*	AGATCAGCTTTGGACGTAGAGC	GAGCCATGTTTTTCCCGAAT
D. galeata	*RpL32*	TGGCAGAACCATAACCAACC	GCTGAAGAGGAACTGGCGTA
C. dubia	*Dsx1*	CGTCGTCTTCGGTCAACAAT	CCGGAAAAGAAATCTCAGCA
C. dubia	*Dsx2*	ATCTCCGTCCTCGCTAAACC	TCGCTCCACCGAAAGAAGTT
C. dubia	*RpL32*	GACAGTACCTGATGCCCAAGA	GCGGTTCTGCATCATAAGGA
M. macrocopa	*Dsx*	GCCTCTCGGAGGTTGTCAAA	GTTTAGCGTTAGGCCCGTCT
M. macrocopa	*RpL32*	AGAGAAACTGGCGCAAACCT	GCTTGGTAGCTTTGGCAGAA

Table 4-4 Estimates of evolutionary divergence between the DSX1 except for DM- and oligomerization-domain and COI

	D. magna	*D. pulex*	*D. galeata*	*C. dubia*	*M. macrocopa*
D. magna	-	0.0288	0.0288	0.0240	0.0721
D. pulex	0.0622	-	0.0192	0.0288	0.0721
D. galeata	0.0533	0.0267	-	0.0240	0.0673
C. dubia	0.1822	0.1956	0.1733	-	0.0625
M. macrocopa	0.3778	0.3911	0.3778	0.3911	-

Table 4-5 Estimates of evolutionary divergence between the DSX2 except for DM- and oligomerization-domain and COI

	D. magna	*D. pulex*	*D. galeata*	*C. dubia*
D. magna	-	0.0288	0.0288	0.0240
D. pulex	0.1238	-	0.0192	0.0288
D. galeata	0.1667	0.0714	-	0.0240
C. dubia	0.2810	0.2667	0.2952	-

Table 4-6 *dsx1-α* TF-map alignment

# meta_v1.1 parameters					
# date Fri Apr 6 05:12:38 2012					
# MAP1 Dpulex_dsx1-a - Length = 396 elems					
# MAP2 Dmagna_dsx1-a - Length = 498 elems					
# ALPHA = 0.50, LAMBDA = 0.10, MU = 0.10					
# Maximum similarity: -76.00					
# SimMatrix: 2903 matches / 197208 positions (1.47 %)					
### Best meta-alignment contains 20 elements					
Column Descriptions					
Sequence ID	Promoter region ID - Species, dsx paralog number, and dsx transcript identifier				
Source	Name of program that generated results				
Type (TF)	Name of transcription factor identified				
Start	Start of transcription factor binding site (TFBS)				
End	End of transcription factor binding site (TFBS)				
Score	Match score between known TFBS (from TFBS database) and identified Daphnia dsx promoter sequence motif				
Sequence ID	**Source**	**Type (TF)**	**Start**	**End**	**Score**
Dpulex_dsx1-a	meta_v1.1	lbe	81	86	0.94
Dmagna_dsx1-a	meta_v1.1	lbe	83	88	1
Dpulex_dsx1-a	meta_v1.1	ara	109	113	0.89
Dmagna_dsx1-a	meta_v1.1	ara	127	131	0.91
Dpulex_dsx1-a	meta_v1.1	ara	153	157	1

Dmagna_dsx1-a	meta_v1.1	ara	184	188	0.89
Dpulex_dsx1-a	meta_v1.1	ara	349	353	0.99
Dmagna_dsx1-a	meta_v1.1	ara	384	388	0.93
Dpulex_dsx1-a	meta_v1.1	ct	403	408	0.9
Dmagna_dsx1-a	meta_v1.1	ct	437	442	0.89
Dpulex_dsx1-a	meta_v1.1	Six4	446	451	0.92
Dmagna_dsx1-a	meta_v1.1	Six4	480	485	1
Dpulex_dsx1-a	meta_v1.1	oc	463	468	0.86
Dmagna_dsx1-a	meta_v1.1	oc	498	503	0.85
Dpulex_dsx1-a	meta_v1.1	ara	469	473	0.91
Dmagna_dsx1-a	meta_v1.1	ara	507	511	0.91
Dpulex_dsx1-a	meta_v1.1	CG42234	475	481	0.87
Dmagna_dsx1-a	meta_v1.1	CG42234	514	520	0.87
Dpulex_dsx1-a	meta_v1.1	C15	484	490	0.93
Dmagna_dsx1-a	meta_v1.1	C15	526	532	0.88
Dpulex_dsx1-a	meta_v1.1	CG4328	570	576	0.87
Dmagna_dsx1-a	meta_v1.1	CG4328	617	623	0.87
Dpulex_dsx1-a	meta_v1.1	caup	593	597	0.9
Dmagna_dsx1-a	meta_v1.1	caup	640	644	0.85
Dpulex_dsx1-a	meta_v1.1	ara	609	613	0.91
Dmagna_dsx1-a	meta_v1.1	ara	656	660	1
Dpulex_dsx1-a	meta_v1.1	C15	657	663	0.93

Dmagna_dsx1-a	meta_v1.1	C15	687	693	0.94
Dpulex_dsx1-a	meta_v1.1	ara	712	716	0.89
Dmagna_dsx1-a	meta_v1.1	ara	743	747	0.91
Dpulex_dsx1-a	meta_v1.1	ara	735	739	0.91
Dmagna_dsx1-a	meta_v1.1	ara	762	766	0.91
Dpulex_dsx1-a	meta_v1.1	ara	790	794	1
Dmagna_dsx1-a	meta_v1.1	ara	818	822	0.91
Dpulex_dsx1-a	meta_v1.1	Eip74EF	818	824	1
Dmagna_dsx1-a	meta_v1.1	Eip74EF	847	853	1
Dpulex_dsx1-a	meta_v1.1	br_Z2	888	895	0.91
Dmagna_dsx1-a	meta_v1.1	br_Z2	907	914	0.86
Dpulex_dsx1-a	meta_v1.1	mirr	965	969	0.89
Dmagna_dsx1-a	meta_v1.1	mirr	967	971	1

Table 4-7 *dsx1-β* TF-map alignments

# meta_v1.1 paramters					
# date Fri Apr 6 05:12:38 2012					
# MAP1 Dpulex_dsx1-b - Length = 441 elems					
# MAP2 Dmagna_dsx1-b - Length = 623 elems					
# ALPHA = 0.50, LAMBDA = 0.10, MU = 0.10					
# Maximum similarity: -79.73					
# SimMatrix: 4962 matches / 274743 positions (1.81 %)					
### Best meta-alignment contains 31 elements					
Column Descriptions					
Sequence ID	Promoter region ID - Species, dsx paralog number, and dsx transcript identifier				
Source	Name of program that generated results				
Type (TF)	Name of transcription factor identified				
Start	Start of transcription factor binding site (TFBS)				
End	End of transcription factor binding site (TFBS)				
Score	Match score between known TFBS (from TFBS database) and identified Daphnia dsx promoter sequence motif				
Sequence ID	**Source**	**Type (TF)**	**Start**	**End**	**Score**
Dpulex_dsx1-b	meta_v1.1	exd	46	53	0.99
Dmagna_dsx1-b	meta_v1.1	exd	55	62	0.99
Dpulex_dsx1-b	meta_v1.1	ara	83	87	0.93
Dmagna_dsx1-b	meta_v1.1	ara	92	96	0.93
Dpulex_dsx1-b	meta_v1.1	ara	111	115	0.99

Dmagna_dsx1-b	meta_v1.1	ara	122	126	0.93
Dpulex_dsx1-b	meta_v1.1	CG4328	119	125	0.87
Dmagna_dsx1-b	meta_v1.1	CG4328	129	135	0.89
Dpulex_dsx1-b	meta_v1.1	CG42234	176	182	0.91
Dmagna_dsx1-b	meta_v1.1	CG42234	185	191	0.91
Dpulex_dsx1-b	meta_v1.1	ems	217	223	0.86
Dmagna_dsx1-b	meta_v1.1	ems	230	236	0.87
Dpulex_dsx1-b	meta_v1.1	CG11617	232	238	0.94
Dmagna_dsx1-b	meta_v1.1	CG11617	241	247	0.92
Dpulex_dsx1-b	meta_v1.1	CG11617	245	251	0.92
Dmagna_dsx1-b	meta_v1.1	CG11617	254	260	0.99
Dpulex_dsx1-b	meta_v1.1	ara	261	265	1
Dmagna_dsx1-b	meta_v1.1	ara	270	274	1
Dpulex_dsx1-b	meta_v1.1	hth	294	299	1
Dmagna_dsx1-b	meta_v1.1	hth	303	308	1
Dpulex_dsx1-b	meta_v1.1	ara	310	314	0.91
Dmagna_dsx1-b	meta_v1.1	ara	313	317	0.91
Dpulex_dsx1-b	meta_v1.1	lbe	331	336	0.91
Dmagna_dsx1-b	meta_v1.1	lbe	328	333	0.92
Dpulex_dsx1-b	meta_v1.1	ara	353	357	0.99
Dmagna_dsx1-b	meta_v1.1	ara	349	353	0.93
Dpulex_dsx1-b	meta_v1.1	CG11617	394	400	0.94

Dmagna_dsx1-b	meta_v1.1	CG11617	393	399	0.89
Dpulex_dsx1-b	meta_v1.1	PHDP	431	437	0.9
Dmagna_dsx1-b	meta_v1.1	PHDP	430	436	0.9
Dpulex_dsx1-b	meta_v1.1	ara	460	464	0.89
Dmagna_dsx1-b	meta_v1.1	ara	460	464	0.89
Dpulex_dsx1-b	meta_v1.1	Six4	495	500	0.92
Dmagna_dsx1-b	meta_v1.1	Six4	493	498	0.92
Dpulex_dsx1-b	meta_v1.1	pan	530	537	0.86
Dmagna_dsx1-b	meta_v1.1	pan	534	541	0.93
Dpulex_dsx1-b	meta_v1.1	caup	594	598	0.85
Dmagna_dsx1-b	meta_v1.1	caup	593	597	0.87
Dpulex_dsx1-b	meta_v1.1	ara	636	640	0.99
Dmagna_dsx1-b	meta_v1.1	ara	645	649	0.93
Dpulex_dsx1-b	meta_v1.1	br_Z2	679	686	0.88
Dmagna_dsx1-b	meta_v1.1	br_Z2	685	692	0.89
Dpulex_dsx1-b	meta_v1.1	lbe	702	707	0.86
Dmagna_dsx1-b	meta_v1.1	lbe	709	714	0.95
Dpulex_dsx1-b	meta_v1.1	ct	719	724	1
Dmagna_dsx1-b	meta_v1.1	ct	724	729	0.86
Dpulex_dsx1-b	meta_v1.1	CG11617	787	793	0.94
Dmagna_dsx1-b	meta_v1.1	CG11617	785	791	0.88
Dpulex_dsx1-b	meta_v1.1	Deaf1	813	818	0.96

Dmagna_dsx1-b	meta_v1.1	Deaf1	808	813	0.91
Dpulex_dsx1-b	meta_v1.1	vvl	821	826	0.9
Dmagna_dsx1-b	meta_v1.1	vvl	822	827	0.88
Dpulex_dsx1-b	meta_v1.1	slbo	857	864	1
Dmagna_dsx1-b	meta_v1.1	slbo	856	863	0.85
Dpulex_dsx1-b	meta_v1.1	lbe	871	876	0.86
Dmagna_dsx1-b	meta_v1.1	lbe	872	877	0.91
Dpulex_dsx1-b	meta_v1.1	ara	878	882	0.91
Dmagna_dsx1-b	meta_v1.1	ara	882	886	1
Dpulex_dsx1-b	meta_v1.1	ara	891	895	0.91
Dmagna_dsx1-b	meta_v1.1	ara	895	899	0.91
Dpulex_dsx1-b	meta_v1.1	mirr	909	913	1
Dmagna_dsx1-b	meta_v1.1	mirr	910	914	0.99

Table 4-8 *dsx2* TF-map alignments

# meta_v1.1 parameters					
# date Fri Apr 6 05:12:38 2012					
# MAP1 Dpulex_dsx2 - Length = 324 elems					
# MAP2 Dmagna_dsx2 - Length = 316 elems					
# ALPHA = 0.50, LAMBDA = 0.10, MU = 0.10					
# Maximum similarity: -37.76					
# SimMatrix: 1942 matches / 102384 positions (1.90 %)					
### Best meta-alignment contains 39 elements					
Column Descriptions					
Sequence ID	Promoter region ID - Species, dsx paralog number, and dsx transcript identifier				
Source	Name of program that generated results				
Type (TF)	Name of transcription factor identified				
Start	Start of transcription factor binding site (TFBS)				
End	End of transcription factor binding site (TFBS)				
Score	Match score between known TFBS (from TFBS database) and identified Daphnia dsx promoter sequence motif				
Sequence ID	**Source**	**Type (TF)**	**Start**	**End**	**Score**
Dpulex_dsx2	meta_v1.1	vis	3	8	0.95
Dmagna_dsx2	meta_v1.1	vis	64	69	0.95
Dpulex_dsx2	meta_v1.1	vis	22	27	0.95
Dmagna_dsx2	meta_v1.1	vis	83	88	0.95
Dpulex_dsx2	meta_v1.1	Six4	40	45	0.95

Dmagna_dsx2	meta_v1.1	Six4	101	106	0.95
Dpulex_dsx2	meta_v1.1	Deaf1	60	65	0.93
Dmagna_dsx2	meta_v1.1	Deaf1	121	126	0.93
Dpulex_dsx2	meta_v1.1	ara	72	76	0.91
Dmagna_dsx2	meta_v1.1	ara	134	138	0.91
Dpulex_dsx2	meta_v1.1	exd	88	95	0.95
Dmagna_dsx2	meta_v1.1	exd	150	157	0.95
Dpulex_dsx2	meta_v1.1	B-H1	105	111	0.96
Dmagna_dsx2	meta_v1.1	B-H1	165	171	0.86
Dpulex_dsx2	meta_v1.1	C15	166	172	0.85
Dmagna_dsx2	meta_v1.1	C15	226	232	0.95
Dpulex_dsx2	meta_v1.1	sd	175	186	0.87
Dmagna_dsx2	meta_v1.1	sd	236	247	0.86
Dpulex_dsx2	meta_v1.1	PHDP	190	196	0.96
Dmagna_dsx2	meta_v1.1	PHDP	251	257	0.96
Dpulex_dsx2	meta_v1.1	mirr	219	223	0.89
Dmagna_dsx2	meta_v1.1	mirr	284	288	0.89
Dpulex_dsx2	meta_v1.1	H2.0	261	267	0.86
Dmagna_dsx2	meta_v1.1	H2.0	333	339	0.9
Dpulex_dsx2	meta_v1.1	Optix	279	283	0.87
Dmagna_dsx2	meta_v1.1	Optix	346	350	0.87
Dpulex_dsx2	meta_v1.1	ct	289	294	0.86

Dmagna_dsx2	meta_v1.1	ct	356	361	0.86
Dpulex_dsx2	meta_v1.1	onecut	318	324	1
Dmagna_dsx2	meta_v1.1	onecut	387	393	1
Dpulex_dsx2	meta_v1.1	caup	325	329	0.85
Dmagna_dsx2	meta_v1.1	caup	394	398	0.85
Dpulex_dsx2	meta_v1.1	Six4	330	335	0.98
Dmagna_dsx2	meta_v1.1	Six4	399	404	0.98
Dpulex_dsx2	meta_v1.1	Gsc	357	362	0.94
Dmagna_dsx2	meta_v1.1	Gsc	417	422	0.94
Dpulex_dsx2	meta_v1.1	Deaf1	429	434	0.96
Dmagna_dsx2	meta_v1.1	Deaf1	463	468	0.98
Dpulex_dsx2	meta_v1.1	hb	440	449	0.92
Dmagna_dsx2	meta_v1.1	hb	470	479	0.95
Dpulex_dsx2	meta_v1.1	pan	478	485	0.95
Dmagna_dsx2	meta_v1.1	pan	493	500	0.95
Dpulex_dsx2	meta_v1.1	B-H1	488	494	0.89
Dmagna_dsx2	meta_v1.1	B-H1	503	509	0.89
Dpulex_dsx2	meta_v1.1	ara	545	549	0.93
Dmagna_dsx2	meta_v1.1	ara	552	556	0.93
Dpulex_dsx2	meta_v1.1	Deaf1	555	560	0.87
Dmagna_dsx2	meta_v1.1	Deaf1	562	567	0.87
Dpulex_dsx2	meta_v1.1	Deaf1	582	587	0.98

Dmagna_dsx2	meta_v1.1	Deaf1	590	595	0.98
Dpulex_dsx2	meta_v1.1	onecut	591	597	0.87
Dmagna_dsx2	meta_v1.1	onecut	599	605	0.87
Dpulex_dsx2	meta_v1.1	vvl	666	671	0.98
Dmagna_dsx2	meta_v1.1	vvl	669	674	0.98
Dpulex_dsx2	meta_v1.1	lbe	692	697	0.95
Dmagna_dsx2	meta_v1.1	lbe	695	700	0.94
Dpulex_dsx2	meta_v1.1	ara	708	712	0.91
Dmagna_dsx2	meta_v1.1	ara	712	716	0.99
Dpulex_dsx2	meta_v1.1	dTCF	716	726	0.91
Dmagna_dsx2	meta_v1.1	dTCF	718	728	0.91
Dpulex_dsx2	meta_v1.1	lbe	740	745	0.86
Dmagna_dsx2	meta_v1.1	lbe	742	747	0.85
Dpulex_dsx2	meta_v1.1	hth	761	766	0.96
Dmagna_dsx2	meta_v1.1	hth	766	771	0.96
Dpulex_dsx2	meta_v1.1	dl	832	842	0.87
Dmagna_dsx2	meta_v1.1	dl	823	833	0.87
Dpulex_dsx2	meta_v1.1	ct	853	858	0.89
Dmagna_dsx2	meta_v1.1	ct	844	849	0.89
Dpulex_dsx2	meta_v1.1	mirr	915	919	1
Dmagna_dsx2	meta_v1.1	mirr	913	917	1
Dpulex_dsx2	meta_v1.1	Deaf1	948	953	0.98

Dmagna_dsx2	meta_v1.1	Deaf1	942	947	0.96
Dpulex_dsx2	meta_v1.1	Lag1	959	965	0.88
Dmagna_dsx2	meta_v1.1	Lag1	957	963	0.88
Dpulex_dsx2	meta_v1.1	Six4	981	986	0.95
Dmagna_dsx2	meta_v1.1	Six4	981	986	0.95
Dpulex_dsx2	meta_v1.1	ara	992	996	1
Dmagna_dsx2	meta_v1.1	ara	992	996	0.89

Table 4-9 TF-map alignments unique TFs comparison

Dsx1-a	Dsx1-b	Dsx2	Total	All	Dsx1-a & Dsx1-b	Dsx1-a & Dsx2	Dsx1-b & Dsx2
ara	ara	ara	ara	ara	br_Z2	C15	Deaf1
br_Z2	br_Z2	B-H1	B-H1	caup	CG42234		exd
C15	caup	C15	br_Z2	ct	CG4328		hth
caup	CG11617	caup	C15	mirr			pan
CG42234	CG42234	ct	caup	lbe			PHDP
CG4328	CG4328	Deaf1	CG11617	Six4			vvl
ct	ct	dl	CG42234				
Eip74EF	Deaf1	dTCF	CG4328				
lbe	ems	exd	ct				
mirr	exd	Gsc	Deaf1				
oc	hth	H2.0	dl				
Six4	lbe	hb	dTCF				
	mirr	hth	Eip74EF				
	pan	Lag1	ems				
	PHDP	lbe	exd				
	Six4	mirr	Gsc				
	slbo	onecut	H2.0				
	vvl	Optix	hb				
		pan	hth				
		PHDP	Lag1				

Dsx1-a	Dsx1-b	Dsx2	Total	All	Dsx1-a & Dsx1-b	Dsx1-a & Dsx2	Dsx1-b & Dsx2
		sd	lbe				
		Six4	mirr				
		vis	oc				
		vvl	onecut				
			Optix				
			pan				
			PHDP				
			sd				
			Six4				
			slbo				
			vis				
			vvl				

Table 4-10 *de novo* conserved regulatory motifs

Motif #			
Seq 1 = DappuDsx1-a			
Seq 2 = DapmaDsx1-a			
Seq 3 = DappuDsx1-b			
Seq 4 = DapmaDsx1-b			
Seq 5 = DappuDsx2			
Seq 6 = DapmaDsx2			
Seq 7 = D. mel (only present if motif found in Dmel)			
		From TSS	
Motif Sequences	**X^2 Score**	**Start**	**Stop**
1			
TGCCTTCC	10.192	-751	-744
GGCTTTTA		-683	
TGCCTTCC		-726	
TGCCTTCC		-717	
TGTTTTCC		-693	
TGACTTGC		-624	
TGCTTTCG		-417	
2			
GACGTTTA	5.1378	-662	-655
GGCTTTTA		-683	
GACGTTTC		-509	
CAGGTTTC		-511	
GACATTTA		-745	
GACGTTTA		-672	
GACGTCAA		-613	
3			
AAACATGG	5.1375	-136	-129
GAACAAGG		-140	
AAACAGGA		-92	
AAACAGCG		-72	
AAACATGG		-86	
AAACATGG		-88	
AAACATTT		-218	

4			
TATATTCA	4.5179	-264	-257
TATATACA		-242	
TATATTCA		-246	
TTAATTTA		-241	
TTTAACCA		-311	
TTTAATCA		-308	
CATATTAA		-255	
5			
TGTTACTA	4.3927	-211	-204
TGCTACTA		-176	
TGTAAATA		-213	
TGTTGCTA		-224	
TGTCAATA		-239	
TGTCAATA		-234	
TGATATTA		-168	
6			
ATCGATCA	4.3504	-324	-317
ATCCATCA		-322	
TTCGTTGA		-286	
ATCGATGA		-281	
ATCGATCA		-526	
ATCGATCA		-511	
ATCGCTCA		-531	
7			
TAATCTCG	4.1444	-545	-538
TAATCTTT		-503	
ACATTTTA		-552	
TCATTTCG		-553	
TAATCTTG		-644	
TAATCTCG		-584	
CACTCTCG		-463	
8			
CTTAGATT	4.0943	-447	-440
CGTAGATT		-437	

CTTCGATT		-564	
CTTTGATT		-565	
CTTTGGTT		-425	
CTTTTGGT		-418	
CTTCGATG		-507	
9			
CATCTTTT	3.8198	-774	-767
AATCTTGG		-712	
CATCTTTC		-806	
CATCTTTT		-797	
GTTCCTTT		-902	
CTTCTTTT		-839	
TATCTTTT		-949	
10			
TTCTAAAA	3.3795	-441	-434
TTCTAAAA		-431	
TTTCAAAA		-376	
TTCTAAAA		-391	
TTCCAATA		-480	
TTCTAATA		-472	
11			
GGCTTTTT	3.3698	-86	-79
AGCTTTTT		-84	
GTCTTTTA		-153	
TGCTTTTG		-151	
GGCTTTTC		-62	
GGCTTTTT		-65	
12			
GATCAAAT	3.2212	-524	-517
GATCAAAT		-486	
TTTCAAAT		-471	
AATCAAAA		-467	
GATCAAAC		-523	
GATCAAAC		-508	
13			

TTCGTGAT	3.1028	-924	-917
TTGGTGAT		-863	
TTCTGGAT		-916	
TTCCGGAT		-907	
TTCCGCTG		-921	
TTCCAATG		-859	
14			
TCTGCATG	3.0511	-493	-486
TCTCCCAG		-453	
TCTATATA		-483	
TCTTCATG		-486	
TCCGCATG		-437	
TCTACATG		-430	

Figures

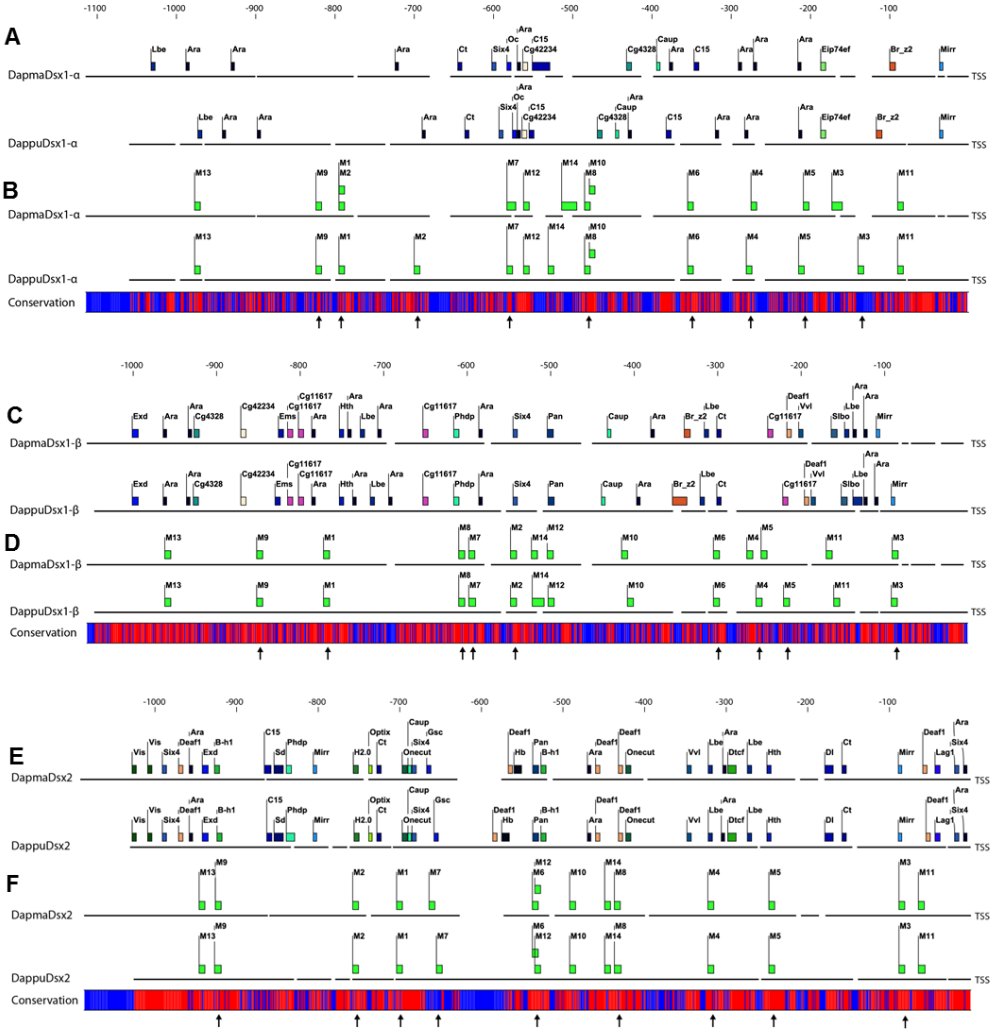
A
DapmaDsx1-α
DappuDsx1-α
B
DapmaDsx1-α
DappuDsx1-α
Conservation
C
DapmaDsx1-β
DappuDsx1-β
D
DapmaDsx1-β
DappuDsx1-β
Conservation
E
DapmaDsx2
DappuDsx2
F
DapmaDsx2
DappuDsx2
Conservation
TSS

Figure 4-1. Annotations mapped onto Pro-Coffee alignment of *dsx1-α*, *dsx1-β* and *dsx2* 5' upstream promoter regions. (A) Putative known transcription factor binding sites in *Daphnia magna* and *D. pulex dsx1-α* promoter regions predicted by TF-map alignment algorithm. (B) *dsx1-α* promoter locations of conserved regulatory motifs predicted in both *D. magna* and *D. pulex dsx* promoter regions. (C) Putative known transcription factor binding sites in *D. magna* and *D. pulex dsx1-β* promoter regions predicted by TF-map alignment algorithm. (D) *dsx1-β* promoter locations of conserved regulatory motifs predicted in all *D. magna* and *D. pulex dsx* promoter regions. (E) Putative known transcription factor binding sites in *D. magna* and *D. pulex dsx2* promoter regions predicted by TF-map alignment algorithm. (F) *dsx2* promoter locations of conserved regulatory motifs predicted in all *D. magna* and *D. pulex dsx* promoter regions. Arrows underneath denote the conserved regulatory motifs also found *D. melanogaster dsx* promoter region.

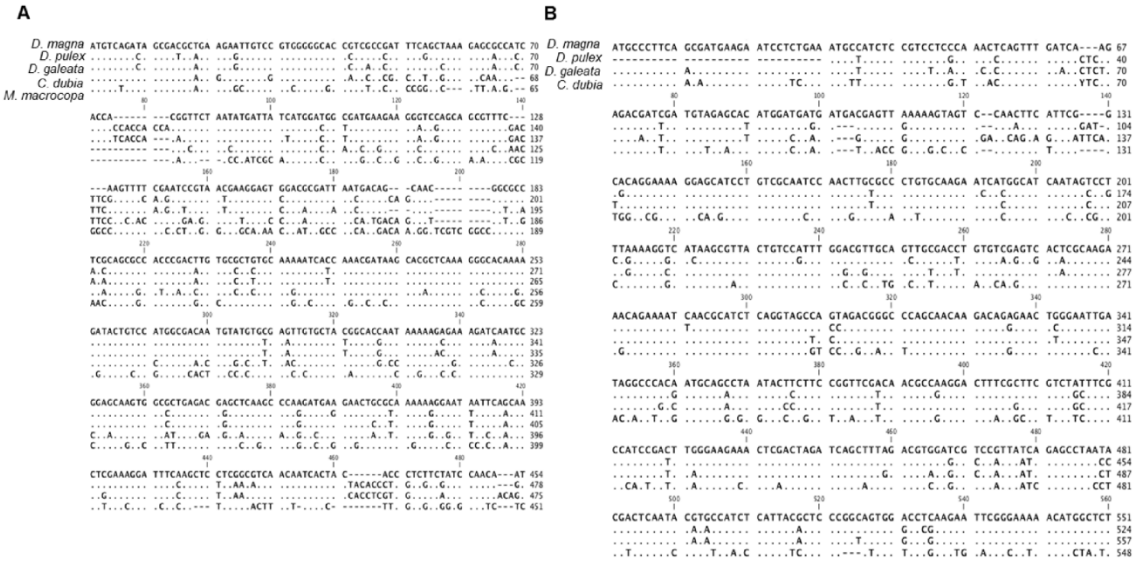

Figure 4-2. Nucleotide sequence comparison of *dsx1* and *dsx2* genes from five cladocerans. (A) Alignment of nucleotide sequence of *dsx1* genes from *Daphnia magna*, *D. pulex*, *D. galeata*, *Ceriodaphnia dubia* and *Moina macrocopa*. (B) Alignment of nucleotide sequence of *dsx2* genes from *D. magna*, *D. pulex*, *D. galeata* and *C. dubia*.

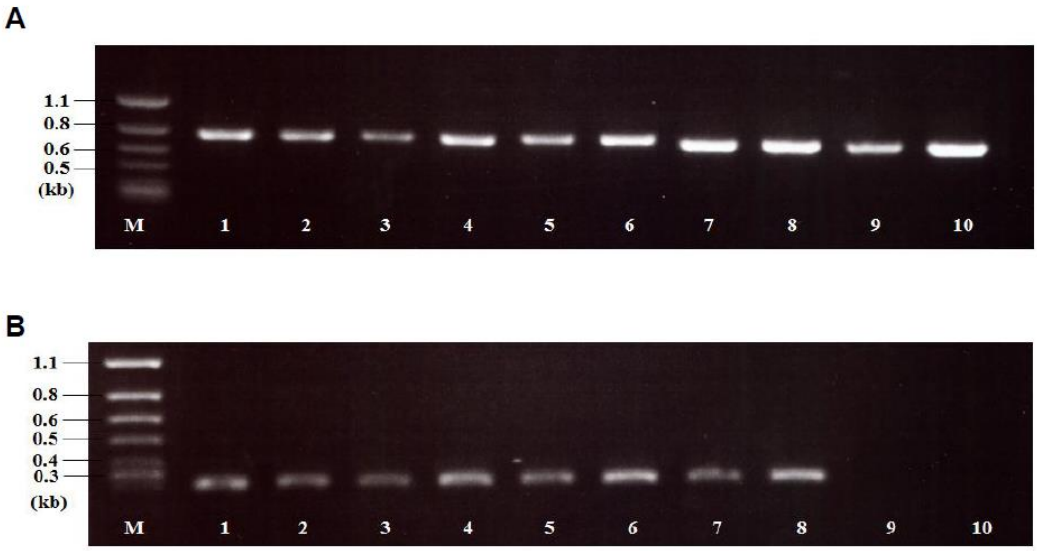

Figure 4-3. RT-PCR of oligonucleotides corresponding to highly conserved region of *dsx1* (A) and *dsx2* (B). The amplified cDNAs were analyzed by agarose gel electrophoresis. Lane M: molecular weight marker. Lane 1 to 10: *D. magna* (female), *D. magna* (male), *D. pulex* (female), *D. pulex* (male), *D. galeata* (female), *D. galeata* (male), *C. dubia* (female), *C. dubia* (male), *M. macrocopa* (female), *M. macrocopa* (male).

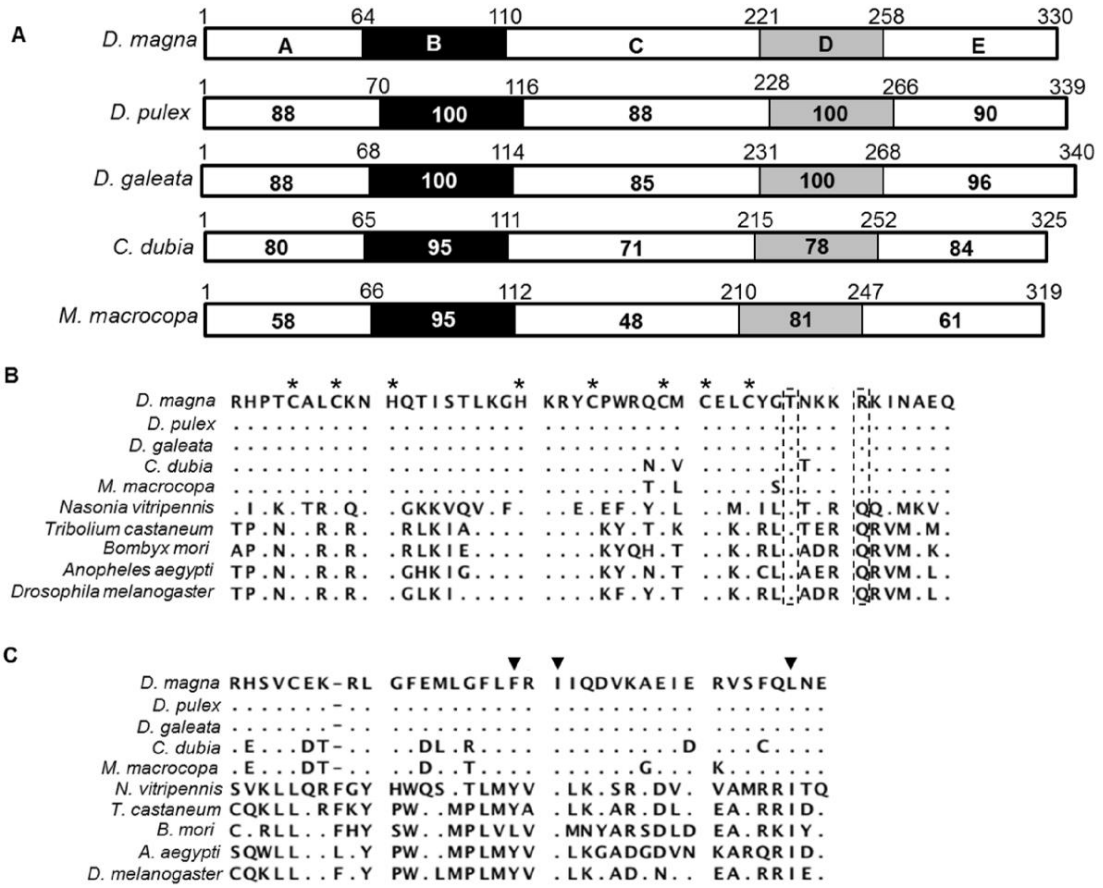

Figure 4-4. Schematic diagrams of the DSX1 structures and its sequence comparison of DM- and oligomerization-domains. (A) Domain structures of DSX1 in *D. magna*, and identity with *D. pulex*, *D. galeata*, *C. dubia* and *M. macrocopa*. DM- and oligomerization-domains are indicated by black and gray boxes, respectively. (B, C) Alignment of predicted amino acid sequences of DM- and oligomerization-domains of DSX1 from five cladocerans, respectively. Amino acid sequences were aligned using CLUSTAL-X. Dotted boxes highlight the conserved threonine (T) residue in the DM-domain, and arginine (R) residue substituted for glutamine (Q), which is conserved amino acid residues of DSX. Asterisks indicate the zinc chelating residues (Oliveira et al., 2009). Position of non-polar amino acids important in formation of the hydrophobic interface between oligomerization domains in *Drosophila* DSX are indicated with solid triangles (Bayrer et al., 2005; Kato et al., 2011a).

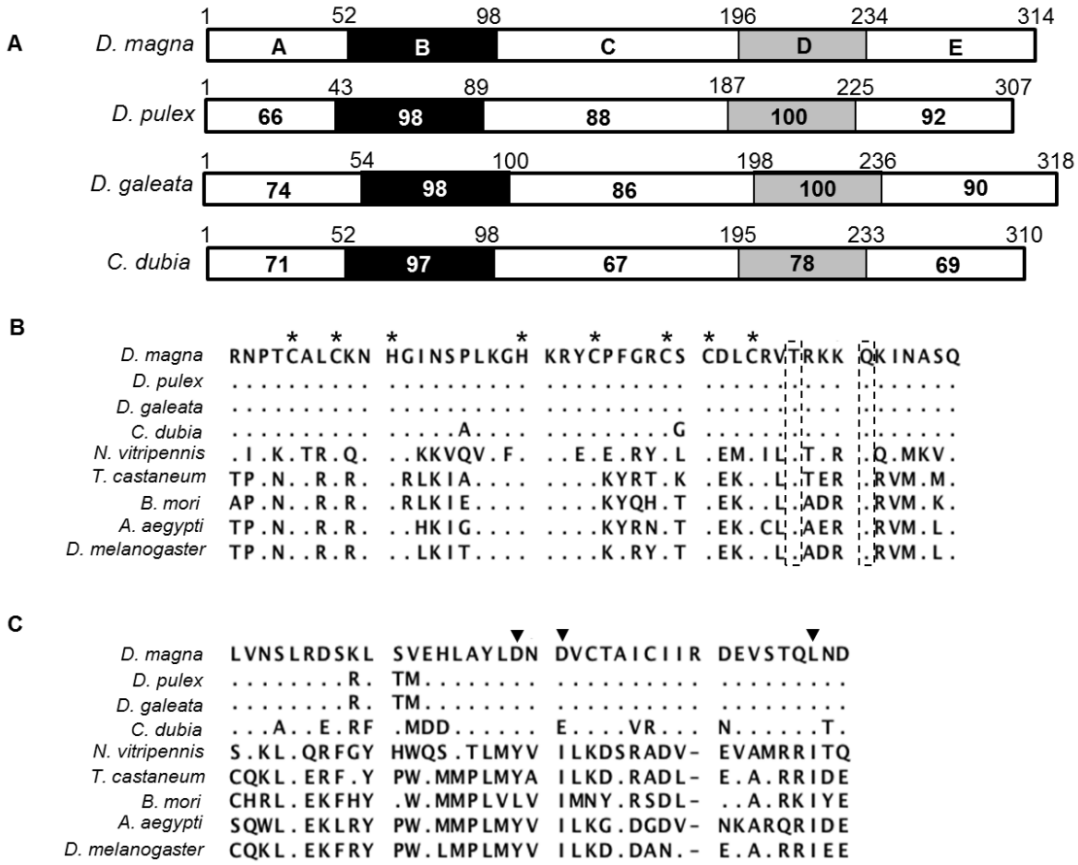

Figure 4-5. Schematic diagrams of the DSX2 structures and its sequence comparison of DM- and oligomerization-domains. (A) Domain structures of the DSX2 of *D. magna*, and identity with *D. pulex*, *D. galeata* and *C. dubia*. DM- and oligomerization-domains are indicated by black and gray boxes, respectively. (B, C) Alignment of predicted amino acid sequences of DM- and oligomerization-domains of DSX2 from four daphniids, respectively. Amino acid sequences were aligned using CLUSTAL-X. Dotted boxes highlight the conserved threonine (T) and glutamine (Q) residues in DSX2. Asterisks indicate the zinc chelating residues. Position of non-polar amino acids important in formation of the hydrophobic interface between oligomerization-domains in *Drosophila* DSX are indicated with solid triangles (Bayrer et al., 2005; Kato et al., 2011a).

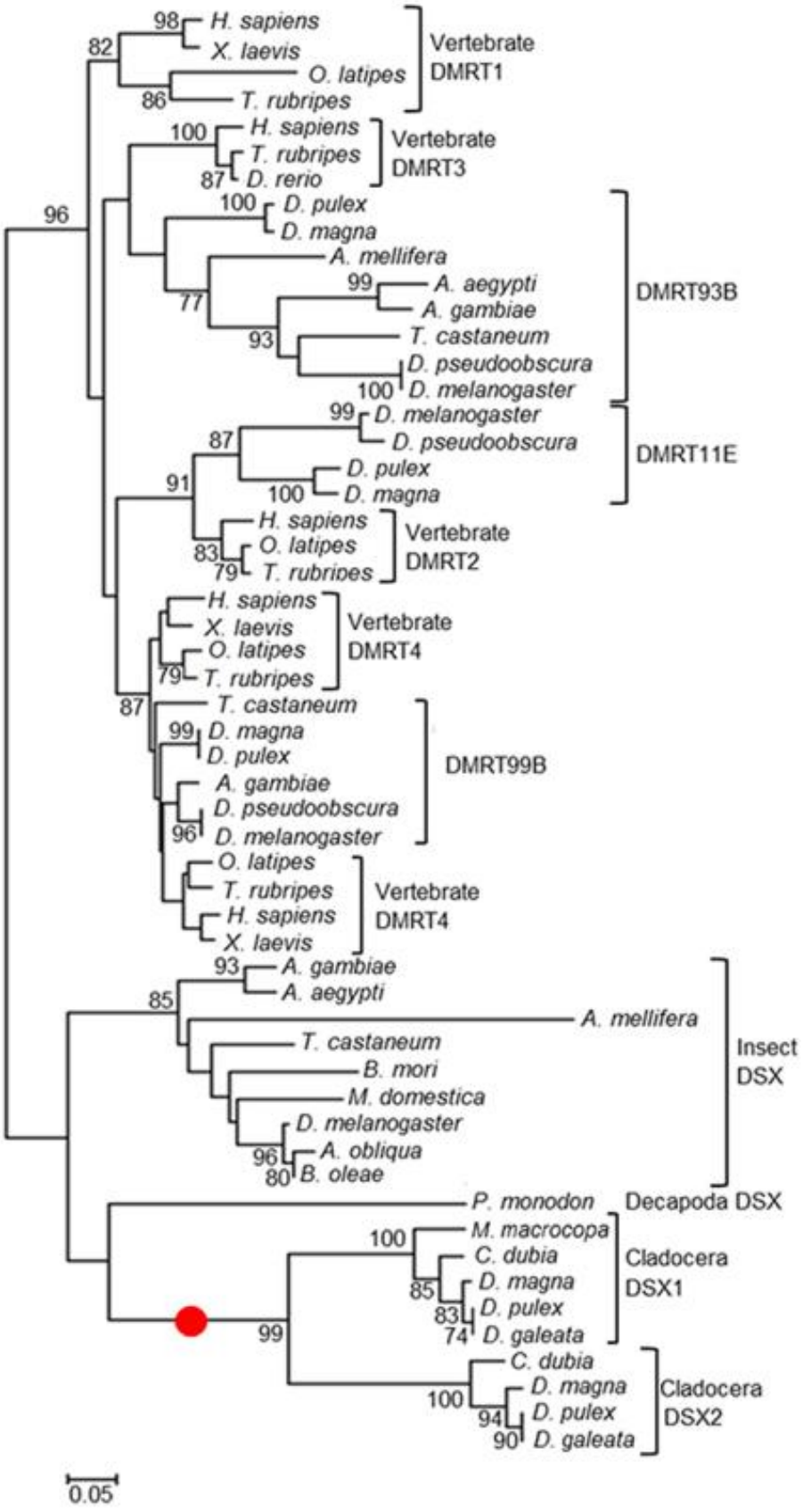
H. sapiens
X. laevis
O. latipes
T. rubripes
Vertebrate DMRT1
H. sapiens
T. rubripes
D. rerio
Vertebrate DMRT3
D. pulex
D. magna
A. mellifera
A. aegypti
A. gambiae
T. castaneum
D. pseudoobscura
D. melanogaster
DMRT93B
D. melanogaster
D. pseudoobscura
D. pulex
D. magna
DMRT11E
H. sapiens
O. latipes
T. rubripes
Vertebrate DMRT2
H. sapiens
X. laevis
O. latipes
T. rubripes
Vertebrate DMRT4
T. castaneum
D. magna
D. pulex
A. gambiae
D. pseudoobscura
D. melanogaster
DMRT99B
O. latipes
T. rubripes
H. sapiens
X. laevis
Vertebrate DMRT4
A. gambiae
A. aegypti
A. mellifera
T. castaneum
B. mori
M. domestica
D. melanogaster
A. obliqua
B. oleae
Insect DSX
P. monodon
Decapoda DSX
M. macrocopa
C. dubia
D. magna
D. pulex
D. galeata
Cladocera DSX1
C. dubia
D. magna
D. pulex
D. galeata
Cladocera DSX2
0.05

Figure 4-6. Phylogeny of DM-domain containing genes based on amino-acid sequence conservation. The evolutionary history of DM-domain containing genes was inferred by using the Neighbor-Joining method. The percentage of replicate trees in which the associated genes clustered together in the bootstrap test (1,000 replicates) is shown next to the branches (Bootstrap values below 70 percent are not shown). The tree is drawn to scale, with branch lengths in the same units as those of the evolutionary distances used to infer the phylogenetic tree. The evolutionary distances were computed using the Poisson correction method and are in the units of the number of amino acid substitutions per site. The analysis involved 55 amino acid sequences. All positions containing gaps and missing data were eliminated. There were a total of 62 positions in the final dataset. Evolutionary analyses were conducted in MEGA5 (Tamura et al., 2011). Red spot indicates duplication period of dsx gene duplication in cladocerans.

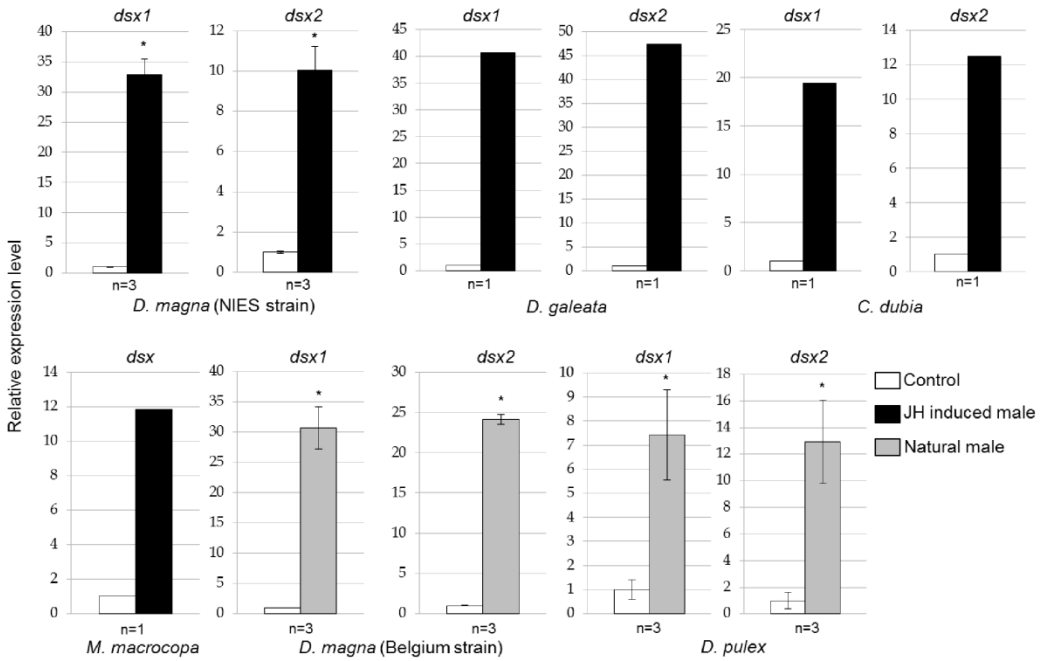

Figure 4-7. Relative transcriptional expression levels of *dsx1* and *dsx2* genes in adult males compared with females. The males of *D. magna* (NIES strain), *D. galeata*, *C. dubia* and *M. macrocopa* were induced by JH analog exposure. *D. magna* (Belgium strain) and *D. pulex* males were induced by environmental cues (see Materials and methods). These genes showed higher expression levels in males using both JHs (black) and natural cues (grey) than in females (white). Y-axes indicate relative expression levels normalized by female expression levels. Bars indicate standard errors. Numbers indicate the biological replicates. Asterisks indicate significant differences ($P < 0.05$, based on Student's *t*-test).

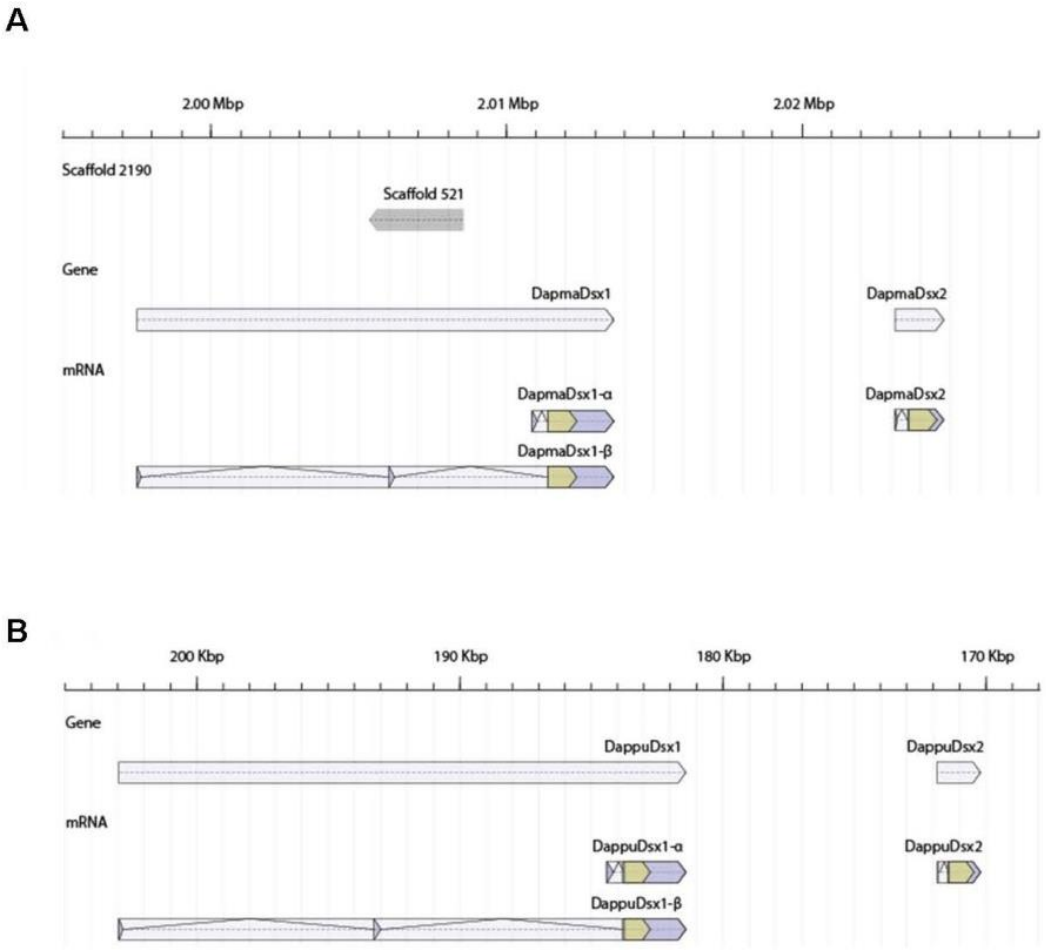

Figure 4-8. Gene model annotations on the *D. magna* and *D. pulex* genome assembly. (A) *D. magna dsx1* and *dsx2* gene model annotations on the *D. magna* genome assembly. (B) *D. pulex dsx1* and *dsx2* gene model annotations on the *D. pulex* genome assembly. Figures were created with AnnotationSketch (Steinbiss et al., 2009).

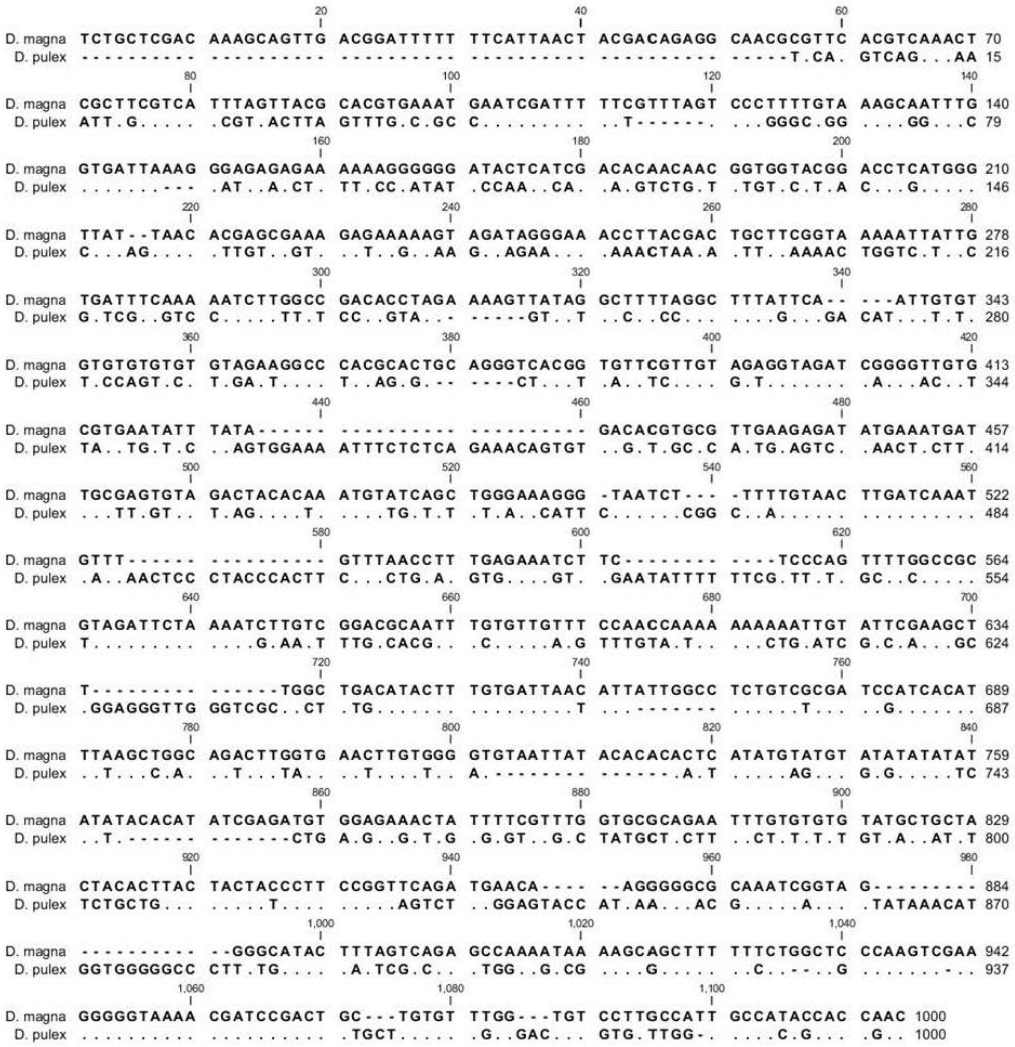

Figure 4-9. Nucleotide sequence comparison of *dsx1-α* promoter regions in *D. magna* and *D. pulex*. Pro-Coffee alignment of *Dsx1-α* 1.0 Kbp upstream promoter region from *D. magna* and *D. pulex*.

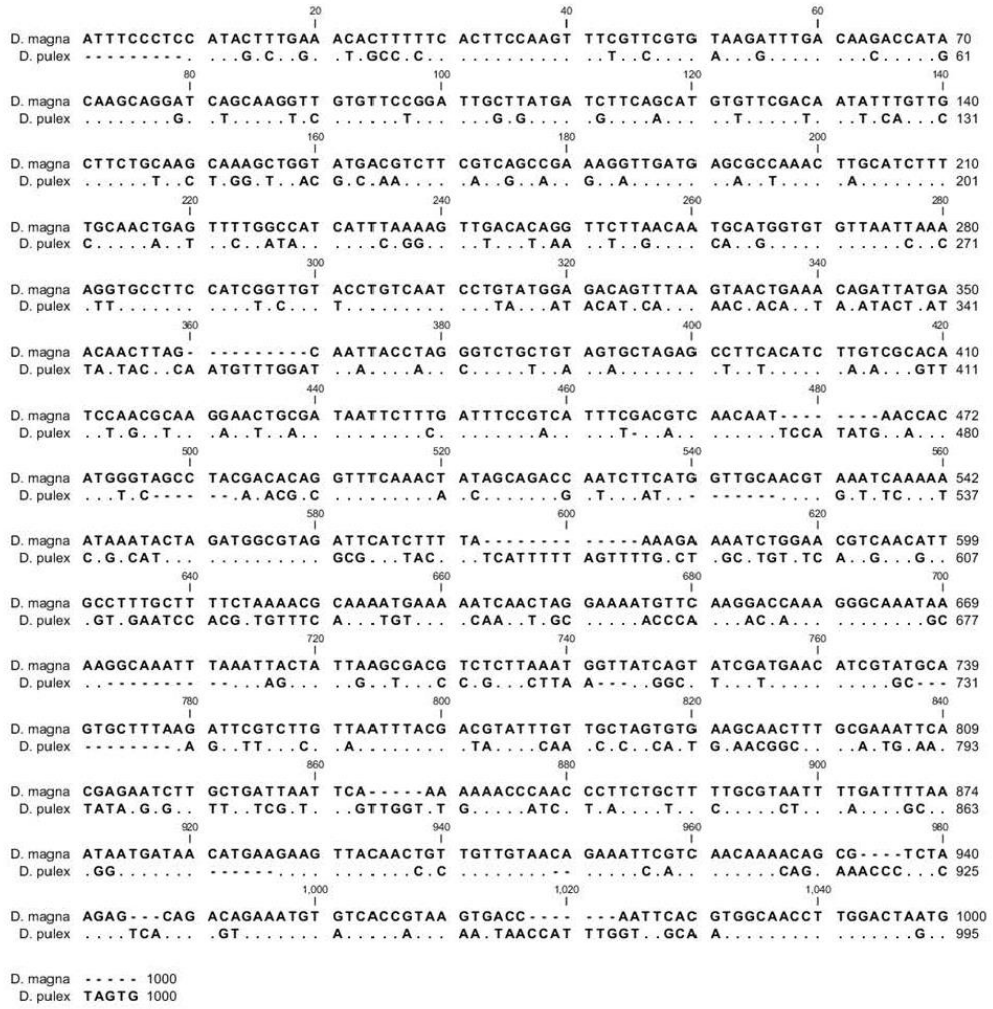

Figure 4-10. Nucleotide sequence comparison of *dsx1-β* promoter regions in *D. magna* and *D. pulex*. Pro-Coffee alignment of *dsx1-β* 1.0 Kbp upstream promoter region from *D. magna* and *D. pulex*.

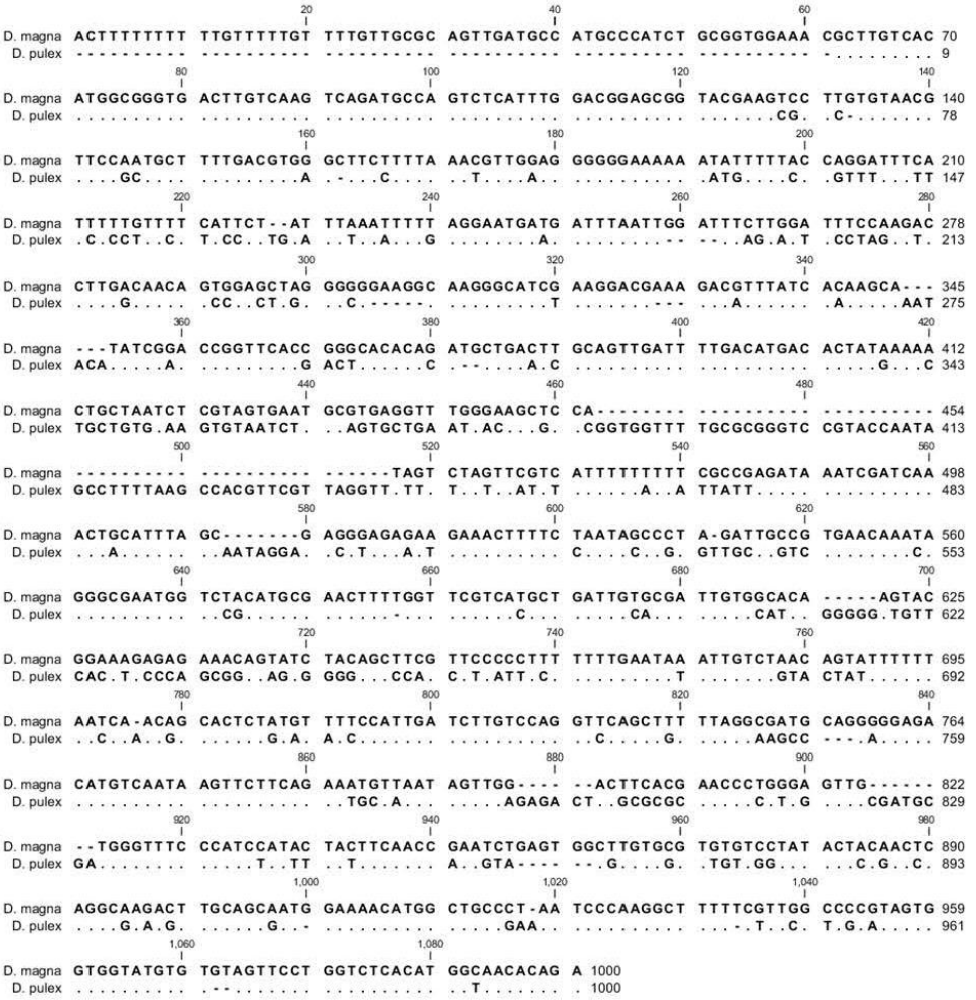

Figure 4-11. Nucleotide sequence comparison of *dsx2* promoter regions in *D. magna* and *D. pulex*. Pro-Coffee alignment of *dsx2* 1.0 Kbp upstream promoter region from *D. magna* and *D. pulex*.

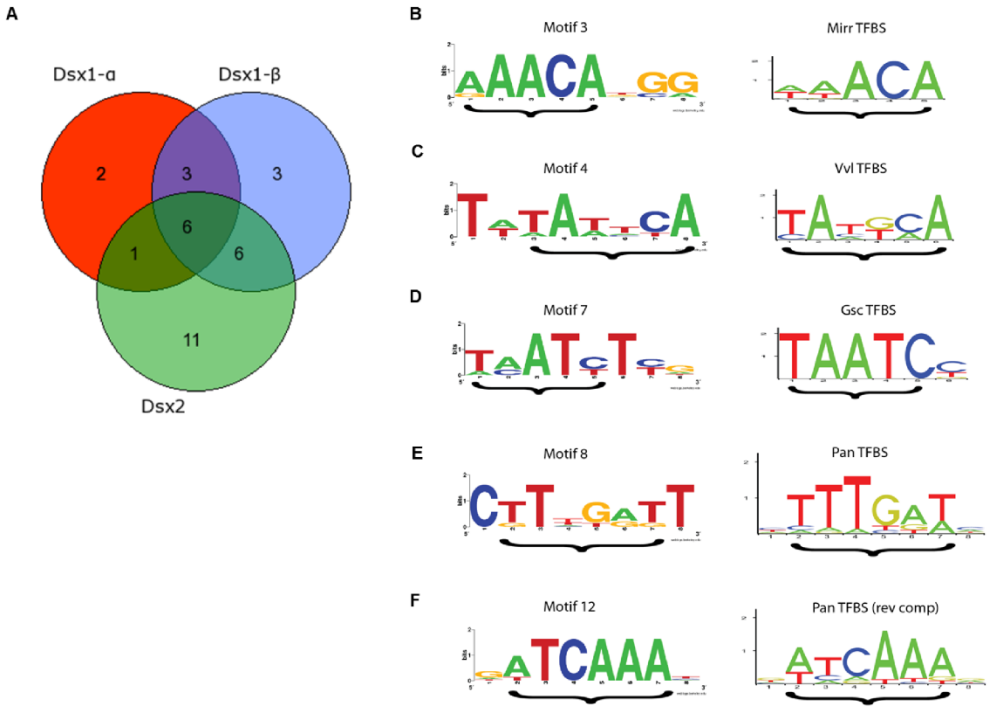

Figure 4-12. Venn diagram of putative transcriptional factors and sequence logos of *de novo dsx* promoter motifs. (A) Venn diagram showing the number of unique putative transcription factors shared amongst the *Daphnia magna* and *D. pulex dsx1-α, dsx1-β,* and *dsx2* TF-map alignments. (B-F) Braces under the sequence logos denote the similar regions between the *de novo* motif and known TFBS. Sequence logos were created with WebLogo (Crooks et al., 2002). (B) Motif 3 and Mirr TFBS (C) Motif 4 and Vvl TFBS (D) Motif 7 and Gsc TFBS (E) Motif 8 and Pan TFBS (F) Motif 12 and Pan reverse complement TFBS.

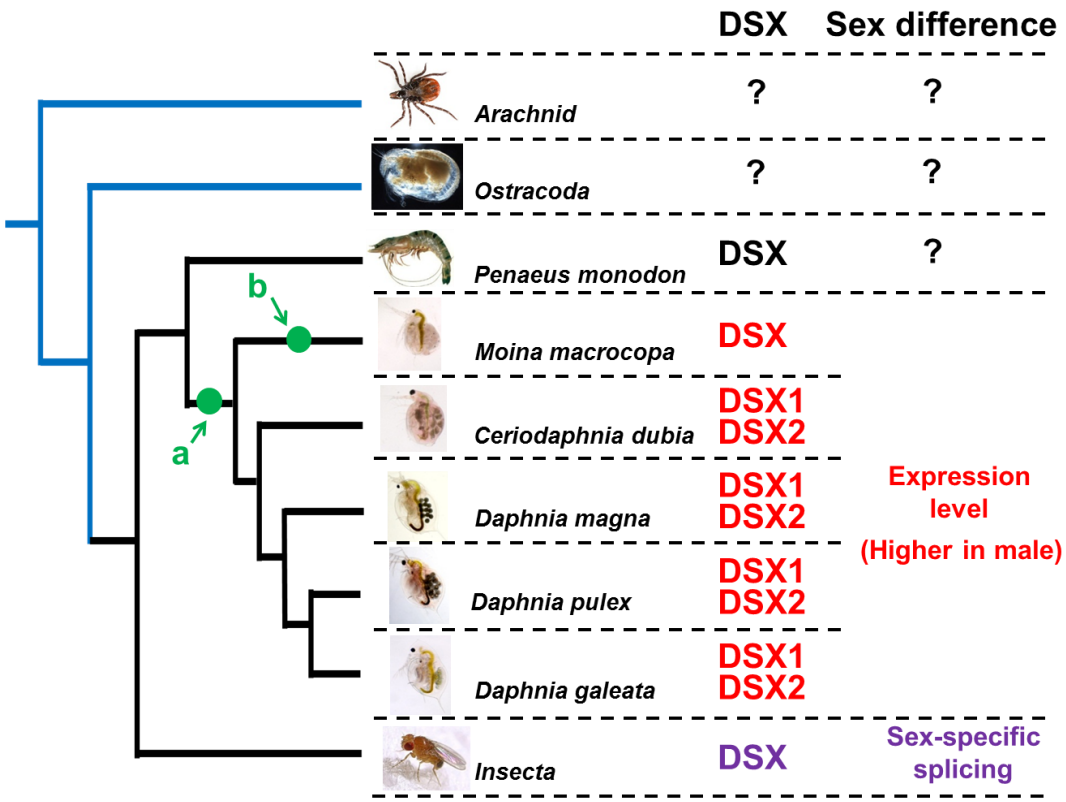

Figure 4-13. Schematic diagram of the phylogeny of arthropods and evolutionary process of acquisition of doublesex genes in the cladoceran species. Based on the phylogenetic relationships, it is suggested that common ancestor of cladocerans-specific duplication of doublesex genes has been occurred (a), and that doublesex2 might have been lost in *M. macrocopa* (b).

General Discussion and Conclusion

In this thesis, comparative, evolutionary, toxicological, biochemical and transcriptomic analyses were performed to understand the molecular signaling around the JH pathway underlying the ESD in daphnids. Throughout my analyses, I demonstrated the key role of JH signaling on the sex determination in daphnids. In chapter I, I established reliable induction system for male and female offspring in a *D. pulex* strain, WTN6, depending on photoperiod differences. Also, I revealed that the MF, which is regulated by JHAMT, is likely an innate JH in daphnids and is responsible for male offspring production (summarized in **Figure 1-20**).

It remained unknown that molecular signaling activating endocrine system (i.e., MF) in response to environmental cues, and the downstream target of MF. In chapter II, I identified the NMDA receptors as primary candidates mediating environmental cues to JH signaling by transcriptome analysis. I also found phosphorylation signaling cascades of the protein kinase C, which might be implied as a downstream signaling of JH (summarized in **Figure 2-6**). These findings provide an overview of the integrated signaling cascades around the JH pathway during sex determination and advance our knowledge for ESD in *D. pulex*. Furthermore, in chapter III, I established a comprehensive catalog of JH-responsive genes. These data provide a good opportunity to survey the genes involving with JH signaling cascades in daphnids, and helpful for investigating various modes of actions of JH agonists including their toxicological effects (summarized in **Figure 3-7**).

Previous study using *D. magna* has been showed that *dsx1* is a key element responsible for male sexually dimorphic development. In chapter IV, I demonstrated that *dsx* genes are evolutionally conserved and exclusively expressed in natural and

JH-induced males among cladoceran species. These results suggested that signaling cascade for male offspring production, which is primarily mediated by parental JH signaling (Kim et al., 2006; Oda et al., 2005b; Sinev and Sanoamuang, 2011), and is lastly elicited male traits by *dsx1* is widely conserved among cladoceran species (summarized in **Figure 4-13**). Based on these findings, I have illustrated the putative molecular signaling regulating sexual fate determination of daphnids depending on environmental conditions **(Figure GD-1)**.

Common principles of molecular mechanism of the ESD

I revealed that transient activation of innate JH signaling in response to external environmental cues is indispensable for male offspring production in daphnids. Interestingly, in the pea aphid *A. pisum* that exhibits cyclical parthenogenesis and ESD manner like daphnids, the decrease in JH III titer by JHE (JH degradation enzyme) is necessary for induction of sexual morph that produces a male and oviparous female (Ishikawa et al., 2012), and topical application of JH to oviparous producer induces the parthenogenetic female in pea aphids (Corbitt and Hardie, 1985). These findings indicate relationship between endogenous JH titer in the mothers and sexual outcome of the offspring is an opposite phenomenon between pea aphids and daphnids: high innate JH titer induces female in pea aphids and male offspring in daphnids **(Figure GD-2)**. It is interesting that JH signaling pathway seems to be co-opted in the sex determination mechanism in both species. Intriguingly, according to my own and other studies using daphnids, aphids, reptiles and fishes, environmental information (*e.g.*, photoperiod and temperature) is translated and integrated into endocrine systems such as, JHs in daphnids (Chapter I) and aphids (Ishikawa et al., 2012), estrogens in reptiles (Crews et

al., 1994; Pieau et al., 1999), and cortisol/estrogens in fish species (Hattori et al., 2009; Hayashi et al., 2010; Yamaguchi et al., 2010), and then facilitating the sexual dimorphic development. Both JHs and steroids (*e.g.*, estrogens and corticosteroids) are lipophilic endocrine factors, because these hormones are thought to permeate promptly and ubiquitously inside of the body. Therefore, a rough overview of signaling pathway of ESD system seems to be shared among organisms even though they are greatly divergent phylogenetically **(Figure GD-2)**.

Reception mechanisms of external environmental cues

Although the present studies focused mainly on JH signaling pathway as a key endocrine factor regulating the ESD system in daphnids, it has been elusive the reception mechanism of primary environmental cues. Previous studies have suggested that several photoreceptors are located in ommatidia of the compound eye of daphnids and are receptive to light signals around 340 nm (ultra violet: UV), 450 nm, 510 nm, and 590 nm (Smith and Macagno, 1990); however, it is still unknown whether these photoreceptors are involved in the primary trigger for sex determination. In the aphid *Megoura viciae*, the photoperiodic signal triggering the switch from parthenogenesis to sexual reproduction is activated in a part of brain (Lees, 1964, 1981). Particularly, a cluster of neurosecretory cells, which located on the dorso-anterior region of the photocerebrum (pars intercerebralis), play an important role in the measurement of scotophase (Gao et al., 1999; Lees, 1964). Therefore, it is postulated that these neurosecretory cells secrete some molecules and alter the developmental fate (viviparous female, oviparous female and male) of the oocytes in aphids. Interestingly, according to the recent morphological study of *Daphnia* nervous system, the compound

eye is directly connected to the protocerebral scaffold by the optic neuropil (Weiss et al., 2012). Based on integration of these findings, photoreceptors localized in ommatidia of the compound eye might be responsible for the short day cue in *D. pulex* WTN6 strain as well as aphids.

In addition to photoperiod cues, various environmental stimuli can trigger the male sexual fate determination in *D. pulex* (crowding and low temperature (Smith, 1915)) and *D. magna* (crowding and short day length (Hobæk and Larsson, 1990), crowding, short day length and oligotrophy (Kleiven et al., 1992)). Accordingly, primary environmental cues regulating the sexual fate determination in daphnids are quite distinct among strains bearing different genetic background. The establishment of stable male-inducing conditions in each strain of daphnids in response to alternative rearing conditions will be useful to clarify this point in the future.

Quantification of endogenous MF titers in daphnids

Recent advances in instrumental analyses enabled us to quantify the endogenous JHs levels from the whole body extract and/or hemolymph in several insect species (Jones et al., 2010; Jones et al., 2013). However, my trials to measure endogenous MF titer from *D. pulex* extracts using LC-MS and GC-MS methods have not been successful at present: I have never detected the MF peaks even though 10 daphnids/sample was extracted. The detection limit of our GC-MS system following the method by Jones et al., 2010 is approximately 5.0 pg. This result suggests that endogenous MF concentration during sex-determining period of *D. pulex* WTN6 strain reared under the male-inducing condition might be less than 0.5 pg/individual. In the case of pea aphid *A. pisum*, although using by LC-MS method, endogenous JH III titer

of male-inducing mother (JH titer is less than half that of viviparous female-inducing mother) is at least 0.5 ng/individual (Ishikawa et al., 2012), indicating there are 1000-fold differences of presumed endogenous JH titer causing alteration of sexual fate determination of next generations between daphnids and aphids. To demonstrate the relationship between endogenous MF titers and sexual fate determination in daphnids, further challenge will be required such as modification of sample preparation methods and use of newly updating equipment.

Transduction of maternal signals during parthenogenetic oogenesis

Sexual fate of daphnids is determined during the oocyte maturation period, prior to ovulation from the mother's ovary (Ignace et al., 2011; Chapter III). Therefore, I postulated that maternal sex determiner in response to JH signaling is supplied in the oocytes. In the case of *D. pulex* WTN6 strain reared under 18°C, once oocytes develop, they ovulate in approximately 70 h. During the oogenesis, cell cluster consisting of an oocyte and three nurse cells, is organized (Rossi, 1980). Both oocyte and nurse cells are morphologically indistinguishable just after ovulation and grow in a similar manner during early stage. Only the oocyte begins to accumulate the yolk granules and oil droplets (24 h after ovulation), whereas nurse cells are finally degenerated (60-70 h after ovulation) (Hiruta and Tochinai, 2011; Rossi, 1980). Tight and continuous association among oocytes, nurse cells and ovarian tissues makes it possible mother to transmit environmental cues into developing oocytes. It is intriguing that a critical JH-sensitive period for sex determination is the middle to late stage of oogenesis (40-60 h after ovulation), when nurse cells are accelerated to be degenerated. Several studies have reported that maternal effects (*e.g.*, food condition, photoperiod and chemical cues

released by the predators, referred to as ‘kairomone’) are associated with regulations of growth rate and fecundity (Alekseev and Lajus, 2009; Gorbi et al., 2011; LaMontagne and McCauley, 2001; Tollrian, 1995), inducibility of resting egg (Alekseev and Lampert, 2001), and acquisition of immune system (Little et al., 2003) in the offspring, however, maternal factors responsible for them are still largely unknown. Recent studies revealed that maternal mRNAs in the ovulated eggs possibly regulate the early embryonic development in daphnids (Asada et al., 2014; Kato et al., 2011a). These findings suggest that external environmental cues associated with sex determination could also be transferred to developing oocytes as maternal factors and they control the sexual fate of the offspring in the next generation, although such maternal substances remains elusive.

Daphnia pulex as an attractive model for the ESD study

Working with nontraditional model species, we usually encounter technological challenges, and experimental tools must be re-optimized for each particular species. We recently established the RNA interference (RNAi) method and transcription activator-like effector nuclease (TALEN) system based on microinjection technique using *D. pulex* embryos just after ovulation (Hiruta et al., 2014; Hiruta et al., 2013). However, the current microinjection-based gene targeting can be only available in early stage embryos and consequently, these techniques cannot be applied for knock-down/out of embryonic lethal genes. To investigate a specific gene function in more depth, a conditional gene targeting system is required for spatio-temporally controlled gene manipulation. In this point, a gene knock-in system based on genome-editing technology would allow the efficient gene modification, and also it will be useful for monitoring the localization of specific genes by expressing as a fusion

protein with fluorescent proteins. Recent progresses in omics and bioinformatics technologies enable us multifaceted views of cells, tissues and organisms in daphnids, such as transcriptomics (Chapter II; Chapter IV; Eads et al., 2008; Colbourne et al., 2011), metabolomics (Poynton et al., 2011), and proteomics (Fröhlich et al., 2009). Gene manipulation technique in combination with these omics data shed light on the novel insight of the pleiotropic aspects of molecular basis of the ESD in daphnids. Finally, I believe that novel findings in my thesis using *D. pulex* yields exciting novel insights of how diversified sex determination mechanisms evolve in animal species.

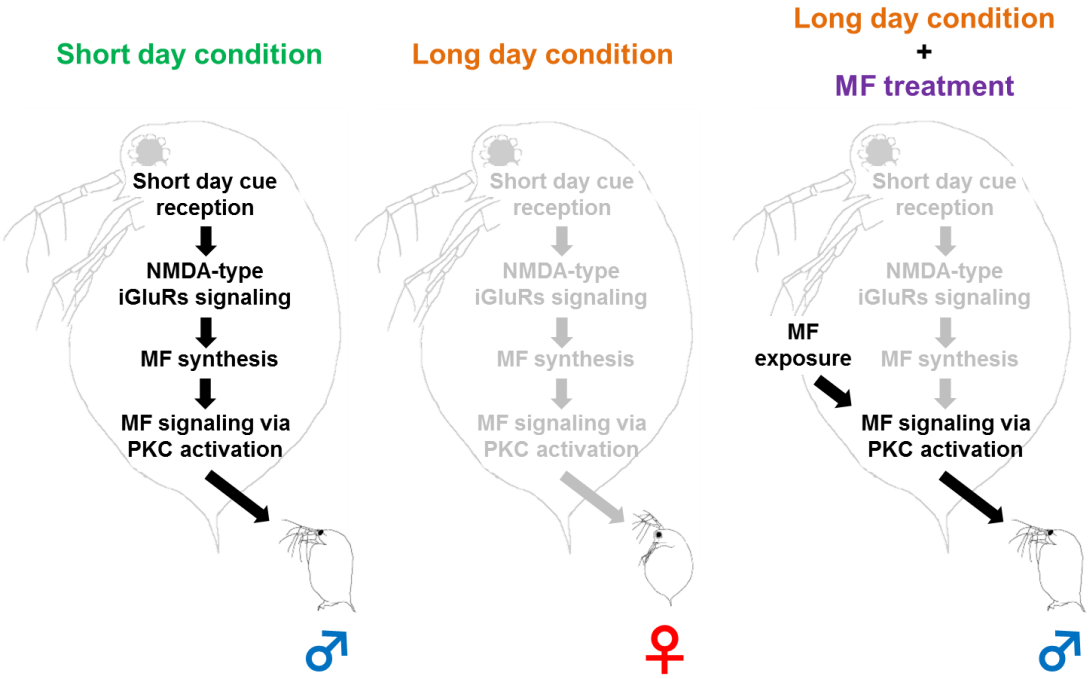

Figure GD-1. Schematic diagram of putative molecular signaling cascades regulating male offspring production responding to the short day stimuli in *D. pulex* WTN6 strain.

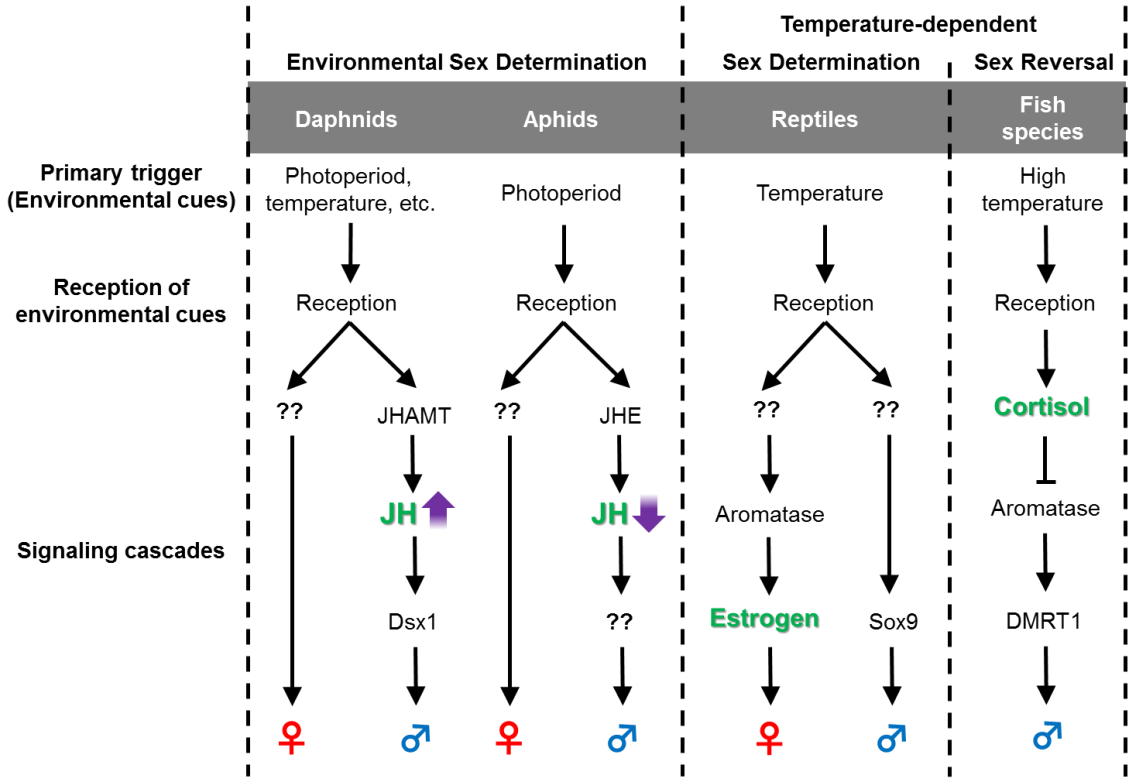

Figure GD-2. Representative ESD system in daphnids (Chapters I, IV), aphids (Ishikawa et al., 2012), reptiles (Crews et al., 1994; Pieau et al., 1999; Yao and Capel, 2005) and fish species (Hayashi et al., 2010; Yamaguchi et al., 2010). Green letters indicate the endocrine factors.

References

Abe, R., Toyota, K., Miyakawa, H., Watanabe, H., Oka, T., Miyagawa, S., Nishide, H., Uchiyama, I., Tollefsen, K.E., Iguchi, T., Tatarazako, N., 2015. Diofenolan induces male offspring production through binding to the juvenile hormone receptor in *Daphnia magna*. Aquat. Toxicol. 159, 44-51.

Adamowicz, S.J., Petrusek, A., Colbourne, J.K., Hebert, P.D.N., Witt, J.D.S., 2009. The scale of divergence: a phylogenetic appraisal of intercontinental allopatric speciation in a passively dispersed freshwater zooplankton genus. Mol. Phylogenet. Evol. 50, 423-436.

Andersen, C.L., Jensen, J.L., Ørntoft, T.F., 2004. Approach to identify genes suited for normalization, applied transcription-PCR data: A model-based variance estimation normalization of real-time quantitative reverse to bladder and colon cancer data sets. Cancer Res. 64, 5245-5250.

Ankley, G.T., Bennett, R.S., Erickson, R.J., Hoff, D.J., Hornung, M.W., Johnson, R.D., Mount, D.R., Nichols, J.W., Russom, C.L., Schmieder, P.K., Serrrano, J.A., Tietge, J.E., Villeneuve, D.L., 2010. Adverse outcome pathways: a conceptual framework to support ecotoxicology research and risk assessment. Environ. Toxicol. Chem. 29, 730-741.

Arand, M., Hemmer, H., Durk, H., Baratti, J., Archelas, A., Furstoss, R., Oesch, F., 1999. Cloning and molecular characterization of a soluble epoxide hydrolase from *Aspergillus niger* that is related to mammalian microsomal epoxide hydrolase. Biochem. J. 344, 273-280.

Banta, A.M., Brown, L.A., 1929a. Control of sex in Cladocera. II. The unstable nature of the excretory products involved in male production. Physiol. Zool. 2, 93-98.

Banta, A.M., Brown, L.A., 1929b. Control of sex in Cladocera. III. Localization of the critical period for control of sex. Proc. Natl. Acad. Sci. U. S. A. 15, 71-81.

Barton, N.H., Charlesworth, B., 1998. Why sex and recombination? Science 281, 1986-1990.

Bayrer, J.R., Zhang, W., Weiss, M.A., 2005. Dimerization of doublesex is mediated by a cryptic ubiquitin-associated domain fold: implications for sex-specific gene regulation. J. Biol. Chem. 280, 32989-32996.

Beguma, M., Breuer, M., Kodrik, D., Rahman, M.M., Loof, A.D., 2004. The NMDA receptor antagonist MK-801 inhibits vitellogenesis in the flesh fly *Neobellieria bullata* and in the desert locust *Schistocerca gregaria*. J. Insect Physiol. 50, 927-934.

Benjamini, Y., Hochberg, Y., 1995. Controlling the false discovery rate: a practical and

powerful approach to multiple testing. Journal of the Royal Statistical Society. Series B (Methodological) 57, 289-300.

Binns, D., Dimmer, E., Huntley, R., Barrell, D., O'Donovan, C., Apweiler, R., 2009. QuickGO: a web-based tool for Gene Ontology searching. Bioinformatics (Oxf) 25, 3045-3046.

Blanco, E., Messeguer, X., Smith, T.F., Guigo, R., 2006. Transcription factor map alignment of promoter regions. PLoS Comp. Biol. 2, e49.

Bryne, J.C., Valen, E., Tang, M.-H.E., Marstrand, T., Winther, O., Piedade, I.d., Krogh, A., Lenhard, B., Sandelin, A., 2008. JASPAR, the open access database of transcription factor-binding profiles: new content and tools in the 2008 update. Nucleic Acids Res. 36, 102-106.

Bull, J.J., 1981. Evolution of environmental sex determination from genotypic sex determination. Heredity 47, 173-184.

Bull, J.J., 1985. Sex determining mechanisms: an evolutionary perspective. Experientia 41, 1285-1296.

Bulmer, M.G., Bull, J.J., 1982. Models of polygenic sex determination and sex ratio control. Evolution 36, 13-26.

Burtis, K.C., Baker, B.S., 1989. Drosophila *doublesex* gene controls somatic sexual differentiation by producing alternatively spliced mRNAs encoding related sex-specific polypeptides. Cell 56, 997-1010.

Caceres, C.E., 1998. Interspecific variation in the abundance, production, and emerence of *Daphnia* diapuasing eggs. Ecology 79, 1699-1710.

Cannon, R., Hooper, H.L., Sibly, R.M., Lim, F.-L., Heckmann, L.-H., Moore, D.J., Watanabe, H., Soetaert, A., Cook, K., Maund, S.J., Hutchinson, T.H., Moggs, J., Coen, W.D., Iguchi, T., Callaghan, A., 2008. Linking molecular and population stress responses in *Daphnia magna* exposed to cadmium. Environ. Sci. Technol. 42, 2181-2188.

Chandler, C.H., P.C.Phillips, F.J.Janzen, 2009. The evolution of sex-determining mechanisms: lessons from temperature-sensitive mutations in sex determination genes in *Caenorhabditis elegans*. J. Evol. Biol. 22, 192-200.

Chang, E.S., Coudron, T.A., Bruce, M.J., Sage, B.A., O'connor, J.D., Law, J.H., 1980. Juvenile hormone-binding protein from the cytosol of *Drosophila* Kc cells. Proc Natl Acad Sci U S A Biol Sci 77, 4657-4661.

Charles, J.-P., Iwema, T., Epa, V.C., Takaki, K., Rynes, J., Jindra, M., 2011. Ligand-binding properties of a juvenile hormone receptor, Methoprene-tolerant. Proc Natl Acad Sci U S A Biol Sci 108, 21128-21133.

Charnier, M., 1966. Action de la température sur la sex-ratio chez l'embryon d'Agama agama (Agamidae, Lacertilien). Comptes Rendus des Séances de la Societé de Biologie de l'Ouest Africain 160, 620-622.

Chauhan, P., Hansson, B., Kraaijeveld, K., Knijff, P.d., Svensson, E.I., Wellenreuther, M., 2014. *De novo* transcriptome of *Ischnura elegans* provides insights into sensory biology, colour and vision genes. BMC Genomics 15.

Chiang, A.-S., Lin, W.-Y., Liu, H.-P., Pszczolkowski, M.A., Fu, T.-F., Chiu, S.-L., Holbrook, G.L., 2002. Insect NMDA receptors mediate juvenile hormone biosynthesis. Proc Natl Acad Sci U S A Biol Sci 99, 37-42.

Colbourne, J.K., Pfrender, M.E., Gilbert, D., Thomas, W.K., Tucker, A., Oakley, T.H., Tokishita, S., Aerts, A., Arnold, G.J., Basu, M.K., Bauer, D.J., Cáceres, C.E., Carmel, L., Casola, C., Choi, J.-H., Detter, J.C., Dong, Q., Dusheyko, S., Eads, B.D., Fröhlich, T., Geiler-Samerotte, K.A., Gerlach, D., Hatcher, P., Jogdeo, S., Krijgsveld, J., Kriventseva, E.V., Kültz, D., Laforsch, C., Lindquist, E., Lopez, J., Manak, J.R., Muller, J., Pangilinan, J., Patwardhan, R.P., Pitluck, S., Pritham, E.J., Rechtsteiner, A., Rho, M., Rogozin, I.B., Sakarya, O., Salamov, A., Schaack, S., Shapiro, H., Shiga, Y., Skalitzky, C., Smith, Z., Souvorov, A., Sung, W., Tang, Z., Tsuchiya, D., Tu, H., Vos, H., Wang, M., Wolf, Y.I., Yamagata, H., Yamada, T., Ye, Y., Shaw, J.R., Andrews, J., Crease, T.J., Tang, H., Lucas, S.M., Robertson, H.M., Bork, P., Koonin, E.V., Zdobnov, E.M., Grigoriev, I.V., Lynch, M., Boore, J.L., 2011. The ecoresponsive genome of *Daphnia pulex*. Science 331, 555-561.

Colbourne, J.K., Singan, V.R., Gilbert, D.G., 2005. wFleaBase: the *Daphnia* genome database. BMC Bioinformatics 6.

Consortium, I.A.G., 2010. Genome sequence of the pea aphid *Acyrthosiphon pisum*. PLoS Biol. 8, e1000313.

Corbitt, T.S., Hardie, J., 1985. Juvenile hormone effects on polymorphism in the pea aphid, *A cyrthosiphon pisum*. Entomol. Exp. Appl. 38.

Crews, D., Bergeron, J.M., Bull, J.J., Flores, D., Tousignant, A., Skipper, J.K., Wibbels, T., 1994. Temperature-dependent sex determination in reptiles: proximate mechanisms, ultimate outcomes, and practical applications. Dev. Genet. 15, 297-312.

Crews, D., Bull, J.J., 2009. Mode and tempo in environmental sex determination in vertebrates. Semin. Cell Dev. Biol. 20, 251-255.

Crooks, G.E., Hon, G., Chandonia, J.-M., Brenner, S.E., 2002. WebLogo: a sequence logo generator. Genome Res. 14, 1188-1190.

Cui, Y., Sui, Y., Xu, J., Zhu, F., Palli, S.R., 2014. Juvenile hormone regulates *Aedes aegypti* Krüppel homolog 1 through a conserved E box motif. Insect Biochem. Mol. Biol. 52, 23-32.

Daimon, T., Shinoda, T., 2013. Function, diversity, and application of insect juvenile hormone epoxidases (CYP15). Biotechnol. Appl. Biochem. 60, 82-91.

Defelipe, L.A., Dolghih, E., Roitberg, A.E., Nouzova, M., Mayoral, J.G., Noriega, F.G., Turjanski, A.G., 2011. Juvenile hormone synthesis: "esterify then epoxidize" or "epoxidize then esterify"? Insights from the structural characterization of juvenile hormone acid methyltransferase. Insect Biochem. Mol. Biol. 41, 228-235.

Denlinger, D.L., 2002. Regulation of diapause. Annu. Rev. Entomol. 47, 93-122.

Dodson, S.I., Merritt, C.M., Shannahan, J.-P., Shults, C.M., 1999. Low exposure concentrations of atrazine increase male production in *Daphnia magna*. Environ. Toxicol. Chem. 18, 1568-1573.

Eads, B., Andrews, J., Colbourne, J., 2008. Ecological genomics in *Daphnia*: stress responses and environmental sex determination. Heredity 100, 184-190.

Eads., B.D., Andrews, J., Colbourne, J.K., 2008. Ecological genomics in *Daphnia*: stress responses and environmental sex determination. Heredity 100, 184-190.

Ebert, D., 2005. Ecology, Epidemiology, and Evolution of Parasitism in Daphnia [Internet]. Bethesda (MD): National Library of Medicine (US), National Center for Biotechnology Information., Available from: http://www.ncbi.nlm.nih.gov/entrez/query.fcgi?db=Books.

Emlen, D.J., Nijhout, H.F., 1999. Hormonal control of male horn length dimorphism in the dung beetle *Onthophagus taurus* (Coleoptera: Scarabaeidae). J. Insect Physiol. 45, 45-53.

Erb, I., lez-Vallinas, J.R.G., Bussotti, G., Blanco, E., Eyras, E., Notredame, C.d., 2012. Use of ChIP-Seq data for the design of a multiple promoter-alignment method. Nucleic Acids Res., 1-11.

Fröhlich, T., Arnold, G.J., Fritsch, R., Mayr, T., Laforsch, C., 2009. LC-MS/MS-based proteome profiling in *Daphnia pulex* and *Daphnia longicephala*: the *Daphnia pulex* genome database as a key for high throughput proteomics in *Daphnia*. BMC Genomics 10, 171.

Gallot, A., Shigenobu, S., Hashiyama, T., Jaubert-Possamai, S., Tagu, D., 2012. Sexual and asexual oogenesis require the expression of unique and shared sets of genes in the insect *Acyrthosiphon pisum*. BMC Genomics 13, 76.

Gao, N., Schantz, M.v., Foster, R.G., Hardie, J., 1999. The putative brain photoperiodic

photoreceptors in the vetch aphid, *Megoura viciae*. J. Insect Physiol. 45, 1011-1019.

Geister, T.L., Lorenz, M.W., Hoffmann, K.H., Fischer, K., 2008. Effects of the NMDA receptor antagonist MK-801 on female reproduction and juvenile hormone biosynthesis in the cricket *Gryllus bimaculatus* and the butterfly *Bicyclus anynana*. J. Exp. Biol. 211, 1587-1593.

Gempe, T., Beye, M., 2011. Function and evolution of sex determination mechanisms, genes and pathways in insects. Bioessays 33, 52-60.

Gentleman, R.C., Carey, V.J., Bates, D.M., Bolstad, B., Dettling, M., Dudoit, S., Ellis, B., Gautier, L., Ge, Y., Gentry, J., Hornik, K., Hothorn, T., Huber, W., Iacus, S., Irizarry, R., Leisch, F., Li, C., Maechler, M., Rossini, A.J., Sawitzki, G., Smith, C., Smyth, G., Tierney, L., Yang, J.Y., Zhang, J., 2004. Bioconductor: open software development for computational biology and bioinformatics. Genome Biol 5, R80.

Ghaffari, N., Sanchez-Flores, A., Doan, R., Garcia-Orozco, K.D., Chen, P.L., Ochoa-Leyva, A., Lopez-Zavala, A.A., Carrasco, J.S., Hong, C., Brieba, L.G., Rudin˜o-Pin˜era, E., Blood, P.D., Sawyer, J.E., Johnson, C.D., Dindot, S.V., Sotelo-Mundo, R.R., Criscitiello, M.F., 2014. Novel transcriptome assembly and improved annotation of the whiteleg shrimp (*Litopenaeus vannamei*), a dominant crustacean in global seafood mariculture. Scientific reports 4, srep07081.

Goodman, W.G., Adams, B., 1984. Semipreparative synthesis and purification of juvenile hormone acids by high-performance liquid chromatography. J. Chromatogr. 294, 447-451.

Goodman, W.G., Cusson, M., 2012. The juvenile hormones. In Insect Endocrinology (Gilbert L.I.). Academic Press, Elsevier, UK, 310-365.

Gorr, T.A., Rider, C.V., Y.Wang, H., Olmstead, A., LeBlanc, G.A., 2006. A candidate juvenoid hormone receptor *cis*-element in the *Daphnia magna* hb2 hemoglobin gene promoter. Mol. Cell. Endocrinol. 247, 91-102.

Gotoh, H., Miyakawa, H., Ishikawa, A., Ishikawa, Y., Sugime, Y., Emlen, D.J., Lavine, L.C., Miura, T., 2014. Developmental link between sex and nutrition; *doublesex* regulates sex-specific mandible growth via juvenile hormone signaling in stag beetles. PLoS Genet. 10, e1004098.

Grabherr, M.G., Haas, B.J., Yassour, M., Levin, J.Z., Thompson, D.A., Amit, I., Adiconis, X., Fan, L., Raychowdhury, R., Zeng, Q., Chen, Z., Mauceli, E., Hacohen, N., Gnirke, A., Rhind, N., Palma, F.d., Birren, B.W., Nusbaum, C.,

Lindblad-Toh, K., Friedman, N., Regev, A., 2011. Full-length transcriptome assembly from RNA-Seq data without a reference genome. Nat. Biotechnol. 29, 644-652.

Guler, Y., Short, S., Kile, P., Ford, A.T., 2012. Integrating field and laboratory evidence for environmental sex determination in the amphipod, *Echinogammarus marinus*. Mar. Biol. 159, 2885-2890.

Haas, B.J., Delcher, A.L., Mount, S.M., Wortman, J.R., Jr, R.K.S., Hannick, L.I., Maiti, R., Ronning, C.M., Rusch, D.B., Town, C.D., Salzberg, S.L., White, O., 2003. Improving the Arabidopsis genome annotation using maximal transcript alignment assemblies. Nucleic Acids Res. 31, 5654-5666.

Hao, W., Zhang, Y., Xu, Y.-S., 2013. Identification of a juvenile hormone esterase binding protein gene and its developmental and hormone regulation in the silkworm, *Bombyx mori*. J. Insect Physiol. 59, 906-912.

Hardie, J., 1981. Juvenile hormone and photoperiodically controlled polymorphism in *Aphis fabae*: Prenatal effects on presumptive oviparae. J. Insect Physiol. 27, 257-265.

Hattori, R.S., Fernandino, J.I., Kishii, A., Kimura, H., Kinno, T., Oura, M., Somoza, G.M., Yokota, M., ssmann, C.A.S., Watanabe, S., 2009. Cortisol-induced masculinization: Does thermal stress affect gonadal fate in Pejerrey, a teleost fish with temperature-dependent sex determination? PLoS ONE 4, e6548.

Hayashi, Y., Kobira, H., Yamaguchi, T., Shiraishi, E., Yazawa, T., Hirai, T., Kamei, Y., Kitano, T., 2010. High temperature causes masculinization of genetically female medaka by elevation of cortisol. Mol. Reprod. Dev. 77, 679-686.

Hebert, P.D., 1987. Genotypic characteristics of cyclic parthenogens and their obligately asexual derivatives. Experientia. Suppl. 55, 175-195.

Hebert, P.D.N., 1997. Cladocera as Model Systems in Biology. J. Exp. Mar. Biol. Ecol. 209, 310-311.

Hiruta, C., Nishida, C., Tochinai, S., 2010. Abortive meiosis in the oogenesis of parthenogenetic *Daphnia pulex*. Chromosome Res. 18, 833-840.

Hiruta, C., Ogino, Y., Sakuma, T., Toyota, K., Miyagawa, S., Yamamoto, T., Iguchi, T., 2014. Targeted gene disruption by use of transcription activator-like effector nuclease (TALEN) in the water flea *Daphnia pulex*. BMC Biotechnol. 14, 95.

Hiruta, C., Toyota, K., Miyakawa, H., Ogino, Y., Miyagawa, S., Tatarazako, N., Shaw, J.R., Iguchi, T., 2013. Development of a microinjection system for RNA interference in the water flea *Daphnia pulex*. BMC Biotechnol. 13, 96.

Hobæk, A., Larsson, P., 1990. Sex determination in *Daphnia magna*. Ecology 71,

2255-2268.

Horst, M.N., Walker, A.N., Bush, P., Wilson, T., Chang, E.S., Miller, T., Larkin, P., 2007. Pesticide induced alterations in gene expression in the lobster, *Homarus americanus*. Comparative Biochemistry and Physiology Part D: Genomics and Proteomics 2, 44-52.

Huang, J., Tian, L., Peng, C., Abdou, M., Wen, D., Wang, Y., Li, S., Wang, J., 2011. DPP-mediated TGFbeta signaling regulates juvenile hormone biosynthesis by activating the expression of juvenile hormone acid methyltransferase. Development 138, 2283-2291.

Hui, J.H.L., Hayward, A., Bendena, W.G., Takahashi, T., Tobe, S.S., 2010. Evolution and functional divergence of enzymes involved in sesquiterpenoid hormone biosynthesis in crustaceans and insects. Peptides 31, 451-455.

Ichikawa, A., Ono, H., Furuta, K., Shiotsuki, T., Shinoda, T., 2007. Enantioselective separation of racemic juvenile hormone III by normal-phase high-performance liquid chromatography and preparation of [2H3]juvenile hormone III as an internal standard for liquid chromatography–mass spectrometry quantification. J. Chromatogr. A 1161, 252-260.

Ignace, D.D., Dodson, S.I., Kashian, D.R., 2011. Identification of the critical timing of sex determination in *Daphnia magna* (Crustacea, Branchiopoda) for use in toxicological studies. Hydrobiologia 668, 117-123.

Iguchi, T., Watanabe, H., Katsu, Y., 2006. Application of ecotoxicogenomics for studying endocrine disruption in vertebrates and invertebrates. Environ. Health Perspect. 114, 101-105.

Ishikawa, A., Ogawa, K., Gotoh, H., Walsh, T.K., Tagu, D., Brisson, J.A., Rispe, C., Jaubert-Possamai, S., Kanbe, T., Tsubota, T., Shiotsuki, T., Miura, T., 2012. Juvenile hormone titre and related gene expression during the change of reproductive modes in the pea aphid. Insect Mol. Biol. 21, 49-60.

Jones, D., Jones, G., Teal, P., Hammac, C., Messmer, L., Osborne, K., Belgacem, Y.H., Martin, J.-R., 2010. Suppressed production of methyl farnesoid hormones yields developmental defects and lethality in *Drosophila* larvae. Gen. Comp. Endocrinol. 165, 244-254.

Jones, G., Teal, P., Henrich, V.C., Krzywonos, A., Sapa, A., Wozniak, M., Smolka, J., Jones, D., 2013. Ligand binding pocket function of *Drosophila* USP is necessary for metamorphosis. Gen. Comp. Endocrinol. 182, 73-82.

Kato, Y., Kobayashi, K., Oda, S., Colbourn, J.K., Tatarazako, N., Watanabe, H., Iguchi, T., 2008. Molecular cloning and sexually dimorphic expression of DM-domain

genes in *Daphnia magna*. Genomics 91, 94-101.

Kato, Y., Kobayashi, K., Oda, S., Tatarazako, N., HajimeWatanabe, Iguchi, T., 2007. Cloning and characterization of the ecdysone receptor and ultraspiracle protein from the water flea *Daphnia magna*. J. Endocrinol. 193, 183-194.

Kato, Y., Kobayashi, K., Oda, S., Tatarazako, N., Watanabe, H., Iguchi, T., 2010. Sequence divergence and expression of a transformer gene in the branchiopod crustacean, *Daphnia magna*. Genomics 95, 160-165.

Kato, Y., Kobayashi, K., Watanabe, H., Iguchi, T., 2011a. Environmental sex determination in the branchiopod crustacean *Daphnia magna*: deep conservation of a *Doublesex* gene in the sex-determining pathway. PLoS Genet. 7, e1001345.

Kato, Y., Shiga, Y., Kobayashi, K., Tokishita, S., Yamagata, H., Iguchi, T., Watanabe, H., 2011b. Development of an RNA interference method in the cladoceran crustacean *Daphnia magna*. Dev. Genes Evol. 220, 337-345.

Kayukawa, T., Minakuchi, C., Namiki, T., Togawa, T., Yoshiyama, M., Kamimura, M., Mita, K., Imanishi, S., Kiuchi, M., Ishikawa, Y., Shinoda, T., 2012. Transcriptional regulation of juvenile hormone-mediated induction of Kruppel homolog 1, a repressor of insect metamorphosis. Proc. Natl. Acad. Sci. U. S. A. 109, 11729-11734.

Kayukawa, T., Tateishi, K., Shinoda, T., 2013. Establishment of a versatile cell line for juvenile hormone signaling analysis in *Tribolium castaneum*. Scientific reports 3, 1570.

Kim, J., Kim, Y., Lee, S., Kwak, K., Chung, W.-J., Choi, K., 2011. Determination of mRNA expression of *DMRT93B, vitellogenin*, and *cuticle 12* in *Daphnia magna* and their biomarker potential for endocrine disruption. Ecotoxicology 20, 1741-1748.

Kim, K., Kotov, A.A., Taylor, D.J., 2006. Hormonal induction of undescribed males resolves cryptic species of cladocerans. Proc R Soc Lond Ser B Biol Sci 273, 141-147.

Kleiven, O.T., Larsson, P., Hobæk, A., 1992. Sexual reproduction in *Daphnia magna* requires three stimuli. Oikos 65, 197-206.

Kodama, Y., Suzuki, H., Dohra, H., Sugii, M., Kitazume, T., Yamaguchi, K., Shigenobu, S., Fujishima, M., 2014. Comparison of gene expression of *Paramecium bursaria* with and without *Chlorella variabilis* symbionts. BMC Genomics 15, 183.

Kopp, A., 2012. *Dmrt* genes in the development and evolution of sexual dimorphism.

Trends Genet. 28, 175-184.
Korpelainen, H., 1990. Sex ratios and conditions required for environmental sex determination in animals. Biol. Rev. Camb. Philos. Soc. 65, 147-184.
Kotov, A., Forró, L., Korovchinsky, N.M., Petrusek, A., 2013. Crustacea-Cladocera checkList. World checklist of freshwater Cladocera species. World Wide Web electronic publication. , http://fada.biodiversity.be/group/show/17
Kuballa, A.V., Guyatt, K., Dixon, B., Thaggard, H., Ashton, A.R., Paterson, B., Merritt, D.J., Elizur, A., 2007. Isolation and expression analysis of multiple isoforms of putative farnesoic acid *O*-methyltransferase in several crustacean species. Gen. Comp. Endocrinol. 150, 48-58.
Langmead, B., Salzberg, S.L., 2012. Fast gapped-read alignment with Bowtie 2. Nat. Methods 9, 357-359.
Le Trionnaire, G., Francis, F., Jaubert-Possamai, S., Bonhomme, J., De Pauw, E., Gauthier, J.P., Haubruge, E., Legeai, F., Prunier-Leterme, N., Simon, J.C., Tanguy, S., Tagu, D., 2009. Transcriptomic and proteomic analyses of seasonal photoperiodism in the pea aphid. BMC Genomics 10, 456.
Lee, H.K., Braynen, W., Keshav, K., Pavlidis, P., 2005. ErmineJ: tool for functional analysis of gene expression data sets. BMC Bioinformatics 6, 269.
Lees, A.D., 1959. The role of photoperiod and temperature in the determination of parthenogenetic and sexual forms in the aphid *Megoura viciae* Buckton - I The influence of these factors on apterous virgmoparae and their progeny. J. Insect Physiol. 3, 92-117.
Lees, A.D., 1964. The location of the photoperiodic receptors in the aphid *Megoura viciae* buckton. J. Exp. Biol. 41, 119-133.
Lees, A.D., 1973. Photoperiodic time measurement in the aphid *Megoura viciae*. J. Insect Physiol. 19, 2279-2316.
Lees, A.D., 1981. Action spectra for the photoperiodic control of polymorphism in the aphid *Megoura viciae*. J. Insect Physiol. 27, 761-771.
Li, M., Mead, E.A., Zhu, J., 2011. Heterodimer of two bHLH-PAS proteins mediates juvenile hormone-induced gene expression. Proc. Natl. Acad. Sci. U. S. A. 108, 638-643.
Li, W., Huang, Z.Y., Liu, F., Li, Z., Yan, L., Zhang, S., Chen, S., Zhong, B., Su, S., 2013. Molecular cloning and characterization of juvenile hormone acid methyltransferase in the honey bee, *Apis mellifera*, and its differential expression during caste differentiation. PLoS ONE 8, e68544.
Liess, M., Ohe, P.C.V.D., 2005. Analyzing effects of pesticides on invertebrate

communities in streams. Environ. Toxicol. Chem. 24, 954-965.

Manar, R., Bessi, H., Vasseur, P., 2009. Reproductive effects and bioaccumulation of chlordane in *Daphnia magna*. Environ. Toxicol. Chem. 28, 2150-2159.

Marin, I., Baker, B.S., 1998. The evolutionary dynamics of sex determination. Science 281, 1990-1994.

Martin, M., 2011. Cutadapt removes adapter sequences from high-throughput sequencing reads. EMBnet.Journal 17, 10-12.

Matson, C.K., Zarkower, D., 2012. Sex and the singular DM domain: insights into sexual regulation, evolution and plasticity. Nat Rev Genet 13, 163-174.

Matys, V., Fricke, E., Geffers, R., Goßling, E., Haubrock, M., Hehl, R., Hornischer, K., Karas, D., Kel, A.E., Kel-Margoulis, O.V., Kloos, D.-U., Land, S., Lewicki-Potapov, B., Michael, H., Munch, R., Reuter, I., Rotert, S., Saxel, H., Scheer, M., Thiele, S., Wingender, E., 2003. TRANSFAC(R): transcriptional regulation, from patterns to profiles. Nucleic Acids Res. 31, 374-378.

Mayoral, J.G., Nouzova, M., Yoshiyama, M., Shinoda, T., Hernandez-Martinez, S., Dolghih, E., Turjanski, A.G., Roitberg, A.E., Priestap, H., Perez, M., Mackenzie, L., Li, Y., Noriega, F.G., 2009. Molecular and functional characterization of a juvenile hormone acid methyltransferase expressed in the corpora allata of mosquitoes. Insect Biochem. Mol. Biol. 39, 31-37.

Merchant-Larios, H., Diaz-Hernandez, V., 2013. Environmental sex determination mechanisms in reptiles. Sexual Development 7, 95-103.

Minakuchi, C., Namiki, T., Yoshiyama, M., Shinoda, T., 2008. RNAi-mediated knockdown of *juvenile hormone acid O-methyltransferase* gene causes precocious metamorphosis in the red flour beetle *Tribolium castaneum*. FEBS J. 275, 2919-2931.

Mitchell, S.E., 2001. Intersex and male development in *Daphnia magna*. Hydrobiologia 442, 145-156.

Miura, T., 2005. Developmental regulation of caste-specific characters in social-insect polyphenism. Evol Dev 7, 122-129.

Miyakawa, H., Gotoh, H., Sugimoto, N., Miura, T., 2013a. Effect of juvenoids on predator-induced polyphenism in the water flea, *Daphnia pulex*. J Exp Zool Part A Comp Exp Biol 319, 440-450.

Miyakawa, H., Imai, M., Sugimoto, N., Ishikawa, Y., Ishikawa, A., Ishigaki, H., Okada, Y., Miyazaki, S., Koshikawa, S., Cornette, R., Miura, T., 2010. Gene up-regulation in response to predator kairomones in the water flea, *Daphnia pulex*. BMC Dev. Biol. 10.

Miyakawa, H., Toyota, K., Hirakawa, I., Ogino, Y., Miyagawa, S., Oda, S., Tatarazako, N., Miura, T., Colbourne, J.K., Iguchi, T., 2013b. A mutation in the receptor Methoprene-tolerant alters juvenile hormone response in insects and crustaceans. Nature Communications ncomms2868.

Miyakawa, H., Toyota, K., Hirakawa, I., Ogino, Y., Miyagawa, S., Oda, S., Tatarazako, N., Miura, T., Colbourne, J.K., Iguchi, T., 2013c. A mutation in the receptor Methoprene-tolerant alters juvenile hormone response in insects and crustaceans. Nature communications 4, 1856.

Miyakawa, H., Toyota, K., Sumiya, E., Iguchi, T., 2014. Comparison of JH signaling in insects and crustaceans. Current Opinion in Insect Science 1, 81-87.

Nagaraju, G.P.C., 2011. Reproductive regulators in decapod crustaceans: an overview. J. Exp. Biol. 214, 3-16.

Nijhout, H.F., 1994. insect Hormones. Princeton, NJ: Princeton University Press.

Nijhout, H.F., 2003. Development and evolution of adaptive polyphenisms. Evol Dev 5, 9-18.

Niwa, R., Niimi, T., Honda, N., Yoshiyama, M., Itoyama, K., Kataoka, H., Shinoda, T., 2008. Juvenile hormone acid *O*-methyltransferase in *Drosophila melanogaster*. Insect Biochem. Mol. Biol. 38, 714-720.

Oda, S., Kato, Y., Watanabe, H., Tatarazako, N., Iguchi, T., 2011. Morphological changes in *Daphnia galeata* induced by a crustacean terpenoid hormone and its analog. Environ. Toxicol. Chem. 30, 232-238.

Oda, S., Tatarazako, N., Dorgerloh, M., Johnson, R.D., Kusk, K.O., Leverett, D., Marchini, S., Nakari, T., Williams, T., Iguchi, T., 2007. Strain difference in sensitivity to 3,4-dichloroaniline and insect growth regulator, fenoxycarb, in *Daphnia magna*. Ecotoxicol. Environ. Saf. 67, 399-405.

Oda, S., Tatarazako, N., Watanabe, H., Morita, M., Iguchi, T., 2005a. Production of male neonates in *Daphnia magna* (Cladocera, Crustacea) exposed to juvenile hormones and their analogs. Chemosphere 61, 1168-1174.

Oda, S., Tatarazako, N., Watanabe, H., Morita, M., Iguchi, T., 2005b. Production of male neonates in four cladoceran species exposed to a juvenile hormone analog, fenoxycarb. Chemosphere 60, 74-78.

Oda, S., Tatarazako, N., Watanabe, H., Morita, M., Iguchi, T., 2006. Genetic differences in the production of male neonates in *Daphnia magna* exposed to juvenile hormone analogs. Chemosphere 63, 1477-1484.

OECD, 1998. *Daphnia magna* reproduction test.

OECD, 2004. Daphnia sp., acute immobilisation test.

Olesen, J., 1998. A phylogenetic analysis of the Conchostraca and Cladocera (Crustacea, Branchiopoda, Diplostraca). Zool. J. Linn. Soc. 122, 491-536.

Oliveira, D.C.S.G., Werren, J.H., Verhuls, E.C., Giebel, J.D., Kamping, A., Beukeboom, L.W., Zande, L.v.d., 2009. Identification and characterization of the *doublesex* gene of *Nasonia*. Insect Mol. Biol. 18, 315-324.

Olmstead, A.W., LeBlanc, G.A., 2000. Effects of endcrine-active chemicals on the development of sex characteristics of *Daphnia magna*. Environ. Toxicol. Chem. 19, 2107-2113.

Olmstead, A.W., LeBlanc, G.A., 2002. Juvenoid hormone methyl farnesoate is a sex determinant in the crustacean *Daphnia magna*. J. Exp. Zool. 293, 736-739.

Organ, C.L., Janes, D.E., 2008. Evolution of sex chromosomes in Sauropsida. Integr. Comp. Biol. 48, 512-519.

Palma, P., Palma, V.L., Fernandes, R.M., Soares, A.M.V.M., Barbosa, I.R., 2009. Endosulfan sulphate interferes with reproduction, embryonic development and sex differentiation in *Daphnia magna*. Ecotoxicol. Environ. Saf. 72, 344-350.

Pavesi, G., Zambelli, F., Pesole, G., 2007. WeederH: an algorithm for finding conserved regulatory motifs and regions in homologous sequences. BMC Bioinformatics 8, 46.

Pieau, C., Dorizzi, M., Richard-Mercier, N., 1999. Temperature-dependent sex determination and gonadal differentiation in reptiles. Cell. Mol. Life Sci. 55, 887-900.

Poynton, H.C., Taylor, N.S., Hicks, J., Scanlan, L., Loguinov, A.V., Vulpe, C., Viant, M.R., 2011. Metabolomics of microliter hemolymph samples enables an improved understanding of the combined metabolic and transcriptional responses of *Daphnia magna* to cadmium. Environ. Sci. Technol. 45, 3710-3717.

Poynton, H.C., Varshavsky, J.R., Chang, B., Cavigiolio, G., Chan, S., Holman, P.S., Loguinov, A.V., Bauer, D.J., Komachi, K., Theil, E.C., Perkins, E.J., Hughes, O., Vulpe, C.D., 2007. Daphnia magna ecotoxicogenomics provides mechanistic insights into metal toxicity. Environ. Sci. Technol. 41, 1044-1050.

Pszczolkowski, M.A., Lee, W.-S., Liu, H.-P., Chiang, A.-S., 1999. Glutamate-induced rise in cytosolic calcium concentration stimulates *in vitro* rates of juvenile hormone biosynthesis in corpus allatum of *Diploptera punctata*. Mol. Cell. Endocrinol. 158, 163-171.

Rachinsky, A., Tobe, S.S., 1996. Role of second messengers in the regulation of juvenile hormone production in insects, with particular emphasis on calcium and

phosphoinositide signaling. Arch. Insect Biochem. Physiol. 33, 259-282.

Raymond, C.S., Murphy, M.W., O'Sullivan, M.G., Bardwell, V.J., Zarkower, D., 2000. *Dmrt1*, a gene related to worm and fly sexual regulators, is required for mammalian testis differentiation. Genes Dev. 14, 2587-2595.

Raymond, C.S., Shamu, C.E., Shen, M.M., Seifert, K.J., Hirsch, B., Hodgkin, J., Zarkower, D., 1998. Evidence for evolutionary conservation of sex-determining genes. Nature 391, 691-695.

Roberts, A., Pachter, L., 2013. Streaming fragment assignment for real-time analysis of sequencing experiments. Nat. Methods 10, 71-73.

Robinett, C.C., Vaughan, A.G., Knapp, J.-M., Baker, B.S., 2010. Sex and the single cell. II. There is a time and place for sex. PLoS Biol. 8, e1000365.

Robinson, M.D., McCarthy, D.J., Smyth, G.K., 2010. edgeR: a Bioconductor package for differential expression analysis of digital gene expression data. Bioinformatics 26, 139-140.

Robinson, M.D., Oshlack, A., 2010. A scaling normalization method for differential expression analysis of RNA-seq data. Genome Biol 11, R25.

Sagawa, K., Yamagata, H., Shiga, Y., 2005. Exploring embryonic germ line development in the water flea, *Daphnia magna*, by zinc-finger-containing VASA as a marker. Gene Expression Patterns 5, 669-678.

Saito, K., Su, Z.H., Emi, A., Mita, K., Takeda, M., Fujiwara, Y., 2006. Cloning and expression analysis of *takeout/JHBP* family genes of silkworm, *Bombyx mori*. Insect Mol. Biol. 15, 245-251.

Sanchez, L., 2008. Sex-determining mechanisms in insects. Int. J. Dev. Biol. 52, 837-856.

Shen, M.M., Hodgkin, J., 1988. *mab-3*, a gene required for sex-specific yolk protein expression and a male-specific lineage in *C. elegans*. Cell 54, 1019-1031.

Shin, S.W., Zou, Z., Saha, T.T., Raikhel, A.S., 2012. bHLH-PAS heterodimer of methoprene-tolerant and Cycle mediates circadian expression of juvenile hormone-induced mosquito genes. Proc Natl Acad Sci U S A Biol Sci 109, 16576-16581.

Shinoda, T., Itoyama, K., 2003. Juvenile hormone acid methyltransferase: a key regulatory enzyme for insect metamorphosis. Proc. Natl. Acad. Sci. U. S. A. 100, 11986-11991.

Shinoda, T., Kobayashi, J., Matsui, M., Chinzei, Y., 2001. Cloning and functional expression of a chitinase cDNA from the common cutworm, *Spodoptera litura*, using a recombinant baculovirus lacking the virus-encoded chitinase gene.

Insect Biochem. Mol. Biol. 31, 521-532.

Shoemaker, C.M., Crews, D., 2009. Analyzing the coordinated gene network underlying temperature-dependent sex determination in reptiles. Semin. Cell Dev. Biol. 20, 293-303.

Shukla, J.N., Nagaraju, J., 2010. *Doublesex*: a conserved downstream gene controlled by diverse upstream regulators. J Genet 89, 341-356.

Shukla, J.N., Palli, S.R., 2012. Sex determination in beetles: Production of all male progeny by Parental RNAi knockdown of *transformer*. Scientific reports 2, srep00602.

Sinev, A.Y., Sanoamuang, L.-O., 2011. Hormonal induction of males as a method for studying tropical cladocerans: description of males of four chydorid species (Cladocera: Anomopoda: Chydoridae). Zootaxa 2826, 45-56.

Smith, G., 1915. The life-cycle of Cladocera, with remarks on the physiology of growth and reproduction in crustacea. Proc. R. Soc. Lond. B. Biol. Sci. 88, 418-435.

Smith, K.C., Macagno, E.R., 1990. UV photoreceptors in the compound eye of *Daphnia magna* (Crustacea, Branchiopoda). A fourth spectral class in single ommatidia. J Comp Physiol A Sens Neural Behav Physiol 166, 597-606.

Snapea, J.R., Maund, S.J., Pickford, D.B., Hutchinson, T.H., 2004. Ecotoxicogenomics: the challenge of integrating genomics into aquatic and terrestrial ecotoxicology. Aquat. Toxicol. 67, 143-154.

Soetaert, A., Moens, L.N., Ven, K.V.d., Leemput, K.V., Naudts, B., Blust, R., Coen, W.M.D., 2006. Molecular impact of propiconazole on *Daphnia magna* using a reproduction-related cDNA array. Comparative Biochemistry and Physiology Part C: Toxicology & Pharmacology 142, 66-76.

Soetaert, A., Vandenbrouck, T., Ven, K.v.d., Maras, M., Remortel, P.v., Blust, R., Coen, W.M.D., 2007a. Molecular responses during cadmium-induced stress in *Daphnia magna*: Integration of differential gene expression with higher-level effects. Aquat. Toxicol. 83, 212-222.

Soetaert, A., Ven, K.v.d., Moens, L.N., Vandenbrouck, T., Remortel, P.v., Coen, W.M.D., 2007b. *Daphnia magna* and ecotoxicogenomics: Gene expression profiles of the anti-ecdysteroidal fungicide fenarimol using energy-, molting- and life stage-related cDNA libraries. Chemosphere 67, 60-71.

Song, J., Zhongxia Wu, Wang, Z., Deng, S., Zhou, S., 2014. Krüppel-homolog 1 mediates juvenile hormone action to promote vitellogenesis and oocyte maturation in the migratory locust. Insect Biochem. Mol. Biol. 52, 94-101.

Soroka, Y., Sagi, A., Khalaila, I., Abdu, U., Milner, Y., 2000. Changes in protein kinase

C during vitellogenesis in the crayfish *Cherax quadricarinatus* -possible activation by methyl farnesoate. Gen. Comp. Endocrinol. 118, 200-208.

Spanier, K.I., Leese, F., Mayer, C., Colbourne, J.K., Gilbert, D., Pfrender, M.E., Tollrian, R., 2010. Predator-induced defences in *Daphnia pulex*: selection and evaluation of internal reference genes for gene expression studies with real-time PCR. BMC Mol. Biol. 11.

Steinbiss, S., Gremme, G., Scharfer, C., Mader, M., Kurtz, S., 2009. AnnotationSketch: a genome annotation drawing library. Bioinformatics 25, 533-534.

Stenderup, J.T., Olesen, J., Glenner, H., 2006. Molecular phylogeny of the Branchiopoda (Crustacea)--multiple approaches suggest a 'diplostracan' ancestry of the Notostraca. Mol. Phylogenet. Evol. 41, 182-194.

Stross, R.G., Hill, J.C., 1965. Diapause induction in Daphnia requires two stimuli. Science 150, 1462-1464.

Suzuki, R., Fujimoto, Z., Shiotsuki, T., Tsuchiya, W., Momma, M., Tase, A., Miyazawa, M., Yamazaki, T., 2011. Structural mechanism of JH delivery in hemolymph by JHBP of silkworm, *Bombyx mori*. Scientific reports 1, srep00133.

Swain, T.D., Taylor, D.J., 2003. Structural rRNA characters support monophyly of raptorial limbs and paraphyly of limb specialization in water fleas. Proc. R. Soc. Lond. B. Biol. Sci. 270, 887-896.

Tamura, K., Peterson, D., Peterson, N., Stecher, G., Nei, M., Kumar, S., 2011. MEGA5: molecular evolutionary genetics analysis using maximum likelihood, evolutionary distance, and maximum parsimony methods. Mol. Biol. Evol. 28, 2731-2739.

Tamura, K., Stecher, G., Peterson, D., Filipski, A., Kumar, S., 2013. MEGA6: Molecular evolutionary genetics analysis version 6.0. Mol. Biol. Evol. 30, 2725-2729.

Tanaka, S., 2001. Endocrine mechanisms controlling body-color polymorphism in locusts. Arch. Insect Biochem. Physiol. 47, 139-149.

Tatarazako, N., Oda, S., 2007. The water flea *Daphnia magna* (Crustacea, Cladocera) as a test species for screening and evaluation of chemicals with endocrine disrupting effects on crustaceans. Ecotoxicology 16, 197-203.

Tatarazako, N., Oda, S., Watanabe, H., Morita, M., Iguchi, T., 2003. Juvenile hormone agonists affect the occurrence of male *Daphnia*. Chemosphere 53, 827-833.

Taylor, D.J., Crease, T.J., Brown, W.M., 1999. Phylogenetic evidence for a single long-lived clade of crustacean cyclic parthenogens and its implications for the evolution of sex. Proc. R. Soc. Lond. B. Biol. Sci. 266, 791-797.

Team, R.C., 2013. R: A Language and Environment for Statistical Computing. R Foundation for Statistical Computing http://www.R-project.org/.

Terashima, J., Bownes1, M., 2005. A microarray analysis of genes involved in relating egg production to nutritional intake in *Drosophila melanogaster*. Cell Death Differ. 12, 429-440.

Thompson, J.D., Higgins, D.G., Gibson, T.J., 1994. CLUSTAL W: improving the sensitivity of progressive multiple sequence alignment through sequence weighting, position-specific gap penalties and weight matrix choice. Nucleic Acids Res. 22, 4673-4680.

Touhara, K., Prestwich, G.D., 1993. Juvenile hormone epoxide hydrolase; Photoaffinity labeling, purification, and characterization tabacco hornworm eggs. The Journal of Biological Chemistry 268, 19604-19609.

Toyota, K., Kato, Y., Miyakawa, H., Yatsu, R., Mizutani, T., Ogino, Y., Miyagawa, S., Watanabe, H., Nishide, H., Uchiyama, I., Tatarazako, N., Iguchi, T., 2014. Molecular impact of juvenile hormone agonists on neonatal *Daphnia magna*. J. Appl. Toxicol. 34, 537-544.

Toyota, K., Kato, Y., Sato, M., Sugiura, N., Miyagawa, S., Miyakawa, H., Watanabe, H., Oda, S., Ogino, Y., Hiruta, C., Mizutani, T., Tatarazako, N., Paland, S., Jackson, C., Colbourne, J.K., Iguchi, T., 2013. Molecular cloning of doublesex genes of four cladocera (water flea) species. BMC Genomics 14, 239.

Toyota, K., Miyakawa, H., Hiruta, C., Furuta, K., Ogino, Y., Shinoda, T., Tatarazako, N., Miyagawa, S., Shaw, J.R., Iguchi, T., in press. Methyl farnesoate synthesis is necessary for the environmental sex determination in the water flea *Daphnia pulex*. J. Insect Physiol.

Trionnaire, G.L., Wucher, V., Tagu, D., 2013. Genome expression control during the photoperiodic response of aphids. Physiol. Entomol. 38, 117-125.

Vandesompele, J., Preter, K.D., Pattyn, F., Poppe, B., Roy, N.V., paepe, A.D., Speleman, F., 2002. Accurate normalization of real-time quantitative RT-PCR data by geometric averaging of multiple internal control genes. Genome Biol 3.

Vermunt, A.M.W., Kamimura, M., Hirai, M., Kiuchi, M., Shiotsuki, T., 2001. The juvenile hormone binding protein of silkworm haemolymph: gene and functional analysis. Insect Mol. Biol. 10, 147–154.

Volff, J.-N., Zarkower, D., Bardwell, V.J., Schartl, M., 2003. Evolutionary dynamics of the DM domain gene family in metazoans. J. Mol. Evol. 57, 241-249.

Ward, V.K., Bonning, B.C., Huang, T., Shiotsuki, T., Griffeth, V.N., Hammock, B.D.,

1992. Analysis of the catalytic mechanism of juvenile hormone esterase by site-directed mutagenesis. Int. J. Biochem. 24, 1933-1941.

Warner, R.R., Fitch, D.L., Standish, J.D., 1996. Social control of sex change in the shelf limpet, *Crepidula norrisiarum*: size-specific responses to local group comparison. J. Exp. Mar. Biol. Ecol. 204, 155-167.

Watanabe, H., Kobayashi, K., Kato, Y., Oda, S., Abe, R., Tatarazako, N., Iguchi, T., 2008. Transcriptome profiling in crustaceans as a tool for ecotoxicogenomics: *Daphnia magna* DNA microarray. Cell Biol. Toxicol. 24, 641-647.

Watanabe, H., Takahashi, E., Nakamura, Y., Oda, S., Tatarazako, N., Iguchi, T., 2007. Development of a *Daphnia magna* DNA microarray for evaluating the toxicity of environmental chemicals. Environ. Toxicol. Chem. 26, 669-676.

Watanabe, H., Tatarazako, N., Oda, S., Nishide, H., Uchiyama, I., Morita, M., Iguchi, T., 2005. Analysis of expressed sequence tags of the water flea *Daphnia magna*. Genome 48, 606-609.

Waters, M.D., Boorman, G., Bushel, P., Cunningham, M., Irwin, R., Merrick, A., Olden, K., Paules, R., Selkirk, J., Stasiewicz, S., Weis, B., Houten, B.V., Walker, N., Tennant, R., 2003. Systems toxicology and the chemical effects in biological systems (CEBS) knowledge base. Environ. Health Perspect. 111, 811-824.

Waters, M.D., Fostel, J.M., 2004. Toxicogenomics and systems toxicology: aims and prospects. Nat Rev Genet 5, 936-948.

Weiss, L.C., Tollrian, R., Herbert, Z., Laforsch, C., 2012. Morphology of the *Daphnia* nervous system: a comparative study on *Daphnia pulex*, *Daphnia lumholtzi*, and *Daphnia longicephala*. J. Morphol. 273, 1392-1405.

Williams, T.M., Carroll, S.B., 2009. Genetic and molecular insights into the development and evolution of sexual dimorphism. Nat Rev Genet 10, 797-804.

Willis, D.K., Wang, J., Lindholm, J.R., Orth, A., Goodman, W.G., 2010. Microarray analysis of juvenile hormone response in *Drosophila melanogaster* S2 cells. Journal of insect science 10.

Yamaguchi, T., Yoshinaga, N., Yazawa, T., Gen, K., Kitano, T., 2010. Cortisol is involved in temperature-dependent sex determination in the Japanese flounder. Endocrinology 151, 3900-3908.

Yamamoto, H., Okino, T., Yoshimura, E., Tachibana, A., Shimizu, K., Fusetani, N., 1997. Methyl farnesoate induces larval metamorphosis of the barnacle, *Balanus amphitrite* via protein kinase C activation. J. Exp. Zool. 278, 349-355.

Yamamoto, K., Chadarevian, A., Pellegrini, M., 1988. Juvenile hormone action mediated in male accessory glands of *Drosophila* by calcium and kinase C.

Science 239, 916-919.

Yanai, H., 2011. Statcel, the Useful Add-in Software Forms on Excel. 3rd edition. Tokyo, OMS.

Yao, H.H.-C., Capel, B., 2005. Temperature, genes, and sex: a comparative view of sex determination in *Trachemys scripta* and *Mus musculus*. J. Biochem. (Tokyo). 138, 5-12.

Zarkower, D., 2001. Establishing sexual dimorphism: conservation amidst diversity? Nat Rev Genet 2, 175-185.

Zhang, Y., Zheng, Y., Li, D., Fan, Y., 2014. Transcriptomics and identification of the chemoreceptor superfamily of the pupal parasitoid of the oriental fruit fly, *Spalangia endius* Walker (Hymenoptera: Pteromalidae). PLoS ONE 9, e87800.

Zhang, Z., Xu, J., Sheng, Z., Sui, Y., Palli, S.R., 2011. Steroid receptor co-activator is required for juvenile hormone signal transduction through a bHLH-PAS transcription factor, methoprene tolerant. J. Biol. Chem. 286, 8437-8447.

Zhou, X., Tarver, M.R., Scharf, M.E., 2007. Hexamerin-based regulation of juvenile hormone-dependent gene expression underlies phenotypic plasticity in a social insect. Development 134, 601-610.

Zhu, J., Busch, J.M., Zhang, X., 2010. Identification of juvenile hormone target genes in the adult female mosquitoes. Insect Biochem. Mol. Biol. 40, 23-29.

Zou, F.-M., Lou, D.-S., Zhu, Y.-H., Wang, S.-P., Jin, B.-R., Gui, Z.-Z., 2011. Expression profiles of glutathione S-transferase genes in larval midgut of *Bombyx mori* exposed to insect hormones. Mol. Biol. Rep. 38, 639-647.

Zou, Z., Saha, T.T., Roy, S., Shin, S.W., Backman, T.W.H., Girke, T., Whitef, K.P., Raikhel, A.S., 2013. Juvenile hormone and its receptor, methoprene-tolerant, control the dynamics of mosquito gene expression. Proc. Natl. Acad. Sci. U. S. A.

Acknowledgements

I wish to express my deepest gratitude to Prof. Taisen Iguchi for his valuable advice, encouragement, support, and critical reading and corrections of this thesis. I also express my gratitude to Prof. Shosei Yoshida, Dr. Eiji Watanabe, and Dr. Toru Miura for their valuable comments on this manuscript, Dr. Akiya Watakabe for his valuable comments in this study, Drs. Shuji Shigenobu, Katsushi Yamaguchi, Tomoko Mori and staffs of NIBB Functional Genomics Facility office for their hospitable support and advices in transcriptome and LC-MS analysis, Drs. John K. Colbourne, Joseph R. Shaw and Norihisa Tatarazako for providing the daphnid strains, Drs. Tetsuro Shinoda and Kenjiro Furuta for providing the data of biochemical assay of JHAMT, Dr. Yasuhiko Kato for his hospitable support in microinjection technique, Drs. Susanne Paland and Craig Jackson for providing the data involved in analysis of promoter regions of *dsx* genes, Kaoru Kobayashi, Masaru Sato and Naomi Sugiura for providing the data of *dsx* genes identified from some cladocerans, Drs. Ikuo Uchiyama and Hiroyo Nishide for their maintenance and update of *D. magna* database in NIBB, Drs. Shinya Maki, Michiaki Mabuchi, Susumu Nakayama, Katsuhiko Nakagawa and staffs of Niihama National College of Technology for their supports and encouragement.

Further, I would like to thank to Drs. Shinichi Miyagawa, Yukiko Ogino, Hitoshi Miyakawa and Chizue Hiruta for their valuable comments in this study, Taeko Imaizumi, Takeshi Mizutani, Tomoko Hayashi, Kayo Inaba, Ryohei Yatsu, Eri Sumiya and Saki Tohyama for their supports, encouragement and friendship. All the member of Department of Basic Biology, School of Life Science, Graduate University for Advanced Studies (SOKENDAI) is thanked for their kind helps.

Finally, I would like to express my great gratitude to my parents, wife (Momoko) and son (Yomei) for the understanding, kind support and encouragement during my Ph.D course.

January 2015, Kenji Toyota

This work was supported by Grant-in-Aid for the Japan Society for the Promotion of Science (JSPS) Fellows (No.12J05579), the Sasakawa Scientific Research Grant from The Japan Science Society, and the Saito Ho-on Kai Scientific Research Grant from The Saito Gratitude Foundation.